Global Reactor Calculations

Makai Mihály & Dániel Péter Kis

2014. február 3.

The present work discusses a segment of the calculational model of reactor calculation, the so called global reactor calculation. The design, the surveillance, safety analysis, the control, and the economic operation is based on models of the nuclear reactor. The models are complex, they require a large amount of input data ranging from the fine details of the geometry to the detailed isotope compositions of the various reactor materials. The input data feed a physical model describing the neutron population in the reactor core. Unfortunately the equations of reactor physics have only numerical solutions in the applications, so the reactor models are computer programs.

The global reactor calculation is the last element of a computation chain which starts with the processing of nuclear data library and continues with the fuel cell calculations, the fuel assembly calculation. All the above mentioned elements contribute to the success or failure of the global calculation.

The present work focuses on the physical and mathematical models of the reactor calculation. The mathematical models determine the problem to be solved, in details the equation, the boundary condition, the numerical procedure used to determine the solution. A practical problem, like the assessment of safety, requires the solution of several mathematical problems. Those working in the nuclear industry, or for a nuclear safety authority, should understand the nature and limit of the involved models.

The Reader is assumed to be familiar with the operation of a nuclear reactor. The treatise focuses on the following topics:

1. The physical and mathematical models used in the global reactor calculation.
2. Provision of input data for the global reactor calculation.
3. The diffusion equation is the corner stone hence we discuss the diffusion theory in details through four Chapters.
4. The numerical methods used to solve the fundamental equations i.e. the Boltzmann equation and the diffusion equation are only mentioned shortly.
5. The iteration process deals with some general problems of large linear equation systems.
6. Immediate applications of the global reactor calculations in the evaluation of in-core measurement processing, in the reactor control and operation as well as in assessing safety issues are dealt with separately.
7. Additional operational questions, like fuel cycle optimization, stability problems, management of transient processes are mentioned only in short.

The material assumes the Reader to be familiar with the basic techniques of linear algebra and matrices, probability theory and statistics, as well as basics of functional analysis. The fission process, the neutron-nucleus interaction, the cross-section of a nuclear reaction is assumed to be known from former nuclear physics studies. Some topics of the applied mathematical tools are summarized in the Appendices. Section 2. is based on the contribution provided by János Végh (Centre of Energy Research, Hungarian Academy of Sciences)

Tartalomjegyzék

Ábrák jegyzéke

Táblázatok jegyzéke

1. fejezet

What is a Nuclear Reactor?

The subject of the present work is the nuclear reactor in which a part of the binding energy of a fissionable nucleus is released in a process called fission. The energy release is accompanied by radioactive radiations. The binding energy is 10^7 times larger than the energy released in chemical reactions therefore the power density in a nuclear reactor is also larger than in the traditional power plants.

Nuclear reactors are classified by their usage as

- energy production;
- propulsion;
- heat source;
- hydrogen production;
- transmutation;
- research;
- education and training.

Energy production takes place in a nuclear power plant, nuclear propulsion is used in ships. Nuclear reactor appears as heat source in district heating plants. Immediate hydrogen production is a recently developing application. The transmutation is a research topic aiming at reducing the storage time of high activity nuclear waste. A nuclear reactor is used as a neutron source in the structure research of complex biological materials, or, in the research of the catalysis. Reactors small in size and low in power are used in education and training.

The heart of the nuclear reactor is the fission process. Some nuclei absorb a neutron and the excitation caused by the binding energy of the absorbed neutron suffices to excite the newly formed nucleus so that it splits into fragments. The process is shown in Fig. 1.1. Some of the fissionable nuclei emit also one or more neutrons. That led Leo Szilárd to the idea that self-sustaining fission, the so called chain reaction, can be established. The fission of ^{235}U shown in Fig. 1.1, results in two fragments of more or less equal mass, and two- or three neutrons. To obtain self-sustaining fission, one needs to arrange the material in such a structure that allows for the neutrons to hit another ^{235}U nucleus before being absorbed by another nucleus. The distribution of the energy released in fission is shown in Table 1.1.

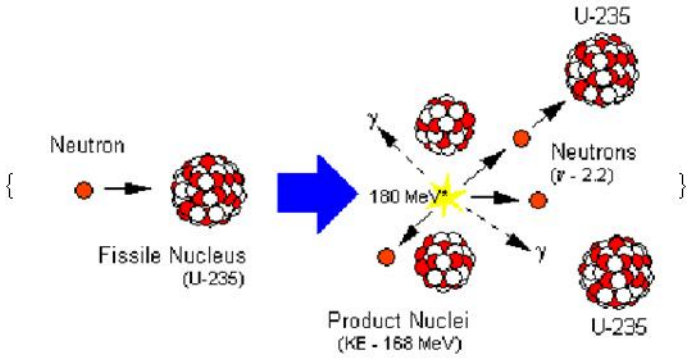

1.1. ábra. Fission process (source: Encyclopedia of Science, internet)

Kinetic energy of fission fragments	162 MeV
Beta decay energy	5 MeV
Gamma decay energy	5 Mev
Neutrino energy	11 MeV
Energy of fission neutrons	6 MeV
Instantaneous gamma-ray energy	6 MeV
Total fission energy	195 MeV

1.1. táblázat. Distribution of fission energy

We see from the table that majority of the energy appears as kinetic energy, i.e. as heat. In order to produce energy, we have to achieve not only the self sustaining fission but also removing the generated heat. In addition, the power released from fission should be kept at a constant level, thus the energy production is also a regulation problem.

The next Chapter gives an overview of nuclear reactors.

2. fejezet

Nuclear Reactors

2.1. Nuclear reactors for electricity production

2.1.1. Fundamentals of nuclear energy production

In this chapter a general overview of the technology applied for energy production in nuclear power stations is outlined, starting with processes taking place in the active core, continuing with heat exchange in the steam generator and ending with the generator supplying electricity to the grid. Description of the various phases of the nuclear fuel cycle is also given, detailing the history of the uranium ore from the mine to the final spent fuel storage, as well as discussing differences between UO2 and MOX fuel. The purpose is to illustrate the main steps in the technology of nuclear electricity production, therefore other type of plants (e.g. for provision of process heat) are not treated here.

Basic principles

The basic process utilized for energy production in any nuclear power station is the controlled and self-sustaining chain reaction of fissile nuclei. The heat generated in the chain reaction is removed by an appropriate coolant material and after suitable conversion the thermal energy is used for producing electricity. The nuclear fuel resides in the so called active core, the fuel consists of fissile isotopes, as well as fertile isotopes that can produce fissile isotopes through nuclear reactions. Generally the fissile material in the fuel is constituted by uranium or by an uranium-plutonium mixture (the latter is called MOX fuel). In nature there exists only one isotope, namely ^{235}U, which undergoes fission induced by low energy (thermal) neutrons, but unfortunately this isotope constitutes only 0,72% of natural uranium. The vast majority (99,275%) of natural uranium is constituted by the ^{238}U isotope: high energy (fast) neutrons induce fission in it, but a self-sustaining chain reaction cannot be maintained in an active core constructed solely from ^{238}U isotope. In the industrial practice the following fissile isotopes are utilized most commonly: ^{235}U, ^{239}Pu, 241Pu and ^{233}U. In nature there exist two important fertile isotopes, ^{238}U and ^{232}Th. The first one produces ^{239}Pu after a neutron-capture event, while the thorium isotope produces ^{233}U. The ^{241}Pu isotope is produced when the ^{240}Pu artificial (i.e. not existing in the nature) fertile isotope undergoes a neutron-capture event. The isotope ^{240}Pu is created by a similar process from ^{239}Pu (see [6] and [7] for details).

Heat is produced by various processes in the active core of a reactor:

- High energy fission products slowdown in the fuel, in the structural materials and in the coolant, and during this process the kinetic energy of the fission products is transformed to heat (thermal energy).
- The gamma radiation produced during the fission process is absorbed and its energy is transformed to heat.
- Heat is also produced by the radioactive decay of the fission products.

The released energy is very large: the energy released during the fission of a single gram of ^{235}U is equivalent to the energy released by burning 3 metric tons of high quality coal.

Reactors commonly operated in nuclear power stations can be classified according to various principles. One possible approach is the classification according to the energy of the neutrons inducing fission in the reactor:

- The chain reaction in the "thermal reactors" is maintained by low energy neutrons, slowed down to the thermal energy region. The vast majority of the energy producing reactors of today belongs to this class. In order to slow down the high energy neutrons produced in the fission process, these reactor types use a so called moderator material (mainly light water or heavy water or graphite is applied as moderator). Thermal neutrons have a very advantageous feature: when fissile isotopes (e.g. ^{235}U or ^{239}Pu) are bombarded by thermal neutrons, these isotopes undergo induced fission with much higher probability compared to the case of fast neutrons. This circumstance makes it possible to use low ($<5\%$) enriched uranium, or even natural uranium as fuel material.
- The chain reaction in the so called "fast reactors" is maintained by high energy neutrons without slowing down, as produced in the fission process. These reactor types do not use moderator and the coolant must not slow down the neutrons either (special coolant applicable in fast reactors is the liquid sodium, for example). Fast reactors use higher fuel enrichment (figures around 20% are typical) in order to compensate the high neutron capture effect (i.e. neutron absorption) of the ^{238}U isotope.

Another commonly used method is to classify according to the material of the moderator used to slow down the neutrons. Generally the following classes are defined:

- Light-water (H_2O) moderated reactors (this is the most widely used type, and generally these reactors use light-water as a coolant, as well), see Fig 2.1.
- Heavy-water (D_2O) moderated reactors (e.g. CANDU, developed by AECL, Canada).
- Graphite moderated reactors (e.g. Advanced Gas Cooled Reactor, AGR).
- Light element (lithium or beryllium) moderated reactors (e.g. Molten Salt Reactor).

Another classification method distinguishes between the reactor types according to the coolant material used for core cooling. According to this method the following types are defined:

- Light-water cooled reactors have two basic types, the pressurized water and the boiling water reactors, Figure 2.1. illustrates the operating scheme of these two types. The water in a pressurized reactor is kept at sufficiently high pressure, to prevent boiling even at the high operation temperature. The coolant flows through the core, then it is led into a large heat exchanger called steam generator, where the coolant looses a considerable fraction of its energy and produces steam. The steam is led to a steam

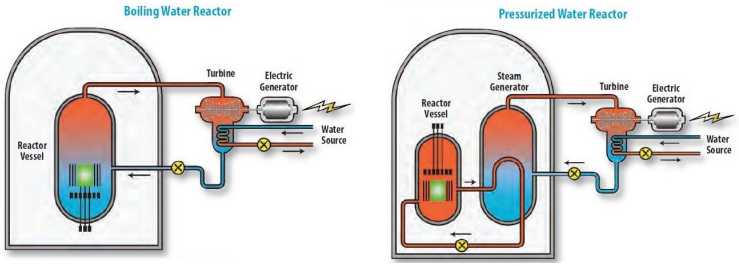

2.1. ábra. Operating scheme of the two most widely used light-water cooled reactor type [8]

turbine and the turbine drives a generator producing electricity. There are no steam generators in a boiling water reactor, because the coolant reaches the boiling state within the active core and this steam is led directly to the turbine.

- In gas cooled reactors the heat is removed from the core by an inert gas, e.g. helium or carbon dioxide. The cooling gas either directly drives a special turbine, or the gas is used for producing steam in a steam generator and the steam is led to a conventional steam turbine.
- Liquid metal (sodium or lead) coolants are used in fast reactors, because these materials are good coolants, but bad moderators, i.e. they do not slow neutrons down.
- Molten salt is used as coolant medium in molten salt reactors (MSR), generally lithium or beryllium salts formed with fluoride are applicable for industrial purposes.

It is also common to define "reactor generations" according to the time interval when reactors were developed and constructed. Reactor generations are treated in 2.2 in detail.

Nuclear fuel cycle

Figure 2.2 shows the history of the uranium ore from the mine to the storage place of radioactive waste or to the fuel reprocessing facility. The history of uranium from the uranium mine to the final spent fuel storage facility or to the reprocessing factory is a long, multi-step process, containing complex chemical, mechanical and other industrial engineering operations. This process is generally called nuclear fuel cycle. Two fuel cycle types are distinguished, depending on what happens with the spent fuel removed from the nuclear power station after the fuel utilization is over. In the so called "open" fuel cycle the fuel is not reprocessed, but after a sufficiently long storage period it is placed in a storage place specially designed and constructed for the safe storage of highly radioactive spent fuel elements. The vast majority of the present nuclear power stations uses this open fuel cycle approach, despite the fact that there is no final spent fuel storage facility in any country yet (design and construction works are going on in several countries). In the so called "closed" fuel cycle the spent fuel is reprocessed in a special factory. During reprocessing plutonium and uranium is extracted from the fuel by using chemical methods, later these materials are used to fabricate new fuel elements. The result is the MOX fuel, see Figure 2.2. In the "closed" cycle the highly radioactive waste - remaining after reprocessing - must be stored at a suitable final repository. In the following Subsections a short description of the "open" fuel cycle is given.

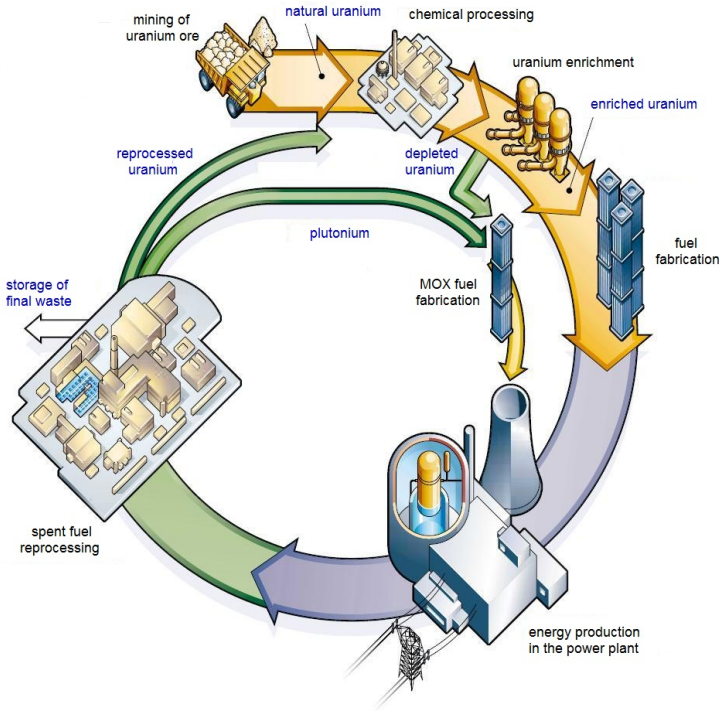

2.2. ábra. The general scheme of the nuclear fuel cycle ([9])

Uranium mining

As of today, the mining of uranium ore is carried out by using three different methods. Open-pit mines are set up at those places where the uranium ore is abundant in layers close to the surface of the Earth. Deep pit mines are constructed at those places where the layers rich in uranium ore are located deep (sometimes several hundred meters) below the surface. Recently the application of a novel method is spreading: the basic principle of this "in situ leaching" method is that a liquid substance containing acidic or alkaline chemicals is being pumped below the surface, into the rock layer containing the uranium ore. The liquid - among others - dissolves the minerals containing uranium, then this liquid (containing dissolved uranium ore) is taken back to the surface where it is further processed to extract uranium. The waste liquid substance remaining after the processing is pumped back, under the surface of the soil. This method does not cause "landscape wounds" as open pit mines do not produce the large amount of waste rock, a well-known characteristics of deep pit mines. In the first phase of processing the uranium ore obtained from the mine is taken through the usual ore processing steps: it is milled into small pieces in an ore mill, then it is selected, cleaned and dried. At the end of this process a fine powder substance is obtained, it is already suitable to start chemical processing, consisting of the following steps:

- by using a suitable chemical solvent material, the uranium present in the ore-powder is solved into an alkaline, acidic or peroxide solution,
- the uranium solution is then separated from the other components,
- in the last step the uranium is precipitated and the precipitate is dried.

The dried uranium precipitate usually has bright yellowish color, this is why the end-product got its well-known name "yellowcake". The uranium heavy metal content of the yellowcake is at least 70%, but for practical reasons its further processing is carried out in U_3O_8 compound form, containing more than 80% uranium.

Uranium enrichment

The next step in the fuel fabrication process is uranium enrichment. "Enrichment" in this context means "increasing the concentration of the ^{235}U isotope in the uranium". However, yellowcake is not an appropriate substance to be used for the enrichment process, so first it is converted to uranium hexafluoride (UF_6) gas. This gas can be enriched in two very different processes: one of the methods relies on diffusion, while the other uses centrifuges, but both methods utilize the small mass difference between the ^{235}U and the ^{238}U isotopes. In case the UF_6 gas diffuses through a porous wall, then the UF_6 molecules containing the lighter ^{235}U isotope move faster and on the other side of the wall their concentration will be higher than that of the UF_6 molecules containing the more heavy ^{238}U isotope. In an industrial application the gas molecules are driven through the porous wall by a high-pressure compressor and the system consists of many diffusion stages. The gas depleted in the ^{235}U isotope is taken back to the previous stages, while the gas enriched in the ^{235}U isotope is forwarded to the next diffusion stages. The parameter called enrichment ratio, characterizing how effectively the enrichment process works, is very small for the gas-diffusion method, therefore approximately 1400 or 1500 diffusion stages are required to achieve the required 4% enrichment (it must be noted that the relative abundance of the ^{235}U isotope is only 0.72% in the natural uranium).

Gas-centrifuges utilize the fact that the centrifugal force acting on a gas molecule with a larger mass is larger compared to a lighter gas molecule. Due to this effect UF_6 molecules

containing the more heavy ^{238}U isotopes tend to increase in number at the outer wall of the centrifuge, while UF_6 molecules with the lighter ^{235}U isotope are more abundant in the region around the middle of the centrifuge. An industrial gas centrifuge is a long vertical cylinder, placed in a closed tank and rotating with very high speed in vacuum. The system is fed by UF_6 gas and as a result of the fast centrifuging the concentration of the more heavy UF_6 molecules is increasing towards the outer wall of the centrifuge. In the long cylinder the flow paths are arranged in such a manner, that the more heavy gas moves towards the bottom of the tank, while the lighter gas moves to the top, allowing a proper separation of the "products" at the bottom and at the top of the centrifuge, respectively. The gas enriched in the ^{235}U isotope is fed to the next centrifugal-stage, while the gas depleted in the ^{235}U isotope is taken back to the beginning of the whole process. At the end of the above described process, 10-15% of the original uranium quantity is obtained as enriched uranium, while 85-90% remains as depleted uranium (note that the ^{235}U concentration in the depleted uranium is much lower than 0.72% characterizing natural uranium). Note that the enrichment ratio of one stage in the centrifugal method is significantly higher than that is for the diffusion method.

Fuel production

After achieving the targeted enrichment (around 4%) fluorine is removed from the UF_6 gas, and the remaining powdery enriched uranium is taken to the next phase of the fuel fabrication process. In this phase first ceramic tablets are made from the powder, then fuel rods are constructed from the tablets and several fuel rods are assembled into a so called fuel assembly (see Figure 2.3). Finally these fuel assemblies are loaded into the active core of the reactor of the nuclear power station. The rods are arranged within the fuel assembly in a lattice (grid). Assemblies have lower- and upper rod-fastening structures and coolant flow-guides, as well as several axial spacer grids in order to keep the geometry of the fuel lattice (see Figure 2.3). In the first manufacturing step the uranium powder is pressed to small, cylindrical tablets (these are often called fuel pellets) by using a power metallurgy technology called sintering. Afterwards ceramic pellets are carefully selected according to size and weight, then they are positioned into a long zirconium-alloy tube. Finally the tube is filled with inert gas (helium) and hermetically sealed. This tubular structure constitutes the so called fuel rod. Zirconium is a suitable material, because it does not absorb neutrons, therefore it does not influence the neutron balance of the core. Ceramic pellets themselves retain the solid fission products produced in the chain reaction, and the primary barrier to prevent the emission of gaseous fission products is the cladding of the fuel rod.

As of today, the vast majority of nuclear fuel utilized in the nuclear power stations all over the world is low-enriched ($<$5%) uranium dioxide used in the form of ceramic pellets. However, recently some countries (e.g. France, United Kingdom and Japan) gradually started to use a new type of fuel, which is called "mixed oxide" (MOX) fuel. The fraction of MOX is not yet significant in the fuel market, according to the numbers of WANO, in 2009 MOX represented only 2% of the manufactured new fuel. The "mixed oxide" name refers to the fact, that this fuel contains various fissile and fertile isotopes. The most important component of the mixture is plutonium, which is either mixed with natural uranium or with depleted uranium obtained from reprocessing or as a by-product of the enrichment process. Plutonium is either obtained through spent fuel reprocessing or from the final dismantling of military nuclear warheads (see the "Megatons to Megawatts" Russian-USA program).

It is a general practice to load 33% or 50% MOX fuel into the active core, but some modern reactor designs can operate even with 100% MOX core. Main differences between MOX and UO_2 fuel characteristics are as follows:

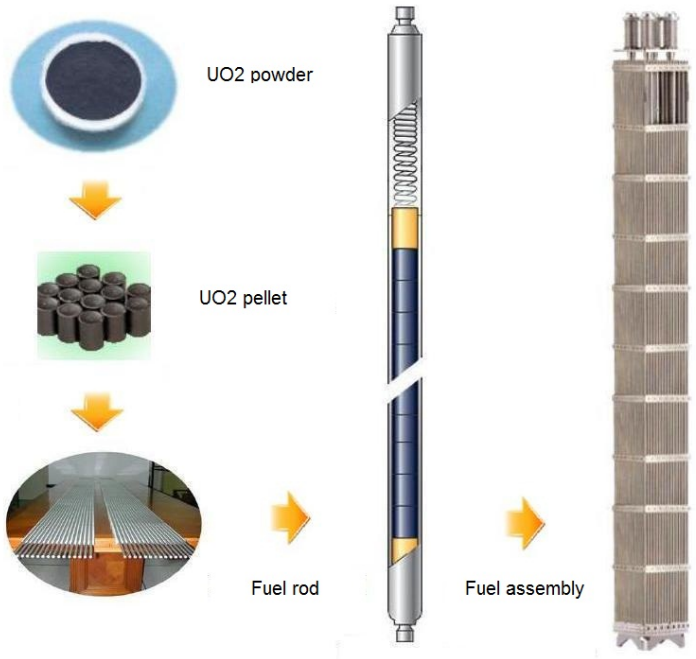

2.3. ábra. Main steps in the nuclear fuel fabrication process

- Due to the higher neutron absorption of plutonium, modifications are necessary in the reactor control system if MOX is used (e.g. more control organs are required).
- The MOX fuel pellet has lower heat conductivity coefficient than the UO_2 tablet, therefore it has higher temperature. This must be taken into account when reactor safety and operation limits are determined.
- The MOX fuel rod has higher fission gas release rate then its UO_2 counterpart, therefore lower maximum burnup levels are achievable with this type of fuel.

During its utilization period approximately 30% of the plutonium originally present in the MOX fuel is burnt out. In today's thermal reactors the plutonium is utilized only one time, as reprocessed product. After its energy production period is over, the burnt out MOX fuel is not reprocessed in a second round, rather it is stored as spent fuel.

Utilization and final disposal of nuclear fuel

The fuel assembly represents the basic transport unit of the nuclear fuel, fresh and spent fuel is handled in this form, as well. For example, the length of a VVER-440 fuel assembly is 2.5 m, it contains 126 fuel rods and there are altogether 349 assemblies in the core. Assemblies reside 4 or 5 years in the core, it depends on the type of the fuel and the reactor. During this period, as a result of nuclear reactions, the uranium content of the fuel gradually decreases, this process is called burnup. In order to compensate the effects caused by the burnup the active core is periodically reshuffled (generally reshuffling is performed after 12, 18 or 24 months of continuous operation). During core reshuffling the fuel assemblies with the

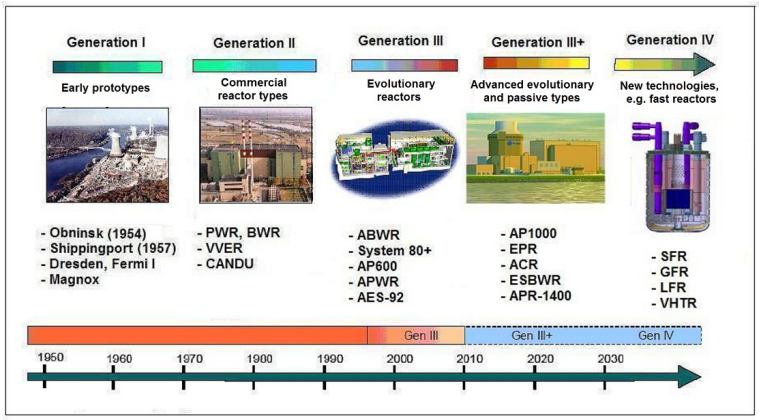

2.4. ábra. The four generation of nuclear power reactors

highest burnup are removed from the core and they are replaced by fresh fuel with zero burnup. This reshuffling is called "refuelling", and the time period between two consecutive refuelling outages is usually called "fuel cycle". The removed burnt fuel is stored for some years close to the reactor in a special storage place called spent fuel storage pool. During this storage period the fuel is kept under water and at the end of the storage the heat production of the fuel decreases to a very low level allowing the transfer of the fuel assemblies to a dry storage facility. In the dry storage facility the spent fuel can be kept safely for decades and its further processing depends on the fuel cycle policy of the owner nuclear utility. In case of an open cycle, at the end of the process spent fuel assemblies are shipped to a final storage place, which generally means a deep geological repository. In case of a closed cycle, spent fuel assemblies are shipped to a reprocessing factory where assemblies are dismantled and pellets are removed from the fuel rods. Then pellets are dissolved in a chemical process to extract uranium and plutonium from the tablets, and finally the extracted fissile and fertile isotopes are used to fabricate MOX fuel elements. Reprocessing also produces a significant amount of highly radioactive waste, this is also stored in a final repository, generally in a vitrified form.

2.2. Nuclear power plant types and generations

It is common to distinguish four reactor generations in the development process of nuclear power stations (see Figure 2.4).

2.2.1. Generation I - prototype and demonstration reactors

The development history of nuclear power stations can be divided into four distinct periods or generations. Generation I contained small scale prototype or demonstration reactors using various technology: the first unit at Obninsk (Soviet Union, 1954) applied graphite moderator and light-water cooling, the Shippingport unit (USA, 1957) had a light-water cooled, thermal breeder reactor, Dresden 1 (USA, 1960) operated the first commercial boiling water reactor, Fermi 1 (USA, 1957) utilized a fast breeder reactor for energy production, while Magnox reactors (UK, 1956) had graphite moderator and CO_2 gas cooling. These units were built in

the 1950s and 1960s and most of them are already closed and decommissioned (apart from some old Magnox units still running in the UK).

2.2.2. Generation II - the power reactors operated today

Generation II reactors were designed in the 1970s and 1980s, based on the experience obtained with Generation I prototype units. During the intense development work several, more or less standard designs were established. The most important types are the pressurized water reactor (PWR), the boiling water reactor (BWR) and the heavy-water moderated, natural uranium fueled CANDU reactor. Needless to say that the vast majority of the currently operated units belongs to Generation II. If classified according to type, the majority belongs to the PWR or BWR class, but a considerable number of units is operated with the Canadian CANDU technology, as well. In March 2012, all over the World 436 units were operated supplying altogether 370.5 GW net electric power, 68% of the reactors were PWR, 21% were BWR and 11% were other types (see 2.5). It must be noted that the Russian-design VVER units belong to the PWR class.

2.2.3. Generation III - the reactors available for construction today

After the severe accidents at Three Mile Island (1979, USA) and Chernobyl (1986, Soviet Union) significant efforts were concentrated to develop new reactor designs all over the World. The basic aim of the design work was to create reactors having considerably better safety indicators than those valid for Generation II types. Generation III was established in the 1990s, mainly through an evolutionary development process starting from selected Generation II reactors. The most important design target was to reduce the probability of severe accidents, as well as to mitigate the consequences of the severe accidents, if they happened. Recently it is common to mention some advanced Generation III designs as Generation III+ reactors. As a rule these Gen III+ reactors apply more passive safety systems than other Gen III designs, to increase the reliability of the safety systems and to decrease core damage frequency. Passive safety systems are extremely reliable, because they use only "natural" driving forces during their functioning. It means that they are operated by gravity, natural circulation or driven by the energy of compressed gas. Due to their operating principles passive systems do not require emergency power supply, and this feature is a considerable advantage in several aspects. The first Generation III units were put into operation in Japan as early as 1996, these were ABWR (Advanced BWR) reactors designed by General Electric and constructed by Hitachi and Toshiba. Today several Gen III types of later design are available on the World market for construction. The most important currently available ("ready for shipment and construction") reactor types are as follows: EPR (European Pressurized Water Reactor) by Areva, AP1000 (Advanced PWR) by Toshiba-Westinghouse, APR-1400 (Advanced Pressurized Reactor) by KEPCO, large APWR (Advanced PWR) by Mitsubishi, ATMEA1 by Areva and Mitsubishi, MIR-1200 (VVER-1200) by Atomstrojexport. In addition to these PWR types, there are some advanced BWR designs on the market, such as ESBWR (Economic Simplified BWR) and ABWR by General Electric, Hitachi and Toshiba, KERENA by Areva (formerly known as Siedewasser Reactor-1000 by Siemens). Atomic Energy of Canada Ltd. also offers a new, higher power and modernized version of its CANDU design under the name of Advanced CANDU Reactor (ACR).

2.2.4. Generation IV - the reactors of the future

The Gen IV project aimed to develop Generation IV reactors was launched in 2000. The basic aim of the development is to create inherently safe reactor types, surpassing present types in practically all aspects of nuclear safety, economical operation, radioactive waste production, as well as proliferation resistance. It is envisaged that some of the Gen IV reactor types presently in the conceptual design phase will be ready for commercial deployment after 2030. In the framework of Generation IV project the following reactor types are being developed: (see [11]):

- sodium cooled fast reactor (SFR)
- gas cooled fast reactor (GFR)
- lead-bismuth cooled fast reactor (LFR)
- high temperature gas cooled thermal reactor (VHTR)
- molten-salt cooled reactor (MSR)
- supercritical pressure, water-cooled reactor (SCWR)

All above listed Gen IV types share ambitious common requirements for safety, reliability, economical and environment-friendly operation, minimization of radioactive waste, and impossibility to use the technology for military purposes. It is also a common target to operate these reactors in a closed fuel cycle. Considering the present status of the associated R&D work it can be firmly stated that none of these reactors can be commercialized before 2030. In the near future the number of investigated Gen IV types will be decreased and the research work will concentrate on only few (two or three) selected designs to ensure success.

As it was stated earlier, on the present World market only Gen III reactors are available: Gen II types are not manufactured any more and one must wait for the Gen IV reactors about two additional decades.

In the further treatment only Generation III PWR types will be discussed, because the PWR type gradually became dominant on the market. Reasons for this dominance are manifold. First of all, PWRs have some design features that makes them superior to BWRs. A PWR unit has three cooling circuits, while a BWR has only two. This technological difference results a considerable difference between the available cooling water inventories, it is mainly due to the large (in certain cases extremely large) water inventory present in PWR steam generators. Larger cooling water masses generally ensure better responses during large transients, i.e. a PWR plant reacts to turbine trips, pipe breaks or even loss of coolant accidents in a more balanced way with larger safety margins during the transient. Another important difference is connected to the reactor pressure vessel (RPV) penetrations: in a BWR control rods are inserted to the core through the bottom of the RPV, while advanced PWR vessels have no penetrations at their bottom part at all. If a core melt accident does happen, in a PWR there are viable means to keep the molten core within the RPV (e.g. by cooling the external wall of the vessel via flooding the reactor cavity by a large amount of water). In a BWR this is not practicable, since the corium will sooner or later pass through the RPV bottom penetrations, and no external cooling can prevent that to happen. An additional fact supporting the PWR type is modern containment technology. Some Generation III PWRs have an extremely robust double containment, constructed with the latest pre-stressed concrete technology. These containments are so strong that they can withstand the crash of a large commercial airplane without loosing critical safety functions.

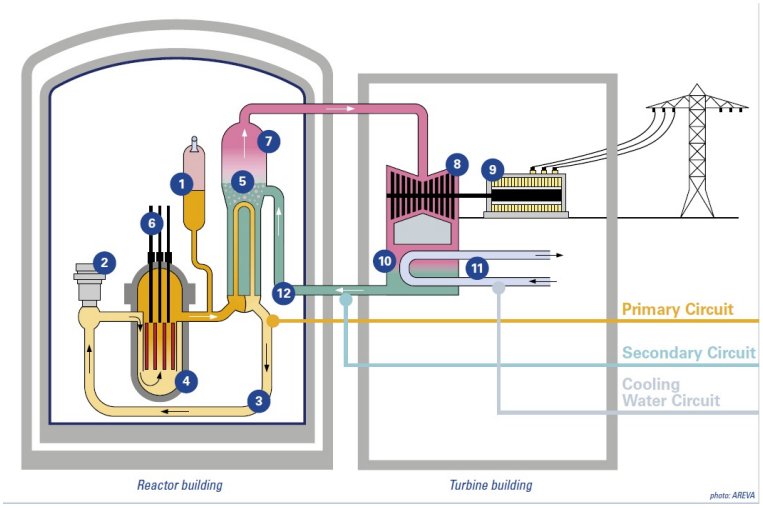

2.5. ábra. Operation scheme of a pressurized water reactor ([13]-[20])

BWR type containments generally have smaller volumes than PWR types and the smaller volume allows faster internal pressure build-up.

As it was mentioned earlier, in March 2012 about 68% of the operating reactors belonged to the PWR type. The PWR dominance is even more pronounced if new builds are considered: 63 new units were under construction in March 2012, and 82% of these units were of PWR type. The tendency is quite clear and one may forecast even more PWRs to be built after Fukushima.

2.3. Technology of nuclear power stations with PWR technology

The present Chapter outlines the main features of the PWR technology, it details the main parts of the nuclear steam generation facility and their operating principles, main buildings of the nuclear power station and describes various possible solutions to ensure site specific ultimate heat sink. Basic features of safety principles applied during plant design are also given briefly (e.g. defense in depth, redundancy, diversity, physical separation) in order to illustrate that the risk represented by Generation III reactors is so small that it is close to the reasonably achievable minimum. In the treatment the emphasis is on Generation III PWRs, concentrating on novel technological solutions developed to achieve a high operational safety level, as well as designs to avoid severe accidents and mitigate their consequences.

The operation scheme of an advanced, large PWR nuclear power station is shown in Fig. 2.5. Legend: 1 - pressurizer, 2 - reactor coolant pump, 3 - primary circuit, 4 - reactor, 5 - secondary circuit, 6 - control assemblies, 7 - steam generator, 8 - turbine, 9 - generator + exciter, 10 - condenser, 11 - cooling water (delivers heat to the ultimate heat sink), 12 - feedwater pump.

The heat production unit of the plant is the reactor, in a PWR type plant the heat is transferred from the reactor to the ultimate heat sink by a cooling system consisting of three cooling circuits. The large amount of heat produced in the active core during the nuclear

fission process is removed by demineralized water circulating in a closed cooling loop called primary circuit. The pressure in the primary circuit is kept by the pressurizer at such a value that the water does not boil even at the high nominal temperature (this is the origin of the "pressurized water reactor" name). The primary circuit must be operated with a very high cooling water flow rate, since the core can have a thermal power value more than 4000 MW. The number of primary circulating loops depends on the design, modern Gen III types generally apply 2, 3 or 4 loop arrangements. The heated up primary circuit cooling water transfers energy to another closed cooling loop called secondary circuit. The heat transfer takes place in very large heat exchangers called steam generators and the generated steam is used to drive a steam turbine. Rotation of the turbine produces electric current in the coupled generator by electromagnetic induction. Finally, through switches and transformers the produced electricity is fed into the national electric grid, where generally 400 kV high voltage level is used.

The exhaust steam leaving the low pressure turbine is condensed to water in the condenser, using the cooling effect of the ultimate heat sink. The ultimate heat sink can be water (taken from the sea, a lake, or a river) or air, if a cooling tower is used. This tertiary cooling circuit is an open circuit, because the large amount of cooling water taken from the water source is led back to the source, although at somewhat higher temperature. The condensed water is heated up and pumped back to the steam generators by using the feedwater pumps.

In addition to the above described main systems the nuclear steam generating system has various auxiliary systems, as well. These auxiliary systems serve for safety purposes, enhance the performance of the plant or clean the above mentioned three cooling circuits. In the following subchapters we illustrate the details of the three cooling circuits with data taken from a large PWR.

2.3.1. Primary circuit

The core is housed by a large vertical, cylindrical steel tank called reactor pressure vessel (RPV). The RPV is made of special steel, for the largest reactors its wall can be as thick as 25 cm in the core region and its outer diameter can be more than 500 cm.

The inner surface of the vessel is coated by a special stainless steel called "plating" to ensure anti-corrosion protection. Modern pressure vessels are designed to have at least 60 years service time, this is ensured by using low carbon austenitic steel alloys as vessel material (this material has low radiation embrittlement behavior). The radiation damage of the RPV wall can be further reduced by a special device called heavy reflector: this steel structure surrounds the core and by reflecting the neutrons back to the core region it decreases the fast neutron flux reaching (and damaging) the wall. The integrity of the RPV is enhanced by the fact that there are no penetrations at the bottom of the vessel and there is no vertical welding at all. Cold leg inlet and hot leg outlet nozzles are located in the upper part of the vessel, their number depends on the number of loops and the design of the primary circuit: there exist designs where there are four cold legs and two hot legs, but in the majority of the reactors the number of hot legs is equal to the number of cold legs. The heat generated in the core is removed by the cooling loops connected to the vessel. The structure of the cooling loops is identical, but one of the loops has an extra equipment called pressurizer, which takes care of the pressure control of the entire primary circuit. When the pressure decreases large heaters are switched on automatically, to keep the pressure at the setpoint (large PWRs operate at 155 or 160 bar nominal pressure). If the primary pressure increases then cold water is injected from one of the cold legs into the pressurizer to lower the pressure according to the setpoint. The circulation of the coolant in the cooling loops is maintained by high-capacity centrifugal pumps called main coolant pumps. The heated up coolant leaves

the pressure vessel through the hot leg nozzles and enters the steam generators. These are large heat exchangers where the heated up primary coolant transfers a large fraction of its energy to the cooling water on the secondary side (this cooling water is called "feedwater"). The cooled down primary coolant is pumped back to the pressure vessel through the cold legs by the main coolant pumps. On the secondary side the feedwater evaporates in the boiling process and the generated steam is led to the steam turbine.

2.3.2. Secondary circuit

The secondary circuit converts the heat produced in the reactor to kinetic and then to electric energy. The feedwater is heated up to boiling by the hot primary water circulating in the steam generator heat exchanger tubes. The steam leaving the steam generator is led to the turbine and rotates the turbine blades by using its kinetic energy. Generation III plants generally have one large turbine, with one high pressure and three low pressure stages and the tendency is to apply "slow" (1500 rpm for 50 Hz grids) machines. In the high pressure stage the steam temperature decreases and its moisture content increases, for this reason a moisture separator and reheater equipment must be applied before the first low pressure stage. This equipment removes water droplets from the steam (these droplets can damage turbine blades) and heats up the steam above the saturation temperature.

2.4. Safety philosophy - defense in depth principle for Generation III plants

The "defense in depth" (often abbreviated as "DiD") principle was already used during the design of the very first nuclear power plants and during the coming decades this principle became a very effective design tool from safety point of view. The proper application of this principle ensures the prevention of various postulated accidents and helps the mitigation of the consequences of severe accidents. Traditionally, when applying the DiD principle, designers tied the postulated accidents and severe accidents to a specific event happened in the technology, called initiating event. Initiating events were selected according to their frequency of occurrence and various DiD levels were defined according to the hypothetical "progression" of the accident: for example if the first level failed then the second level took over, etc. The basic rationale behind this level system was to ensure redundancy, in order to maintain critical safety functions* as long as possible during the escalation of an accident (*critical safety functions are subcriticality, fuel cooling and limiting radioactive releases). The original concept of DiD contained three levels (details can be found in Ref. [17], [18], [19]): As a further development, in the nineties the so called "beyond design basis accident" (BDBA) category was introduced. Basically those accidents belong to this category, that were not included in the original plant design base, such as accidents resulting as a consequence of multiple failures and severe accidents. In order to handle this new category systematically, two new levels of defense were introduced, see Table 2.2.

2.4.1. Application of defense in depth for new reactor designs

The defense in depth concept proposed for the new reactor designs already contains five levels of defense (see [18] for details):

1. Level 1. The aim is to prevent deviations from normal operation and faulty actuations. That goal is achieved by conservative design, high quality construction and safe operation.

2.1. táblázat. Defense in depth concept

	Level of defense	Basic aim of level	Means for achieving basic aim	Corresponding plant states
Original plant design state	Level 1	Prevention of deviations from normal operation and prevention of faulty actuation	Conservative design, high quality construction and safe operation	Normal operation
	Level 2	Detection of abnormal plant states and prevention of anticipated operational occurrences from developing into design basis accidents	Control, limitation and protection systems, monitoring systems, operating procedures	Anticipated operational occurrences
	Level 3	Handling design basis accidents according to the plant design	Safety systems handling design basis accidents, emergency operating procedures	Design basis accidents (postulated individual initiating events)

2.2. táblázat. Additional defense in depth levels

	Level of defense	Basic aim of the level	Means for achieving basic aim	Corresponding plant states
Beyond design basis scenarios	Level 4	Prevention of BDBA situations and mitigation of their consequences	Application of additional measures and devices, and accident management guides	Multiple failures, severe accidents
Accident mitigation plan	Level 5	Mitigation of radiological consequences in case of large radioactive releases	On-site and off-site emergency mitigation measures	

2. Level 2. The aim is to detect abnormal plant states and anticipated operational occurrences from developing into design basis accidents. That goal is achieved by protection systems, monitoring systems, operating procedures.

3. Level 3. The aim is to handle an accident in order to limit radioactive releases and to prevent core damage. The goal is achieved by safety systems and emergency operating procedures.

4. Level 4. The aim is to limit radioactive releases and to prevent core damage. The goal is achieved by safety systems and emergency operating procedures dedicated for handling design base accidents.

5. Level 5.The aim is to mitigate radiological consequences of large radioactive releases. The goal is achieved by prevention measures in the plant's vicinity.

As a consequence of the new design philosophy, the design base of the new reactors includes such accidents that are considered as BDBA events for the presently operating plants (such events are for example the accidents resulting from multiple failures). This means, that for the presently operating plants and for the new designs the meaning of the "beyond design basis accidents" category is different. A further enhancement is the fact that while for the present reactors the DiD deals with the nuclear fuel mainly in those plant states when the fuel resides in the reactor, then for the new designs it includes all possible states of the nuclear fuel (e.g. it includes also those situations when the fuel is stored in the spent fuel storage pool). Characteristic multiple failure cases are, for example:

- anticipated transients without scram (ATWS events),
- station blackout,
- total loss of feedwater,
- small-break LOCA with loss of medium-head safety injection or loss of low-head safety injection system,
- small-break LOCA with loss of component cooling system
- total loss of the spent fuel storage pool cooling system.

The safety analysis of postulated initiating events - combined with the fulfilment of the single failure criterion - can prove the correct functioning of the design solutions applied to ensure proper redundancy. In addition, the analysis of multiple failure scenarios provides information on the fact, whether diverse design solutions applied on the third level of DiD function properly or not.

2.4.2. Special safety design features of Generation III reactors

The most important design features of Generation III reactors are as follows (see e.g. Ref. [13]):

- There is a strong tendency for equipment standardization, system simplification and more robust manufacturing practice, and for a significant reduction of the number of plant components. This tendency reduces the number of potential failure modes (according to the "simpler is safer" principle) and potentially reduces licensing and construction time.

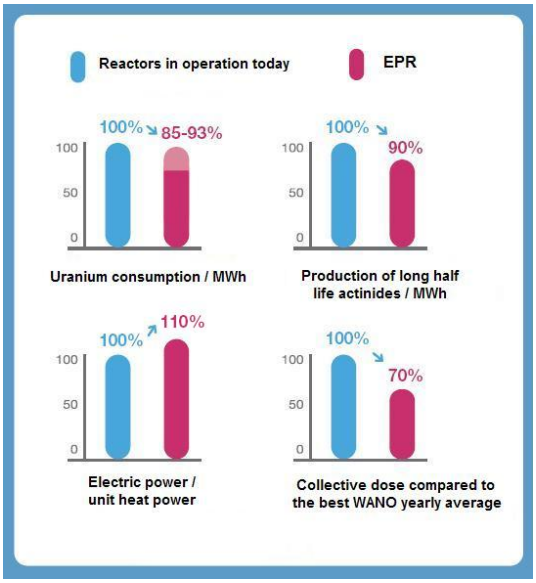

2.6. ábra. Comparison of selected features of currently operating reactors with the features of EPR ([14])

- Enhanced safety features, achieved mainly by applying passive safety systems. Basic safety design targets defined by nuclear utilities in the European Utility Requirements (EUR) document are fulfilled by these Generation III plants with large margins.
- Basic safety design targets are as follows: CDF (core damage frequency) 10^{-5} /year and LRF (Large Release Frequency) 10^{-6} /year.
- The design service time of these units is generally 60 years and the design load factor exceeds 90% (the latter was achieved by enhancing system maintainability and by shortening the time required for refueling).
- The maneuverability of the plants was enhanced significantly, to ensure flexible and safe plant reaction to fast changes in grid load requirements, by controlling the power of the unit and the grid frequency.
- The nuclear fuel was enhanced, as well, resulting in higher fuel burnup levels and more economic fuel utilization. These enhancements result less radioactive waste per unit energy production.

Figure 2.6 shows the comparison of the Generation II reactors currently in operation and the EPR unit:

Generation III reactor design improvements were mainly concentrated on two basic areas: to avoid hypothetical severe accidents and to mitigate their consequences if they happened. New designs contain solutions that prevent the dispersion of radioactive materials into the environment even during severe accident scenarios. One frequently used solution is the so called "core catcher" aimed to prevent the melt-through of the concrete located below the reactor pressure vessel during severe accidents with core melt. The core catcher utilizes special compartments located at the bottom of the reactor cavity in order to spread the molten

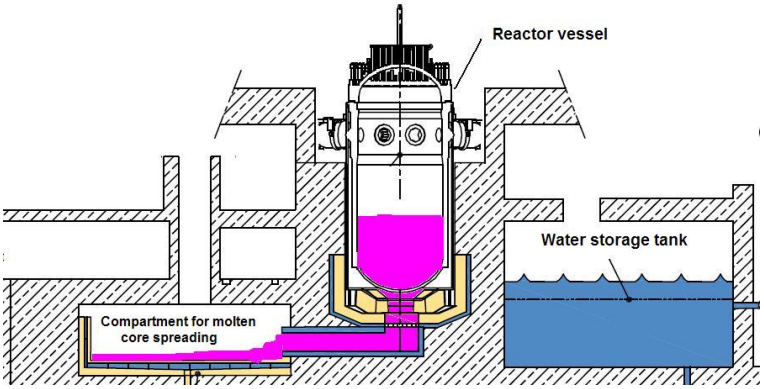

2.7. ábra. Scheme of the EPR "core catcher" ([14])

core to facilitate its cooling-down. These compartments may also contain special materials (tiles) that prevent corium-concrete interaction to happen. Cooling and stabilization of the spread corium is carried out by a passive method, using water inventory of a very large water tank located inside the containment. The water is led from this tank to the spread corium by gravitational flooding (see Figure 2.7). Long term cooling of the containment system is then performed by using a high-capacity spray system. This design solution is applied in the standard EPR, ATMEA1 and MIR-1200 units. The standard design of the Korean APR-1400 unit does not contain a core catcher, but the version to be shipped for European installations will be constructed with core catcher.

The AP1000 design uses a different approach called "in-vessel retention" to handle the molten core during severe accidents. The basic aim of the Westinghouse-approach is to keep the molten core inside the pressure vessel. This is achieved by an external cooling of the vessel, the cooling is ensured by flooding the reactor cavity with a large amount of water. The water surrounding the external wall of the pressure vessel provides an intense cooling to the vessel, while the evaporated water escapes to the internal area of the containment (see Figure 2.8). Continuous cooling water supply is ensured by a passive - gravitational - method, using the water inventory of a large water tank located inside the containment (see [8-10] for details). Note that the standard design of the Korean APR-1400 reactor uses a similar solution.

The containment is a very important part of the plants' defense in depth, since it represents the last barrier between radioactive materials and the environment. Generation III reactor designs introduced several innovative solutions to reinforce the containment retention capabilities, as well as to maintain the long term integrity of the containment structure. One remarkable approach is the AP1000 passive containment that is designed to be intact even during severe accidents and thus prevents the dispersal of radioactive materials. The ultimate heat sink is ensured by a passive containment cooling system: in the first phase of an accident this system ensures that the containment pressure remains below its design limit, then it provides a gradual containment pressure decrease. The heat generated within the containment is primarily removed by the internal - stainless steel - containment wall, the wall itself is being cooled by air driven by natural circulation. If required, this air cooling is backed up by water cooling exerted on the external surface of the containment wall, the makeup of cooling water is ensured by a passive - gravitational - method, using the water

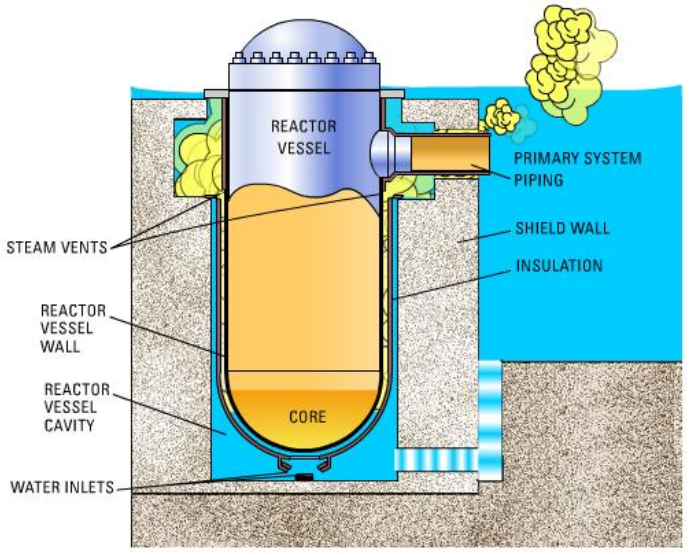

2.8. ábra. Cooling of the external surface of the vessel by flooding the reactor cavity ([16])

inventory of a large water tank located at the top of the containment.

The integrity of the containment is also protected by special devices intended to handle the hydrogen generated in large quantities during severe accidents. Hydrogen is mixed with the containment air and when its concentration reaches a certain value it may explode and this explosion may damage or destroy the structure of the containment. Two basic methods are used to prevent this explosion: the passive method utilizes catalytic recombiners, while the active method uses hydrogen burners. The catalytic recombiners continuously eliminate the hydrogen from the containment atmosphere, thus ensuring that the hydrogen cannot reach its critical concentration in any region of the containment. Active hydrogen burners are usually located in the "dome" (upper part) of the containment and they are operated from time to time to decrease the amount of hydrogen in the containment atmosphere.

The containment design takes into account external threats due to natural phenomena such as earthquakes and extreme weather conditions, as well as threats due to human activities, with the airplane crash event at the first place. In most countries recent safety regulations demand that the containment be able to withstand the effect resulting from the impact of a large passenger airplane. Regulations prescribe that the unit shall reach safe shut-down state after such an event, despite extensive fires that can potentially be ignited by the large amount of liquid fuel (kerosene) spilled out in the crash. The effectiveness of the increased containment protection measures can be illustrated by the fact that the EPR containment is designed to withstand the crash of an Airbus A380, the largest passenger carrier plane of today.

As the result of the above outlined safety design enhancements, Generation III reactors do not exert a substantial influence on the public and on the environment even in those extremely improbable cases, when a severe accident does occur.

2.5. Problems

1. Compare the PWR and BWR technology. Which one is simpler? Find their respective advantages and disadvantages.
2. Compare the advantage and disadvantage of the following coolants: natural water, heavy water, graphite.
3. How is the initial excess reactivity compensated? What are the characteristics of each compensation?
4. What is the possible fuel of the fission power plants? Is it possible to produce fissionable material in a nuclear power plant?
5. What was the motivation of the search for new nuclear power plant generations?
6. How is realized the defense in depth principle in a nuclear power plant?
7. Estimate the amount of spent fuel required in your country to produce the average per capita electric power. Compare it to the required amount of coal, wood, oil or gas.
8. What do you think, which technological units determine the life time of a nuclear power plant?
9. What is the approximate share in the nuclear energy production of the following items: investment, operation, and fuel?
10. Is the nuclear power plant suitable for the so called load follow operation, when the produced electric power is decreased or increased according to the actual energy demand?

3. fejezet

On Reactor models

When speaking of reactor models, one may have in mind various aspects of the energy production: how to achieve or maintain the self-sustaining fission, how to provide lasting heat balance, how to control various aspects of heat production. In the first subsection of the next Section we present a simple model.

3.1. Control theory models

Let us consider a device $\mathfrak{D}$ that we regulate by an m parameter vector $\mathbf{u} = (u_1, u_2, \ldots, u_m)$. Let vector $\mathbf{x} = (x_1, x_2, \ldots, x_n)$ characterize the possible states of $\mathfrak{D}$. But we get information on $\mathfrak{D}$ only by measurements, and the measured quantities are $\mathbf{y} = (y_1, y_2, \ldots, y_p)$. In the frame of system theory, the following relationship is assumed between $\mathbf{x}, \mathbf{u}$, and $\mathbf{y}$:

$$\frac{dx}{dt} = \mathcal{A}\mathbf{x} + \mathcal{B}\mathbf{u} \tag{3.1}$$

and

$$\frac{dy}{dt} = \mathcal{C}\mathbf{x} + \mathcal{D}\mathbf{u}. \tag{3.2}$$

Operators $\mathcal{A}, \mathcal{B}$, and $\mathcal{C}, \mathcal{D}$ depend on the properties of $\mathfrak{D}$.

When they are linear operators, e.g. matrices, model (3.1), (3.2) are called linear model. Since $\mathbf{u}$ is independent of $\mathcal{D}$, it may be applicable to influence the behavior of $\mathcal{D}$. In control theory, it is studied whether it is possible to give a regulation $\mathbf{u}(t)$ to move the system into a predetermined state.

There are several forms of modeling $\mathcal{D}$. Some of the most frequently used models include:

- linear algebra model: $\mathcal{A}, \mathcal{B}, \mathcal{C}$ are represented by matrices;
- differential equation model: $\mathcal{A}, \mathcal{B}, \mathcal{C}$ are represented by differential operators;
- integral equation model: $\mathcal{A}, \mathcal{B}, \mathcal{C}$ are represented by integral operators;
- feed-back model: when the regulation $\mathbf{u}$ is formed from the system state $\mathbf{x}$ or the observed $\mathbf{y}$.

In connection with the model (3.1)-(3.2) the following questions have to be investigated:

1. realization problem: it should be investigated if the relevant features of $\mathcal{D}$ are reproduced by the model (3.1)-(3.2). This is an ubiquitous problem of model making. The usual technique is to study simple states of $\mathcal{D}$ and to compare the behavior of the real model to the behavior of the mathematical model. This process is called benchmarking.

2. Observability. In control theory, observability is a measure for how well internal states of a system can be inferred by knowledge of its external outputs

3. Controllability describes the existence of an external input u such that it moves the internal state $\mathbf{x}$ of $\mathcal{D}$ from any initial state $\mathbf{x}_i$ to any final state $\mathbf{x}_f$ in a finite time interval.

Systems can be built by coupling subsystems. System theory is capable of modeling not only small biological entities like a cell or a bacterium but such a complex phenomenon like the economy or human society.

3.1.1. A simple system theoretic model of a reactor

The following model is taken from Ref. [4]. Our model reactor is a thin rod of length a. In the rod the neutrons move with unit velocity along the rod. When a neutron collides with a nucleus of an atom in the rod, the neutron is instantaneously replaced by $0, 1, \ldots, N$ neutrons with respective probabilities $c_k, k = 0, 1, \ldots, N$. Casti's simple model is necessarily a probabilistic one.

The collisions follow Poisson distribution so the probability of a collision in the interval $(x, x + \Delta)$ is Δ/λ, where λ is the mean free path of the neutron in the rod. The no collision probability under a path of length s is $e^{-s/\lambda}$. When the neutron arrives at the end of the rod, it leaks out.

The simple reactor is triggered by a single neutron (input) and its output is the number of neutrons alive after infinitely long time. The input-output relation, the heart of the system theoretic model, is derived below.

We introduce a single neutron moving to the right at $t = 0$ at x. Let $u(x)$ be the probability that at $t = \infty$ at least one neutron is alive. When at $t = 0$ we start a neutron at x to the left, the probability that at $t = \infty$ at least one neutron is alive be $v(x)$. A neutron emerging from a collision moves to the left/right with the probability $1/2$. We introduce the extinction probability $p(y)$ as

$$p(y) = \sum_{k=0}^{N} c_k p_k(y) \tag{3.3}$$

where $p_k(y)$ is the probability that all of the k new born neutrons extinct before causing fission. Then if no neutrons are alive at $t = \infty$ they either leaked out or vanished therefore

$$1 - u(x) = e^{-(a-x)/\lambda} + \int_x^a e^{-(y-x)/\lambda} p(y) dy/\lambda. \tag{3.4}$$

With k neutrons produced,

$$\binom{k}{n} \left(\frac{1}{2}\right)^k$$

is the probability that n will move to the right and the rest to the left. The extinction probability is then

$$(1 - u(y))^n (1 - v(y))^{k-n}.$$

A similar equation holds for $v(x)$. Let

$$z(x) = (u(x) + v(x))/2, \tag{3.5}$$

and the following equation holds for $z(x)$:

$$z(x) = \int_0^a E(x,y)G(z(y))dy, \quad 0 \le x \le a, \tag{3.6}$$

where

$$E(x,y) = \frac{1}{2\lambda} e^{-|x-y|/\lambda} \tag{3.7}$$

and

$$G(r) = cr - \sum_{k=2}^{N} c_k[c_k(1-r)^k - 1 + kr] = 1 - \sum_{k=0}^{N} c_k(1-r)^k, \tag{3.8}$$

$$c = \sum_{k=1}^{N} kc_k \tag{3.9}$$

is the average neutron number multiplication. When $c < 1$ the reactor is subcritical, when $c = 1$ critical and with $c > 1$ supercritical.

Equation (3.6) is a nonlinear relationship between the input and the output. It can be shown that (3.6) is equivalent to the following nonlinear differential equation:

$$-\frac{d^2z}{dx^2} + \frac{z}{\lambda^2} = \frac{G(z(x))}{\lambda^2}, \quad 0 < x < a \tag{3.10}$$

with the boundary conditions

$$z'(0) - \frac{z(0)}{\lambda} = 0; \;\; z'(a) + \frac{z(a)}{\lambda} = 0. \tag{3.11}$$

The model is simple, the reactor has two features: the mean free math λ and the number of secondary neutrons per collision, see (3.9). The Reader may compare this simple model with the one given in the subsequent Section.

3.1.2. Control theory model

The reader may have noted, control theory is a part of the system theory. When the system is sufficiently simple, there is a hope that we can solve this problem: what kind of regulation is needed to achieve a given behavior of a given device? When the system is simple, it can be modeled by simple techniques, like linear differential or integral equations although even those simple models address serious theoretical problems.

Our starting point is a simple differential equation with one parameter, and using classical examples we study the behavior of the solutions in terms of the value of that parameter. We present a few basic terms used in uncertainty and stability analysis. Consider the following ordinary differential equation:

$$\frac{dr}{dt} = -(\Gamma r + r^3). \tag{3.12}$$

Here Γ is the free parameter. When $\Gamma > 0$ the solution has a fixed point (attractor) it is the origin because from any starting point $r \to 0$ when $t \to \infty$. This case is shown in Fig. 3.1. When $\Gamma < 0$ the solution winds up on a circle of radius $\sqrt{|\Gamma|}$. This case is shown in Fig.

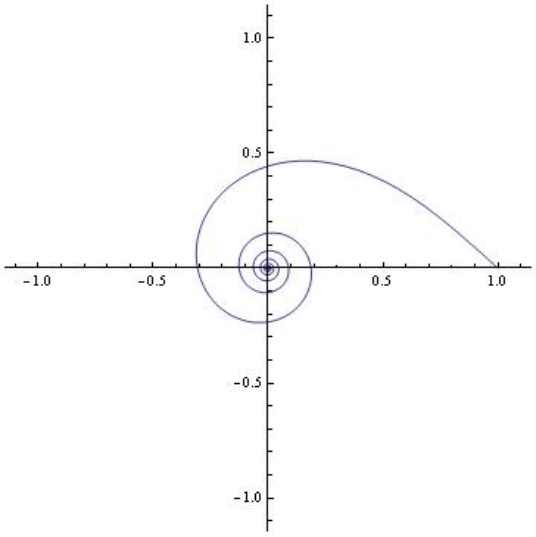

3.1. ábra. Attractor

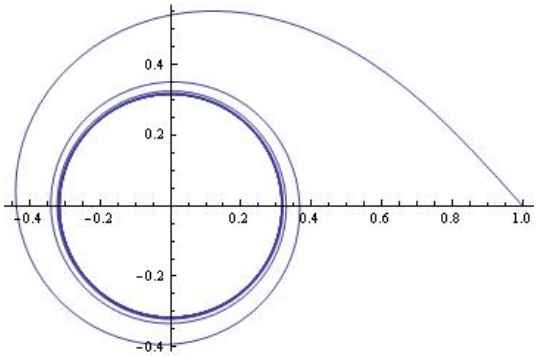

3.2. ábra. Limit Cycle

3.2.

There are situations, when the iteration ends up not in a single point of the phase space but in a bounded region. The state of the studied system crosses every point of the strange attractor but there is no subset in the strange attractor which would enclose the orbit of the system.

We seek characteristics by which a given map can be classified. Since the numerical solution is actually an iteration, it is usual to consider the following map:

$$x_{n+1} = f(x_n), \quad n = 0, 1, 2, \ldots . \tag{3.13}$$

The iteration usually maps a vector to vector, hence $f : \mathbb{R}^m \to \mathbb{R}^m$ for some positive integer m. The result of the iteration depends on the initial point x_0 and the map f. The stability of the map f is characterized by the Liapunov exponent. We start the iteration from x_0 and $x_0 + \varepsilon$. When f is continuous, $f(x_0)$ and $f(x_0 + \varepsilon)$ are close. Applying that thought of line to the iteration process, the Liapunov exponent $\lambda_0(x_0)$ is defined as

$$\begin{aligned} \lambda(x_0) &= \lim_{N\to\infty} \frac{1}{N} \log \left| \frac{d}{dx_0} f^N(x_0) \right| = \lim_{N\to\infty} \frac{1}{N} \log \left| \sqcap_{i=0}^{N-1} f'(x_1) \right| \\ &= \lim_{N\to\infty} \frac{1}{N} \sum_{i=0}^{N-1} \log |f'(x)| . \end{aligned} \tag{3.14}$$

It can be shown [26], that the mean loss of information ΔI is connected to the Liapunov exponent as

$$\lambda(x_0) = (\log 2)|\Delta I|. \tag{3.15}$$

In stability studies, a real reactor is too complex to be studied in its full complexity, therefore so called reduced order models [24] are used. Reduced order means a simplified description of the relevant feed-back processes, so that the resulting ordinary differential equation set is tractable by simple techniques. Below we present [25] a simple mathematical model formulated as a regulation problem.

Let the unknown vector be $\mathbf{x} = (x_1, x_2, \ldots, x_5)$ and we write its evolution in time as

$$\frac{d\mathbf{x}}{dt} = \mathbf{G}(\mathbf{a}, \mathbf{x}) \tag{3.16}$$

where $\mathbf{G} = (G_1, G_2, \ldots, G_5)$ is a nonlinear expression of $\mathbf{x}$, the constant vector $\mathbf{a} = (a_1, a_2, \ldots, a_{11})$ depends on the physical properties of the process to be modeled. The reduce order model we are going to discuss, is the following:

$$\begin{pmatrix} \frac{dx_1}{dt} \\ \frac{dx_2}{dt} \\ \frac{dx_3}{dt} \\ \frac{dx_4}{dt} \\ \frac{dx_5}{dt} \end{pmatrix} = \begin{pmatrix} x_1(a_1x_4 + a_2x_3 - a_3)/a_4 + a_5x_2 + (a_1x_4 + a_2x_3)/a_4 \\ x_1a_3/a_4 - a_5x_2 \\ a_6(x_1 + a_7H(t)) - a_8x_3 \\ x_5 \\ -a_9x_5 - a_{10}x_4 - a_{11}x_3 \end{pmatrix}. \tag{3.17}$$

Here $H(t)$ is Heaviside's step function. The first order differential equation set is nonlinear because of the terms $a_1x_1x_4$ and $a_2x_1x_3$ in the first equation.

The stability of the solution depends on the eigenvalues of the matrix

$$\mathbf{L}_{ij} = \frac{\partial G_i(x)}{\partial x_j}, \quad 1 \le i, j \le 5. \tag{3.18}$$

That matrix is

$$\mathbf{L}_{ij} = \begin{pmatrix} (a_1x_4 + a_2x_3 - a_3)/a_4 & a_5 & a_2x_1 + a_2/a_4 & a_1x_1 + a_1/a_4 & 0 \\ a_3/a_4 & -a_5 & 0 & 0 & 0 \\ a_6 & 0 & -a_8 & 0 & 0 \\ 0 & 0 & 0 & 0 & 1 \\ 0 & 0 & -a_{11} & -a_{10} & -a_9 \end{pmatrix}. \quad (3.19)$$

As we see, the derivative matrix $\mathbf{L}$ depends on the solution. In the linear approximation, the stability is analyzed as follows. Assume that we have a solution $\mathbf{x}_0$ of the problem

$$0 = \mathbf{G}(\mathbf{a}, \mathbf{x}_0), \quad (3.20)$$

then $\mathbf{x}_0$ is an equilibrium solution as it never quits that point. The equilibrium solution depends on the parameter vector $\mathbf{a}$. The solution of (3.16) is called stable if a solution starting in the vicinity of an equilibrium solution remains close to it. This is the case when all the eigenvalues of matrix $\mathbf{L}$ have negative real parts.

Unfortunately only numerical calculations are available, the eigenvalue problem requires solving fifth order equations. The problem becomes a control problem, however, when we assume that one of the parameters can be varied. We return to the problem in the Chapter where kinetics is discussed.

3.2. Physical model

In the history, the favored models varied as our understanding of the natural laws has been evolving. Today engineers prefer to build small mockup models of a dam, or a bridge to study specific problems. When the motions of various mechanical systems have been understood, engineers built mechanical models[1]. Later, when the electric circuitries became available, electric models have been built. Today the computer simulation is in fashion, like the Monte Carlo method.

The equation governing the neutron distribution involves cross-sections that depend on the neutron energy. A good example of model making is the variety of models elaborated to specific parts of the neutron spectrum. Those models have made it possible to acquire effective models in the entire energy spectrum. Those models are discussed in Chapter 5.

Whatever is the model we use, its aptness basically depends on the understanding of the physical processes which determine the relevant phenomena of the device under consideration. Unfortunately it is a less attractive and laborious task, but there is no alternative but to lay down a solid model based on the latest achievements of science. Such a model is described in the following Sections.

3.3. Realistic reactor models

The simple model of Section 3.1.1 accounts for the criticality, but to design and manage the reactor operation, one needs a more realistic model. In order to assess what one has to know to design the reactor operation, we have to go back to the description of the physical process of fission.

There are free neutrons in the reactor, they collide with the nucleus of the fuel and of the other materials, and some collisions lead to fission and neutron release. Self-sustaining fission requires fissionable material (fuel) and free neutrons. The neutron population is described by the Boltzmann transport equation.

[1] Maxwell studied the electromagnetism on mechanical models.

3.4. Nuclear physics of fission

Reactor physics is based on the nuclear physics, such basic quantities as decay constant, cross-section, reaction energy, reaction mechanism, etc. are defined and provided by nuclear physics. It is therefore important to get acquainted with the basics of nuclear physics. This Chapter presents the fundamentals of nuclear physics used throughout the theoretical and experimental reactor physics.

3.4.1. Nuclear Properties

This Section describes the basic measurable properties of the nucleus in a nutshell. The most important properties including the composition of the nucleus, its electric charge, radius, mass, binding energy, excited and ground states. The above mentioned features are the static properties of a nucleus.

Composition and mass of stable nuclei

After the discovery of the neutron (in 1932, James Chadwick) the nuclear structure was complete: the nucleus consists of protons and neutrons bound by the short-range attractive nuclear force. So a nucleus can be identified clearly by the number of its protons and neutrons. The number of protons is denoted Z, which equals to the atomic number in the periodic table. The chemical features of the atom is determined by Z. The number of neutrons is denoted N, and the mass number A which is the number of nucleons in the nucleus is $A = Z + N$. The specification of a nucleus is

$$ {}^{A}_{Z}X_{N} \tag{3.21}$$

where X is the symbol for the chemical element. Naturally an element occurring in the nature may have different mass numbers referring to different number of neutrons in the nucleus. These nuclei are called *isotopes*. The different isotopes may be either stable or unstable against radioactive decay (see below), for example the three hydrogen isotopes are: ${}^{1}_{1}H$ is stable (hydrogen), ${}^{2}_{1}H_1$ is stable (deuteron) and ${}^{3}_{1}H_2$ is unstable (triton). Nuclear physics point of view there are special formation of nuclei, which have the same mass number (A =constant), this are called *isobars*.

Let us now consider the total energy and total mass of a nucleus. Consider a nucleus made up from Z protons and $A - Z$ neutrons. In the first approximation, the total mass of the nucleus is the sum of the total mass of the protons plus the total mass of the neutrons:

$$ Zm_p + (A - Z)\, m_n, \tag{3.22}$$

where m_p and m_n is the mass of the free proton and of the free neutron, respectively. But in the nucleus the nucleons are in bound state thus the total mass of the bound system of nucleons will be less than the total mass of the free particles would be:

$$ M(Z, A) = Zm_p + (A - Z)\, m_n - B(Z, A)/c^2, \tag{3.23}$$

where $B(Z, A)$ is the *binding energy* of the nucleus with mass number A and atomic number Z. The factor $B(Z, A)/c^2$ is known as the *mass defect* of the nucleus. The fundamental reason for the *mass defect* is Albert Einstein's famous formula $E = mc^2$, expressing the equivalence of energy and mass.

The nuclear binding energy

The formal definition of the nuclear binding energy is derived from the strong nuclear force and is the energy required to disassemble a nucleus into free, unbound nucleons. After rearranging (3.23), we obtain an expression for the binding energy:

$$B(Z,A) = [Zm_p + (A-Z)\,m_n - M(Z,A)]\,c^2. \tag{3.24}$$

(3.24) shows that the binding energy to depend on two independent variables: the mass number and the atomic number. In nuclear physics, the binding energy per nucleon (or the mean binding energy) is used:

$$\varepsilon(Z,A) = \frac{B(Z,A)}{A}. \tag{3.25}$$

Figure 3.3 shows the $\varepsilon(Z,A)$ of β-stable nuclei as a function of the mass number A. The β-stable means that the function of the binding energy per nucleon of the variable Z is close to the local maximum. In general, the greater is the binding energy per nucleon, the more stable is the nucleus. The function of $\varepsilon(Z,A)$ is saturated about 7 to 8 MeV/nucleon values. In the range above $A = 20$ the binding energy per nucleon can be seen roughly constant around 8 MeV with a maximum of about 8.8 MeV, and decreasing monotonically to about 7.5 MeV at $A \cong 240$. The binding energy per nucleon curve is rapidly rising between $A = 1$ and $A = 30$ with a superimposed oscillation (for example at ${}^4He$ and ${}^{16}O$). The oscillation is due to the high stability of nuclei at the number of nucleons (either protons or neutrons) equal to $2, 8, 20, 28, 50, 82, 126$. These numbers are known as *magic numbers* in nuclear physics. When nuclei have equal neutron number and proton (atomic) number, and that number is one of the magic numbers, are called "double magic", and are especially stable against decay.

It follows from the definition of the binding energy that the energy of nucleus is less than zero (just like the gravitational energy of the planets in the solar system), and the binding energy is given by

$$E = -B(Z,A). \tag{3.26}$$

Every physical system, thus also the nucleus, minimize its total energy. This manifests in a maximal binding energy.

The liquid drop model of the nucleus

The liquid drop model is based on the observation that the nucleus and the liquid droplet are similar, both are incompressible: $\rho \approx constant$ in the asymptotic region $r \ll R$ and the attractive interaction between the their components are *short-ranged forces*. The radius of nucleus: $R = 1.25 \cdot 10^{-13} A^{1/3}\ cm$, where A is the mass number [37],[38],[39].

It follows that the short-ranged nuclear interaction between nucleons must be limited to the nearest neighbors. So the total binding energy would increase as the total number of nucleons increases, the binding energy must include a term B_v, which is proportional to the volume of the nucleus. For this component of binding energy we may write

$$B_v = a_v A, \tag{3.27}$$

where a_v is an empirically determined constant and we have used the relation $V \sim A$. This term is called *volume energy* .

Nucleons close to the surface must be more weakly bound as they have less neighbors than those in the inner region of the nucleus. That weakening in the binding energy is given by

$$B_s = -a_s A^{2/3}, \tag{3.28}$$

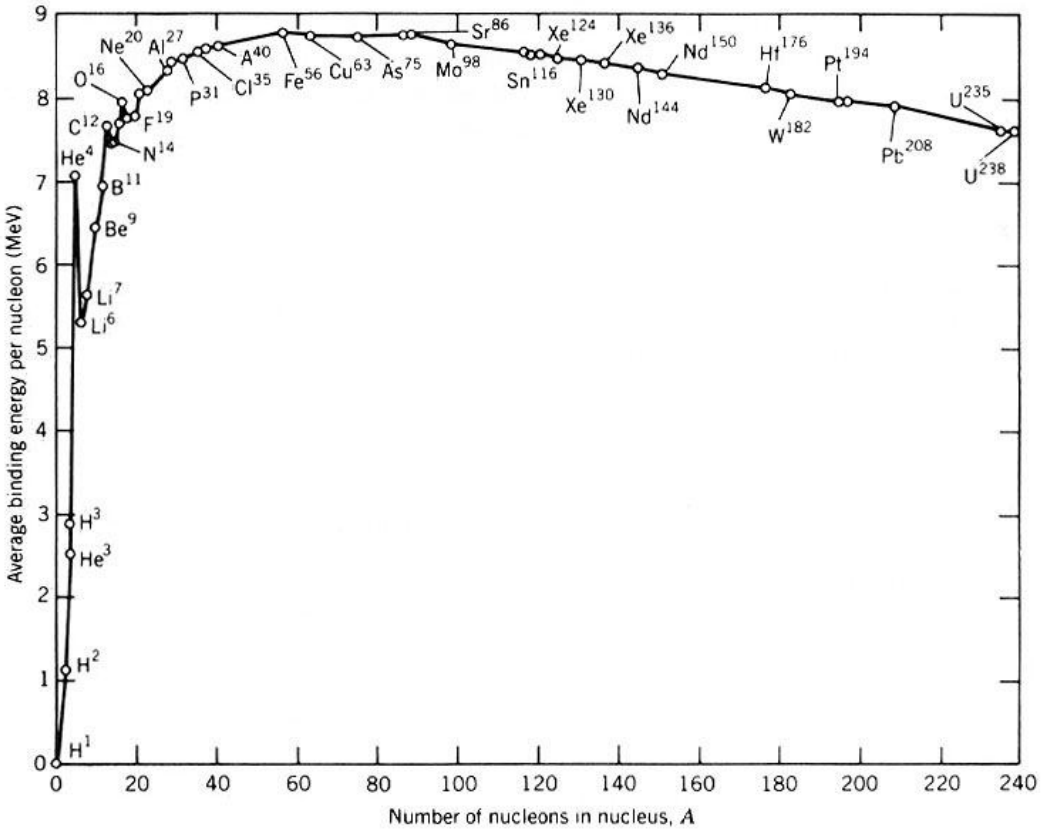

3.3. ábra. The nuclear binding energy per nucleon

where we exploited the relation $R^2 \sim S \sim A^{2/3}$. This term is called *surface energy*, which corresponds to the surface tension of a liquid drop.

Protons, having positive electric charges, repel each other by the electrostatic Coulomb potential. The repulsive force depends on the charge distribution, if the nucleus is considered as a homogeneous sphere with a net charge Ze and radius $R \sim A^{1/3}$, according to the electrostatic theory the total electrostatic energy is given by

$$B_c = -a_c \frac{Z(Z-1)}{A^{1/3}} \approx -a_c \frac{Z^2}{A^{1/3}}, \tag{3.29}$$

where a_c includes the electron charge e, and the r_0 parameter from radius of nuclei:

$$a_c = \frac{3}{5}\frac{e^2}{r_0}, \tag{3.30}$$

this relation holds in the center of mass coordinate system. The obtained approximation is suitable for heavy nuclei. This term is referred to as *Coulomb energy*, which also weakens the binding energy.

There are two more terms influencing the binding energy. One of them expresses the effect of neutron excess, because the excess number of neutrons over the number of protons can destabilize the nucleus [37] (this phenomenon can be observed in the fission fragments). This may be written as

$$B_a = -a_a \frac{(N-Z)^2}{A}, \tag{3.31}$$

a_a being an empirical constant. It is known as *asymmetry energy*. The last term in the binding energy is called *pairing energy*. The nuclei are found to display a systematic trend in that those having even-even number of neutrons and protons (e-e nuclei) are more stable than even-odd, or, odd-even number of neutrons and protons (o-e nuclei), and those having odd-odd Z and N are mainly unstable [37]. Taking into account that pairing effect a new term B_p is added to the binding energy formula:

$$B_p = a_p \delta(Z,A) A^{-3/4}, \tag{3.32}$$

where

$$\delta(Z,A) = \begin{cases} +1 & \text{for e-e nuclei} \\ 0 & \text{for o-e nuclei} \\ -1 & \text{for o-o nuclei} \end{cases} \tag{3.33}$$

Finally adding all the terms together, we get the *semi-empirical binding energy formula*:

$$B(Z,A) = a_v A - a_s A^{2/3} - a_c \frac{Z(Z-1)}{A^{1/3}} - a_a \frac{(N-Z)^2}{A} + a_p \delta(Z,A) A^{-3/4}, \tag{3.34}$$

which is often referred to as *Bethe-Weizsacker formula*. The incorporated empirical constants in this formula are numerically determined by fitting [37]:

$$\begin{cases} a_v \approx 14.1 & \text{MeV} \\ a_s \approx 13 & \text{MeV} \\ a_c \approx 0.595 & \text{MeV} \\ a_a \approx 19 & \text{MeV} \\ a_v \approx 33.5 & \text{MeV} \end{cases} \tag{3.35}$$

The Bethe-Weizsacker formula generally furnishes values of binding energies within 1 percent of values determined experimentally. Discrepancies of fitted and measured binding energies have been observed for magic nuclei having a specific number of neutrons and protons. The *shell model* is more appropriate to determine the binding energy of those nuclei.

The radioactive decay law

The radioactivity was discovered in 1896 by Henry Becquerel. He found that photographic materials wrapped in black paper, i.e. isolated from light, blackened when brought close to uranium salts. These salts were emitting radiations, that could pass through paper and were absorbed by the photographic emulsion. In the next few years other researchers discovered that different types of decay can occur. The Curies were the first to isolate a new element called the polonium, and to separate the new element from barium. In the years following 1899 Rutherford and his colleagues showed that the radioactive radiations have three different components, α-, β- and γ-radiation.

The radioactive (unstable) nuclei can be described by the *mean lifetime*, designated by τ. The *mean lifetime* means the average time of an unstable nucleus before decay. This is a random variable, but the decay constant more directly carries the random purport: it gives the probability that the nucleus decays in unit time. It is given by

$$\lambda = \frac{1}{\tau}, \tag{3.36}$$

in $1/s$ unit. It follows that it is impossible to say exactly when a nucleus decays.

A large population of radioactive atoms (nuclei) is needed to define average quantities. Let us consider a homogenous radioactive material containing a large number $N(t)$ of nuclei. The $N(t)$ function decreases monotonous, because the radioactive nuclei are continuously decaying. The probability of nucleus decaying per Δt time is given by $\lambda \cdot \Delta t$, therefore the number of decayed nuclei from $N(t)$ per Δt time is equal to $N(t) \cdot \lambda \cdot \Delta t$. The decrease of $N(t)$ is

$$N(t + \Delta t) - N(t) = -\lambda N(t) \cdot \Delta t, \tag{3.37}$$

the negative sign indicates that N decreases with time. After reordering, we obtain

$$\frac{N(t + \Delta t) - N(t)}{\Delta t} = -\lambda N(t), \tag{3.38}$$

We have in limit $\Delta t \to 0$, the above expression is given by

$$\frac{dN(t)}{dt} = -\lambda N(t). \tag{3.39}$$

This is the differential equation of decay. The solution of equation (3.39) is simple, the integration of this differential equation with initial condition $N(0) = N_0$ gives:

$$N\left(t\right) = N_0 e^{-\lambda t} = N_0 e^{-\frac{t}{\tau}}. \tag{3.40}$$

(3.40) is called *exponential decay law.* In practice, it is much easier to measure the activity $A\left(t\right)$ than $N(t)$, where

$$A\left(t\right) = \lambda N\left(t\right), \tag{3.41}$$

after multiplying the (3.39) with λ the exponential decay law for the activity is given as

$$A\left(t\right) = A_0 e^{-\lambda t} = A_0 e^{-\frac{t}{\tau}}. \tag{3.42}$$

The SI unit of radioactive activity is the becquerel (Bq), 1 Bq is one decay per second. Therefore the activity A gives the number of decays per second.

It is convenient to define a special quantity $T_{1/2}$ which corresponds to the mean time required for the activity (or number of nuclei) to reduce to one half of its value. This is called the *half-life*. Substituting $N = \frac{N_0}{2}$ at $t = T_{1/2}$ in relation (3.40) shows that

$$T_{1/2} = \frac{\ln(2)}{\lambda}. \tag{3.43}$$

It is associated with the statistically random behavior of the population of nuclei. In consequence, predictions using half-life is less accurate for small number of atoms.

The chains of radioactive decays

Now we consider the case of a chain of two decays: one nuclide 1 decaying into another 2 by one process, then 2 decaying into another 3 by a second process, where 3 is a stable nuclide. The process is

$$1 \to 2 \to 3 \tag{3.44}$$

We assume that $N_1 = N_{10}$, $N_2 = N_{20} = 0$ and $N_3 = N_{30} = 0$ at the time $t = 0$, the decay constants of 1 nuclide (it is referred to *parent* nuclide) and 2 nuclide (it is referred to *daughter* nuclide) are λ_1 and λ_2 and naturally $\lambda_1 \neq \lambda_2$. The equation for change of parent nuclei is

$$\frac{dN_1(t)}{dt} = -\lambda_1 N_1(t), \tag{3.45}$$

for daughter nuclei is

$$\frac{dN_2(t)}{dt} = -\lambda_2 N_2(t) + \lambda_1 N_1(t). \tag{3.46}$$

and finally the equation for the stable isotope is

$$\frac{dN_3(t)}{dt} = \lambda_2 N_2(t). \tag{3.47}$$

The solution of (3.45) is already known from equation (3.39)

$$N_1(t) = N_{10} e^{-\lambda_1 t}, \tag{3.48}$$

so re-writing equation (3.46)

$$\frac{dN_2(t)}{dt} = -\lambda_2 N_2(t) + \lambda_1 N_{10} e^{-\lambda_1 t}. \tag{3.49}$$

The solution of this inhomogeneous differential equation with the boundary conditions $N_1 = N_{10}$ and $N_2 = 0$ at time $t = 0$ is

$$N_2(t) = \frac{\lambda_1}{\lambda_2 - \lambda_1} N_{10} \left(e^{-\lambda_1 t} - e^{-\lambda_2 t}\right). \tag{3.50}$$

Using the definition of activity 3.41 gives a relation for the daughter activity:

$$A_2(t) = \frac{\lambda_2}{\lambda_2 - \lambda_1} 1_{10} \left(e^{-\lambda_1 t} - e^{-\lambda_2 t}\right), \tag{3.51}$$

where $A_2(t) = \lambda_2 N_2(t)$ and $1_{A0} = \lambda_1 N_{10}$. After reordering may be written

$$A_2(t) = A_1(t) \frac{\lambda_2}{\lambda_2 - \lambda_1} \left(1 - e^{-(\lambda_2 - \lambda_1)t}\right). \tag{3.52}$$

Let us now consider the daughter activity in special cases. The first case is when the decay constant of parent nuclide is less than decay constant of daughter nuclide $\lambda_2 > \lambda_1$. Then the exponent factor is positive all the time in (3.52) $(\lambda_2 - \lambda_1) > 0$, so after a sufficiently long time the exponential factor approaches to zero in this expression. In this asymptotic limit the (3.52) can be written as

$$A_2(t) \approx A_1(t) \frac{\lambda_2}{\lambda_2 - \lambda_1}. \tag{3.53}$$

The next case when the inequality between parent and daughter decay constant is much stronger than in the previous case: $\lambda_2 \gg \lambda_1$. In this case we may use relation $(\lambda_2 - \lambda_1) > 0$, of course. However, due to the stronger condition we may write

$$\frac{\lambda_2}{\lambda_2 - \lambda_1} = \frac{1}{1 - \frac{\lambda_1}{\lambda_2}} \approx 1. \tag{3.54}$$

Using this approximation in expression (3.53), we obtain

$$A_2(t) \approx A_1(t). \tag{3.55}$$

This case is called *secular equilibrium* .

Finally we consider the general case, which includes any number of consecutive decays in a decay chain, i.e.

$$A_1 \to A_2 \to \cdots \to A_i \to \cdots \to A_M \tag{3.56}$$

where M is the number of decays. N_i denotes the number of nuclide of i-th isotope, the population equation for N_i nuclide is given by

$$\frac{dN_i(t)}{dt} = -\lambda_i N_i(t) + \lambda_{i-1} N_{i-1}(t). \tag{3.57}$$

The initial conditions are $N_1 = N_{i0}$ and $N_i = 0$ if $N \geq i > 1$ at the reference time $t = 0$. The general solution to the recursive problem are given by *Bateman's equations* [40]:

$$N_M(t) = \frac{N_{10}}{\lambda_M} \sum_{i=1}^{M} c_i e^{-\lambda_i t} \tag{3.58}$$

$$c_i = \prod_{j=1, i \neq j}^{M} \frac{\lambda_j}{\lambda_j - \lambda_i} \tag{3.59}$$

These solutions are useful in burn-up problems.

3.4.2. Nuclear reactions

General description and Energetics of nuclear reactions

The nuclear reactions are formally considered as a process in which two nuclei and either subatomic particles (for examples neutrons, protons, electrons) collide to produce two or

more new particles (nuclei), which are different from the initial particles. The standard notation of nuclear reaction which involves two initial and two produced particles is

$$\begin{array}{ccc} a + A & \rightarrow & b + B \\ A & (a,b) & B \end{array} \tag{3.60}$$

In nuclear reactions one of the initial particle is referred as a projectile, while the other is taken a target, for example in above process the projectile is a while the target is A. The nuclear reactions are caused by strong- (or other words nuclear), electromagnetic- and weak-interactions between the collided particles.

The fundamental principle of conservation laws has a decisive influence upon the nuclear reactions, so the reactions are categorized as forbidden and allowed reactions. Most important conservation quantities are:

- energy
- momentum
- angular-momentum
- parity (except for weak-interaction)
- electric charge
- number of barions (neutrons, protons, etc)
- number of leptons (electron, neutrino, etc)

We consider the energetics in this section. Most nuclear reactions involve two-body interactions as showed the relation (3.60). Because of energy conservation the total energy of initial and final system must be equal, it follows that

$$E^{(a)} + E^{(A)} = E^{(b)} + E^{(B)}, \tag{3.61}$$

using the relation $E^{(i)} = E^{(i)}_{kin} + E^{(i)}_0$, (3.61) may be written as

$$\left(E^{(a)}_{kin} + E^{(a)}_0\right) + \left(E^{(A)}_{kin} + E^{(A)}_0\right) = \left(E^{(b)}_{kin} + E^{(b)}_0\right) + \left(E^{(B)}_{kin} + E^{(B)}_0\right), \tag{3.62}$$

where E_{kin} is the kinetic energy of the particle (can be relativistic or non-relativistic), $E_0 = m_0c^2$ is the rest energy of particle, c is velocity of light in vacuum. Separating the variables, we can re-write this equation

$$\left(E^{(b)}_{kin} + E^{(B)}_{kin}\right) - \left(E^{(a)}_{kin} + E^{(A)}_{kin}\right) = \left(E^{(a)}_0 + E^{(A)}_0\right) - \left(E^{(b)}_0 + E^{(B)}_0\right). \tag{3.63}$$

Now we can introduce a new variable Q, it is defined by

$$Q = \left(E^{(a)}_0 + E^{(A)}_0\right) - \left(E^{(b)}_0 + E^{(B)}_0\right), \tag{3.64}$$

it is called *reaction energy*, whence

$$\left(E^{(b)}_{kin} + E^{(B)}_{kin}\right) = Q + \left(E^{(a)}_{kin} + E^{(A)}_{kin}\right). \tag{3.65}$$

The reaction energy is the energy, which is released in nuclear reaction, the definition and relation (3.24) follow that Q involves the changing of binding energy between the initial and final system. The (3.64) model- and coordinate-system–independent formula can be applied to all types of two-body nuclear reaction processes. Q can be utilized for:

- $Q = 0 \longrightarrow E_{kin}^{(initial)} = E_{kin}^{(final)}$ and $a = c$, $b = d$: *elastic scattering*, in which collided particles keep their identity, and the total kinetic energy remains.
- $Q \neq 0 \longrightarrow E_{kin}^{(initial)} < E_{kin}^{(final)}$ but $a = c$, $b = d$: *inelastic scattering*, in which in which collided particles keep their identity, but the total kinetic energy changes by Q, where Q is equal to excitation energy given to the target nucleus.
- $Q < 0 \longrightarrow E_{kin}^{(initial)} < E_{kin}^{(final)}$ but $a \neq c$, $b \neq d$: *endothermic reaction*: which is energy-absorbing process
- $Q > 0 \longrightarrow E_{kin}^{(initial)} > E_{kin}^{(final)}$ but $a \neq c$, $b \neq d$: *exothermic reaction*: which is energy-producing interaction

The endothermic reactions are special among the nuclear processes, because the minimal incident energy is required for the reaction to take place. This minimal energy is called *threshold energy* E_{thres}. It follows the connection between Q value and initial velocities depends on the choice of coordinate system [37]. Finally we show some nuclear reactions from the Q point of view:

$$^3He + n \rightarrow {}^3H + p + (Q = 764 \text{ keV}) \tag{3.66}$$
$$^6Li + {}^2H \rightarrow 2\,{}^4He + (Q = 22.4 \text{ MeV}) \tag{3.67}$$
$$^{12}C + {}^2H \rightarrow {}^{13}N + n + (Q = -3.82 \text{ MeV}) \tag{3.68}$$

Direct and compound nucleus reactions

The nuclear reactions may also be classified according to reaction mechanism, which have two possible ways: the direct and the compound nuclear reactions. In the direct reactions (for example $A(a,b)B$) the interaction between two collided nuclei is considered to be a single very quick event, these characteristic time is about 10^{-22} s. The energy and momentum transfer are relatively small. The angular distribution of direction of reaction products is significantly different from the uniform distribution (anisotropic process), therefore the cross section strongly dependents on the "scattering" angular (it means the angular between the direction of incident particle (a) and direction of outgoing particle (b)). Generally, the forward scattering is typical.

In the case of compound nuclear reactions the process will be a two-step, schematically: $a+A \rightarrow C \rightarrow b+B$, first step the compound nucleus C is created by collision of a and A, than second step the compound nucleus in the excited state decays to possible ways. These decay differs from the radioactive decay, because this is determined by nuclear interaction, thus in this case two or more nuclei (nucleons) are produced. The first theory of compound nuclear reactions were developed by *N. Bohr*. The characteristic time of interaction is equal to the lifetime of compound nucleus ($10^{-15}s - 10^{-19}s$) which is compared to the time for the incident energy to be shared among nucleus C, therefore particle a has energy transfers with nucleons in the target nucleus A. Thus the nucleus C forgets that which was the incident particle, in other words nucleus C retains no memory of how it was formed. Another consequence the final state is independent of the initial state. The angular distribution of direction of outgoing reaction products is approximately uniform, the cross section weakly depends on the angular (isotropic process).

Reaction cross sections

Nuclear reactions are stochastic processes described by statistical laws. A single elementary reaction is characterized by the *transition probability* and the *cross-section*, these can

be determined[37] by using quantum mechanics. The solutions of the quantum mechanics problems are not the subject of this book, so we introduce the cross section with a simple physical meaning. Accordingly the cross section gives the amount of reactions (R) occur per second while ϕ incident particles collide with the surface element of target:

$$R = \sigma N_t \phi, \tag{3.69}$$

where N_t is the number of target nucleus, ϕ denotes the flux of incident particle in dimension $cm^{-2}s$ and R is the *reaction rate* in dimension s^{-1}. So σ is a physical quantity which determines the probability of a nuclear reaction event. Based on these the cross section is defined as

$$\sigma = \frac{R}{N_t \phi}. \tag{3.70}$$

σ is usually called *microscopic cross-section*. The unit of the cross-section is area cm^2, but in nuclear and reactor physics is also used the *barn* unit. One barn is equal to $10^{-24}cm^2$. Note that the cross-section is not identical with the surface of the target nucleus, the latter being a geometric data whereas the former depends strongly on the total initial kinetic energy of the projectile, in the *laboratory coordinate system* where the target nucleus is at rest.

For the experimental determination of a cross-section, a thin target is manufactured from the homogeneous material made of the target nuclei and the attenuation of the projectile beam Φ through a target of thickness x is measured. Let the number of target nuclei per unit volume be N, then the number of target atoms in an infinitesimal dx thick layer parallel to the the surface of the target is Ndx. The number of reactions is $R = \Phi N \sigma dx$ per unit surface and per unit time in this layer. Obviously the attenuation of the projectile beam equals to R:

$$d\Phi = -\Phi(x) N \sigma dx. \tag{3.71}$$

Integrating this equation, we obtain

$$\Phi(x) = \Phi_0 e^{-N\sigma x} = \Phi_0 e^{-\Sigma x}, \tag{3.72}$$

the initial condition is $\Phi(0) = \Phi_0$. This is the *exponential attenuation law*. In (3.72) a new variable has been introduced: $\Sigma = N\sigma$, where N is the nuclide density of the target. Σ is usually called *macroscopic cross-section*, its dimension is cm^{-1}. Let ρ designate the density of the target material. To determine N, we have to recall [2] that $N_{Av} = 6.023 \cdot 10^{23}$ atom is in A gram material hence

$$N = \frac{\rho}{A} N_{Av}. \tag{3.73}$$

The target may contain several isotopes, the macroscopic cross-section is the sum of the cross-sections of the isotopes:

$$\Sigma = N_1\sigma_1 + N_2\sigma_2 + \ldots, \tag{3.74}$$

where N_i is the number of nuclei per unit volume of isotope i, σ_i is the microscopic cross-section of isotope i.

The material under consideration may be a chemical compound in which the constituting atoms have a fixed ratio. Let M be the molecular weight and the compound contain n_i atoms of type i. Then

$$\Sigma = \frac{\rho N_{Av}}{M} \sum_i n_i \sigma_i, \tag{3.75}$$

[2] N_{Av} is the Avogadro constant.

where σ_i is the microscopic cross-section of isotope i.

Let us now consider the main reaction types. The same reaction partners can produce several different nuclear reactions however, these reactions are mutually exclusive, distinct events. If different reactions are induced by the same projectile then Φ and N cannot change in (3.70), thus the total reaction rate R_t is given by

$$R_t = R_1 + R_2 + R_3 + \ldots, \tag{3.76}$$

using 3.70 in the above relation, we find that the microscopic cross-sections are additive:

$$\sigma_t = \sigma_1 + \sigma_2 + \sigma_3 + \ldots, \tag{3.77}$$

where σ_i designates the microscopic cross-section for reaction of type i and σ_t is the total microscopic cross-section. In the general case when a homogeneous material contains several chemical compounds and all the different nuclei are involved in the compounds have some disjoint reaction with the same projectile (for example neutron), the Σ_t can be written

$$\Sigma_t = \sum_i \frac{\rho_i N_{Av}}{M_i} \sigma_t^i, \tag{3.78}$$

where ρ_i is the partial density of nuclei of type i, σ_t^i is the total microscopic cross-section of nuclei of type i (3.77).

In nuclear and reactor physics the most important nuclear reaction types are the neutron-nucleus interactions, where the neutron is referred to projectile. The likelihood of interaction between an incident neutron and a target nuclide is characterized by the total microscopic cross section σ_t. Two possible things can happen in the neutron-nucleus interaction, on one hand an incident neutron bounces off the target and continues moving, that interaction is called scattering. On the other hand the neutron may be absorbed in the target nucleus, that interaction is called absorption. The total cross-section is the sum of the scattering σ_s and absorption σ_a cross-sections.

$$\sigma_t = \sigma_s + \sigma_a. \tag{3.79}$$

The following reactions are distinguished within the main interaction types:

1. the *inelastic scattering* reaction with cross-section $\sigma_{s,e}$, in which the total kinetic energy is preserved in the scattering;

2. the *elastic scattering* reaction with cross-section $\sigma_{s,in}$, in which the total kinetic energy is reduced;

3. the *capture* process with cross-section σ_c, in which the incident neutron is absorbed in target without fission, but produced other particle (for examples proton (n,p), gamma photon (n,γ), deuteron (n,d), another neutron (n,n'), etc.) ;

4. the *fission* reaction with cross-section σ_f, which that we will discuss in detail in the next Section.

Thus the σ_t can be written

$$\sigma_t = \sigma_{s,e} + \sigma_{s,in} + \sigma_c + \sigma_f. \tag{3.80}$$

where $\sigma_c + \sigma_f = \sigma_a$ because the incident neutron disappears in both reaction processes.

Neutron induced direct reactions

The neutron-nucleus reactions without *resonances* (see below) can be approximately written by first-order time dependent perturbation theory in quantum mechanics. In this model the cross section of $A(a,b)B$ direct reaction can be written (see details in [37]) as

$$\sigma_{(a,b)} = C\frac{P_b^2}{v_a v_b}, \tag{3.81}$$

where C denotes a special constant, which includes the quantum mechanical details, v_a is velocity of projectile, v_b and P_b are the velocity and momentum of outgoing particle b, respectively. (3.81) formula is true if conditions $M_A \gg m_a$ and $M_B \gg m_b$ are satisfied, and the interaction operator is approximately constant at infinitesimal energy interval $[E_b, E_b + dE_b]$. Below is shown the cross section of some of the neutron induced nuclear reaction (without resonances).

The first reaction type is the (n,γ) in other words γ-absorbtion. This process usually is strongly exothermic, thus around $Q \sim 1MeV$ energy produced, which shared between the γ-photon and remanent nuclide. Can be seen from (3.81) that the cross section decreases when the speed of neutron (as incident particle) increases, so this reaction preference for very slow neutrons which are called *thermal neutrons*. The average energy of thermal neutrons $\tilde{E} \simeq 0.025eV$. The reaction energy is much more than initial neutron energy $Q \gg \tilde{E}$, therefore neutron energy cannot affect the energy of the $\gamma-$photon, so can be considered to $P_\gamma^2/v_\gamma = \text{const}$. Finally the cross-section of (n,γ) can be written

$$\sigma_{(n,\gamma)} = C\frac{P_\gamma^2}{v_n v_\gamma} \sim \frac{1}{v_n}. \tag{3.82}$$

This formula is known as "1/v" cross section.

An other process is (n,n) elastic scattering. If the M_A mass of target nucleus is greater than m_n neutron mass then the scattering cannot alter the (v_n) absolute value of neutron speed can only alter the direction of moving, that is $v_a = v_b = v_n$. The cross section approximately can be

$$\sigma_{(n,n)} = C\frac{P_n^2}{v_n v_n} = C\frac{m_n^2 v_n^2}{v_n^2} = Cm_n^2 = \text{const.} \tag{3.83}$$

Interesting process when the incident neutron knocks out another bounded neutron from the target nucleus: (n,n'). Consider just threshold process in which the incoming neutron energy E_n is just greater than the binding energy E^* of bounded neutron. In this case the outgoing neutron point of view the speed of incoming neutron is regarded as be constant, so the cross section

$$\sigma_{(n,n')} = C\frac{P_{n'}^2}{v_n v_n'} \sim v_n' \sim \sqrt{E_n - E^*}, \tag{3.84}$$

where we used the energy conversation law $E_n = E_n' + E^*$, the reaction energy is negligible in threshold process.

A similar process in which the incoming neutron knocks out a bounded proton (n,p) or a nuclear cluster (for example α-cluster) (n,α). The difference is that in those cases the outgoing particle has electric charge, thus these must go through the Coulomb-barrier of remanent nucleus. So we have to complement the (3.84) formula the factor T_b which describes how particle b can go through the Coulomb-barrier. In case of the threshold process the cross section of (n,p):

$$\sigma_{(n,p)} = CT_p\frac{P_p^2}{v_n v_p} \sim T_p v_p \sim T_p\sqrt{E_n - E^*}, \tag{3.85}$$

where T_p is depends on the energy of proton.

As we have previously mentioned, the cross-section may depend strongly on the neutron's kinetic energy or neutron speed. For example, the cross section can be, at low energies, either near or equal to zero. Such an example can be seen in the fission cross-section of ^{238}U, see Fig. 3.4. On the other hand, the cross-section usually has a number of local maxima which may be considerable larger than the cross-sections at most of the energies. An example for that can be observed in the fission cross-section of ^{235}U in Fig. 3.4.

Resonances and compound nucleus interactions

At intermediate energies i.e. in the range $1\ \ eV \leq E \leq 10\ \ keV$, there can be resonances in the cross-sections, which are actually peaks where the cross-section strongly jumps to a higher value (up to several 100 times) from the background at inside of narrow energy range. The reason is the result of the neutron-nucleon collision, the compound nucleus gets into one of its excited states. The excitation energy equals the E_n kinetic energy of the incident neutron[[37],[38]]). Then the energy of resonance $E_r = \hbar\omega_r$ (using Planck's relation, where $\hbar = \frac{h}{2\pi}$ is reduced Planck constant) is equal to the kinetic energy of neutron E_n. This phenomenon may be similar to the classical physics known as excited oscillator, where the oscillator is excited by external periodic force with frequency ω. If the frequency ω is near (or equal) to the resonance frequency ω_0 of oscillator, large amplitude oscillation can be produced by the external force. The amplitude corresponds to the cross section in this analogy.

Let E be the kinetic energy of the neutron (in the laboratory system), E_r be the energy of resonance, then the cross section of reaction type i near resonance is given by *single level Breit-Wigner formula* [37]

$$\sigma_i(E) = \sigma_l \frac{\Gamma\Gamma_i}{(E - E_r)^2 + \left(\frac{\Gamma}{2}\right)^2}, \tag{3.86}$$

where Γ it the total resonance width (FWHM)[3], Γ_i is the partial width of reaction i (i can be scattering, capture or fission), $\sigma_l = \frac{\pi}{k_n^2}(2l+1)$ is the maximum value of total cross section at $E = E_r$ and k_n is the wave number of incoming neutron. Actually the Breit-Wigner formula describes the cross section of emergence of compound nucleus from the collided particles. Hence we have the opportunity to characterize the compound nucleus reactions.

As we mentioned the typical compound nuclear reactions looks like this: $a + A \to C \to b + B$. The final state is not definite, it depends on the excited state of compound nucleus. Similarly to the resonance the formation of the C compound nucleus can be written as

$$\sigma_{a+A\to C}(E) = \frac{\pi}{k_a^2} \frac{\Gamma\Gamma_i}{(E - E_r)^2 + \left(\frac{\Gamma}{2}\right)^2}, \tag{3.87}$$

where index i is specialized by the initial reaction in which produced the compound nucleus (for example $a + A$) and $\Gamma = \sum_i \Gamma_i$. The second stage is decay of the compound nucleus:

$$P_{C\to b+B} = \frac{\Gamma_j}{\Gamma}, \tag{3.88}$$

where index j denotes the one of the possible final state of decay (for example $b + B$). So the cross section of total process can be written as

$$\sigma_{(a,b)}^{comp}(E) = \sigma_{a+A\to C}(E) P_{C\to b+B} = \frac{\pi}{k_a^2} \frac{\Gamma_i\Gamma_j}{(E - E_r)^2 + \left(\frac{\Gamma}{2}\right)^2}. \tag{3.89}$$

[3]FWHM- Full Width at Half Maximum

This result shows similarity between the resonance and compound nucleus reaction, so in any case the resonance is considered as formation of compound nucleus.

In thermal reactors, primarily the resonances of the even-even nuclei are significant, these nuclei such as ^{238}U, ^{232}Th,^{240}Pu etc., but can not be disregarded the even-odd nuclei, for example ^{235}U,^{239}U. Resonances play an outstanding role in the description of the slowing down of neutrons.

The nuclear fission

In nuclear physics nuclear fission is a special nuclear reaction in which the nucleus of an atom splits into smaller parts (lighter nuclei), often producing free neutrons and high energy photons (in the form of gamma rays), and releasing a very large amount of energy. It is schematically shown in figure 1.1.

The energetic preference for nuclei to fission can be understood from the binding energy per nucleon, see Fig. 3.3. A heavy nucleus with $Z \geq 90$ has a binding energy of about 7.6 MeV/nucleon. If ^{238}U splits two equal fragments with $A \simeq 119$ [39], their binding energy per nucleon would be about 8.5 MeV. The energy must be released in splitting of ^{238}U from (3.64):

$$Q = \Delta E = E\left(^{238}U\right) - 2 \cdot E\left(^{119}Pb\right) = -B\left(^{238}U\right) + 2 \cdot B\left(^{119}Pb\right), \tag{3.90}$$

i.e.:

$$\Delta E = -238 \cdot 7.6 + 2 \cdot 119 \cdot 8.5 = 214 \text{ MeV}. \tag{3.91}$$

As we see, the fission of a heavy nucleus is an *exothermic reaction*, where the released reaction energy can appear both as neutron, β and γ emission ($\sim 10\%$) and as kinetic energy of the fragments ($\sim 80\%$).

The *spontaneous fission* of ^{238}U is very rare event. What inhibits the fission process? The answer is the Coulomb barrier. If a ^{238}U is divided into two equal fragments that are just touching at their surfaces, the Coulomb barrier is 250 MeV [[39]]. But the released reaction energy is just 214 MeV, so the Coulomb barrier can prevent the fragments from disruption, therefore the likelihood of fission process is determined by quantum mechanics tunneling as the *Gamow-factor*. The energy difference is required for the spontaneous fission is called as *activation energy*. With those nuclei which in separated states do not have energy enough to cross the Coulomb barrier, the spontaneous fission is rare or not observable. Notwithstanding, absorption of a small amount of energy, such as from a free neutron or a γ photon, may create an intermediate, quasi bound state called (*compound nucleus*). The compound nucleus may have larger energy than the the Coulomb barrier so the fission process may occur. This process is usually known as *induced fission*.

The simplest and most instructive description of fission is obtainable from the liquid drop model of nucleus. The ground state nucleus has spherical geometry in the model. Absorbing an incident particle, for example a neutron, the nucleus gets into an excited state. Then the nucleus stretches while the volume remains constant, but the deformation changes the surface and Coulomb terms in (3.34). The deformed nucleus may be represented as a rotational ellipsoid, let ϵ designate the distortion parameter (deviation from the sphere), then the ellipsoid axes are given by

$$a = R(1+\epsilon) \tag{3.92}$$

$$b = R(1+\epsilon)^{-1/2}, \tag{3.93}$$

where R is the radius of the non-deformed nucleus. As the volume is constant:

$$R^3 = ab^2. \tag{3.94}$$

After the deformation the surface is

$$S = 4\pi R^2 \left(1 + \frac{2}{5}\epsilon^2\right)$$

which reduces the binding energy while the surface energy increases in contrast to the Coulomb term, which is multiplied by the factor $\left(1 - \frac{1}{5}\epsilon^2\right)$ increasing the binding energy [39]. Taken into account all these, the deformation energy is

$$\Delta E = B(\epsilon) - B(\epsilon = 0) = \left(-\frac{2}{5}a_s A^{2/3} + \frac{1}{3}a_c Z^2 A^{-1/3}\right)\epsilon^2, \tag{3.95}$$

where we have used the *semi-empirical mass formula* (3.34). If the second term is larger than the first, the activation energy is negative, then arbitrary small deformation produces energy. Such a nucleus is unstable against this deformation and the spontaneous fission is possible. Therefore the condition for spontaneous fission is

$$\left(\frac{2}{5}a_s A^{2/3} > \frac{1}{3}a_c Z^2 A^{-1/3}\right)\epsilon^2, \tag{3.96}$$

using the numerical values from Ref.[39]

$$\frac{Z^2}{A} > 47. \tag{3.97}$$

Among other things, this is the reason that the periodic system includes finite number of elements.

The cross section of induced fission reaction strongly depends on the energy variable and the type of isotopes (composition of nuclide). For example the ^{235}U is already split by absorption a low-energy neutron, but the splitting of ^{238}U requires high-energy neutron absorption, although the activation energy is the same in both cases, it is shown in Figure 3.4. The latter process is a threshold reaction. The reason is that the fission of ^{235}U includes transition from even-odd nucleus ($^{235}U + n$) to even-even nucleus ((^{236}U)), because the even-even nuclei are more bounded than even-odd nuclei so energy is gained in this process which is enough to fission process. In contrast the fission of ^{238}U includes transition from even-even nucleus ($^{238}U + n$) to even-odd nucleus (^{239}U), where the final state is less bounded than the initial state, so there is no energy release. In this case the energy required for fission is provided by the absorption of high-energy neutron.

The fission fragments and other particles (as neutrons, β and γ particles, etc.) are emitted in fission process. The typical neutron-induced fission is

$$^{235}U + n \rightarrow ^{93}Rb + ^{141}Cs + 2n + \text{energy}. \tag{3.98}$$

Nevertheless the fission products are not determined, there are a lot of possible final states in a fission process, this is typical of the compound nucleus reactions. The distribution of masses of two fission products are shown in Figure 3.5. The distribution is approximately symmetric about the nearly equal fragments ($A_1 \approx A_3$). The fragments are extremely rich in neutrons, so the fragments are typically unstable against β^--decay. Besides the fragments, one or more neutrons appear at the instant of fission, in this manner the neutron excess is reduced. These neutrons are known as *the prompt neutrons*. The number of prompt neutrons is determined by the types of the two fission fragments, so may vary in each fission event. The average number of prompt neutrons ν is characteristic of particular fission process. For example the experimentally observed value of ν are 2.42 for ^{235}U, 2.86 for ^{239}Pu [39], [37].

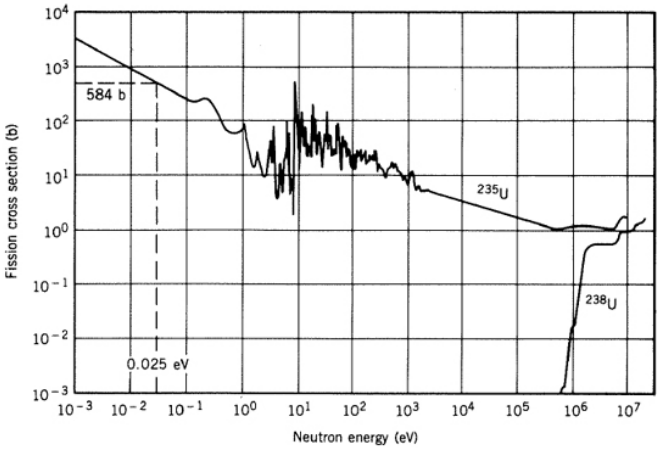

3.4. ábra. The neutron induced fission process

In addition to the prompt neutron, so-called *delayed neutrons* are also emitted in a fission process. These neutrons are emitted after the β-decay of fragments. The fragments will often be in an excited state even after the β-decay, a part of the the excitation energy is released by neutron emission.

3.5. The physical background of chain reaction

The volume in which the energy is produced in a nuclear power plant is called core. The energy is produced by fission [2]. In the reactor core, neutrons are either bound in a nucleus or in a free state. The free neutrons behave like a dilute gas in which the neutron-neutron collisions are negligible, the neutron-nucleus collisions dominate. The quantitative description of the neutron gas is based on the concept of cross-section introduced in the previous Section.

In reactor physics, the neutron-nucleus reactions are classified according to their effect on the number of neutrons. Each reaction type is characterized by a cross-section. The cross-sections are:

1. the capture cross-section Σ_c is associated with the reaction when the neutron is captured and a new nucleus is formed. Details are given in the first Subsection of Section 3.3.

2. the scattering cross-section Σ_s is associated with such neutron-nucleus collision from which one neutron emerges. If the kinetic energies of the neutron and nucleus is preserved the scattering is elastic, otherwise inelastic.

3. in the fission, the neutron-nucleus collision is inelastic, the binding energy of the neutron excites the nucleus, which eventually splits into two parts, and in the reaction also a random number of neutrons are emitted. Usually in the neutron balance only the mean value ν of the released neutrons is used unless we are interested in the fluctuations of the neutron density.

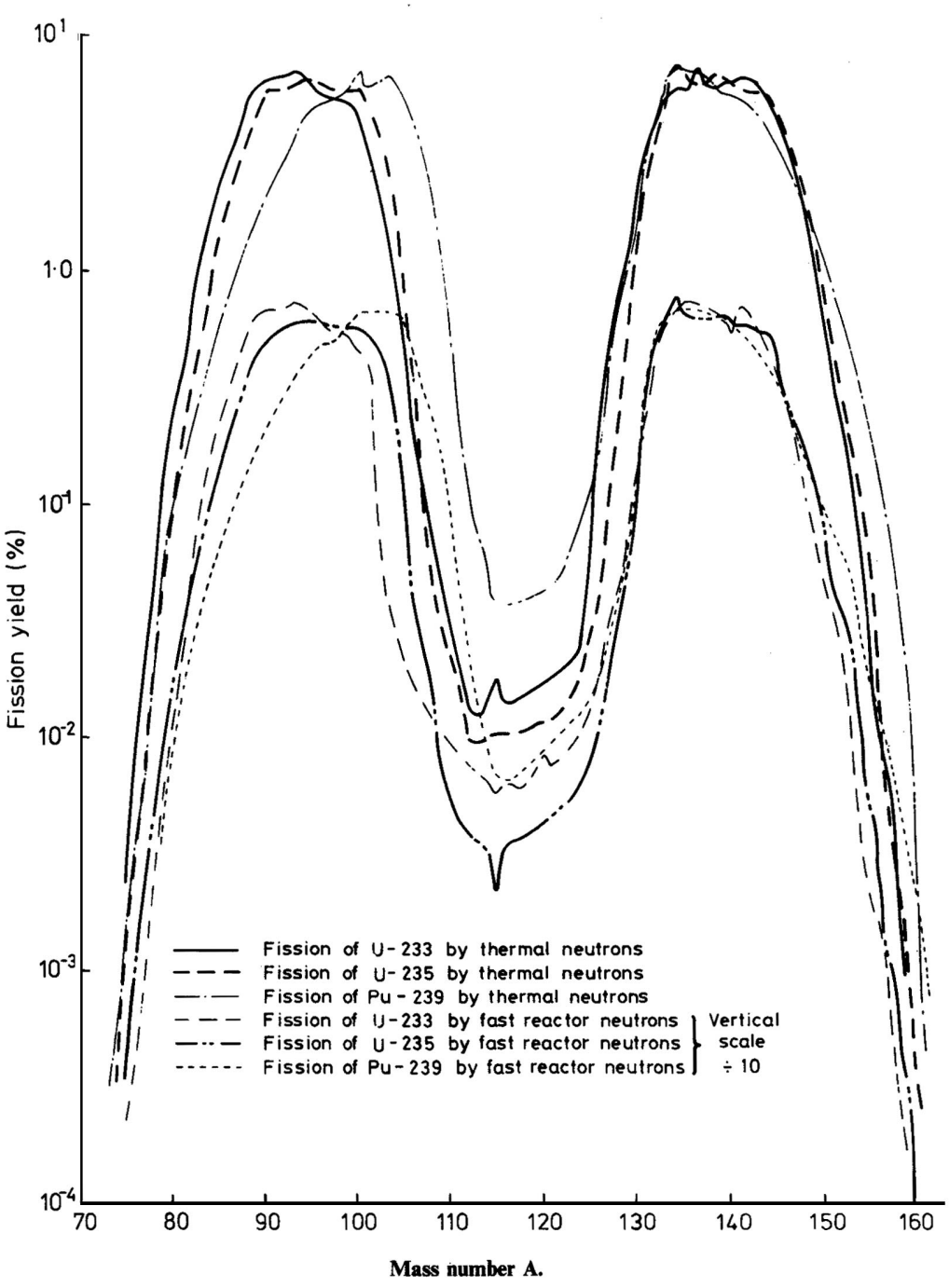

3.5. ábra. The distribution of fragments for neutron induced fission process

4. The cross-sections of the $(n, 2n), (n, 3n)$ reactions are usually negligible, but in specific

problems they may have to taken into account.

We have to generalize the description of the neutron-nuclei interaction because in scattering and fission reactions neutrons may emerge. In those processes first a neutron is absorbed in the collision event and one or more secondary particles are emitted. To account for the mentioned collision types, we introduce two more terms in connection with the cross-section. $c(\mathbf{r},t)$ is the mean of secondary particles emitted in a collision event at $(\mathbf{r},\mathbf{v})$ point of the phase space and $f(\mathbf{v}\to\mathbf{v}')d^3\mathbf{v}'$ is the probability that any secondary particle emitted in the collision of a neutron having velocity $\mathbf{v}$ will have velocity in $d^3\mathbf{v}'$ around $\mathbf{v}'$. The fission cross-section is often written as

$$\Sigma_f(E\to E',\mathbf{\Omega}\to\mathbf{\Omega}')=\frac{\nu(E)f(E)\Sigma_f(E)}{4\pi}, \tag{3.99}$$

where $f(E)$ is the fission spectrum because the angular distribution of the neutrons emerging from fission is isotropic [4]. The energy and angle distribution of neutrons emerging from scattering is often written as

$$\Sigma(E\to E',\mathbf{\Omega}\to\mathbf{\Omega}')=\Sigma(E\to E',\mathbf{\Omega}\mathbf{\Omega}'), \tag{3.100}$$

because the angular distribution depends only on the angle between the neutron directions. The scattering cross-section is

$$\Sigma_s(E,\mathbf{\Omega})=\int dE\int d\mathbf{\Omega}'\Sigma(E\to E',\mathbf{\Omega}\to\mathbf{\Omega}'). \tag{3.101}$$

The cross-section libraries give the cross-section in the center of mass coordinates. Notwithstanding, in reactor physics, the laboratory coordinate system is used, in which the neutron velocity is $\mathbf{v}$ and the nucleus velocity is $\mathbf{V}$. The library data refer to the relative velocity

$$v_r=|\mathbf{v}-\mathbf{V}|.$$

To resolve the contradiction, we introduce the effective cross-section. The nucleus velocity follows the Maxwell-Boltzmann distribution in thermal equilibrium. Let $P(\mathbf{V})d\mathbf{V}$ the probability density of the nucleus velocity being in $d^3\mathbf{V}$ around $\mathbf{V}$. The number of collisions is

$$\int v_r\sigma(v_r)P(\mathbf{V})d^3\mathbf{V}\cdot dt$$

under dt time. The effective cross-section σ_{eff} is defined by

$$v\sigma_{eff}(v)dt=\int v_r\sigma(v_r)P(\mathbf{V})d^3\mathbf{V}\cdot dt. \tag{3.102}$$

Only the so called $1/v$ cross-section[5] has the same σ_{eff} cross-section as the one given in the library.

The kinetics of the neutron population is partly determined by the atom-neutron collisions. In the interaction only the nucleus of the atom plays role but the position of the nucleus is determined by the dimension of the atom. It is clear that the diameter of the atom is determined by the state of the electron shell. The diameter of an atom is in the order of $10^{-8}\,cm$, that of the nucleus appr. $10^{-12}\,cm$. That ratio is like a nut placed in the middle of a stadium. Imagine an aligned string of atoms. One would think that the first

[4] An exception is the large crystal structure.

[5] When $\sigma(v_r)\sim 1/v_r$ the cross-section is of $1/v$ type.

nucleus captures the neutron impinging from the direction of the atom string. But practically the 10000 times smaller nuclei are randomly distributed and each atom may enter into a collision with a neutron unless the cross-section of the nucleus increases, which is the case in the resonance capture. Then the self-shielding should be taken into account.

The different reaction types exclude each other thus a neutron can enter into one given nuclear reaction type. When we account for all the possible reaction types, however, we have to add the cross-sections.

Individual nuclear reactions are random by the very nature of particle interactions. Remember, the cross-section is obtained from a large number of collision events, and says nothing about individual collisions. (3.72) means that the number of neutrons avoiding a collision with the host atoms exponentially decreases with the path of the neutron. This makes it possible to give a probabilistic interpretation to (3.72). Follow the path of the neutron. The fraction of neutrons suffering a collision between path s and $s+ds$ is $\Sigma_x ds$. The average distance λ_x that a neutron will travel before being absorbed is

$$\lambda_x = \frac{\int_0^\infty s e^{-\Sigma_x s}\Sigma_x ds}{\int_0^\infty e^{-\Sigma_x s}\Sigma_x ds} = \frac{1}{\Sigma_x}, \tag{3.103}$$

which is called mean free path or relaxation length (the average distance traveled by the neutron without entering x type collision). Using the mean free path, (3.72) is rewritten as

$$\phi(s) = \phi_0 e^{-\frac{s}{\lambda_x}}. \tag{3.104}$$

Now we are able to derive an equation for the neutron density. To this, first we have to clear the details of neutron distribution. We consider the neutrons as classical particles that can be characterized by specifying the particle position $\mathbf{r}$ and velocity $\mathbf{v}$. Internal variables of the neutron, like spin or polarization are assumed not to influence the motion. Our goal is to find the neutron density function $n(\mathbf{r},\mathbf{v},t)$ in the phase space spanned out by the neutron position $\mathbf{r}$ and velocity $\mathbf{v}$ at time t. Let $n(\mathbf{r},\mathbf{v},t)d^3\mathbf{r}d^3\mathbf{v}$ be the average number of neutrons in the infinitesimal volume $d^3\mathbf{r}$ about $\mathbf{r}$ having velocity in $d^3\mathbf{v}$ about $\mathbf{v}$ at time t. The neutron density $N(\mathbf{r},t)$ at position $\mathbf{r}$ and time t is the integral of $n(\mathbf{r},\mathbf{v},t)$:

$$N(\mathbf{r},t) = \int n(\mathbf{r},\mathbf{v},t)d^3\mathbf{v}, \tag{3.105}$$

where the integration extends over the possible velocities. In cases it is expedient to use the function

$$f(\mathbf{r},\mathbf{v},t) = \frac{n(\mathbf{r},\mathbf{v},t)}{N(\mathbf{r},t)}, \tag{3.106}$$

the probability distribution or density function, which is normalized as

$$\int f(\mathbf{r},\mathbf{v},t)d^3\mathbf{v} = 1 \tag{3.107}$$

for every $\mathbf{r},t$. $n(\mathbf{r},\mathbf{v},t)$ and $f(\mathbf{r},\mathbf{v},t)$ carry information only about the expected number of neutrons in an infinitesimal volume $d^3\mathbf{r}d^3\mathbf{v}$ of the phase space.

It is often convenient to use another independent variables in the phase space. We introduce the

$$\boldsymbol{\omega} = (\mathbf{r}, E, \boldsymbol{\Omega}) \tag{3.108}$$

variable and then $n(\boldsymbol{\omega},t)d^3\mathbf{r}dE$ is the average number of neutrons in $d^3\mathbf{r}$ about $\mathbf{r}$ with kinetic energy in dE about E moving in direction $\boldsymbol{\Omega}$ in solid angle $d\boldsymbol{\Omega}$. The neutron energy E and

velocity $\mathbf{v}$ is related by the well known formula

$$E = \frac{1}{2} m_n \mathbf{v}^2, \tag{3.109}$$

where m_n is the neutron mass. A few further useful concepts are the angular current density $\mathbf{j}(\mathbf{r}, \mathbf{v}, t)$ by the definition

$$\begin{aligned} \mathbf{j}(\mathbf{r}, \mathbf{v}, t) dS d^3\mathbf{v} \quad = \quad & \text{expected number of particles crossing area dS per second} \\ & \text{with velocity } \mathbf{v} \text{ in } d^3\mathbf{v} \text{ at time } t., \end{aligned} \tag{3.110}$$

the net current density $\mathbf{J}(\mathbf{r}, t)$ which is

$$\mathbf{J}(\mathbf{r}, t) = \int \mathbf{j}(\mathbf{r}, \mathbf{v}, t) d^3\mathbf{v} = \int \mathbf{v} n(\mathbf{r}, \mathbf{v}, t) d^3\mathbf{v}, \tag{3.111}$$

and the partial current densities $J_\pm(\mathbf{r}, t)$ at a surface S:

$$J_\pm(\mathbf{r}, t) = \pm \int_\pm \mathbf{n}_S \mathbf{j}(\mathbf{r}, \mathbf{v}, t) d^3\mathbf{v} \tag{3.112}$$

where $\mathbf{n}_S$ is the unit normal to S, and the integration is taken over only the neutron directions in the positive or negative direction. Comparing (3.112) and (3.111) we find

$$\mathbf{n}_s \mathbf{J}(\mathbf{r}, t) = J_+ - J_-. \tag{3.113}$$

Now we derive an exact equation for the phase space density $n(\mathbf{r}, \mathbf{v}, t)$. The distribution in the phase space changes because the neutrons fly and collide with the nuclei of the host material. Consider a neutron at point $(\mathbf{r}, \mathbf{v})$ at time t. After δt the neutron will be at $(\mathbf{r} + \delta t \mathbf{v}, \mathbf{v})$ and covers $\delta t \mathbf{v}$ distance. There are $n(\mathbf{r}, \mathbf{v}, t)$ neutrons in the infinitesimal volume $d^3\mathbf{r} d^3\mathbf{v}$, and after δt they either move to $(\mathbf{r} + \delta t \mathbf{v}, \mathbf{v})$ or suffer a collision, therefore

$$n(\mathbf{r}, \mathbf{v}) = n(\mathbf{r} + \delta t \mathbf{v}, \mathbf{v}) d^3\mathbf{r} d^3\mathbf{v} + \mathbf{v} \delta t (\Sigma_t) n(, \mathbf{r}, \mathbf{v}, t) d^3\mathbf{r} d^3\mathbf{v} + Q(\mathbf{r}, \mathbf{v}, t) d^3\mathbf{r} d^3\mathbf{v} \tag{3.114}$$

where $Q(\mathbf{r}, \mathbf{v}, t)$ is the number of neutrons produced in the collisions. The source term Q has contributions from the scattering and fission nuclear reactions, and from an external source S:

$$\begin{aligned} Q(\mathbf{r}, \mathbf{v}, t) = & S(\mathbf{r}, \mathbf{v}, t) \delta t + \int \Sigma_s(\mathbf{r}, \mathbf{v}' \to \mathbf{v}) v' n(\mathbf{r}, \mathbf{v}', t) d^3\mathbf{v}' \cdot \delta t \\ & + \frac{f(v)}{4\pi} \int \nu \Sigma_f(\mathbf{r}, \mathbf{v}', t) v' n(\mathbf{r}, \mathbf{v}', t) d^3\mathbf{v}' \cdot \delta t. \end{aligned} \tag{3.115}$$

Subtracting $n(\mathbf{r}, \mathbf{v}, t)$ from both side and in the limit $\delta t \to 0$ we get the neutron transport equation:

$$\begin{aligned} \frac{\partial n(\mathbf{r}, \mathbf{v}, t)}{\partial t} = & - \mathbf{v} \boldsymbol{\nabla} n(\mathbf{r}, \mathbf{v}, t) - \Sigma_t(\mathbf{r}, \mathbf{v}, t) v n(\mathbf{r}, \mathbf{v}, t) + S(\mathbf{r}, \mathbf{v}, t) \\ & + \int \Sigma_s(\mathbf{r}, \mathbf{v}' \to \mathbf{v}) v' n(\mathbf{r}, \mathbf{v}', t) d^3\mathbf{v}' \cdot \\ & + \frac{f(v)}{4\pi} \int \nu \Sigma_f(\mathbf{r}, \mathbf{v}', t) v' n(\mathbf{r}, \mathbf{v}', t) d^3\mathbf{v}'. \end{aligned} \tag{3.116}$$

The physical meanings of the terms on the right hand side are as follows. We rearrange the term $-\mathbf{v}\boldsymbol{\nabla}n(\mathbf{r},\mathbf{v},t) = -\boldsymbol{\nabla}\mathbf{v}n(\mathbf{r},\mathbf{v},t)$ and integrate it over an infinitesimal volume V:

$$\int_V -\boldsymbol{\nabla}\mathbf{v}n(\mathbf{r},\mathbf{v},t)d^3\mathbf{r} = \oint_{\partial V} \mathbf{v}n(\mathbf{r},\mathbf{v},t)d\mathbf{S}$$

what gives the number of neutrons leaving V per unit time. That quantity is called the leakage. The term $-\Sigma_t(\mathbf{r},\mathbf{v},t)vn(\mathbf{r},\mathbf{v},t)$ is the neutron loss at phase space point $(\mathbf{r},\mathbf{v})$ due to collisions, and is called removal. Note that the neutrons entering into a scattering reaction reappear at another velocity in the source term. We remark here that the loss apart from the scattering has two component: the capture, its cross-section is Σ_c and the fission with cross-section Σ_f. Their sum is called absorption cross-section:

$$\Sigma_a = \Sigma_c + \Sigma_f. \tag{3.117}$$

Accordingly, the total cross-section Σ_t has the following two components:

$$\Sigma_t = \Sigma_a + \Sigma_s, \tag{3.118}$$

where at a given neutron energy E

$$\Sigma_s(E) = \int_0^\infty \Sigma_s(E \to E')dE' \tag{3.119}$$

The last three terms in (3.116) are the sources but only the first one is independent of the neutron density, the other terms are the scattering source and the fission source.

The (3.116) is applicable if the assumptions we have made in the derivation are fulfilled:

- the neutron density is low and the neutron-neutron collisions can be neglected;
- the neutron density is large enough to speak of the mean value of neutron density and neutron-host nuclei interactions. That assumption is needed to use the mean number of secondary neutrons in the fission term.
- We assumed that the nuclear reactions are prompt, the neutrons emerging from fission or scattering appear at the position of the collision. That assumption fails in kinetic problems, see Chapter 8, Section 7.1.

The reaction rate, see (3.69), is proportional to $vn(\mathbf{r},\mathbf{v},t)$ and because the reaction rates are independent of the direction of $\mathbf{v}$. We often deal with reaction rates so introduce the neutron flux $\Phi(\mathbf{r},v,t)$ with the definition:

$$\Phi(\mathbf{r},v,t) = v\int_{4\pi} n(\mathbf{r},v,\boldsymbol{\Omega},t)d\boldsymbol{\Omega}, \tag{3.120}$$

which is the distance traveled by the neutrons under unit time at position $\mathbf{r}$ having absolute velocity v. The flux in energy variable is

$$\Phi(\mathbf{r},E,t) = \int_{4\pi} vn(\mathbf{r},E,\boldsymbol{\Omega})d\boldsymbol{\Omega}. \tag{3.121}$$

Traditionally, the quantity

$$\Phi(\mathbf{r},E,\boldsymbol{\Omega},t) = vn(\mathbf{r},E,\boldsymbol{\Omega},t) \tag{3.122}$$

Name	Formula	Interrelation
Angular flux	$\Phi(\mathbf{r}, E, \mathbf{\Omega})$	-
Flux or scalar flux	$\Phi(\mathbf{r}, E) = \int_{4\pi} \Phi(\mathbf{r}, E, \Omega) d\mathbf{\Omega}$	$\Phi(\mathbf{r}, E) = 2(J^+(\mathbf{r}, E) + J^-(\mathbf{r}, E))$
Normal component of net current	$J_n(\mathbf{r}, E) = \int_{4\pi} \mathbf{\Omega} n \Phi(\mathbf{r}, E, \boldsymbol{\omega}) d\mathbf{\Omega}$	$J_n(\mathbf{r}, E) = J^+(\mathbf{r}, E) - J^-(\mathbf{r}, E)$
Partial current $(+\mathbf{n})$	$J^+(\mathbf{r}, E) = \int_{\mathbf{\Omega n}>0} \mathbf{\Omega} n \Phi(\mathbf{r}, E, \mathbf{\Omega}) d\mathbf{\Omega}$	$J^+(\mathbf{r}, E) = \frac{1}{4}\Phi(\mathbf{r}, E) + \frac{1}{2} J_n(\mathbf{r}, E)$
Partial current $(-\mathbf{n})$	$J^-(\mathbf{r}, E) = -\int_{\mathbf{\Omega n}<0} \mathbf{\Omega} n \Phi(\mathbf{r}, E, \mathbf{\Omega}) d\mathbf{\Omega}$	$J^-(\mathbf{r}, E) = \frac{1}{4}\Phi(\mathbf{r}, E) - \frac{1}{2} J_n(\mathbf{r}, E)$

3.1. táblázat. Characteristics of the neutron distributions

is called angular flux, which gives the distance traveled under unit time by the neutrons flying in direction $\mathbf{\Omega}$. The flux and the angular flux are related as

$$\Phi(\mathbf{r}, E, t) = \int_{4\pi} \Phi(\mathbf{r}, E, \mathbf{\Omega}) d\mathbf{\Omega}. \tag{3.123}$$

Before passing on to the neutron balance, we summarize the relationships between the characteristics of the neutron field using the $(\mathbf{r}, E, \mathbf{\Omega}, t)$ variables. In the table the partial and net currents are given with respect to a surface, $\mathbf{r}$ is a point on that surface, n is the outward normal to the surface, see Table 3.1.

The angular variable is a unit vector, its Cartesian components are

$$\Omega_x = \sin\theta\cos\varphi \tag{3.124}$$
$$\Omega_y = \sin\theta\sin\varphi \tag{3.125}$$
$$\Omega_z = \cos\theta. \tag{3.126}$$

The infinitesimal element on the surface of the unit sphere is

$$d\mathbf{\Omega} = \sin\theta d\theta d\varphi. \tag{3.127}$$

The following integrals are useful in the calculations:

$$\int_{4\pi} d\mathbf{\Omega} = \int_0^{\pi}\int_0^{2\pi} sin\theta d\varphi d\theta = 4\pi \quad \int_{4\pi} \mathbf{\Omega} d\mathbf{\Omega} = 0, \tag{3.128}$$

$$\int_{\mathbf{\Omega}_z>0} \mathbf{\Omega}_i \mathbf{\Omega}_i d\mathbf{\Omega} = \int_{\mathbf{\Omega}_z<0} \mathbf{\Omega}_i \mathbf{\Omega}_i d\mathbf{\Omega} = \frac{2\pi}{3}, \quad i = x, y, z. \tag{3.129}$$

$$\int_{\mathbf{\Omega}_z>0} \mathbf{\Omega}_i \mathbf{\Omega}_j d\mathbf{\Omega} = \int_{\mathbf{\Omega}_z<0} \mathbf{\Omega}_i \mathbf{\Omega}_j d\mathbf{\Omega} = 0; \quad i \neq j. \tag{3.130}$$

$$\int_{\mathbf{\Omega}_z>0} \mathbf{\Omega}_z d\mathbf{\Omega} = -\int_{\mathbf{\Omega}_z<0} \mathbf{\Omega}_z d\mathbf{\Omega} = \pi. \tag{3.131}$$

It is convenient to introduce the neutron flux in (3.116). In the removal, scattering, and fission terms we just replace vn, in the leakage term we substitute $\mathbf{v} = \mathbf{\Omega} v$ and multiply the time derivative by v and divide it by v to arrive at

$$\begin{aligned}\frac{1}{v}\frac{\partial \Phi(\mathbf{r}, \mathbf{v}, t)}{\partial t} =& -\mathbf{\Omega}\boldsymbol{\nabla}\Phi(\mathbf{r}, \mathbf{v}, t) - \Sigma_t(\mathbf{r}, \mathbf{v}, t)\Phi(\mathbf{r}, \mathbf{v}, t) + S(\mathbf{r}, \mathbf{v}, t) \\ &+ \int \Sigma_s(\mathbf{r}, \mathbf{v}' \to \mathbf{v})\Phi(\mathbf{r}, \mathbf{v}', t) d^3\mathbf{v}' \cdot \\ &+ \frac{f(v)}{4\pi}\int \nu\Sigma_f(\mathbf{r}, \mathbf{v}', t)\Phi(\mathbf{r}, \mathbf{v}', t) d^3\mathbf{v}'.\end{aligned} \tag{3.132}$$

Let us investigate the cross-sections in the transport equation more closely. As mentioned above, we may sum the cross-sections of various isotopes. Thus a macroscopic cross-section Σ_x in equation 3.132 is

$$\Sigma_x(\mathbf{r}, E) = \sum_i n_i(\mathbf{r})\sigma_i(E). \tag{3.133}$$

Such a physical feature of Σ_x as its variation with the energy, is determined by the microscopic cross-section. But the number of isotopes may vary between 3 and 150, the former for example in the water moderator, which contains two hydrogen and one oxygen isotope, the latter in a fuel where various fission products may be present. The nuclide density n_i depends on the temperature, the temperature depends on the position in the core. Therefore it is not a trivial task how to determine the cross-sections effectively in the transport equation. A further problem is that some cross-sections are used in different models and the model may depend on the mass number, see the slowing down models. As we will see later, a parametrized library is prepared, where it is easy to look up the actual cross-sections.

The neutron transport equation differs from the general particle transport equation (e.g. photon transport, plasma transport) in the collision term, and in the force acting on the particle. When the particle-particle interactions can not be neglected, the transport equation becomes nonlinear.

3.5.1. The mathematical problem

Either form of the transport equation is linear, when Φ_1 and Φ_2 are solutions, so is $c_1\Phi_1 + c_2\Phi_2$. Either form is an integro-differential equation as it contains derivation with respect to time and space, and integrals over the energy. The differentials in the equations entail that we have to fix an initial condition at every $\mathbf{r}$ and a boundary condition along the boundary ∂V of a volume V.

Symbolically the transport equation (3.132) has the following structure:

$$\begin{aligned}\frac{\partial\Phi(\boldsymbol{\omega}, t)}{\partial t} &= -\mathcal{L}\Phi(\boldsymbol{\omega}, t) - \mathcal{R}\Phi(\boldsymbol{\omega}, t) + \mathcal{S}\Phi(\boldsymbol{\omega}, t) + \mathcal{F}\Phi(\boldsymbol{\omega}, t) + S(\boldsymbol{\omega}, t) \\ &\equiv \mathcal{T}\Phi(\boldsymbol{\omega}, t) + S(\boldsymbol{\omega}, t),\end{aligned} \tag{3.134}$$

where $\mathcal{L}, \mathcal{R}, \mathcal{S}, \mathcal{F}$ are the leakage, removal, scattering, and fission operators, respectively; and S is the external source. We have introduced the $\mathcal{T}$ transport operator:

$$\mathcal{T} = -\mathcal{L} - \mathcal{R} + \mathcal{S} + \mathcal{F}, \tag{3.135}$$

which is a linear operator and using $\mathcal{T}$, we write the transport equation as

$$\frac{\partial\Phi(\boldsymbol{\omega})}{\partial t} = \mathcal{T}\Phi(\boldsymbol{\omega}, t). \tag{3.136}$$

Assume for a moment that φ is an eigenfunction of $\mathcal{T}$:

$$\mathcal{T}\varphi(\boldsymbol{\omega}) = \tau\varphi(\boldsymbol{\omega}), \tag{3.137}$$

then

$$\Phi(\boldsymbol{\omega}, t) = e^{\tau t}\varphi(\boldsymbol{\omega}) \tag{3.138}$$

is a solution of (3.136); here τ is an eigenvalue of the transport operator. When the eigenfunctions φ of $\mathcal{T}$ form a complete system, we can expand a possible solution $\Psi(\boldsymbol{\omega}, t)$ in terms of the eigenfunctions:

$$\Psi(\boldsymbol{\omega}, t) = \sum_i c_i(t)\varphi_i(\boldsymbol{\omega}), \tag{3.139}$$

where

$$c_i(t) = c_i(0)e^{\tau_i t}\varphi_i(\boldsymbol{\omega}). \tag{3.140}$$

At $t = 0$ we also expand the given $\Phi(\boldsymbol{\omega}, 0)$ as

$$\Phi(\boldsymbol{\omega}, 0) = \sum_i c_i(0)\varphi_i(\boldsymbol{\omega}). \tag{3.141}$$

Order the eigenvalues in a monotonously decreasing order of $Re(\tau_i)$:

$$\Phi(\boldsymbol{\omega}, t) = e^{\tau_0 t}\left(c_i(0)e^{(\tau_i-\tau_0)t}\varphi_i(\boldsymbol{\omega})\right). \tag{3.142}$$

Because $Re(\tau_i - \tau_0) < 0$ the exponentials are negative for $i > 0$, and

$$\lim_{t\to\infty} \Phi(\boldsymbol{\omega}, t) = e^{\tau_0 t}\varphi_0(\boldsymbol{\omega}), \tag{3.143}$$

i.e. the asymptotic form (c.f. Subsection XX) of the solution tends to the eigenfunction $\varphi_0(\boldsymbol{\omega})$. $\tau_0, \varphi_0(\boldsymbol{\omega})$ are called the fundamental eigenvalue and the fundamental eigenfunction of the transport operator. The material composition of V, the boundary condition along ∂V and the initial condition together determine the fundamental eigenvalue τ_0. When $\tau_0 > 0, \tau < 0$ we call V supercritical and subcritical, respectively. When $\tau_0 = 0$, V is critical. Note that in (3.136) the external source is zero.

The transport operator $\mathcal{T}$ has a fundamental eigenvalue which is real and the associated eigenfuction is positive.

3.5.2. Boundary conditions

To obtain the boundary conditions along an internal boundary, we integrate the static (3.116) over an ϵ thick box so that the upper half of the box is in material 1 the lower part in material 2. Let the material interface be at $\mathbf{r}_s$. The time derivative is zero in a static case. We integrate (3.116) over the box and in the resulting expression we let ϵ tend to zero. The integrals involving the absorbtion, scattering, and fission will tend to zero. Only the leakage term remains that can be transformed into a surface integral. The integrals over the faces of length ϵ give zero, and remains two integrals, one over S_1, that side of the box which lays in material 1, that surface be at $\mathbf{r}_s + 0$. The other surface S_2 be at $\mathbf{r}_s - 0$ and let that lay in material 2. The integrated transport equation now takes the form

$$\lim_{\epsilon\to 0}\int_{S_1} \boldsymbol{\Omega}\mathbf{n}_1\Phi(\boldsymbol{\omega})dS + \lim_{\epsilon\to 0}\int_{S_2} \boldsymbol{\Omega}\mathbf{n}_2\Phi(\boldsymbol{\omega})dS = 0, \tag{3.144}$$

where $\mathbf{n}_1$ and $\mathbf{n}_2$ are the outward normals to surfaces S_1 and S_2, respectively. Obviously $\mathbf{n}_1 = -\mathbf{n}_2$. From (3.144), we get that at every $\mathbf{r}_s$ point of the surface must hold

$$\boldsymbol{\Omega}\mathbf{n}\Phi(\mathbf{r}_s - 0, \boldsymbol{\Omega}) = \boldsymbol{\Omega}\mathbf{n}\Phi(\mathbf{r}_s + 0, \boldsymbol{\Omega}). \tag{3.145}$$

Note that this expression entails that for $\boldsymbol{\Omega}\mathbf{n} \neq 0$ the angular flux must be continuous:

$$\Phi(\mathbf{r}_s + 0, \boldsymbol{\Omega}) = \Phi(\mathbf{r}_s - 0, \boldsymbol{\Omega}), \tag{3.146}$$

whereas when $\boldsymbol{\Omega}\mathbf{n} = 0$ any finite discontinuity is allowed at the boundary $\mathbf{r}_s$.

There are to views regarding the internal boundary conditions. In the mathematical literature, it is assumed that the cross-sections are smooth functions and the solution must

belong to the class of smooth functions, usually continuous first derivative with respect to spatial variables. In the physical literature, however, the volume under consideration is composed of homogeneous material blocks, the cross-sections are discontinuous at material boundaries, but the quantities having a physical meaning, obey some suitable continuity condition.

The boundary values prescribed on the external boundary of V fall into one of the two categories. The inhomogeneous boundary condition fixes a given entering current on the boundary and the subcriticality theorem (see below) assures the existence and uniqueness of the solution. The second category is the homogeneous boundary condition that sets a linear relationship on the boundary between entering and exiting currents. The most general form is

$$J_-(\boldsymbol{\omega}) = \int_{\partial V} \int_{\boldsymbol{\Omega}'\mathbf{n}>0} \int_0^\infty (\boldsymbol{\Omega}'\mathbf{n}(\mathbf{r}'))\Gamma(\boldsymbol{\omega};\boldsymbol{\omega}')J_+(\boldsymbol{\omega}')dE'd\boldsymbol{\Omega}'d^3\mathbf{r}', \tag{3.147}$$

where $\boldsymbol{\Omega}\mathbf{n}(\mathbf{r}) < 0$, and $J_-(\boldsymbol{\omega})$ is the entering current, which is a linear expression of the exiting current at phase point $\boldsymbol{\omega}'$, the albedo matrix is $\Gamma(\boldsymbol{\omega};\boldsymbol{\omega}')$. The general form considerably reduces in the practical applications. We mention here four particular cases:

1. Black boundary condition: $\Gamma \equiv 0$, no neutrons enter into V through the boundary.
2. White boundary condition: $\Gamma \equiv 1$, all the exiting neutrons reenter V.
3. Reflective boundary condition: $\Gamma(\boldsymbol{\omega};\boldsymbol{\omega}') = \delta_{\boldsymbol{\omega},\boldsymbol{\omega}_r}$ where δ is Kronecker's delta function, and $\boldsymbol{\omega}_r = \boldsymbol{\omega} - 2\mathbf{n}\boldsymbol{\omega}$, the reflected direction of $\boldsymbol{\omega}$.
4. Local albedo: $\Gamma = constant$, a given fraction of the exiting neutrons returns to V.
5. Periodic boundary condition. Let V stand for the volume under consideration, such that an approximate infinite volume can be created by repeating V. Let the boundary ∂V composed of faces and assume that face A is opposite to face B. The periodic boundary condition assumes that faces A and B are adjacent and the corresponding internal boundary condition should be applied to them.

Note that although the boundary condition has been formulated using partial currents, using the relationships

$$J_+(\mathbf{r},E) = \frac{1}{4}\Phi(\mathbf{r},E) + \frac{1}{2}J_n(\mathbf{r},E) \tag{3.148}$$

$$J_-(\mathbf{r},E) = \frac{1}{4}\Phi(\mathbf{r},E) - \frac{1}{2}J_n(\mathbf{r},E) \tag{3.149}$$

any linear boundary condition relating the partial currents can be formulated as a relationship between fluxes $\Phi(\mathbf{r},E)$ and the normal component of the net current $J_n(\mathbf{r},E)$. A particular case is the $\Gamma = 1$ when

$$\Phi(\mathbf{r},E) = 0; \mathbf{r} \in \partial V. \tag{3.150}$$

Since $\Phi(\mathbf{r},E,\boldsymbol{\Omega}) \geq 0$ that is equivalent to no neutrons being at $\mathbf{r}$. This assumption is unphysical therefore the boundary condition is fixed not along the boundary but along an extrapolated boundary $\mathbf{r} + \lambda\mathbf{n}_\mathbf{r}$ where λ is the extrapolation distance.

Taking into account the possible forms of the static transport equation (3.116) and the boundary conditions, the possible particular cases fall into one of the following four categories:

1. Homogeneous transport equation with homogeneous boundary condition when we solve

$$\mathcal{T}\Phi(\boldsymbol{\omega}) = 0; \quad \mathbf{r} \in V; \tag{3.151}$$

$$\Phi(\boldsymbol{\omega}_-) = \Gamma\Phi(\boldsymbol{\omega}_+), \quad \mathbf{r} \in \partial V, \tag{3.152}$$

where $\boldsymbol{\Omega}\mathbf{n} < 0$ in $\boldsymbol{\omega}_-$ i.e. the entering directions; and $\boldsymbol{\Omega}\mathbf{n} > 0$ in $\boldsymbol{\omega}_+$. Nontrivial solution exists only if operator $\mathcal{T}$ maps some functions into zero, that requires some relationship between the cross-sections. Such a V in which equations (3.151) and (3.152) have non-trivial solutions is called critical. In order to make it possible to treat non-critical V, we introduce a free parameter in $\mathcal{T}$. Such a V is called conditionally critical as it is critical at specific values of the parameter, see (3.163).

2. Homogeneous transport equation with inhomogeneous boundary condition when we solve

$$\mathcal{T}\Phi(\boldsymbol{\omega}) = 0, \quad \mathbf{r} \in V; \tag{3.153}$$

$$\Phi(\boldsymbol{\omega}_-) = q(\boldsymbol{\omega}_-), \quad \mathbf{r} \in \partial V, \tag{3.154}$$

where $q(\boldsymbol{\omega}_-)$ is a given function. The problem has a solution that can be given with the help of the Green's function, see Chapter 11.

3. Inhomogeneous transport equation with source and homogeneous boundary condition when we solve

$$\mathcal{T}\Phi(\boldsymbol{\omega}) = Q(\boldsymbol{\omega}) \quad \mathbf{r} \in V; \tag{3.155}$$

$$\Phi(\boldsymbol{\omega}_-) = \Gamma\Phi(\boldsymbol{\omega}_+), \quad \mathbf{r} \in \partial V, \tag{3.156}$$

the solution can be given with the help of the Green's function, see Chapter 11.

4. Inhomogeneous transport equation with inhomogeneous boundary condition when we solve

$$\mathcal{T}\Phi(\boldsymbol{\omega}) = Q(\boldsymbol{\omega})\mathbf{r} \in V; \tag{3.157}$$

$$\Phi(\boldsymbol{\omega}_-) = q(\boldsymbol{\omega}_-), \mathbf{r} \in \partial V. \tag{3.158}$$

By means of the linearity of the transport operator, the solution of (3.157)-(3.158) is the sum of the solutions of problems (3.155)-(3.156) with $\Gamma = 0$ and (3.153)-(3.154).

The inhomogeneous problems are uniquely solvable when the source term satisfies some conditions, see Chapter 11 for details.

Consider the time dependent transport equation

$$\frac{\partial\Phi(\boldsymbol{\omega}, t)}{\partial t} - \mathcal{T}\Phi(\boldsymbol{\omega}, t) = Q(\boldsymbol{\omega}, t) \tag{3.159}$$

in a volume V. The initial condition is $\Phi(\boldsymbol{\omega}, t_0) = 0$ for $\mathbf{r} \in V$. Note that operator $\mathcal{T}$ is linear.

3.1 Theorem (Uniqueness theorem) *[147][p.18] The neutron angular density within a given volume V of space bounded by the surface ∂V is uniquely determined by*

1. *the initial angular density $f(\boldsymbol{\omega})$ in V;*
2. *the sources $Q(\boldsymbol{\omega})$ in V;*
3. *the angular density incident on ∂V.*

Proof: Assume that we have two solutions of the time dependent transport equation with a given source term $Q(\boldsymbol{\omega})$:

$$\frac{\partial \Phi_1}{\partial t} + \mathcal{T}\Phi_1(\boldsymbol{\omega}) = Q(\boldsymbol{\omega})\mathbf{r} \in V;$$

and

$$\frac{\partial \Phi_2}{\partial t} + \mathcal{T}\Phi_2(\boldsymbol{\omega}) = Q(\boldsymbol{\omega}) \;\; \mathbf{r} \in V;$$

Subtracting the two equations, and using that operator $\mathcal{T}$ is linear, we see that

$$\frac{\partial(\Phi_1(\boldsymbol{\omega}) - \Phi_2(\boldsymbol{\omega}))}{\partial t} - \mathcal{T}(\Phi_1(\boldsymbol{\omega}) - \Phi_2(\boldsymbol{\omega})) = 0, \mathbf{r} \in V; \tag{3.160}$$

and the difference of the two solutions is identically zero in V at t_0, and is also identically zero along the boundary of V. Introducing

$$\Psi(\boldsymbol{\omega}, t) = \Phi_1(\boldsymbol{\omega}, t) - \Phi_2(\boldsymbol{\omega}, t) \tag{3.161}$$

we multiply (3.160) by Ψ and integrate the resulting equation over t from t_0 to $t_1 > t_0$, over V, and over $\boldsymbol{\Omega}$. The resulting expression is quadratic in Ψ. This statement is not trivial for the scattering term in $\mathcal{T}$ but there we can use the inequality

$$\int \left[\Psi(\mathbf{r}, \boldsymbol{\Omega}, t) - \Psi(\mathbf{r}, \boldsymbol{\Omega}', t)\right]^2 g(\boldsymbol{\Omega}, \boldsymbol{\Omega}', \mathbf{r}) d\boldsymbol{\Omega} d\boldsymbol{\Omega}' \geq 0$$

provided $g \geq 0$. From the terms involving time derivative, we get

$$\int \frac{1}{2} \left(\Psi^2(\mathbf{r}, \boldsymbol{\Omega}, t_1) - \Psi^2(\mathbf{r}, \boldsymbol{\Omega}, t_0)\right) d^3\mathbf{r} d\boldsymbol{\Omega} \geq 0$$

because the angular flux is zero at t_0. In a subcritical region, the other terms are all positive, their sum is zero only when $\Psi(\boldsymbol{\omega}) \equiv 0$, from this follows $\Phi_1(\boldsymbol{\omega}) = \Phi_2(\boldsymbol{\omega})$. Otherwise, one substitutes $\tilde{\Psi}(\mathbf{r}, \boldsymbol{\Omega}, t) \to e^{-\alpha t}\Psi(\mathbf{r}, \boldsymbol{\Omega}, t)$ and the above presented procedure is applicable to $\tilde{\Psi}$. Q.E.D.

In a stationary subcritical region the solution of the transport equation is also unique [147][Chapter 2]:

3.2 Theorem (Subcriticality) *Let volume V be subcritical. Then the flux distribution in V is uniquely determined by the time-independent incident distribution.*

Proof: We omit the integration over time in the proof of the Uniqueness theorem. Q.E.D.

The transport operator is linear, and it has a stationary solution only if its fundamental eigenvalue is zero, see (3.143). Such a volume V in which the external source free transport equation has a stationary solution is called critical volume. Any volume can be made conditionally critical, if we introduce an additional parameter into the transport operator. Two such eigenvalues are used in reactor physics: the time absorption and the effective multiplication factor k_{eff}. The first one is an additive constant in the removal operator, we replace $\mathcal{R}$ by $\mathcal{R} + \alpha$:

$$(\mathcal{L} + \mathcal{R} + \alpha)\Phi(\boldsymbol{\omega}) = \mathcal{F}\Phi(\boldsymbol{\omega}) \tag{3.162}$$

and we seek an α by which (3.162) has non-trivial solution. V is called supercritical, critical, and subcritical, when $\alpha > 0, \alpha = 0$, and $\alpha < 0$, respectively. Any volume (i.e. subcritical, critical, or supercritical) has a time absorption type eigenvalue.

The second kind of eigenvalue is written in the form of a multiplier in the fission term, using the substitution $\mathcal{F} \to 1/k_{eff}\mathcal{F}$ and we have to find k_{eff} with which the equation

$$(\mathcal{L} + \mathcal{R})\Phi(\boldsymbol{\omega}) = \frac{1}{k_{eff}}\mathcal{F}\Phi(\boldsymbol{\omega}). \tag{3.163}$$

has non-trivial solution. When $k_{eff} > 1$, V is called supercritical, when $k_{eff} = 1$, critical, when $k_{eff} < 1$, subcritical. If V has no fissionable material, the effective multiplication factor can not be defined. The reactivity ρ is obtained from the k_{eff} by the following relation:

$$\rho = 1 - \frac{1}{k_{eff}} \tag{3.164}$$

therefore the reactivity of a subcritical/supercritical volume is negative/positive, and the reactivity of a critical volume is zero. In neutron kinetics, see Chapter 7, Section 7.1, a new unit for the criticality is introduced, it is measured in delayed neutron fraction unit.

In an industrial equipment, self-sustaining fission has to be established. As we have seen in Fig. 1.1, this is possible if we have a large amount of fissionable nuclei arranged in such a manner that the number of neutrons remains constant in time. That state is called criticality, we discussed it in details in Chapter 3. In a thermal reactor, the criticality can be estimated by the four-factor formula [2]. Estimate the number of neutrons in two consecutive generations in an infinite in extent multiplying system. The neutrons emerging from fission have large energies. Fast neutrons are absorbed both in ^{235}U and ^{238}U, let the average number of secondary neutrons be ϵ which is defined as the ratio of the total number of fast neutron produced by fissions due to neutrons of all energies to the number resulting from thermal neutron fissions. The latter number is

$$\eta = \nu\frac{\Sigma_f}{\Sigma_{fuel}}, \tag{3.165}$$

where ν is the average number of fast neutrons released per slow neutron fission, Σ_f is is the macroscopic cross-section for slow neutron fission, Σ_{fuel} is the total absorbtion cross-section of thermal neutrons. When n thermal neutrons are captured in fuel, $n\eta\epsilon$ fast neutrons are produced. A fraction $p < 1$ of those neutrons escape capture while being slowed down, thus $n\eta\epsilon p$ neutrons become thermalized. A fraction $f < 1$ of the thermalized neutrons are absorbed in fuel, thus the ratio of neutrons in two consecutive generations is

$$k = k_\infty = \frac{n\eta\epsilon pf}{n}, \tag{3.166}$$

which is just the multiplication factor. A further loss of neutrons is due to leakage. Let $P < 1$ denote the non-leakage probability, i.e. the fraction of neutrons not leaking out. The criticality condition is

$$k_\infty P = 1. \tag{3.167}$$

This expression is suitable to comprehend the reactor operation but for core design the four-factor formula is inappropriate.

Note that the equations of the neutron balance alone are linear, therefore the balance equation in itself does not determine the power of the reactor. When the thermal-hydraulics equations are also taken into account, the feedback makes the equations nonlinear and determine the power level.

Nuclear reactors have been operated at various power levels. In research reactors or training reactors the power is low as the main point is to carry out measurements or teaching

reactor operation. The measurements on research reactors have played an important role in checking the calculation methods (see validation and verification). When a new reactor type emerges, possible cores are studied on zero or low power experimental facilities. This has been the case among others with the source driven subcritical system [3].

Other research reactors serve as neutron source, the neutrons are exploited in a number of experimental facilities installed around the research reactors. The experimental technique has been applied in studying the structure of the matter (solid state physics, molecular interactions, catalysts, large molecules, protein, lipid and other important compounds in biology, new forms of matter like ferrofluids etc.).

3.5.3. Reactor control

The operator sitting in the control room is able to alter state of devices (open or close valves, etc.) in the technology. Operator actions may affect:

- the position H of the control rods;
- the boron concentration c_B in the coolant;
- the coolant flow rate G;
- the temperature of the inlet coolant T_{in}.

All the reactor parameters that the operator is capable of regulating must depend on the mentioned four parameters. For example, to increase the reactor power, the operator may withdraw the control rods. That increases the reactivity, the reactor power grows. The growing power raises the average temperature in the core, that initiates a negative feedback. At a given power level a new equilibrium is set up.

Now we are interested in the reactivity control, the most important reactor parameter that should always be controllable. Clearly it means

$$\rho = \rho(H, c_B, G, T_{in}). \tag{3.168}$$

Every argument is in a noisy environment thus subject to fluctuations. Stable reactor operations require negative feedback, thus

$$\frac{\partial \rho}{\partial H} < 0 \tag{3.169}$$

meaning that insertion of a control rod should decrease the reactivity;

$$\frac{\partial \rho}{\partial c_B} < 0, \tag{3.170}$$

adding boron to the coolant should decrease the reactivity. When the coolant flow rate is reduced, the average temperature increases in the core, moreover, the change of the inlet temperature also leads to an increase in the average temperature. The increased temperature may lead to bubbles appearing in the coolant. To account of that, two more partial derivatives should provide negative feedback:

$$\frac{\partial \rho}{\partial x} < 0 \tag{3.171}$$

where x is the steam concentration in the coolant, and

$$\frac{\partial \rho}{\partial T_{av}} < 0, \tag{3.172}$$

an increase in the average core temperature should lead to decreasing reactivity.

These are only the main design principles rendering stability to the reactor operation. We only mention here that the temperature change leads to irreversible changes in the metal structural elements, including the reactor vessel itself. The four arguments of the reactivity in (3.168) clearly shows that remote technological elements may influence the reactivity. Interested reader may find further details in the literature.

3.6. Alternative formulations

As we have seen, the neutron density is the solution of the Boltzmann equation (3.116), which is an integro-differential equation. The features of the material types appear in the macroscopic cross-sections. The macroscopic cross-sections depend on the neutron energy, since the number of isotopes in a spent fuel may exceed one hundred, and there are energy ranges where the cross-sections vary rapidly, the storage and retrieval of the cross-section has to be carefully prepared. In the present Section, we discuss two equations which may serve in some sense as alternative for the Boltzmann equation. The first one is the integral form of the transport equation, but the second form discussed here, the so called adjoint transport equation reflects a radically different physical model although it is mathematically strictly related to the Boltzmann equation. The latter form is especially important in the perturbation theory, the universal tool in the numerical discussion of the consequences following minor alterations in geometry, material composition or temperature.

3.6.1. Integral transport equation

Formally, we can easily transform the integro-differential form of the transport equation (3.116) into an integral equation. To this end we consider the neutron density in V, and select a point $\mathbf{r}_0 \in \partial V$ on the boundary and introduce the following distance and time:

$$t = t_0 - s/v; \quad \mathbf{r} = \mathbf{r}_0 - s\mathbf{\Omega}, \tag{3.173}$$

that means we consider a point $\mathbf{r} \in V$ and neutrons flying with velocity v from the boundary point $\mathbf{r}_0$ towards $\mathbf{r}$ in the direction $\mathbf{\Omega}$. The neutron starting at t_0 from the point $\mathbf{r}_0$ will reach position $\mathbf{r}$ at time t given by (3.173). We show that

$$\frac{1}{v}\frac{\partial \Phi(\boldsymbol{\omega}, t)}{\partial t} + \mathbf{\Omega}\boldsymbol{\nabla}\Phi(\boldsymbol{\omega}, t) = -\frac{\partial \Phi(\mathbf{r}, \mathbf{\Omega}, t)}{\partial s}.$$

Using the chain rule, and (3.173), we get the straightforward result:

$$\frac{\partial \Phi}{\partial s} = \frac{\partial \Phi}{\partial t}\frac{dt}{ds} + \boldsymbol{\nabla}\Phi\frac{d\mathbf{r}}{ds} = -\frac{1}{v}\frac{\partial \Phi}{\partial t} - \mathbf{\Omega}\boldsymbol{\nabla}\Phi.$$

That simple transformation can be used to write the transport equation for

$$\Phi(\mathbf{r}_0 - s\mathbf{\Omega}, \mathbf{\Omega}, t_0 - \frac{s}{v})$$

and the resulting equation is

$$\begin{aligned}
&\frac{\partial \Phi(\mathbf{r}_0 - s\mathbf{\Omega}, \mathbf{\Omega}, t_0 - \frac{s}{v})}{\partial s} - \Sigma_t \Phi(\mathbf{r}_0 - s\mathbf{\Omega}, \mathbf{\Omega}, t_0 - \frac{s}{v}) = \\
&-\frac{1}{4\pi}\Big(\mathcal{S}\Phi\big(\mathbf{r}_0 - s\mathbf{\Omega}, \mathbf{\Omega}, t_0 - \frac{s}{v}\big) \\
&+ \mathcal{F}\Phi(\mathbf{r}_0 - s\mathbf{\Omega}, \mathbf{\Omega}, t_0 - \frac{s}{v}) + S(\mathbf{r}_0 - s\mathbf{\Omega}, \mathbf{\Omega}, t_0 - \frac{s}{v})\Big).
\end{aligned} \tag{3.174}$$

When $\mathbf{r}_0, \mathbf{\Omega}$ and t_0 are given, (3.174) is a first order ordinary differential equation, its solution is

$$\begin{aligned}&\Phi\Big(\mathbf{r}_0 - s\mathbf{\Omega}, \mathbf{\Omega}, t_0 - \frac{s}{v}\Big) = \\ &\Phi(\mathbf{r}_0, \mathbf{\Omega}, t_0)e^{s\Sigma_t}\frac{1}{4\pi}\int_0^s -\frac{1}{4\pi}\Big(\mathcal{S}\Phi(\mathbf{r}_0 - s'\mathbf{\Omega}, \mathbf{\Omega}, t_0 - \frac{s'}{v}) \\ &+ \mathcal{F}\Phi\big(\mathbf{r}_0 - s'\mathbf{\Omega}, \mathbf{\Omega}, t_0 - \frac{s'}{v}\big) + S(\mathbf{r}_0 - s'\mathbf{\Omega}, \mathbf{\Omega}, t_0 - \frac{s'}{v})\Big)ds'.\end{aligned} \tag{3.175}$$

Equation (3.175) has the following physical meaning. The neutrons at point $\mathbf{r} \in V$ can be decomposed according to the place of the last collision. With regard to the free flight of neutrons between collisions, the place of the collision must be along the straight line starting from $\mathbf{r}$ and parallel to $\mathbf{\Omega}$.

Now we reverse the above reasoning. Consider the neutrons at position $\mathbf{r} \in V$, their last collision must happen at $\mathbf{r} - s\mathbf{\Omega}$ for $0 < s \leq s_0$ where s_0 is the distance between point $\mathbf{r}$ and the closest boundary point in the direction $\mathbf{\Omega}$. The probability that no collision occurs between $\mathbf{r} - s\mathbf{\Omega}$ and $\mathbf{r}$ is given by

$$e^{-\Sigma_{opt}(s',s)} = \exp - \int_0^s \Sigma_t(\mathbf{r} - (s - s')\mathbf{\Omega})ds, \tag{3.176}$$

where the exponent $\Sigma_{opt}(s)$ in (3.176) is called the optical thickness length. Thus the flux at $\mathbf{r}$ is

$$\Phi(\boldsymbol{\omega}, t) = \int_0^{s_0} \exp -\Sigma_{opt}(s', s)Q\big(\mathbf{r} - s\mathbf{\Omega}, E, \mathbf{\Omega}, t - \frac{s' - s}{v}\big)ds', \tag{3.177}$$

where Q is the source term:

$$Q(\mathbf{r}', E, t) = \mathcal{S}(\mathbf{r}', E, \mathbf{\Omega}, t) + (\mathcal{S}(\mathbf{r}', E, \mathbf{\Omega}, t) + \mathcal{F}(\mathbf{r}', E, \mathbf{\Omega}, t))\Phi. \tag{3.178}$$

Note that the scattering and fission operators contain an integration over the energy, thus the source term at energy E may contain a contribution from $E' \neq E$.

The integral form (3.177) of the transport equation also needs an initial condition and a boundary condition along ∂V.

3.6.2. Adjoint transport equation

Consider the reaction rate or detector current in a subcritical volume V in which an external source $Q(\boldsymbol{\omega})$ maintains the stationary neutron field. In V, we calculate the reaction rate R as an integral over the phase space:

$$R = \int \Sigma_d(\boldsymbol{\omega})\Psi(\boldsymbol{\omega})d\boldsymbol{\omega}. \tag{3.179}$$

Only those phase space points contribute to R where the detector cross-section Σ_d differs from zero. The flux $\Psi(\boldsymbol{\omega})$ obeys the transport equation:

$$\mathcal{T}\Psi(\boldsymbol{\omega}) = Q(\boldsymbol{\omega}), \tag{3.180}$$

and because the transport operator is linear, we know that the angular flux is linear also in the source term in the following sense:

$$\mathcal{T}(c_1\Psi_1(\boldsymbol{\omega}) + c_2\Psi_2(\boldsymbol{\omega}) = c_1Q_1(\boldsymbol{\omega}) + c_2Q_2(\boldsymbol{\omega}) \tag{3.181}$$

provided

$$\mathcal{T}\Psi_i(\boldsymbol{\omega}) = Q_i(\boldsymbol{\omega}), \quad i = 1, 2. \tag{3.182}$$

But then R, which is linear in the angular flux, also must be linear in Q and can be expressed as

$$R = \int w(\boldsymbol{\omega})Q(\boldsymbol{\omega})d\boldsymbol{\omega}. \tag{3.183}$$

In (3.183) $w(\boldsymbol{\omega})$ is the contribution to reaction rate R of a single neutron emitted from the source at $\boldsymbol{\omega}$. When we select another detector, we need a new $w(\boldsymbol{\omega})$ function. Thus it is reasonable to name $w(\boldsymbol{\omega})$ importance as it gives the contribution of a neutron emitted from the source.

A new born neutron makes no immediate contribution to the reaction rate, rather it flies, collides, and its contribution to R is made by its progenies. In order to shorten the discussion, we resort to some mathematical tools. The integral in the reaction rate is a kind of scalar product of two functions: $\Sigma_d(\boldsymbol{\omega})$ and $\Psi(\boldsymbol{\omega})$. The natures of the two terms in the scalar product are different, to emphasize that, we choose the possible detector cross-sections from a different function space that we call adjoint, and introduce the following notation for the scalar product:

$$R = (\Sigma(\boldsymbol{\omega}), \Psi(\boldsymbol{\omega})). \tag{3.184}$$

The sequence of the two components in the scalar product is fixed, the first one is the adjoint, the second one is the flux. The introduced notation makes it easy to introduce formal operations acting on the adjoint functions. The formal rule is

$$(\Sigma(\boldsymbol{\omega}), \mathcal{T}\Psi(\boldsymbol{\omega})) = (\mathcal{T}^+\Sigma(\boldsymbol{\omega}), \Psi). \tag{3.185}$$

Later we specify how to determine $\mathcal{T}^+$ that we call the adjoint operator to $\mathcal{T}$.

Now we have

$$R = (w(\boldsymbol{\omega}), Q(\boldsymbol{\omega})) = (w(\boldsymbol{\omega}), \mathcal{T}\Phi(\boldsymbol{\omega})) = (\mathcal{T}^+w(\boldsymbol{\omega}), \Phi(\boldsymbol{\omega})) = (\Sigma_d(\boldsymbol{\omega}), \Phi(\boldsymbol{\omega})),$$

therefore the newly introduced $w(\boldsymbol{\omega})$ satisfies the equation

$$\mathcal{T}^+w(\boldsymbol{\omega}) = \Sigma(\boldsymbol{\omega}). \tag{3.186}$$

Determine the adjoint of a few operators. The adjoint of the leakage operator is:

$$\mathcal{L}^+\Phi^+(\boldsymbol{\omega}) = -\boldsymbol{\Omega}\boldsymbol{\nabla}\Phi^+(\boldsymbol{\omega}), \tag{3.187}$$

of the removal operator:

$$\mathcal{R}\Phi^+(\boldsymbol{\omega}) = \Sigma_t(\boldsymbol{\omega})\Phi^+(\boldsymbol{\omega}), \tag{3.188}$$

of the fission operator:

$$\mathcal{F}\Phi^+(\boldsymbol{\omega}) = \int d\boldsymbol{\Omega}' \int dE' \Phi^+(\mathbf{r}, E', \boldsymbol{\Omega}')\nu\Sigma_f(\mathbf{r}, E, \boldsymbol{\Omega} \to \boldsymbol{\Omega}')\chi(\mathbf{r}, E \to E') \tag{3.189}$$

of the scattering operator

$$\mathcal{S}\Phi^+(\boldsymbol{\omega}) = \int d\boldsymbol{\Omega}' dE' \Phi(\mathbf{r}, E', \boldsymbol{\Omega}')\Sigma_s(\mathbf{r}, E \to E', \boldsymbol{\Omega} \to \boldsymbol{\Omega}'). \tag{3.190}$$

Note that the integration in $\mathcal{F}^+, \mathcal{S}^+$ goes the opposite way as in the transport equation. Note that the leakage term has opposite sign and finally the removal operator is self adjoint.

The boundary conditions to be applied for the adjoint flux are obtained from the definition of the adjoint flux and the leakage operator $\mathcal{L}$:

$$(\Phi^+, \mathcal{L}\Phi) = (\mathcal{L}^+\Phi^+, \Phi),$$

after rearranging we get

$$(\Phi^+, \mathcal{L}\Phi) - (\mathcal{L}^+\Phi^+, \Phi) = 0, \tag{3.191}$$

in details, using the derivation rules and partial integration we get

$$\int_V \Phi^+(\boldsymbol{\omega})\mathcal{L}\Phi(\boldsymbol{\omega})d^3\mathbf{r} = -\int_V \Phi(\boldsymbol{\omega})[\boldsymbol{\Omega}\boldsymbol{\nabla}]\Phi^+(\boldsymbol{\omega}) + \int_{\partial V} \Phi(\boldsymbol{\omega})[\boldsymbol{\Omega}\mathbf{n}]\Phi(\boldsymbol{\omega})\Phi^+(\boldsymbol{\omega})d\boldsymbol{\omega}, \tag{3.192}$$

and now immediately follows that

$$(\Phi^+, \mathcal{T}\Phi) - (\mathcal{T}^+\Phi^+, \Phi) = \int_{\partial V} \Phi(\boldsymbol{\omega})[\boldsymbol{\Omega}\mathbf{n}]\Phi(\boldsymbol{\omega})\Phi^+(\boldsymbol{\omega})d\boldsymbol{\omega} \tag{3.193}$$

We decompose the surface integral into two integrals, the first one, over $\boldsymbol{\omega}^+$ involving $\boldsymbol{\Omega}\mathbf{n} > 0$ directions, goes over the exiting $\boldsymbol{\Omega}$ directions, the other, $\boldsymbol{\omega}^-$ involving $\boldsymbol{\Omega}\mathbf{n} < 0$ directions,, for the entering directions, and the space variable is confined to the boundary in either integral. The resulting expression takes the form

$$\int_{\partial V} \Phi(\boldsymbol{\omega})[\boldsymbol{\Omega}\mathbf{n}]\Phi(\boldsymbol{\omega})\Phi^+(\boldsymbol{\omega})d\boldsymbol{\omega} = \int_{\boldsymbol{\omega}^+} \Phi(\boldsymbol{\omega})[\boldsymbol{\Omega}\mathbf{n}]\Phi(\boldsymbol{\omega})d\boldsymbol{\omega} - \int_{\boldsymbol{\omega}_-} \Phi(\boldsymbol{\omega})|\boldsymbol{\Omega}\mathbf{n}|\Phi^+(\boldsymbol{\omega})d\boldsymbol{\omega}, \tag{3.194}$$

where $d\boldsymbol{\omega} = dEd\boldsymbol{\Omega}dS$. Here dS is an infinitesimal element of the boundary ∂V.

We are seeking the boundary condition to be applied to the adjoint flux on the boundary provided we know the boundary condition to be applied to the flux in the last term of (3.194). We define the adjoint boundary condition Γ^+ by requiring the following relationship to hold for any Φ and Φ^+:

$$\int_{\boldsymbol{\omega}^-} \Phi^+(\boldsymbol{\omega})\Gamma\Phi(\boldsymbol{\omega})|\boldsymbol{\Omega}\mathbf{n}|d\boldsymbol{\omega} = \int_{\boldsymbol{\omega}^+} \left(\Gamma^+\Phi^+(\boldsymbol{\omega})\right)\Phi(\boldsymbol{\omega})(\boldsymbol{\Omega}\mathbf{n})d\boldsymbol{\omega} \tag{3.195}$$

and (3.191) is met when

$$\Phi^+(\boldsymbol{\omega}^+) = \Gamma^+\Phi^+(\boldsymbol{\omega}^-). \tag{3.196}$$

The boundary condition for the adjoint flux gives the angular flux for the exiting directions in terms of the angular flux for the entering directions. The relation is linear, the matrix Γ^+ is the adjoint to Γ, the matrix in the boundary condition for the flux. The adjoint means that the energy group indices in matrix Γ should be changed compared to the original matrix.

The usual boundary conditions for the adjoint operator are:

- for the white boundary condition: $J_n^+(\mathbf{r}, E) = 0$;
- for the black boundary condition: $\Phi^+(\mathbf{r}_s, E, \boldsymbol{\Omega}) = 0$ for $\boldsymbol{\Omega}\mathbf{n}_s < 0$, just for the entering directions;
- albedo: $J^-(E') = \sum \Gamma(E' \to E)J^+(E)$;
- the given entering current is replaced by the given exiting current.

We explain the physical meaning of the adjoint through the following example. Let appear a neutron at phase space point $\mathbf{r}_0, E_0, \mathbf{\Omega}_0$. Then the flux in the new situation is

$$\Phi'(\boldsymbol{\omega}) = \Phi(\boldsymbol{\omega}) + \delta(E - E_0)\delta(\mathbf{r} - \mathbf{r}_0)\delta(\mathbf{\Omega}\mathbf{\Omega}_0), \tag{3.197}$$

but the new neutron distribution varies with time. Using the expansion in terms of the eigenfunctions of the transport operator, and observing that all the higher modes die out after long time, we find that a new static equilibrium establishes with the flux

$$\Phi'(\boldsymbol{\omega}) = (1 + c_0)\Phi(\boldsymbol{\omega}) \tag{3.198}$$

where we get c_0 by expanding the perturbation in (3.197) in terms of the eigenfunctions of the adjoint transport operator, and c_0 is the coefficient of the fundamental solution. Therefore

$$c_0 = (\Phi^+(\boldsymbol{\omega}), \delta(E - E_0)\delta(\mathbf{r} - \mathbf{r}_0)\delta(\mathbf{\Omega}\mathbf{\Omega}_0)) = \Phi^+(E_0, \mathbf{r}_0, \mathbf{\Omega}_0). \tag{3.199}$$

We got that injecting a single neutron, the establishing static distribution will be proportional to the fundamental solution, the increase of the amplitude is proportional to the adjoint at the phase space point at which the neutron has been injected.

With the help of the worth function, a given reaction rate can be estimated immediately from the source. Since the neutrons exiting from the source interact with the detector mostly through their progenies, the worth of a neutron should be equal to the total amount of worth of its progenies. This allows for deriving a simple equation for the neutron worth.

Let the source emit $Q(\mathbf{r})$ neutrons per second, the neutron not entering into interaction will be at $\mathbf{r} + v\mathbf{\Omega}dt$ after dt time, but their uncollided fraction $(1 - vdt\Sigma_t)$ reaches $\mathbf{r} + v\mathbf{\Omega}dt$ so the total worth of the uncollided neutrons is

$$Q(q - vdt\mathbf{\Omega})\Psi^+(\mathbf{r} + vdt\mathbf{\Omega}, v, \mathbf{\Omega}, t + dt). \tag{3.200}$$

From among the neutrons suffering a collision, the number of scattering interaction is $Qvdt\Sigma_s(v)$ and the scattering will result in appearing

$$Qvdt\Sigma_s(v)g(v \to v', \mathbf{\Omega} \to \mathbf{\Omega}') \tag{3.201}$$

neutrons in the infinitesimal volume $dv'd\mathbf{\Omega}'$ around $(\mathbf{r}, v', \mathbf{\Omega}')$. The number of neutrons entering into fission reaction is $Qvdt\Sigma_f(v)$ and the neutrons emerging from the fission are assumed to be isotropically distributed, their energy distribution is $f(v')$ and the number of secondaries, $\nu(v)$, depends on the neutron energy.

The sum of the worth of the progenies equals the worth of the neutrons emitted from the fission thus

$$\begin{aligned}
&Q\Phi^+(\mathbf{r}, v, \mathbf{\Omega}, t) = \\
&Qvdtp(\mathbf{r}, v, \mathbf{\Omega}, t) + Q(1 - vdt\Sigma_t)\Phi^+(\mathbf{r} + vdt\mathbf{\Omega}, v, \mathbf{\Omega}, t + dt) \\
&+ Qvdt\int_0^\infty \int_{4\pi} \Sigma_s(v)g(v' \to v, \mathbf{\Omega} \to \mathbf{\Omega}')\Phi^+(\mathbf{r} + vdt\mathbf{\Omega}, v', \mathbf{\Omega}', t + dt)d\mathbf{\Omega}'dv' \\
&+ Qvdt\frac{\nu(v)}{4\pi}\Sigma_f(v)\int_0^\infty \int_{4\pi} f(v')\Phi^+(\mathbf{r} + vdt\mathbf{\Omega}, v', \mathbf{\Omega}', t + dt)d\mathbf{\Omega}'dv'.
\end{aligned} \tag{3.202}$$

We immediately obtain from this the following differential equation for the worth Φ^+:

$$\begin{aligned}
&-\frac{1}{v}\frac{\partial\Phi^+(\mathbf{r}, v, \mathbf{\Omega}, t)}{\partial t} = \mathbf{\Omega}\boldsymbol{\nabla}\Phi^+(\mathbf{r}, v, \mathbf{\Omega}, t) + \Sigma_t(v)\Phi^+(\mathbf{r}, v, \mathbf{\Omega}, t) \\
&+ \Sigma_s(v)\int_0^\infty \int_{4\pi} g(v')\Phi^+(\mathbf{r}, v', \mathbf{\Omega}', t)d\mathbf{\Omega}'dv' \\
&+ \frac{\nu(v)}{4\pi}\Sigma_f(v)\int_0^\infty f(v')\Phi^+(\mathbf{r}, v', \mathbf{\Omega}', t)d\mathbf{\Omega}'dv' + p(\mathbf{r}, v, \mathbf{\Omega}, t).
\end{aligned} \tag{3.203}$$

Here $p(\mathbf{r}, v, \mathbf{\Omega}, t)$ is the contribution of a neutron emitted from the source with parameters $(\mathbf{r}, v, \mathbf{\Omega}, t)$ to the reaction rate R.

Perturbation theory

When we wish to know the flux distribution, we have to solve a form of the transport equation. When some parameter slightly changes, it is not economic to solve the transport equation again. This is the case when we are interested in the consequence of the small scale change in the material parameters or control variables. The present Subsection deals with the analysis of small changes in the core structure.

The first kind of problems adhere to the reactor state, the operational state of the reactor is always critical but there are continual disturbances caused by the automatic control rod motion, the fluctuations in the coolant flow, or local temperature fluctuations. When we measure the flux in an experimental reactor, the detector material perturbs the flux, when there are air gaps between the fuel pellets, their effect is also treated as a perturbation. If we know the perturbation of the flux, we may identify the cause of the perturbation, hence we encounter perturbations also in diagnostics.

Let us consider the transport equation (3.136), and decompose the transport operator as

$$\mathcal{T} = \mathcal{P} - \mathcal{D} \tag{3.204}$$

where $\mathcal{P}$ is the fission (production) operator, $\mathcal{D}$ is the destruction operator

$$\mathcal{D} = \mathcal{L} + \mathcal{R} \tag{3.205}$$

where $\mathcal{L}$ is the leakage, $\mathcal{R}$ is the removal operator. We investigate the general neutron balance

$$\frac{\partial \Phi(\boldsymbol{\omega}, t)}{\partial t} = (\mathcal{F} - \mathcal{D})\Phi(\boldsymbol{\omega}, t) + Q(\boldsymbol{\omega}, t) \tag{3.206}$$

in its general form. In a static problem the left hand side is zero. Now when the core is perturbed, $\mathcal{F}$, $\mathcal{D}$, and S may change. As a consequence, the solution also changes. In the perturbed case we have

$$0 = (\mathcal{F} + \delta\mathcal{F} - (\mathcal{D} + \delta\mathcal{D}))(\Phi(\boldsymbol{\omega}, t) + \delta\phi) + Q(\boldsymbol{\omega}, t) + \delta Q. \tag{3.207}$$

There are two kinds of perturbation problems: the first kind: we know the changes in the operators and wish to find the change in the flux. The second kind: we know the change of the flux, and find out what may be the change of the operators.

In a perturbation of the first kind, the transport operator becomes $\mathcal{T} + \delta\mathcal{T}$ the flux changes to $\Phi + \delta\Phi$ the flux before perturbation satisfies (3.206) with time derivative equal to zero, and we keep only first order variations in the balance equation:

$$(\mathcal{P} - \mathcal{D})\delta\phi = (\delta\mathcal{D} - \delta\mathcal{P})\Phi. \tag{3.208}$$

In accordance with the Fredholm alternative theorem, that equation is solvable, when the source on the right hand side is orthogonal to the solution of the homogeneous equation

$$(\mathcal{P}^+ - \mathcal{D}^+)\phi^+ = 0, \tag{3.209}$$

and the imposed orthogonality is expressed with the scalar product as

$$(\phi^+, (\delta\mathcal{D} - \delta\mathcal{P})\phi) = 0, \tag{3.210}$$

which is a restriction on the applied perturbations when the adjoint equation has non-trivial solution. In a subcritical volume $\phi^+ \equiv 0$, thus the solvability condition is always fulfilled.

Note that the source term depends only on the solution in the unperturbed state and the perturbation of the cross-sections. On the left hand side of (3.208), we find the operators of the unperturbed state. If the Green's function of the operators on the left hand side is known, the solution can be expressed as an integral.

The second kind of perturbation occurs when a source appears. This happens if a control rod starts vibrating, or bubbles appear in a zone of the reactor. Then the new, perturbed situation is characterized by the change of the source:

$$Q = Q_0 + \delta Q. \tag{3.211}$$

Since the transport equation and its approximations are linear when feedback can be neglected, the solution will be the sum

$$\Phi = \Phi_0 + \delta\Phi, \tag{3.212}$$

where

$$\mathcal{T}\Phi = Q_0; \;\; \mathcal{T}\delta\Phi = \delta Q. \tag{3.213}$$

From that we immediately see, the ratio

$$\frac{\delta\Phi}{\Phi_0} = \frac{\delta Q}{Q_0},$$

offering an immediate estimation for the magnitude of the source perturbation.

When the cross-section changes in V, the k_{eff} also may change. We start out from the neutron balance:

$$(\mathcal{L} + \mathcal{R})\Phi = \frac{1}{k_{eff}}\mathcal{P}\Phi + \mathcal{Q}. \tag{3.214}$$

From (3.214), we get the eigenvalue k_{eff} which is required for stationary solution to exist when $Q = 0$:

$$k_{eff} = \frac{(\Phi^+, \mathcal{F}\Phi)}{(\Phi^+, (\mathcal{L} + \mathcal{R})\Phi)}, \tag{3.215}$$

and the reactivity

$$\rho = 1 - \frac{1}{k_{eff}} = \frac{(\Phi^+, \mathcal{T}\Phi)}{(\Phi^+, \mathcal{F}\Phi)}. \tag{3.216}$$

Before continuing the analysis of perturbations, we remark that (3.206) is a local neutron balance hence valid at every point of the phase space. When multiplied by any reasonable function, the resulting equation will also be valid. This fact is extensively exploited in reactor physics. When multiplied by the weight function $w^+ \equiv 1$, we get an integrated balance:

$$\frac{\partial(w^+, \Phi(\boldsymbol{\omega}, t))}{\partial t} = (w^+, (\mathcal{P} - \mathcal{D})\Phi(\boldsymbol{\omega}, t)) + (w^+, Q(\boldsymbol{\omega}, t)). \tag{3.217}$$

Furthermore, appropriate choice of the weight function helps investigate a reaction rate type that may be of distinguished importance in a given problem. Therefore below we retain in the scalar product the notation w^+ to retain generality.

A perturbation makes the following changes in the operators:

$$\mathcal{L} \to \mathcal{L} + \delta\mathcal{L}; \;\; \mathcal{R} \to \mathcal{R} + \delta\mathcal{R}; \;\; \mathcal{F} \to \mathcal{F} + \delta\mathcal{F}; \;\; \mathcal{S} \to \mathcal{S} + \delta\mathcal{S}. \tag{3.218}$$

In the perturbed state the new eigenvalue is $k_{eff} \to k_{eff} + \delta k_{eff}$ and the neutron balance equation in the perturbed state is

$$\begin{aligned} &[(\mathcal{L}+\mathcal{R}) + (\delta\mathcal{L}+\delta\mathcal{R})]\,(\Phi+\delta\Phi) = \\ &\frac{1}{[k_{eff}+\delta k_{eff}]}\,[\mathcal{F}+\delta\mathcal{F}]\,(\Phi+\delta\Phi), \end{aligned} \tag{3.219}$$

in which the second order terms have been neglected. Before proceeding, we investigate the consequence of an error in the eigenvalue. The stationary state is

$$\mathcal{T}(p)\Phi(p) = \tau(p)\Phi(p),$$

where $p = \alpha$ or $p = k_{eff}$ depending on the eigenvalue problem under consideration, and p is chosen so that

$$\tau(p) \approx 0.$$

When $\tau(p) \neq 0$, the solution will depend on time:

$$\Phi(t) = ce^{\tau(p)vt},$$

where v is a typical neutron speed, $v \approx 10^5 \;\; cm/s$. In other words, when the error of the eigenvalue is of the order 10^{-5}, the flux grows by a factor of e in every second. Thus the perturbations should be calculated as precisely as possible. That question is the subject of the next Subsection.

One is tempted to estimate the reactivity perturbation from (3.216) by subtracting the reactivity of the unperturbed state from the reactivity of the perturbed state:

$$\delta\rho = \frac{(w^+, (\mathcal{T}+\delta\mathcal{T})(w^+, \delta\Phi))}{(w^+, (\mathcal{F}+\delta\mathcal{F})\Phi)} - \frac{(w^+, \mathcal{T}\Phi)}{(w^+, \mathcal{F}\Phi)}. \tag{3.220}$$

This direct way of calculation is the every day praxis in power plants so that w^+ is a chosen weight function, often $w^+(\boldsymbol{\omega}) = 1$ is chosen. That approach has two drawbacks. First, it requires two core calculations: one for the unperturbed, one for the perturbed core. The second drawback is more important, in a practical calculation the accuracy of any result is limited by the convergence limit, the applied numerical approximations, the approximate models. An advantage of applying the adjoint Φ^+ as the weight w^+ in (3.220) is that the result is stationary with respect to the first order variations of the neutron flux. To see that [152], we note that

$$\delta\rho = \delta\frac{1}{k_{eff}},$$

therefore when Φ changes to $\Phi + \delta\Phi$ the change in the reactivity is

$$\begin{aligned} \delta\rho &= \frac{(\Phi^+, \mathcal{D}(\Phi+\delta\Phi))}{(\Phi^+, \mathcal{F}(\Phi+\delta\Phi))} - \frac{(\Phi^+, \mathcal{D}\Phi)}{(\Phi^+, \mathcal{F}\Phi)} \\ &\approx \frac{(\Phi^+, \mathcal{D}\Phi)}{(\Phi^+, \mathcal{F}\Phi)} - \frac{(\Phi^+, \mathcal{D}\Phi)}{(\Phi^+, \mathcal{F}\Phi)}(\Phi^+, \mathcal{F}\delta\Phi) \\ &= \frac{\left(\Phi^+, \left[\mathcal{D} - \frac{1}{k_{eff}}\mathcal{F}\right]\delta\Phi\right)}{(\Phi^+, \mathcal{F}\Phi)} \\ &= \frac{\left(\left[\mathcal{D} - \frac{1}{k_{eff}}\mathcal{F}\right]^+\Phi^+, \delta\Phi\right)}{(\Phi^+, \mathcal{F}\Phi)} = 0. \end{aligned} \tag{3.221}$$

In the first transformation we exploited that

$$\frac{(\Phi^+, \mathcal{D}(\Phi + \delta\Phi))}{(\Phi^+, \mathcal{F}(\Phi + \delta\Phi))} = \frac{(\Phi^+, \mathcal{D}\Phi) + (\Phi^+, \mathcal{D}\delta\Phi)}{(\Phi^+, \mathcal{F}(\Phi)) + (\Phi^+, \mathcal{F}\delta\Phi)}$$

and in the denominator

$$(\Phi^+, \mathcal{F}(\Phi)) >> (\Phi^+, \mathcal{F}\delta\Phi)$$

therefore the following approximation is applicable:

$$\frac{A}{B + \delta B} \simeq A(B - \delta B), \tag{3.222}$$

and the error of the approximation is $O([\delta B]^2)$. The perturbation of ρ is symmetric in[6] Φ and Φ^+, thus the above considerations are also valid for the adjoint and the error of determining the reactivity by

$$\rho = \frac{(\Phi^+, \mathcal{T}\Phi)}{(\Phi^+, \mathcal{F}\Phi)} \tag{3.223}$$

is proportional to $\delta\Phi^+\delta\Phi$, thus is of second order. As to the perturbation of k_{eff}, the following expression is correct to first order:

$$\delta\left(\frac{1}{k_{eff}}\right) = -\frac{\left(\Phi^+, \left[\frac{1}{k_{eff}}\delta\mathcal{F} - \delta\mathcal{D}\right]\Phi\right)}{(\Phi^+, \mathcal{F}\Phi)}. \tag{3.224}$$

As we see, in (3.223) and (3.224) we need only the perturbations of the involved operator, and the flux and adjoint flux in the unperturbed state.

Perturbation theory is often used in reactor physics. In Chapter 7 we discuss the time dependent perturbation theory and apply perturbation theory to time dependent problems. The operators involved in the discussed formulas may be applied in various approximate models. Thus in Chapter 6, applications in diffusion theory are given.

3.6.3. Formal inverse

Consider the stationary transport operator that we obtain from (3.155) by substituting $\partial\Phi\partial t = 0$:

$$\mathcal{T}\Phi = Q \tag{3.225}$$

or

$$\Phi = \mathcal{T}^{-1}Q. \tag{3.226}$$

The inverse operator in (3.226) is readily available. Let us solve the equation

$$\mathcal{T}\mathcal{G}(\boldsymbol{\omega}, \boldsymbol{\omega}_0) = \delta(\boldsymbol{\omega}_0) \tag{3.227}$$

to obtain the Green's function $\mathcal{G}$. We multiply equation (3.227) by $Q(\boldsymbol{\omega}_0$ and integrate over $\boldsymbol{\omega}_0$, we get

$$\mathcal{T}\int_{\boldsymbol{\omega}_0} \mathcal{G}(\boldsymbol{\omega}, \boldsymbol{\omega}_0)Q(\boldsymbol{\omega}_0)d\boldsymbol{\omega}_0 = Q(\boldsymbol{\omega}). \tag{3.228}$$

Comparing (3.228) with (3.225), we immediately find

$$\Phi(\boldsymbol{\omega}) = \int_{\boldsymbol{\omega}_0} \mathcal{G}(\boldsymbol{\omega}, \boldsymbol{\omega}_0)Q(\boldsymbol{\omega}_0)d\boldsymbol{\omega}_0. \tag{3.229}$$

Thus the integral in (3.229) is the formal inverse of operator $\mathcal{T}$. We derive the boundary condition associated with (3.227) from the adjoint equations, see the first part of the present subsection.

[6] Confer the next Subsection.

3.6.4. Variational formulation

Several phenomena in physics can be explained by extremum principles. The best known such principles are that physical processes drive a physical system towards the energy minimum and the entropy maximum. In classical mechanics, the principle of least action is a widely used formulation of the law of motion.

The mathematical formulation of variation is an extremum of a definite integral depending on a function

$$F[q] = \int_a^b L(q(t))dt, \tag{3.230}$$

where function $q(t)$ should be chosen so that $F[q]$ is minimal. In a more general formulation, the integrand L may depend not only on $q(t)$ but also on its derivatives $q'(t), q''(t), \ldots$. To measure the sensitivity of $F[q]$ on q, we may use

$$\delta F[q,h] = \lim_{\varepsilon \to 0} \frac{F[q+\varepsilon h] - F[q]}{\varepsilon}, \tag{3.231}$$

which is called the first variation of functional F. When $\delta F[\bar{q},h] = 0$ for all h we say that $F[q]$ is stationary at $\bar{q}$.

When $F[q]$ depends on q and q', a case typical in classical mechanics, the expression

$$F[q] = \int_a^b L(q(t), \dot{q}(t))dt, \tag{3.232}$$

the stationary condition imposes a first order differential equation, the Euler-Lagrange equation on $q(x)$:

$$\frac{\partial L}{\partial q} - \frac{d}{dt}\left(\frac{\partial L}{\partial \dot{q}}\right) = 0. \tag{3.233}$$

Note, that here the derivative $\dot{q}$ is regarded as a function independent of q. It is tempting to render an extremum to a given Euler-Lagrange equation because then instead of solving a differential equation we have to find the minimum of an integral, which is a well studied problem. This idea has led to a number of applications in numerical mathematics.

It is possible to find a variational problem corresponding to a given Euler equation by using the so called functional derivative, i.e. a derivative of functional F with respect to q:

$$\frac{\delta F}{\delta q} \equiv \lim_{\varepsilon \to 0} \frac{F[q+\varepsilon h] - F[q]}{\varepsilon}. \tag{3.234}$$

The name is appropriate as can be see from the following example. Let

$$F[q] = \int g(t)q(t)dt \tag{3.235}$$

then

$$\frac{\delta F}{\delta q} = g(t). \tag{3.236}$$

Further details are available for example in Ref. [153]. We give a short list of variational problems used in transport theory [59][p. 388]. Eigenvalue problems are the Euler-Lagrange equation of the variational problem, viz. the variational problem of self-adjoint operator $\mathcal{L}$

$$F[\Psi] = \frac{(\Psi, \mathcal{L}\Psi)}{(\Psi, \Psi)} \tag{3.237}$$

has the Euler-Lagrange equation

$$\mathcal{L}\Psi = \lambda\Psi; \mathcal{L} = \mathcal{L}^+. \tag{3.238}$$

This variational property of the eigenvalue is called Ritz principle. When $\mathcal{L}$ is not self adjoint, we get two Euler-Lagrange equations:

$$\mathcal{L}\Psi = \lambda\Psi \tag{3.239}$$
$$\mathcal{L}^+\Psi^+ = \lambda^+\Psi^+, \tag{3.240}$$

where λ^+ is the complex conjugate of λ.

When $\mathcal{L}$ is self-adjoint, the non-homogeneous equation

$$\mathcal{L}\Psi = q \tag{3.241}$$

is the Euler-Lagrange equation of the functional

$$F[\Psi] = 2(\Psi, q) - (\Psi, \mathcal{L}\Psi). \tag{3.242}$$

Finally, we mention that the Euler-Lagrange equation of the variational problem

$$F[\Psi] = \int_a^b \left[p(t) \left(\frac{d\Psi}{dt} \right)^2 + q(t)[\Psi(t)]^2 + 2f(t)\Psi(t) \right] dt \tag{3.243}$$

is the Sturm-Liouville equation

$$-\frac{d}{dt}\left[p(t)\frac{d\Psi}{dt} \right] + q(t)\Psi(t) + f(t) = 0. \tag{3.244}$$

The variational principle will be used in the finite element method, in Chapter 8 and in the nodal methods.

3.7. Response matrices

When calculating the neutron distribution in a large core, one often has to solve the stationary transport equation (or one of its approximations) in a part of the core, which is obviously subcritical. Then the stationary solution is zero unless there is an entering current along the boundary. The problem is tractable when we use the Green's function to handle that problem: using the surface Green's function, the solution is given by (3.227). It is straightforward to determine either the angular flux or the scalar flux, or alternatively the entering or exiting currents on the boundary. All these quantities are expressed as linear functions of the angular flux at the boundary for the incoming directions. The structure of the solutions originates from the Green's function. In connection with the response matrices, we use the Green's function with the angular flux given for the entering directions. Then the scalar flux at the phase space point $\mathbf{r}, E$ due to a neutron entering the boundary at $\mathbf{r}'$ is given by

$$\Phi(\mathbf{r}', E' \to \mathbf{r}, E) = \int_{\mathbf{\Omega}'\mathbf{n}(\mathbf{r}')<0} \int_{4\pi} \mathcal{G}(\boldsymbol{\omega}' \to \boldsymbol{\omega})\Phi(\mathbf{r}', E', \mathbf{\Omega}')d\mathbf{\Omega}'d\mathbf{\Omega} \tag{3.245}$$

The Green's function is the contribution made by one neutron entering the boundary to the angular flux at the phase space point $\boldsymbol{\omega}$. As we have seen in (3.184), a reaction rate is a linear function of the angular flux. Hence the Green's function immediately leads to the

determination of the contribution from a neutron entering the boundary. Contribution to the reaction rate at energy E is

$$\Sigma(\mathbf{r}, E) \int_0^\infty \Phi(\mathbf{r}', E' \to \mathbf{r}, E) dE'; \quad \mathbf{r} \in V. \tag{3.246}$$

We are seeking relations between various quantities on the boundary caused by one neutron crossing the boundary, so we introduce the following notation:

$$\boldsymbol{\omega}_+ = (\mathbf{r}_b, E, \boldsymbol{\Omega}), \quad \mathbf{r}_b \in \partial V, \boldsymbol{\Omega} n(\mathbf{r}_b) > 0, \tag{3.247}$$

$$\boldsymbol{\omega}_- = (\mathbf{r}_b, E, \boldsymbol{\Omega}), \quad \mathbf{r}_b \in \partial V, \boldsymbol{\Omega} n(\mathbf{r}_b) < 0, \tag{3.248}$$

$$\boldsymbol{\omega}_b = (\mathbf{r}_b, E, \boldsymbol{\Omega}) \tag{3.249}$$

The angular fluxes for the entering and exiting directions are $\Phi(\boldsymbol{\omega}_-)$, and $\Phi(\boldsymbol{\omega}_+)$, respectively. The angular flux at a boundary point $\mathbf{r}_b$ is given by

$$\Phi(\mathbf{r}_b, E, \boldsymbol{\Omega}) \equiv \Phi(\boldsymbol{\omega}_b). \tag{3.250}$$

Using the formulas introduced above, we are able to express any reaction rate in V. First, let us write the terms in the local balance at $\mathbf{r} \in V$, an internal point. In the absorption rate $R_a(\mathbf{r}', E' \to \mathbf{r}, E)$ we use (3.246):

$$R_a(\mathbf{r}' \to \mathbf{r}, E) = \Sigma_a(\mathbf{r}, E) \Phi(\mathbf{r}', E' \to \mathbf{r}, E) \tag{3.251}$$

In the fission source the neutrons emerge with a fission spectrum of energies $f(E)$ and fissions at every energy E'' contribute to the neutron production, with the process taking place in two steps. In the first step the neutron entering the boundary at $\mathbf{r}'$ having energy E' goes to $\mathbf{r}$ and its energy may be arbitrary $0 \le E'' \le \infty$. That step is described by $\Phi(\mathbf{r}', E' \to \mathbf{r}, E)$. In the second step that neutron enters a fission reaction and the neutrons produced in the fission emerge with energy E.

$$R_f(\mathbf{r}', E' \to \mathbf{r}, E) = \frac{f(E)}{4\pi} \int_0^\infty \nu \Sigma_f(\mathbf{r}, E'') \Phi(\mathbf{r}', E' \to \mathbf{r}, E'') dE''. \tag{3.252}$$

Here we have assumed that the angular distribution of the fission source is isotropic.

Scattering plays two roles in the balance: the out-scattering at energy E contributes to removal by

$$R_s(\mathbf{r}', E' \to \mathbf{r}, E) = \Sigma_s(\mathbf{r}, E) \Phi(\mathbf{r}', E' \to \mathbf{r}, E) \tag{3.253}$$

where $\Sigma_s(\mathbf{r}, E)$ is obtained by integrating over the final energy of the scattering process, see (3.119). We introduce the contribution to removal as

$$R_r(\mathbf{r}', E' \to \mathbf{r}, E) = R_a(\mathbf{r}' \to \mathbf{r}, E) + R_s(\mathbf{r}', E' \to \mathbf{r}, E). \tag{3.254}$$

On the other hand, the scattered neutrons appear as a source $R_{ss}(\mathbf{r}', E' \to \mathbf{r}, E)$, a process that is analogous to fission, takes place in two steps. In the first step the neutron gets from the boundary to $\mathbf{r}$ at energy E'', and in the second step the neutron is scatted to energy E:

$$R_{ss}(\mathbf{r}, E, \boldsymbol{\Omega}) = \int_0^\infty \int_{4\pi} \Sigma_s(\mathbf{r}, E'', \boldsymbol{\Omega}'' \to E, \boldsymbol{\Omega}) \Phi(\mathbf{r}', E' \to \mathbf{r}, E'', \boldsymbol{\Omega}'') d\boldsymbol{\Omega}'' dE''. \tag{3.255}$$

Finally, the neutron balance at $\mathbf{r} \in V$ takes the following form:

$$\boldsymbol{\Omega} \boldsymbol{\nabla} \Phi(\mathbf{r}', E' \to \boldsymbol{\omega}) + \Sigma_t(\mathbf{r}, E) \Phi(\mathbf{r}', E' \to \boldsymbol{\omega}) = R_{ss}(\mathbf{r}', E' \to \boldsymbol{\omega}) + R_f(\mathbf{r}', E' \to \boldsymbol{\omega}). \tag{3.256}$$

Equation (3.256) has the following meaning. The neutrons at position $\mathbf{r}$ originate from a boundary point $\mathbf{r}'$. When we decompose the reaction rates according to the origin of the neutron, the neutron balance should hold. On the other hand, the balance at $\mathbf{r}, E$ involves integration over $\mathbf{r}'$ and E'.

The formalism we have obtained has a number of disadvantages. First of all, the reaction rates depend on the boundary angular flux as each term involves integrations over the boundary angular flux. To overcome that, we introduce well-defined model boundary fluxes and include the integration into the operator, with only partial the amplitudes of the basis functions appearing as multiplicative constants. Formally, we express $\Phi(\boldsymbol{\omega}_{b-})$ as given linearly independent functions along the boundary ∂V and express the angular flux at the boundary for the entering directions as

$$\Phi(\mathbf{r}_b, E, \mathbf{\Omega}) = \sum_j I_j \tilde{F}_j(\mathbf{r}_b, E, \mathbf{\Omega}); \;\; \mathbf{\Omega n} < 0 \tag{3.257}$$

where the $\tilde{F}_j$ functions are linearly independent. Then we get the reaction rate R_x as

$$R_x(\mathbf{r}, E, \mathbf{\Omega}) = \sum_j I_j \int_{\partial V} \int_0^\infty \int_{\mathbf{\Omega}' n(\mathbf{r}')<0} \mathcal{G}(\mathbf{r}', E', \mathbf{\Omega}' \to \mathbf{r}, E, \mathbf{\Omega}) \tilde{F}_j(\mathbf{r}', E', \mathbf{\Omega}') d\mathbf{\Omega}' dE' d\mathbf{r}', \tag{3.258}$$

indicating that any reaction rate is a linear: function of the amplitudes I_j. Thus we can precalculate the integral once $\tilde{F}_j$ and $\mathcal{G}$ are known. When the volume V under consideration is large, it is expedient to subdivide V into sub-volumes. Among the independent variables the space coordinate $\mathbf{r}$ has a distinguished role because at the joint boundary of two sub-volumes the angular flux must be continuous; see the Boundary Conditions Subsection in this Chapter. If it is possible to find functions $\tilde{F}_j$ such that the physical parameters determined on the boundaries such as scalar flux, entering current, exiting current, and net current retain their spatial forms on either side of the boundary, the calculations considerably simplify.

The rest of the present Subsection is devoted to finding functions $\tilde{F}_j$ that are advantageous as boundary conditions. The first step in our investigation is to decompose the boundary ∂V as

$$\partial V = \cup_{m=1}^{N_f} F_m \tag{3.259}$$

and we call F_m a face of the volume V. When V is a three-dimensional volume, F_m is a surface; when V is two-dimensional, F_m is just a line. For the sake of simplicity, we deal only with regular volumes the boundary of which are formed by N_f congruent faces. In three dimensions such a regular volume is a cube whose surface is six congruent squares. We have also to analyze less symmetric volumes such as a pile of square or regular hexagonal bases, but in such situations we confine the analysis to the regular but two-dimensional square or regular hexagonal base. The discussion below refers to two-dimensional V.

A coordinate-system is laid out in V so that the origin is placed at the symmetry center of V. Then any point P on the boundary ∂V is uniquely labeled by the angle α between the x axis and the line segment connecting the origin and P and $0 \le \alpha \le 2\pi$. Points on the N_f faces are labeled by segments $2\pi/N_f(m-1) \le \alpha \le 2\pi/N_f m$. Any function along the boundary can be given as $f_m(\alpha), m = 1, \ldots, N_f$, with $2\pi/N_f(m-1) \le \alpha \le 2\pi/N_f m$. This picture can be used also in the case of Wigner-Seitz cells of a lattice. When we investigate the neutron distribution in an extended volume the variation of material properties over a sub-volume is small. This enables us to deal with symmetric sub-volumes, so we investigate the boundary conditions in a symmetric sub-volume that we denote by V. Furthermore, if the sub-volume is small, it suffices to prescribe the incoming neutron flux at one point per

face, say at the face centers. Then the boundary condition is equivalent to four or six values when the sub-volume is a square, or a hexagon, respectively. Consider a square shaped sub-volume. Let the four values be given in the following four-tuple

$$\underline{\varphi}(E,\mathbf{\Omega}) \equiv \begin{pmatrix} \varphi_1(E,\mathbf{\Omega}) \\ \varphi_2(E,\mathbf{\Omega}) \\ \varphi_3(E,\mathbf{\Omega}) \\ \varphi_4(E,\mathbf{\Omega}) \end{pmatrix}, \tag{3.260}$$

and introduce the following basis vectors

$$\underline{e}_1 = \begin{pmatrix} 1 \\ 1 \\ 1 \\ 1 \end{pmatrix}, \quad \underline{e}_2 = \begin{pmatrix} 1 \\ 0 \\ -1 \\ 1 \end{pmatrix}, \quad \underline{e}_3 = \begin{pmatrix} 0 \\ 1 \\ 0 \\ -1 \end{pmatrix}, \quad \underline{e}_4 = \begin{pmatrix} 1 \\ -1 \\ 1 \\ -1 \end{pmatrix}. \tag{3.261}$$

Using the notation just introduced,

$$\underline{\varphi}(E,\mathbf{\Omega}) = A_1(E,\mathbf{\Omega})\underline{e}_1 + A_2(E,\mathbf{\Omega})\underline{e}_2 + A_3(E,\mathbf{\Omega})\underline{e}_3 + A_4(E,\mathbf{\Omega})\underline{e}_4 \tag{3.262}$$

where

$$A_1 = \frac{1}{4}\sum_{j=1}^{4}\varphi_j(\mathbf{r},E,\mathbf{\Omega}) \tag{3.263}$$

$$A_2 = \frac{1}{2}(\varphi_1(\mathbf{r},E,\mathbf{\Omega}) - \varphi_3(\mathbf{r},E,\mathbf{\Omega})) \tag{3.264}$$

$$A_3 = \frac{1}{2}(\varphi_2(\mathbf{r},E,\mathbf{\Omega}) - \varphi_4(\mathbf{r},E,\mathbf{\Omega})) \tag{3.265}$$

$$A_4 = \frac{1}{4}\sum_{j=1}^{4}\varphi_j(\mathbf{r},E,\mathbf{\Omega})(-1)^{j-1}. \tag{3.266}$$

We number the faces of the sub-volume starting from the face with normal parallel with the $+x$ axes, the numbering being counter clock-wise. The first terms in (3.261) and (3.263) represent uniform surroundings, the second ones a gradient along the x axes, the third ones a gradient along the y axes, and the fourth one is a kind of second gradient. A boundary value problem in the case under consideration provides a solution of the transport equation with the given boundary condition. Thus, we may write the solution to the general boundary condition problem as

$$\mathcal{T}u(\boldsymbol{\omega}) = 0 \quad \mathbf{r} \in V \tag{3.267}$$

$$u(\boldsymbol{\omega}_{j-}) = f_j(\boldsymbol{\omega}_-) \quad \mathbf{r} \in F_j, \quad j = 1,2,3,4; \tag{3.268}$$

where the four-tuples built from $f_j(\boldsymbol{\omega}_-),\ j = 1,\ldots,4$ are functions given along the four faces for the entering directions as

$$\mathcal{T}u_0 = 0 \quad \mathbf{r} \in V \tag{3.269}$$

$$u(\boldsymbol{\omega}_{j-}) = A_1(E,\mathbf{\Omega})\underline{e}_{1j}, j = 1,4; \tag{3.270}$$

the solution of which is a symmetric u_0 function;

$$\mathcal{T}u_x = 0 \tag{3.271}$$

$$u_x(\boldsymbol{\omega}_{j-}) = A_2(E,\mathbf{\Omega})\underline{e}_{2j}, j = 1,4; \tag{3.272}$$

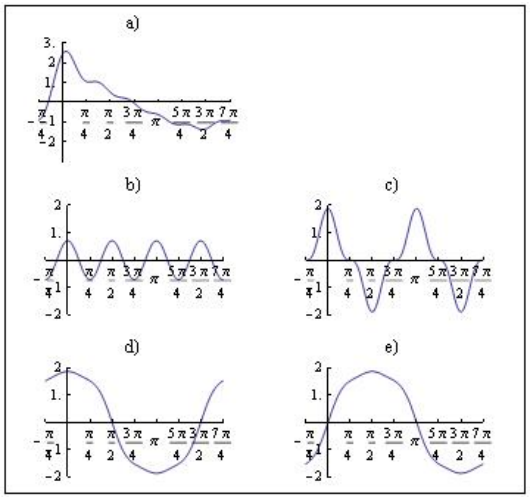

3.6. ábra. Fourier transforms at the boundary of a square

$$\mathcal{T}u_y = 0 \tag{3.273}$$
$$u_y(\boldsymbol{\omega}_{j-}) = A_3(E,\boldsymbol{\Omega})\underline{e}_{3j}, j = 1,4; \tag{3.274}$$

$$\mathcal{T}u_{xy} = 0 \tag{3.275}$$
$$u_{xy}(\boldsymbol{\omega}_{j-}) = A_4(E,\boldsymbol{\Omega})\underline{e}_{4j}, j = 1,4; \tag{3.276}$$

Now we refer to asymptotic theory, where we can express the solution (4.36) to the transport equation in a periodic structure as a macroflux multiplied by a microflux, plus the x component of the gradient of the macroflux multiplied by a microflux, plus the x component of the gradient of the macroflux multiplied by a microflux etc. Asymptotic theory deals with the neutron flux in a lattice; now we discuss the neutron flux in a cell. The analogy is immediate. Below we discuss the consequences of the finite-cell diameter.

Symmetry means that we see that same distribution in V after a rotation of $2\pi/N_f$. On a finite interval, the only possible symmetry transformation is the inversion to the middle of the interval, placing the origin there. Then any function can be decomposed into an even and an odd component. The symmetry components have a physical interpretation when V is a square. Any function $f(\alpha)$ given along the boundary can be decomposed into Fourier components:

$$f(\alpha) = \sum_{i=1}^{4}\sum_{k=1}^{\infty} a_{ik}\sin[(4k+i)\alpha] + b_{ik}\cos[(4k+i)\alpha] \tag{3.277}$$

If we plot the function $f(\alpha)$ and its four components, we get Figure 3.6. Part a) of Figure 3.6 shows a curve given along the boundary of the square. Curves b), c), d), and e) show the components $\underline{e}_1, \underline{e}_2, \underline{e}_3$ and $\underline{e}_4$ of curve a). The first component models a square embedded into a homogeneous surrounding, the second a gradient along the x axis, the third a gradient along the y axis, the fourth one is a kind of second derivative. Here we only mention that if we solve either the transport equation or the diffusion equation with a boundary condition of such a type, the boundary, flux, net current and exiting current will preserve the symmetry of the original boundary condition.

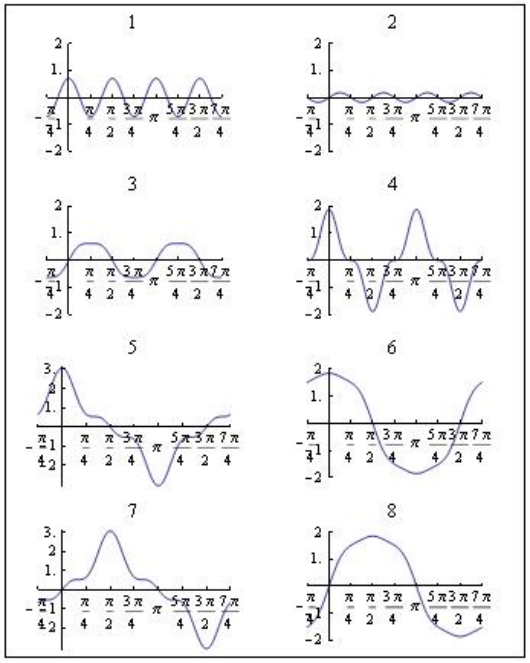

3.7. ábra. Fourier transforms along half-boundaries of a square

If we look at the curves b), c), d), and e), we can observe that only b) contributes to any reaction rate integrated over V, because the other three components give equal positive and negative contributions to the 1/8-th areas of the square. In other words, the integrated neutron balance depends only on the symmetric component of the solution. When V is small, it suffices to average over a face the function prescribed along the boundary. Then the odd components give no contribution. This approximation is satisfactory in cell calculations but in a larger assembly the odd components should also be taken into account. Then the number of components is eight; see Fig. 3.7, where the function shown in Fig. 3.6 under a) is decomposed, the components being labeled from 1 to 8. Note that components 2, 3, 5, and 7, are odd on all the four faces making no contribution to the face averages.

To handle the decomposition formally, we have to look at the boundary condition more closely. First note that the components can be even and odd along a given face. The formal treatment is done by using Walsh functions: see Appendix A. The Walsh functions are step functions, taking discrete values $-1, 0, +1$. The four components of the boundary value used in Fig. 3.6 include the four Walsh functions shown in Fig. 3.8. The Walsh functions are independent in the following sense. Whenever the initial boundary condition belongs to a given type of Walsh- function family, for example type A with quadratic space-dependence along each face, the response of the cell also will belong to an A type Walsh function but the face-wise distribution may have constant, linear, etc. components.

In reactor calculation, the response matrices are used following the below given seven steps:

1. Assume that we plan to determine the flux in volume V. The first step is discretization; we subdivide V into N_s congruent regular subvolumes, triangles, squares, or hexagons.

2. The model spatial distributions on the boundaries of a subvolume have to be deter-

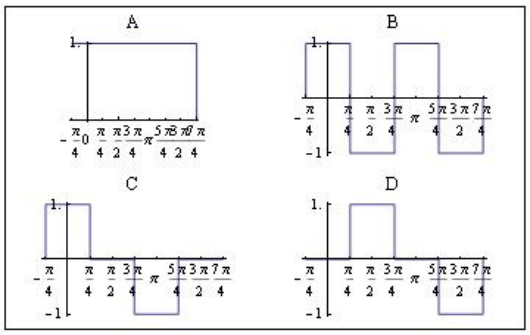

3.8. ábra. Fourier transforms at the boundary of a square

mined. A component to be used in the decomposition of the boundary condition will be an N_F-tuple, where N_F is the number of faces of a subvolume. A systematic way to determine the N_F -tuples is using group theory [55]. Laletin [57][Chapter 7] came to the same idea by heuristics. The reader may find further practical applications in [178].

3. The representation of the spatial distribution depends on the mesh size, the distance between two adjacent subvolumes. When the diameter of a subvolume is comparable to the mesh size, the boundary value may be taken as constant. When the diameter is larger by an order of magnitude or more, a quadratic spatial shape should be used.

4. The neutronics model to be used also should be determined. That model is either diffusion or transport theory. Diffusion theory is simpler and results in a faster algorithm. In the models used at the Kurchatov Institute (Moscow), transport theory has been chosen. In the KARATE code [146], diffusion theory is applied as a possible option. Those models are used in 3D production codes.

5. The response matrix may depend on a number of parameters. Among others, the burnup in a fuel assembly may vary with location, the void fraction, and hence moderator density may depend on the position inside the assembly, etc. All those parameters can be taken into account by a suitable parametrized library, a must of a production code.

6. Using numerical methods, see Chapter 8, we set up an iteration scheme to determine the boundary values at subvolume boundaries.

7. When the iteration has converged, the flux distribution inside the subvolumes is obtained from a type 2 assembly calculation. In that calculation the internal structures of the subvolumes are taken into account and the local power, and flux distributions, nuclide densities are determined.

The response matrix will be used in diffusion theory calculations, see Chapter 6.

3.8. Input data

One of the simplest models is the input-output model. We write a computer program, provide it with some input and it calculates functions depending on position or time, the output.

Such a model makes sense if we are able to produce the required input, set up an algorithm having all the desired features of a physical model and capable of deriving the output from a finite amount of input data in a finite amount of time. Throughout the rest of the present Chapter, we deal with the problem of providing input data for a reactor calculation.

3.9. Creation of input data

In the present Section, we deal with the problem of input data. A nuclear reactor is a human made device, in contrast with the ready made nuclei. Indeed, geometrical data along with some material parameters can be measured. Measurements are always inexact, but now we disregard that. An essential component of the input data, viz. the nuclear material properties are measured indirectly using sophisticated models and evaluation techniques. The problem is theoretical from the point of view of the structure of the energy levels of a given nucleus, but practical from the point of view of the usage of parametrized nuclear data libraries in practical calculations. This makes evident that the reactor calculation model must be stable with respect to the input data, and the models used in the derivation of the input data. The calculational model must be robust with respect to the models involved.

The model and the input data are not well defined. Casti's model is a good example for a simple model reflecting some features of a nuclear reactor and the input is λ-the mean free path in the rod, p_k-the probability of k neutrons emerging from a collision. The real reactors don't have the shape of a rod, contain several materials so if we wish to use Casti's model to describe a real reactor we have to give a recipe for preparing p_k and λ.

An alternative is to describe the reactor as a homogeneous material, in Chapter 6 the reader finds that kind of models. As a general rule, we pay the price of a simple model in the narrower applicability and smaller accuracy. It is a good policy to keep an arsenal of models and to use that one which gives reasonable results in a given task. That needs expertise which is acquired only by experience.

3.10. Validation and verification

We have to prove that the computational model is robust, stable, reasonably insensitive to the input data. The validation and verification process (V&V) is based on the following principles:

- defense in depth;
- independent multiple control;
- equal opportunities for the participants.

The V&V process uses the following tools:

1. Mathematical verification: Since the reactor model is an algorithm on a computer, it has to be verified if the algorithm obeys the same features as the programmed equations. A production code embodies appr. one hundred man-years of work in programming, and testing. The code development has its specific order in the nuclear industry, see [27],[28], [29], [30], [31], [32], [33], [34], [35], [36].
2. Physical validation: following the defense-in-depth principle, the validation starts with the input data. Under the auspices of the International Atomic Energy Agency, the library of nuclear data are continually checked and revised. Users of a given reactor type exchange their experience, improve their data and code when needed.

3. Benchmarking: sets of tests problems have been defined to find out how a computer model solves well defined specific problems. The tests problems range from the theoretical to the industrial problems.

4. Operational benchmarks: nuclear facilities compile a large amount of measured data from experiments. There are special power plants well equipped with measurements to provide data on operating power plants. The utility can collect its own benchmark data provided it complies with the [34] regulation.

5. The IAEA organizes meetings where reactor designers, utility staff, researchers, and representatives of the nuclear authorities can exchange their views on safety or technical issues.

The theoretical background of the V&V process is explained as follows. We have a device $\mathfrak{D}$, we have built a model (this time a computer code) that is capable of predicting some features of $\mathfrak{D}$ and we wish to see how accurate is the prediction.

In the V& V process, we use the input-output model, i.e. we use the computer code as a device to transform the input data to the output data. First we have to give a wish list: which data must be on the output list.

3.11. Problems

1. What features of a nuclear reactor are reflected by Casti's the simple control theory model?

2. What is the amount of remanent heat in a 1000 MW nuclear power plant? How can it be removed from the reactor core?

3. The average rise of the coolant temperature in a reactor is 31 C. What flow rate is required in a 1000 MW power plant to avoid overheating?

4. Assume the average coolant temperature rise is 31 C° and the flow rate in each assembly is the same, the maximum assembly power rate is 1.35. What is the maximum coolant temperature rise?

5. In the fuel certificate the error of the enrichment is $\pm 5\%$. Assuming normal distribution of the enrichment, what is the mean value of the enrichment in the core? What is its variance?

6. Estimate the heat deposit in the coolant due to the neutron slowing down in the coolant.

7. What is the ratio of the geometrical diameter of the ^{135}Xe nucleus to its effective cross-section $\sigma_a = 10^6$ barn? (Hint: use the $r = 1.5 \times 10^{-12} A^{1/3}$ formula to get the radius in cm from the mass number A.)

8. What is the ratio of the hydrogen $\sigma = 0.001$ barn cross-section and its actual radius?

9. How varies the angular flux at the boundary of two materials? How varies the angular flux at the joint boundary of three materials?

10. Estimate the effect of 10 % bubbles are a neutron radiation shield.

11. What would you build from a shield against slow neutrons? Against fast neutrons?

12. The first two eigenvalues of the TE are $\lambda_1 = -0.01 \ \ 1/s$ and $\lambda_2 = -0.2 + 10i$. Is this possible? After how long time will the first eigenvalue become dominant?

13. Assume that $\Phi(\mathbf{r})$ varies slowly in the integral transport equation. Give an estimate for the diffusion constant.

14. The density of water is 0.99799 g/cm^3, what is the atomic density of hydrogen and oxygen?

15. The density of UO_2 is 10.4 g/cm^3. Calculate the atomic density of U-235, and of U-238 and of oxygen, if the enrichment is 3.6%.

16. The thermal power of a reactor is 3000 MW. How much hydrogen is produced in neutron decay in one day? The neutron half-life is 11 min., the average lifetime of neutron is 25 μs in the reactor. One fission emits average 2.4 pieces of neutrons. $3.1 \cdot 10^{10}$ fissions products 1 J energy.

4. fejezet

Providing Input

As we have seen in Section 1, we need the following information to control the fission process:

- the relevant characteristics of the material placed into the reactor;
- the position of the material composition, i.e. the geometry;
- the physical laws governing the fission process.

Various reactor models differ in the way they describe the above mentioned three items. When speaking about the material distribution, the following models are used:

1. continuous position dependence, when material properties like the density are considered as continuous functions of the position, for example the mass density is given as $\rho(\mathbf{r}), \mathbf{r} \in V$.
2. homogeneous regions filled with a given material type, and the regions are connected by suitable boundary conditions. The boundary conditions are deduced from the physical description of the neutron field.
3. when the material composition is periodic, the geometry may be approximated by a lattice, i.e. an infinite periodic structure.
4. phenomena occurring at material interfaces are studied on finite geometries, like two adjacent half places.
5. even the simplest geometry may render a good service, for example the attenuation of a field is often studied in an infinite homogeneous material.

The nuclear properties of nuclei have been collected in so called evaluated nuclear data files. Such files are accessible through the Nuclear Data Section of the International Atomic Energy Agency, Vienna. Those files are based on nuclear models and a large amount of expertise is required to interpret and use properly the nuclear data.

Note, that nuclear data vary for each isotope consequently it is insufficient to have the material composition of various materials in the core. The source of those data is usually the vendor, and it is expensive to determine the isotope composition of a structural material or insulator.

Far the input preparation appears as a trivial matter. When we have to provide input for a given physical model the complexity of the problem becomes apparent. Some of the problems to be solved are:

1. How to replace a heterogeneous material with a homogeneous one? That problem is known under the term homogenization.
2. How to replace an energy dependent material by an energy independent one? That problem is known as energy condensation.
3. How can we simplify the boundary condition?

4.1. Energy condensation

The number of problems where the Boltzmann equation is solvable analytically, is rather small, to solve the majority of the problems we must rely on numerical methods which are computer programs running on a large capacity computer. Some problems should be solved in a limited time frame, see the real-time reactor simulation. Therefore we have the following available choices:

1. The simplification of the transport equation (3.116) itself. That choice means that approximations are used in the theory and those restrict the validity and accuracy of the solution. An advantage of that choice is that specific phenomena may be treated nearly exactly, and some general features of the solution may be transplanted to other, more complex problems.

2. We retain the original form of the equation and resort to numerical solution methods. Here special care is needed because the numerical solution must accord with the problem under consideration. In engineering practice, this approach is the most widely used one.

3. We refrain from attacking the original problem, simplify it by enhancing its features and create a simpler but solvable problem by introducing a model. The goal is to create models with manageable analytical or numerical solutions.

In the application of the transport equation to reactor physics, all the three mentioned choices are encountered. The present Chapter is devoted to two problems solvable analytically, and the subsequent Chapter is devoted to numerical methods. To be just with the model problem, we cite [59][p. 45] a list of the usual models in a classification of the energy variable:

Common approximations of energy dependence:

1. One-speed approximation in which all particles are characterized by a single kinetic energy or speed.

2. Multigroup energy description, in which the neutron energy is broken into intervals or groups, and each group is characterized by a single energy.

3. Simple models of the cross-section energy dependence (e.g. expansion in polynomial functions of energy).

4. Simple models of the collision kernels (e.g. separable or degenerate kernels).

A considerable simplification would originate from eliminating the energy variable. The idea has been generalized so that the energy range is broken into finite intervals called energy groups. Traditionally the numbering of the energy groups starts from the highest energy and proceeds downward, the boundaries of the energy groups are given as

$$E_g < E < E_{g-1}, g = 1, 2, \ldots, G \tag{4.1}$$

and G is the number of energy groups. The reason of the downward group numbering is that the neutrons lose energy in collisions, see Section 5.2 in Chapter 5. In the transport equation, we encounter the angular flux, cross-sections, and external sources. The angular flux is replaced by the group flux

$$\Phi_g(\mathbf{r}) = \int_{E_g}^{E_{g-1}} \Phi(\mathbf{r}, E) dE, \tag{4.2}$$

the cross-sections are averaged by the group angular flux as

$$\Sigma_{ag}(\mathbf{r}) = \frac{\int_{E_g}^{E_{g-1}} \Phi(\mathbf{r}, E)\Sigma_a(\mathbf{r}, E) dE}{\Phi_g(\mathbf{r})}, \tag{4.3}$$

and

$$\Sigma_{tg}(\mathbf{r}) = \frac{\int_{E_g}^{E_{g-1}} \Phi(\mathbf{r}, E)\Sigma_t(\mathbf{r}, E) dE}{\Phi_g(\mathbf{r})}, \tag{4.4}$$

$$\Sigma_{sg}(\mathbf{r}) = \frac{\int_{E_g}^{E_{g-1}} \Phi(\mathbf{r}, E, \mathbf{\Omega})\Sigma_s(E)dE}{\Phi_g(\mathbf{r}, \mathbf{\Omega})}. \tag{4.5}$$

There are cross-sections associated with energy change. The fission cross-section in group g is

$$\nu\Sigma_{fg}(\mathbf{r}) = \frac{\int_{E_g}^{E_{g-1}} \Phi(\mathbf{r}, E, \mathbf{\Omega})\nu\Sigma_f(\mathbf{r}, E)dE}{\Phi_g(\mathbf{r}, \mathbf{\Omega})}, \tag{4.6}$$

and the fission spectrum that gives the fraction of neutrons emerging in group g is

$$f_g = \int_{E-g}^{E_{g-1}} f(E)dE. \tag{4.7}$$

The scattering cross-section is averaged with the flux of the group in which the collision happens:

$$\Sigma_{s,g'\to g}(\mathbf{r}) = \frac{\int_{E_g}^{E_{g-1}} \Sigma_s(E' \to E)\Phi(\mathbf{r}, E')dE'}{\Phi_{g'}}. \tag{4.8}$$

Note that the reaction rates are often calculated by the scalar flux, thus the angular flux may be replaced by the scalar flux, although the group condensation relates only the energy variable. Finally, the group velocity is

$$v_g^{-1}(\mathbf{r}, \mathbf{\Omega}) = \frac{\int_{E_g}^{E_{g-1}} \frac{\Phi(\mathbf{r}, E, \mathbf{\Omega})}{v} dE}{\Phi_g(\mathbf{r})} \tag{4.9}$$

The last expression is rather surprising, usually the averaging is done to attain simplifications, now we got that even the averaged speed depends on $\mathbf{\Omega}$ and position $\mathbf{r}$.

As to the external source, it is replaced by

$$Q_g(\mathbf{r}, \mathbf{\Omega}) = \int_{E_g}^{E_{g-1}} Q(\mathbf{r}, E, \mathbf{\Omega})dE. \tag{4.10}$$

With the help of the group fluxes and group cross-sections, the transport equation takes the form of

$$\begin{aligned}\frac{1}{v_g}\frac{\partial\Phi_g(\mathbf{r}, \mathbf{\Omega})}{\partial t} = &-\mathbf{\Omega}\boldsymbol{\nabla}\Phi_g(\mathbf{r}, \mathbf{\Omega}) - \Sigma_{tg}(\mathbf{r})\Phi_g(\mathbf{r}, \mathbf{\Omega}) + \sum_{g'=1}^{G} \Sigma_{s,g'\to g}(\mathbf{r})(\mathbf{\Omega}' \to \mathbf{\Omega})\Phi_g(\mathbf{r}, \mathbf{\Omega}) \\ &+ \frac{f_g}{4\pi}\sum_{g'=1}^{G} \nu\Sigma_{fg'}(\mathbf{r})\Phi_{g'}(\mathbf{r}) + Q_g(\mathbf{r}, \mathbf{\Omega}),\end{aligned} \tag{4.11}$$

called multigroup transport equation, in which the dependent variables are G functions: $\Phi_g(\mathbf{r}, \mathbf{\Omega}), g = 1, \ldots, G$. In reactor physics calculation the multigroup transport equation is often used. The associated boundary and initial conditions are analogous to the continuous energy dependent case: we have to fix the initial values of $\Phi_g(\mathbf{r}, \mathbf{\Omega}, t_0), g = 1, \ldots, G$ and one of the boundary conditions at the boundary ∂V of volume V. The albedo boundary condition for the multigroup transport equation is

$$\Phi_g(\mathbf{r}_b, \mathbf{\Omega}^-) = \sum_{g'=1}^{G} \Gamma_{gg'}\Phi_{g'}(\mathbf{r}_b, \mathbf{\Omega}^+), \quad \mathbf{r}_b \in \partial V, \tag{4.12}$$

where $\Gamma_{gg'}$ is the local albedo matrix.

The multigroup form of the transport equation is applicable with any other approximation (diffusion theory, see Chapter 6, P_n, and S_n methods, or collision probabilities, see 8).

The multigroup model is based on the assumption that the flux is a slowly varying function of the energy, an assumption not valid if one of the involved isotopes has a resonance line in the energy group under consideration. In such a group resonance integrals are used, see Section 5.3 in Chapter 5.

4.2. Homogenization, asymptotic theory

There are geometrical structures in which the solution to the Boltzmann equation or its approximations can be found particularly simply. These are simple geometries, like a large homogeneous material. When seeking the above mentioned problems in a complex geometry, we may attempt to preserve features of those solutions. The solution simplifies if characteristics of the geometry (e.g. using symmetry consideration, we can reduce the domain of the solution) may be transplanted from the geometry to the solution. This is because the symmetries of the transport equation (and its approximations) are determined by the space dependence of the cross-section, in other words, by the space dependence of the material properties. Below we enlist such simple geometries.

1. Homogeneous material. The material properties of the volume under consideration are equivalent, the solution will share the symmetries of the volume. When the considered volume is infinite, there is no distinguished direction or position, the material properties are invariant under rotations and translations. When we place a point neutron source into the material, the position of the source is distinguished and the positions in the volume are classified according to their distance from the source. The homogeneous material has one characteristic distance, the mean free path. That constant determines the variation of the neutron distribution. There are no internal material boundaries where the material properties would change. This observation makes the homogeneous material attractive in reactor physics. That approximation is applied even when there are internal material boundaries provided the homogeneous regions are several mean free path thick.

2. A homogeneous half space is a homogeneous material plus an external boundary. There the positions may be classified in term of their distance from the external boundary. The solution in a half space problem often has a gradient orthogonal to the external boundary. The position parallel to the external boundary brings in no distinguished direction but if an external source is present, the space points are classified according to their positions with respect to the distance from the source and from the boundary.

3. One dimensional material distribution. There the material properties vary with one parameter. Such a geometry is the slab, the spherical geometry, and the axially infinite cylinder. The name of the geometry suggests the suitable coordinate system. Note that in the case under consideration the material properties are constant along the coordinates perpendicular to the to the axis along which the material properties vary. This is the simplest model to study the effect of space dependent material properties.

4. Periodic lattice. The structure of the matter is ab ovo hierarchical. There is a specific structure at the lower level and the next level may have a different structure. Modern engineering extensively has been using the so called composite material that has just the mentioned type structure. The reactor is made up from fuel assemblies, an array

of fuel pins constitute the fuel assemblies, each level has its own geometry. It is evident to experiment with the model of a periodic lattice as an approximating structure. The periodic lattice is invariant under translations by given vectors.

5. Lack of symmetry. When a structure shows no symmetry at all, one may try the random material approximation. That approach has been used mainly in structures varying randomly in time, like the chaotic motion of a liquid.

The transport operator is linear, and it has a stationary solution only if its fundamental eigenvalue is zero, see (3.143). Such a volume V in which the external source free transport equation has a stationary solution is called critical volume. Any volume can be made conditionally critical, if we introduce and additional parameter into the transport operator. Two such eigenvalues are used in reactor physics: the time absorption and the effective multiplication factor k_{eff}. The first one is an additive constant in the removal operator, we replace $\mathcal{R}$ by $\mathcal{R} + \alpha$:

$$(\mathcal{L} + \mathcal{R} + \alpha)\Phi(\boldsymbol{\omega}) = \mathcal{F}\Phi(\boldsymbol{\omega}) \tag{4.13}$$

and we seek an α by which (4.13) has non-trivial solution. V is called supercritical, critical, and subcritical, when $\alpha > 0, \alpha = 0$, and $\alpha < 0$, respectively. Any volume has a time absorption type eigenvalue.

The second kind of eigenvalue is written in the form of a multiplier in the fission term, using the substitution $\mathcal{F} \to 1/k_{eff}\mathcal{F}$ and we have to find k_{eff} with which the equation

$$(\mathcal{L} + \mathcal{R})\Phi(\boldsymbol{\omega}) = \frac{1}{k_{eff}}\mathcal{F}\Phi(\boldsymbol{\omega}). \tag{4.14}$$

has non-trivial solution. When $k_{eff} > 1$, V is called supercritical, when $k_{eff} = 1$, critical, when $k_{eff} < 1$, subcritical. If V has no fissionable material, the effective multiplication factor can not be defined. The reactivity ρ is obtained from the k_{eff} by the following relation:

$$\rho = 1 - \frac{1}{k_{eff}} \tag{4.15}$$

therefore the reactivity of a subcritical/supercritical volume is negative/positive, and the reactivity of a critical volume is zero. In neutron kinetics, see Chapter 7, a new unit for the criticality is introduced, it is measured in delayed neutron fraction unit.

4.2.1. Asymptotic analysis

Consider the integral- differential form of the neutron transport equation [177], see 3.3 in Chapter 3 and gather the prompt neutron-nucleus reactions into a single operator $\mathcal{L}$. For the sake of simplicity we disregard the delayed neutrons. Larsen's derivation has been based on the following assumptions:

1. We consider a domain D composed of nearly identical cells, the cells are arrange periodically.

2. A typical mean free path in D is assumed to be of the same order as a cell diameter.

3. The ratio of a typical mean free path to a typical dimension of D is small of order ϵ.

4. The material properties i.e. the cross-sections, are periodic in space and independent of time except for a perturbation term of order ϵ^2.

5. External sources are small of order ϵ.

All nuclear reactions leading to energy change, including the fission, are included in the collision operator. We write the neutron balance in terms of scaled space and time variables:

$$\tau = \frac{t}{\epsilon^2}; \;\; \mathbf{r}' = \frac{\mathbf{r}}{\epsilon}, \tag{4.16}$$

where $\mathbf{r}'$ is the fast space variable. Note that the cell diameter is of the same order as $\mathbf{r}'$. The slow time variable is t. The scaled form of the neutron transport equation is

$$\left(\frac{1}{\epsilon}\frac{\partial}{\partial\tau} + \mathbf{v}\boldsymbol{\nabla} - \frac{1}{\epsilon}\mathcal{L}\right)\Phi(\mathbf{r},\mathbf{v},\tau,\epsilon) = \epsilon S(\mathbf{r},\frac{\mathbf{r}}{\epsilon},\mathbf{v},\epsilon t), \tag{4.17}$$

where the source is assumed to be of order $\epsilon << 1$ and it depends both on the slow spatial variable $\mathbf{r}$ and the fast spatial variable $\mathbf{r}/\epsilon$. At the same time the source varies slowly in time so depends on ϵt. The collision operator $\mathcal{L}$ has two components:

$$\mathcal{L}f = \int v'\Sigma_S(\mathbf{r},\frac{\mathbf{r}}{\epsilon},\mathbf{v}'\to\mathbf{v},\epsilon^2\tau,\epsilon)f(\mathbf{r},\mathbf{v}',\tau,\epsilon)d\mathbf{v}' - v'\Sigma_T(\mathbf{r},\frac{\mathbf{r}}{\epsilon},v,\epsilon^2\tau,\epsilon)f(\mathbf{r},\mathbf{v},\tau,\epsilon). \tag{4.18}$$

Here $\mathbf{r} = (x,y,z)$, $\mathbf{v} = (v_x,v_y,v_z)$. In (4.17), we clearly indicated that the cross-sections Σ_S and Σ_T are small of order ϵ.

We introduce the Taylor expansions in the last variable of Σ_S and Σ_T as

$$\Sigma_S(\mathbf{r},\frac{\mathbf{r}}{\epsilon},\mathbf{v}'\to\mathbf{v},\epsilon^2\tau,\epsilon) = \sum_{n=0}^{\infty}\epsilon^n\Sigma_{Sn}(\mathbf{r},\frac{\mathbf{r}}{\epsilon},\mathbf{v}'\to\mathbf{v},\epsilon^2\tau) \tag{4.19}$$

and

$$\Sigma_T(\mathbf{r},\frac{\mathbf{r}}{\epsilon},v,\epsilon^2\tau,\epsilon) = \sum_{n=0}^{\infty}\epsilon^n\Sigma_{Tn}(\mathbf{r},\frac{\mathbf{r}}{\epsilon},v,\epsilon^2\tau). \tag{4.20}$$

Note that Σ_T depends only on the energy therefore in its argument only (v) is encountered, whereas in the argument of Σ_S we find $\mathbf{v}$.

We consider a volume V composed of cells of identical geometry. The cell has a symmetry center at $\mathbf{r} = 0$. We also assume that the material distribution in the cell is symmetric function of position. We also assume Σ_T and Σ_S to be rotationally symmetric in $\mathbf{v}$ and $\mathbf{v}'$ to order ϵ:

$$\Sigma_{Tn}(\mathbf{r}'\epsilon,\mathbf{r}',v,t) = \Sigma_{Tn}(-\mathbf{r}'\epsilon,-\mathbf{r}',v,t), n = 0,1. \tag{4.21}$$

$$\Sigma_{Sn}(\mathbf{r}'\epsilon,\mathbf{r}',\mathbf{v}'\to\mathbf{v},t) = \Sigma_{Sn}(-\mathbf{r}'\epsilon,-\mathbf{r}',-\mathbf{v}'\to-\mathbf{v},t), n = 0,1. \tag{4.22}$$

We also assume that when $\epsilon = 0$, Σ_S és Σ_T as well as the source are periodic in $\mathbf{r}'$. Be the center of a given cell at $\mathbf{r}' = 0$, and $\mathbf{r}' = \mathbf{a}$ is the center of any other cell. Then

$$\Sigma_{S0}(0,\mathbf{r}',\mathbf{v}'\to\mathbf{v},t) = \Sigma_{S0}(0,\mathbf{r}'+\mathbf{a},\mathbf{v}'\to\mathbf{v},t); \Sigma_T(0,\mathbf{r}',v,t) = \Sigma_T(0,\mathbf{r}'+\mathbf{a},v,t) \tag{4.23}$$

holds for any $\mathbf{r}'$ inside the cell (translational invariance).

We are interested in the solution at positions far from the boundaries of D at time long after the initial time.

We introduce the $\mathbf{r}' = \mathbf{r}/\epsilon$ fast space variable and the slow time variable $t = \epsilon\tau$. In the new variables, we write the dependent variable in (4.17) as $\Phi(\mathbf{r},\mathbf{r}',\mathbf{v},t,\epsilon)$, where variables $\mathbf{r}$ and $\mathbf{r}'$ are considered as independent therefore the leakage is:

$$\mathbf{v}\nabla\Phi = (\mathbf{v}\boldsymbol{\nabla} + \frac{1}{\epsilon}\mathbf{v}\nabla')\Phi(\mathbf{r},\mathbf{r}',\mathbf{v},t,\epsilon). \tag{4.24}$$

Expand the collision operator $\mathcal{L}$ in (4.18) into a power series of ϵ:

$$\mathcal{L} = \sum_n \epsilon^n \mathcal{L}_n, \tag{4.25}$$

where in operator $\mathcal{L}_n$ the following substitutions have been carried out: $\Sigma_T \to \Sigma_{Tn}$ és $\Sigma_S \to \Sigma_{Sn}$, c.f. (4.19)-(4.20). Now the transport equation takes the form of

$$\left(\frac{1}{\epsilon}\partial_\tau + \mathbf{v}\nabla + \epsilon^{-1}\mathbf{v}\nabla' - \sum_{n=0}^{\infty} \epsilon^{n-1}\mathcal{L}_n \right) \Phi = \epsilon S, \tag{4.26}$$

where, as has been mentioned, $\mathbf{r}$ and $\mathbf{r}'$ are independent variables. Inside V, we seek the solution in the form of a power series:

$$\Phi \sim \sum_{n=0}^{\infty} \epsilon^n \Phi_n(\mathbf{r}, \mathbf{r}', \mathbf{v}, t) \tag{4.27}$$

where $t = \epsilon^2\tau$. Further notation:

$$\mathcal{T} = v\nabla' - \mathcal{L}_0 \tag{4.28}$$

Using that in (4.27):

$$\mathcal{T}\Phi_n = \sum_{j=0}^{n-1} \mathcal{L}_{n-j}\Phi_j - v\nabla\Phi_{n-1} - \partial_t\Phi_{n-2} + \delta_{n2}S. \tag{4.29}$$

The terms with negative subscript (Φ_{-2}, Φ_{-1}) are zero.

We solve (4.29) recursively. Note that operator $\mathcal{T}$ includes derivatives with respect to $\mathbf{r}'$, which is the fast spatial variable. When $n = 0$ the equation becomes

$$\mathcal{T}\Phi_0 = 0, \tag{4.30}$$

its general solution is

$$\Phi_0 = F(\mathbf{r}, t)u_0(\mathbf{r}, \mathbf{r}', \mathbf{v}, t). \tag{4.31}$$

u_0 is periodic in $\mathbf{r}'$, $\mathbf{r}$ is the slow space variable referring to a location in V and t are parameters. u_0 satisfies the following homogeneous equation:

$$\begin{aligned} 0 =& \mathbf{v}\nabla' u_0(\mathbf{r}, \mathbf{r}', \mathbf{v}, t) + v\Sigma_{T0}(\mathbf{r}, \mathbf{r}', v, t)u_0(\mathbf{r}, \mathbf{r}', \mathbf{v}, t) \\ & - \int v'\Sigma_{S0}(\mathbf{r}, \mathbf{r}', \mathbf{v}' \to \mathbf{v}, t)u_0(\mathbf{r}, \mathbf{r}', \mathbf{v}, t)d\mathbf{v}'. \end{aligned} \tag{4.32}$$

Nontrivial, unique solution exists only if operator $\mathcal{T}$ has a one-dimensional null space. This assumes a relationship among the cross-sections fixing the criticality of the infinite lattice. When (4.32) is solvable with the normal component of the current equal to zero boundary condition, the infinite lattice is critical. In general, criticality is achieved by introducing a free parameter into the cross-sections, usually the fission cross-section is multiplied by $1/k$ and the parameter resulting in criticality is called effective multiplication factor or simply k_{eff}.

Now we pass on to the case $n = 1$. From (4.29) we get

$$\mathcal{T}\Phi_1 = F\mathcal{L}_1 u_0 - \mathbf{v}\boldsymbol{\nabla}(Fu_0), \tag{4.33}$$

where the null space of operator $\mathcal{T} = \mathbf{v}\boldsymbol{\nabla}' - \mathcal{L}_0$ as well as the null space of its adjoint are one-dimensional ones. Unique solution exists if the right hand side of (4.33) is orthogonal to the solution of the adjoint flux Φ^+:

$$0 = F(u_0^+, \mathcal{L}_1 u_0) + (u_0^+, \mathbf{v}\nabla F u_0), \tag{4.34}$$

where the scalar product is the following integral:

$$(a^+, b) = \int_{cell} a^+(\mathbf{v}, \mathbf{r}') b(\mathbf{v}, \mathbf{r}') d\mathbf{v} d\mathbf{r}'. \tag{4.35}$$

The second integral in (4.34) is zero because u_0 is symmetric in $\mathbf{v}$ and $\mathbf{r}'$ once the cross-sections are symmetric. Therefore the solvability condition is

$$(u_0^+; \mathcal{L}_1 u_0) = 0,$$

which is a condition on[1] operator $\mathcal{L}_1$. The general solution of (4.33) is:

$$\Phi_1 = F_1 u_0 - F\mathcal{T}^{-1}\mathcal{L}_1 u_0 - \mathcal{T}^{-1}\mathbf{v}\nabla F u_0, \tag{4.36}$$

where $\mathcal{T}^{-1}$ is the inverse of $\mathcal{T}$. $\mathcal{T}^{-1}$ possesses the following property:

$$\int_{cell} u_0^+ \mathcal{T}^{-1} f d\mathbf{v} d\mathbf{r}' = 0$$

for every functions such that

$$\int_{cell} u^+ f d\mathbf{v} d\mathbf{r}' = 0.$$

Let us pass on to the $n = 2$ case in the investigation of (4.29). We have to solve

$$\mathcal{T}\Phi_2 = F\mathcal{L}_2 u_0 + (\mathcal{L}_1 - \mathbf{v}\nabla)(F_1 u_0 - \mathcal{T}^{-1}\mathbf{v}\nabla F u_0 - F\mathcal{T}^{-1}\mathcal{L}_1 u_0) - \partial_t(F u_0) + S_0. \tag{4.37}$$

(4.37) is solvable when

$$\frac{dF}{dt} = \boldsymbol{\nabla}(M_0 \boldsymbol{\nabla} F) + \mathbf{M}_1 \boldsymbol{\nabla} F + M_2 F + S_0, \tag{4.38}$$

where

$$M_0(\mathbf{r}, t) = (\mathbf{v} u_0^+, \mathcal{T}^{-1} u_0 \mathbf{v}) \tag{4.39}$$

$$\mathbf{M}_1(\mathbf{r}, t) = (u_0^+ \mathbf{v}, \nabla \mathcal{T}^{-1} \mathbf{v} \nabla u_0) - (\mathbf{v}\nabla u_0 \mathcal{T}^{-1} \mathbf{v} \nabla u_0) \tag{4.40}$$

$$\mathbf{M}_2(\mathbf{r}, t) = (u_0^+ \mathbf{v}, \nabla \mathcal{T}^{-1}(\mathbf{v}\nabla u_0)) + (u_0^+, \mathcal{L}_2 u_0) - (u_0^+, \mathcal{L}_1 \mathcal{T}^{-1} \mathcal{L}_1 u_0) - (u_0^+, \partial_t u_0) \tag{4.41}$$

$$S_0(\mathbf{r}, t) = (S, u_0). \tag{4.42}$$

(4.38) is a second order differential equation for the slowly varying $F(\mathbf{r})$ function. The solution of the neutron transport equation in a periodical material (lattice) has two components: a slow varying function $F_0(r)$ and a periodic u_0, the components should be multiplied. When the cell is homogeneous, $F_0(\mathbf{r})$ is purely space dependent, u_0 is purely energy dependent. That is the so called asymptotic assumption of reactor physics. That solution dominates far from the material interfaces and from the external boundary. Note, that F_0 is not constant

[1] That condition holds for any operator which is odd in space.

inside a cell but varies slowly. That has made it possible to derive from the microfluxes the coefficients in the equation for F_0. The above discussed asymptotic theory has been extended and has proven successful in various branches of physics.

The neutron distribution is determined in the following manner using the asymptotic theory.

1. We solve equation (4.32) in a cell for $u_0(\mathbf{r}, \mathbf{r}', t)$, the space variable is considered as constant in a cell;
2. In the next step we solve (4.39)-(4.41) to determine the matrices in equation (4.38);
3. Then equation (4.38) is solved for the macroflux F;
4. We build up the flux from F and u_0, using (4.31).

4.2.2. Finite lattice

Below we present a simple model for the finite lattice. The idea is that we consider an infinite lattice, at the boundary of the finite lattice define a boundary condition and derive a solution of the infinite lattice satisfying the transport equation and the boundary condition.

We study the static solution of the neutron transport equation that we write as

$$\mathbf{\Omega}\boldsymbol{\nabla}\Phi(\mathbf{r}, E, \mathbf{\Omega}) + \Sigma(\mathbf{r}, E) = \int dE' d\mathbf{\Omega}' \mathcal{S}(\mathbf{r}, E' \to E, \mathbf{\Omega}' \to \mathbf{\Omega})\Phi(\mathbf{r}, E', \mathbf{\Omega}'), \tag{4.43}$$

where $\mathcal{S}(\mathbf{r}, E' \to E, \mathbf{\Omega}' \to \mathbf{\Omega})$ comprises every processes changing the energy or the direction of the neutron. $\mathcal{S}$ involves the scattering and the fission, see Section 4.1 in the present Chapter. In order to make equation (4.43) solvable, in the latter the fission cross-section is replaced by Σ_f/k where appropriate value of k makes equation (4.43) solvable. Our intention is to build up the neutron flux from infinite core solutions. To this end, the core is extended to infinity by exploiting the periodicity of the cross-section:

$$\Sigma(\mathbf{r} + \mathbf{a}, E, \mathbf{\Omega}) = \Sigma(\mathbf{r}, E, \mathbf{\Omega}), \tag{4.44}$$

here $\mathbf{a}$ is a lattice vector that connects two cell centers, Σ stands for any cross-section in (4.43). The cross-sections are assumed symmetric in $\mathbf{r}$.

The Bloch theorem guarantees the existence of a particular solution in the for,

$$\Phi_{\mathbf{B}}(\mathbf{r}, E, \mathbf{\Omega}) = e^{i\mathbf{B}\mathbf{r}} u_{\mathbf{B}}(\mathbf{r}, E, \mathbf{\Omega}), \tag{4.45}$$

where $u_{\mathbf{B}}(\mathbf{r}, E, \mathbf{\Omega})$ is periodic in space. We introduce the following shorthand notation for the transport equation:

$$[\mathbf{\Omega}\boldsymbol{\nabla} + \mathcal{H}(k)]\Phi(\mathbf{r}, E, \mathbf{\Omega}) = 0, \tag{4.46}$$

where operator $\mathcal{H}(k)$ includes every cross-sections. We substitute (4.45) into (4.46) and obtain the following equation for the periodic part of the solution:

$$[\mathbf{\Omega}\boldsymbol{\nabla} + \mathcal{H}(k)]u_{\mathbf{B}}(\mathbf{r}, E, \mathbf{\Omega}) = -i\mathbf{B}\mathbf{\Omega}\mathbf{u}_{\mathbf{B}}(\mathbf{r}, \mathbf{E}, \mathbf{\Omega}). \tag{4.47}$$

We can see from this equation that $k = k(\mathbf{B})$. We are interested in a solution with physical meaning, that belongs to the so called fundamental eigenvalue. That restricts the $\mathbf{B}$ vectors to a set R_0. The infinite lattice is invariant under a set of transformations (reflections, rotations, translations). Those transformations may not change k. Since the transformations

map according to the transformation rule of a vector identically $\mathbf{B}, \mathbf{r}, \mathbf{\Omega}$ into some $\mathbf{B}', \mathbf{r}', \mathbf{\Omega}'$ i.e.

$$\mathbf{B}' = \mathbf{P}\mathbf{B};\ \mathbf{r}' = \mathbf{P}\mathbf{r};\ \mathbf{\Omega}' = \mathbf{P}\mathbf{\Omega}. \tag{4.48}$$

But then follows

$$k(\mathbf{B}') = \mathbf{k}(\mathbf{B}), \tag{4.49}$$

since the equation has remained invariant. The translation in $\mathbf{r}$ corresponds to a translation by a reciprocal lattice vector $\mathbf{q}$ in $\mathbf{B}$, thus

$$k(\mathbf{B} + \mathbf{q}) = \mathbf{k}(\mathbf{B}) \tag{4.50}$$

also must hold far any reciprocal lattice[2] vector $\mathbf{q}$.

In an infinite lattice the solution is periodic thus there $\mathbf{B} = \mathbf{0}$. We are interested in lattices consisting of a large number of cells when $|\mathbf{B}| << \mathbf{1}$ and the following expansion is applicable:

$$u_{\mathbf{B}}(\mathbf{r}, E, \mathbf{\Omega}) = u_0(\mathbf{r}, E, \mathbf{\Omega}) + u_1(\mathbf{r}, E, \mathbf{\Omega}) i\mathbf{B} + \mathbf{B}\mathbf{u_2}(\mathbf{r}, \mathbf{E}, \mathbf{\Omega})\mathbf{B} + \ldots \tag{4.51}$$

and

$$k(\mathbf{B}) = \kappa_{\mathbf{0}} + \sum_{\mathbf{k}} \kappa_{\mathbf{2j}} \mathbf{B}_{\mathbf{j}}^{\mathbf{2}} + \ldots. \tag{4.52}$$

Note that the terms odd in components of $\mathbf{B}$ are missing because the $\mathbf{r} \to -\mathbf{r}$ is also a possible symmetry in the lattice therefore all the odd components equal to zero. We use (4.51) and (4.52) in (4.47), in the resulting equation the coefficients of power of $\mathbf{B}$ components should be equal hence we get the following set of equations:

$$\begin{aligned}
[\mathbf{\Omega}\boldsymbol{\nabla} + H(\kappa_0)]u_0(\mathbf{r}, E, \mathbf{\Omega}) &= 0 && (4.53)\\
[\mathbf{\Omega}\boldsymbol{\nabla} + H(\kappa_0)]u_{1i}(\mathbf{r}, E, \mathbf{\Omega}) &= -\mathbf{\Omega}_i u_0(\mathbf{r}, E, \mathbf{\Omega}) && (4.54)\\
[\mathbf{\Omega}\boldsymbol{\nabla} + H(\kappa_0)]u_{2i}(\mathbf{r}, E, \mathbf{\Omega}) &= -\Omega_i u_{1i}(\mathbf{r}, E, \mathbf{\Omega}) - H(\kappa_{2i}) u_0(\mathbf{r}, E, \mathbf{\Omega}). && (4.55)
\end{aligned}$$

Note that the source term in (4.54) is odd and is orthogonal to $u_0(\mathbf{r}, E, \mathbf{\Omega})$ therfore (4.54) is solvable. The right hand side of (4.55) must be orthogonal to $u_0(\mathbf{r}, E, \mathbf{\Omega})$ resulting in

$$\int_{4\pi} \int_0^\infty \int_{V_{cell}} \mathbf{\Omega}_i u_{1i}(\mathbf{r}, E, \mathbf{\Omega}) u_0^+(\mathbf{r}, E, \mathbf{\Omega}) + u_0^+(\mathbf{r}, E, \mathbf{\Omega}) H(\kappa_{2i}) u_0(\mathbf{r}, E, \mathbf{\Omega}) d^3\mathbf{r} dE d\mathbf{\Omega} = 0 \tag{4.56}$$

which is an equation to determine κ_{2i}.

The general solution of (4.46) is a linear combination of the Bloch functions therefore

$$\Phi(\mathbf{r}, E, \mathbf{\Omega}) = \sum_{i=0}^{\infty} \boldsymbol{\nabla}^i [\Phi_M(\mathbf{r})] u_i(\mathbf{r}, E, \mathbf{\Omega}) \tag{4.57}$$

where[3] the macroflux $\Phi_M(\mathbf{r})$ is

$$\Phi_M(\mathbf{r}) = \int_{R_0} W(\mathbf{B}) \mathbf{e}^{\mathbf{i(Br)}} \mathbf{dB}. \tag{4.58}$$

The weight function $W(\mathbf{B})$ is to be determined from the boundary condition fixed along the boundary of the finite lattice.

[2] If $\mathbf{q}$ is a reciprocal lattice vector and $\mathbf{r}$ is a lattice vector then $\mathbf{qr} = 2\pi n$ where n is an integer.

[3] Note that u_0 is one function, u_1 is a vector and u_2 is a tensor.

We can determine κ_0 and κ_2 either from the microflux equations (4.53)-(4.55), or from the macroflux that obeys the equation

$$\bar{D}\boldsymbol{\nabla}^2\Phi_M(\mathbf{r}) + (\nu\bar{\Sigma}_f - \bar{\Sigma}_a)\Phi_M(\mathbf{r}) = 0 \tag{4.59}$$

and the two criticality eigenvalues are equal provided

$$\bar{\Sigma}_a = \frac{(\Sigma_a(\mathbf{r})u_0, u_0^+)}{(u_0, u_0^+)} \tag{4.60}$$

$$\nu\bar{\Sigma}_f = \frac{(\nu\Sigma_f(\mathbf{r})u_0, u_0^+)}{(u_0, u_0^+)} \tag{4.61}$$

$$\bar{D}_i = \frac{-(\boldsymbol{\Omega}_i u_{1i}, u_0^+)}{(u_0, u_0^+)}. \tag{4.62}$$

This is the homogenization recept we wanted to get. The calculation scheme goes as follows.

1. First we determine the periodic u_0, u_1 and u_2 functions from (4.53)-(4.55);
2. With those functions the homogenization is carried out using (4.60)-(4.62);
3. Using the homogenized cross-sections, determine the macroflux from (4.59);
4. In the final step the flux distribution is reconstructed using the microflux and the macroflux according to (4.57).

4.2.3. Heterogeneous lattices

An important application of the diffusion (and the transport) equation is the assembly calculation, where a set of assemblies are composed of a number of homogeneous cells of identical geometry. As we have seen to describe the neutron distribution in a periodic structure we need a macroflux and a microflux. The former helps in fulfilling the boundary condition at external boundaries, the latter is a consequence of the periodicity of the geometry. The asymptotic theory offers a recipe for preparing the coefficients in the equation fulfilled by the macroflux. Here it suffices to separate the most symmetric component (the so called unit representation).

We wish to modify the asymptotic theory so that it applies to lattices made up from cells of diverse material compositions. For the light water reactors the following theory [145] was elaborated[4]. The material properties of the cells may differ thus equation (4.63) is different from cell to cell. The boundary of the cell is subdivided into n_F edges. We write the equation under consideration in the concise form of

$$\mathbf{T}_k(k_{eff})\psi_k(\mathbf{r}, E, \Omega) = 0. \tag{4.63}$$

Here operator $\mathbf{T}$ acts on the neutron flux ψ in cell k. To ensure the solvability of the homogeneous equation, we need an additional parameter k_{eff} which divides the fission cross-section. In cell k, the boundary condition fixes the flux for the entering directions:

$$\psi_k(\mathbf{r}, E, \Omega) = \psi_{kb}(\mathbf{r}, E, \Omega) \text{ for } \Omega\mathbf{n} < 0. \tag{4.64}$$

[4]The method is applicable for transport and diffusion theory as well. The notation follows the more general transport theory

We assume that the energy range can be discretized into energy groups. We assume the diffusion approximation at the boundary, therefore for edge i in energy group superscript g is

$$\psi_{ki}^{g} = \frac{1}{4\pi}\left[\Phi_{ki}^{g} + 3\Omega_{r}^{(i)} J_{ki}^{rg} + 3\Omega_{\alpha}^{(i)} J_{ki}^{\alpha g}\right], \tag{4.65}$$

where $\Omega_r^{(i)}$, $\Omega_\alpha^{(i)}$ are the radial and tangential component of the direction vector Ω along the ith edge; Φ_{ki}^g is the scalar flux and J_{ki}^{rg}, $J_{ki}^{\alpha g}$ are the radial and tangential components of the net current. Later we show that the current components are determined by the fluxes.

In the proposed method for global reactor calculation and the solution of the Boltzmann equation for a cell are coupled. The quantities Φ_{ki}^g and k_{eff} are determined in the global reactor calculation. As we will see in Section 8.4, any reaction rate integrated over a cell depends only on the symmetric solution, which, in turn belongs to a symmetric boundary condition. Therefore we separate the symmetric part from the boundary fluxes:

$$\Phi_{ki}^{g} = F_{k0}^{g} + \hat{F}_{ki}^{g}, \tag{4.66}$$

where

$$F_{k0}^{g} = \frac{1}{n_F}\sum_{i=1}^{n_F} \Phi_{ki}^{g}. \tag{4.67}$$

A reaction rate is a linear expression of F_{k0}^g. We express it with the help of $\Gamma_{xk}^{gg'}$ to be introduced below. $\Gamma_{xk}^{gg'}$ is a straightforward generalization of the response matrix. Let R_{xm}^k be the x type reaction rate in energy group k, in cell m, then

$$R_{xm}^{k} = \sum_{k'=1}^{G} \Gamma_{xm}^{kk'} F_{m0}^{g'}, \tag{4.68}$$

where G is the number of energy groups. The net currents[5] may differ from face to face thus there

$$J_{mi}^{rk} = \sum_{k'=1}^{G}\sum_{\ell'=1}^{n_F} \Gamma_{m\ell\ell'}^{kk'} \Phi_{m\ell'}^{k'}. \tag{4.69}$$

We need a special reaction rate, the average flux $\bar{\phi}_m^k$.

At an internal boundary, the fluxes on the shared face should be equal and the net current should be continuous, i.e. the current leaving one cell enters the adjacent cell. Let the subscript m' of cell neighboring to cell m at face ℓ be $m'(m\ell)$ and the common edge of cell $m'(m\ell)$ be ℓ'. Then, at an internal boundary

$$\Phi_{m\ell}^{k} = \Phi_{m'(m\ell)\ell'} \tag{4.70}$$

and

$$J_{m\ell}^{rk} = -J_{m'(m\ell)\ell'}^{rk}. \tag{4.71}$$

From the boundary current we also separate the symmetric component:

$$J_{m\ell}^{rk} = G_{m0}^{k} + \hat{G}_{m\ell}^{k}. \tag{4.72}$$

With the new variables, the continuity conditions (4.70)–(4.71) read as

$$F_{m0}^{k} + \hat{F}_{m\ell}^{k} = F_{m'0}^{k} + \hat{F}_{m'\ell'}^{k} \tag{4.73}$$

[5]The tangential current does not contribute to the balance.

and

$$G^k_{m0} + \hat{G}^k_{m\ell} = G^k_{m'0} + \hat{G}^k_{m'\ell'}. \tag{4.74}$$

Now the boundary current is a linear expression of the symmetric fluxes:

$$J^{rk}_{m\ell} = \frac{2}{h}\,\frac{\alpha^k_{m\ell}\alpha^k_{m'\ell'}}{\alpha^k_{m\ell}+\alpha^k_{m'\ell'}}\left[\left(F^k_{m'0} - \frac{h}{2}\,\frac{G^k_{m'0}}{\alpha^k_{m'\ell'}}\right) - \left(F^k_{m0} - \frac{h}{2}\,\frac{G^k_{m0}}{\alpha^k_{m\ell}}\right)\right]. \tag{4.75}$$

Here we introduced

$$\alpha^k_{m\ell} = \frac{h}{2}\,\frac{\hat{G}^k_{m\ell}}{\hat{F}^k_{m\ell}}\,, \tag{4.76}$$

and h is the lattice pitch. We need one more additional parameter:

$$\epsilon^k_{m\ell} = \frac{F^k_{m0} - \frac{h}{2}\,\frac{G^k_{m0}}{\alpha^k_{m\ell}}}{\bar{\phi}^k_m}\,, \tag{4.77}$$

with which the boundary current can be expressed by the average fluxes of the adjacent cells as

$$J^{rk}_{m\ell} = \frac{2}{h}\,\frac{\alpha^k_{m\ell}\alpha^k_{m'\ell'}}{\alpha^k_{m\ell}+\alpha^k_{m'\ell'}}\left(\epsilon^k_{m'\ell'}\bar{\phi}^k_{m'} - \epsilon^k_{m\ell}\bar{\phi}^k_m\right). \tag{4.78}$$

and the boundary flux as

$$\Phi^k_{m\ell} = \frac{\alpha^k_{m'\ell'}}{\alpha^k_{m\ell}+\alpha^k_{m'\ell'}}\,\epsilon^k_{m'\ell'}\bar{\phi}^k_{m'} + \frac{\alpha^k_{m\ell}}{\alpha^k_{m\ell}+\alpha^k_{m'\ell'}}\,\epsilon^k_{m\ell}\bar{\phi}^k_m. \tag{4.79}$$

The neutron balance reads as

$$\sum_{\ell=1}^{n_F} J^{rk}_{m\ell} - V_m R^k_{am} + \frac{1}{k_{eff}}\,\chi^k V_m \sum_{k'=1}^{K} R^{k'}_{fm} + V_m \sum_{k'\neq k} R^{k'\to k}_{sm} = 0. \tag{4.80}$$

Comparing equations (4.79) and (4.78) with the corresponding finite difference expressions

$$\Phi^k_{m\ell} = \frac{D_m\Phi_m + D_{m'}\Psi_{m1}}{D_m + D_{m'}} \quad J^{rk}_{m\ell} = -\frac{D_m D_{m'}}{h(D_m+D_{m'})}(\Phi_m - \Phi_{m'}).$$

we see the only difference that „α" replaces the diffusion constant D and $\epsilon\Phi$ replaces Φ. It can be shown [145] that in a finite uniform lattice

$$\alpha^k_{m\ell} \to D_k$$

and

$$\epsilon^k_{m\ell} \to 1,$$

and equations (4.79)–(4.78) tend to the FDM equations as $h \to 0$. Based on the above considerations, a coherent calculation scheme has been set up that has been implemented in the KARATE system [146] as one of the available options.

The reader may have observed that symmetry considerations simplify the calculations mostly in simple cases. Now, in the discussion of reactor lattices, more simplifications came from symmetries in a uniform lattice where a translation invariant basis leads to recognize the micro- and macro components in the solution. In a lattice made up from a number of cells, the result is less spectacular.

4.2.4. Homogenization methods

The goal of cell calculation is to find the parameters in the equation for the macroflux. As we have seen in the previous Subsection, the macroflux is obtained from a diffusion like equation even if the equation to be solved in a periodic structure is the transport equation. Early works relied on the principle used in the energy group approach, see Chapter 4 Section 4.1: if the terms in the equation for the macroflux have their respective physical meanings, then it is self-evident to determine the reaction rates in the cell and define the associated homogenized cross-section so that the reaction rate be preserved. Unfortunately, the diffusion constant does not exists also in the transport theory but we will see its definition below. Now we recall that the objective of cell homogenization is to get a simplified cell description hence a homogenization method. In principle we would need individual cross-sections for each cell, thus we should have create a parametrized cross-section library for each cell. Therefore, in a practical calculation the actual constants of each cell should have been looked up in a separate cell library[6]. Even if we store cell cross-sections for a given cell type[7] in a parametrized library, the production codes serving a power reactor spend 60-70 % of the time with looking up the actual parameters in the parametrized library. Power reactor calculation needs a few types of diffusion theory parameter sets with possible corrections for those cells located in a specific ambiance, e.g. in the immediate vicinity of a control rod or reflector.

The diffusion constant is especially problematic as it adheres to the streaming of neutrons, which is the only non-local phenomenon. Streaming is not only non-local but may be highly anisotropic. It is well known that the axial direction may completely differ from any radial direction concerning the streaming of neutrons. In a fast reactor, there exist specific directions along which the neutrons stream without restraint whereas frequent collisions slow the neutron flow in other directions. We have to remember also that a non-negligible fraction of the cells resides in a heterogeneous surroundings either because the neutron spectrum changes in a short distance or because of the large spatial gradient in the neutron flux. The coefficients derived in Section 4.2.3 of the present Chapter clearly indicate that in a heterogeneous lattice more is needed than a single set of diffusion parameters, see matrices $M_0, \mathbf{M}_1, M_2$ in (4.38) and $\epsilon^k_{ml}, \alpha^k_{ml}$ in (4.78) and (4.79).

What is the benefit of theoretical investigations in such a situation? Theory certainly provides insight into the problem and may point out the weakness of practical procedures, or, may offer improvements in reactor analysis codes that engineers need in practice to large amount of numerical work needed in practice.

In the previous subsections we have introduced two theoretical approaches: Larsen's asymptotic analysis and a method based on the so called gamma matrices. A good survey of homogenization methods is given by Deniz in the second volume of [5] handbook. Now we add further examples starting with the Benoist cross-section set, and the response matrices proposed by N. I. Laletin [53]. In transport theory, the Bloch functions are written as

$$\Phi(\mathbf{r}, E, \Omega) = u_B(\mathbf{r}, E, \Omega) e^{i\mathbf{Br}}, \tag{4.81}$$

only the periodic part of the Bloch function depends on the energy and the angle. Benoist's method expresses the solution with Bloch functions, the balance equation is expanded in a power series of B. The $O(B^2)$ cell integrated balance equation reads as

$$\left[\sum_k B_k^2 D_k^{BC} + \Sigma_a^{BC} - \frac{1}{k_{eff}} \nu \Sigma_f^{BC} \right] (u_0, 1) \approx 0(B^2). \tag{4.82}$$

[6]The number of cells is of the order 10^4, in a core it is the number of assemblies multiplied by the number of cells in an assembly.

[7]The number of cell types is a few times ten.

Superscript BC refers to the Benoist corrected coefficients.

$$D_k^{BC} = \frac{-(\boldsymbol{\nabla}\boldsymbol{\Omega} r_{cell,k} u_{1k}, 1)}{(u_0, 1)} \tag{4.83}$$

$$\Sigma_x^{BC} = \frac{(\Sigma_x(u_0 - (\mathbf{B}\mathbf{r}_{cell}(\mathbf{B}\mathbf{u}_1)) + \mathbf{B}\mathbf{u}_2\mathbf{B}) - u_0 \frac{(\mathbf{B}\mathbf{r}_{cell})^2}{2}, 1)}{(u_0, 1)} \tag{4.84}$$

Here subscript x refers to the type of the cross-section. The expansion of the periodic part of the Bloch function is written as

$$u_{\mathbf{B}} = u_0 + \mathbf{B}^+\mathbf{u}_1 + \mathbf{B}^+\mathbf{u}_2\mathbf{B} + \ldots \tag{4.85}$$

where $\mathbf{u}_1 = (u_{1x}, u_{1y}, u_{1z})$ is a vector, $\mathbf{u}_2 = u_{2ij}, i = 1,3; j = 1,3$ is a tensor. The space position is

$$\mathbf{r} = \mathbf{r}_0 + \mathbf{r}_{cell}, \tag{4.86}$$

here $\mathbf{r}_0$ is the position of the cell center, $\mathbf{r}_{cell}$ is the position inside the cell.

The Deniz-Gelbard diffusion coefficient

$$D_k^{DG} = -\frac{(u_0^+, \boldsymbol{\Omega}_k u_{1k})}{(u_0^+, \mathcal{P}u_0)} \frac{(1, \mathcal{P}u_0)}{(1, u_0)} \tag{4.87}$$

The Larsen diffusion coefficient

$$D_k^L = -\frac{(u_0^+, \boldsymbol{\Omega}_k u_{1k})}{(u_0^+, u_0)} \tag{4.88}$$

$$\Sigma_x^L = \frac{(u_0^+, \Sigma_x u_0)}{(u_0^+, u_0)} \tag{4.89}$$

The Benoist uncorrected diffusion coefficient

$$D_k^{BU} = -\frac{(1, \boldsymbol{\Omega}_k u_{1k})}{(1, u_0)} \tag{4.90}$$

$$D_k^{2BU} = -\frac{(1, \boldsymbol{\Omega}_k)}{(1, (u_0 + \mathbf{B}^+\mathbf{u}_2\mathbf{B}))} \tag{4.91}$$

$$\Sigma_x^{2BU} = \frac{(1, \Sigma_x(u_0 + \mathbf{B}^+\mathbf{u}_2\mathbf{B}))}{(1, u_0)} \tag{4.92}$$

The Benoist corrected diffusion coefficient

$$D_k^{BC} = -\frac{(1, \boldsymbol{\nabla}(\boldsymbol{\Omega}\mathbf{r}_{cell} u_{1k})}{(1, u_0)} \tag{4.93}$$

$$\Sigma_x^{2BC} = \frac{(1, \Sigma_x R_2)}{(1, u_0)} \tag{4.94}$$

$$R_2 = u_0 - (\mathbf{B}\mathbf{r}_{cell}(\mathbf{B}^+\mathbf{u}_1) + B^+ u_2 B - u_0 \frac{(\mathbf{B}\mathbf{r}_{cell})^2}{2}. \tag{4.95}$$

We have chosen an illustration from among the available homogenization recipes. A more complete list can be found in [5]. We mention only those equivalent homogeneous regions that are used in a number of places in the calculational method, for example in the resonance treatment.

4.3. Simplified boundary condition

4.3.1. Simplifications

The goal of the reflector calculation is the determination of the albedo in few (2-6) energy group diffusion theory. Normally ex-core materials contain no fissionable material, the physical process in the reflector is that fast neutrons leak out of the core, slow down in the reflector, and a fraction of the neutrons re-enters the core.

The reflector softens the spectrum, the fuel assemblies at the core-reflector boundary may feel that effect. The neutron flux in the core diminishes approaching the core edge. It is an option in the calculation to include a part of the reflector but the effect of the reflector albedo is so local that it does not justify the inclusion of the reflector into the power iteration.

The albedo boundary condition relates the entering current J_g^+ to the exiting current J_g^- as

$$J_g^- = \Gamma_{gg} J_g^+ + \sum_{g' \neq g} \Gamma_{gg'} J_{g'}^+. \tag{4.96}$$

Note that J_g^+ depends on core properties as it is the exiting current of the core, it exits from a fuel assembly at the core edge. The albedo matrix $\Gamma_{gg'}$ depends on the material composition and geometry of the ex-core region, shortly called reflector.

At the boundary of the reactor a boundary condition is to be applied. This is usually a local albedo that is an input of the core calculation. To learn the albedo, a detailed calculation of the region surrounding the core is carried out. Features of that calculation are:

- The geometry is irregular because structural elements, holes etc. make it irregular. In the region above the reactor core the structure is only known by-and-large, because control rod drives, cables, in some cases moving parts make that area complex. Often the albedo is obtained from a fitting in the lack of detailed information. Note that the leakage from the core directly influences the reactivity and hence the safety.
- The material composition of the elements placed around the zone are often not given by the vendor (such a problem is the isotope composition of the steel elements).
- A part of the ex-core region also includes coolant. If the regulation uses boron, the albedo varies with the progress of the fuel cycle. That may require repeated recalculations of the albedo.

To determine the albedo matrix, the few group diffusion equation has to be solved with the same number of energy group used in the core calculation. To carry out the diffusion calculation, few group cross-sections of the 5-10 mean-free-path reflector region should be determined in an approximate regular geometry. The boundary condition is the given entering current at the faces of the fuel assemblies. Those entering currents are get from a core calculation. When the migration of the neutrons is taken into account, we have to label also the boundary faces and several faces may contribute to the reflector albedo:

$$J_{gk}^- = \sum_{\ell} \left[\Gamma_{gg,k\ell} J_{g\ell}^+ + \sum_{g \neq g'} \Gamma_{gg',k\ell} J_{g'\ell}^+ \right]. \tag{4.97}$$

That calculation accounts for the neutron wandering.

The second method is a Monte Carlo calculation in which neutrons are randomly started from the core edge, and the score is the number of neutrons returning to the reactor boundary.

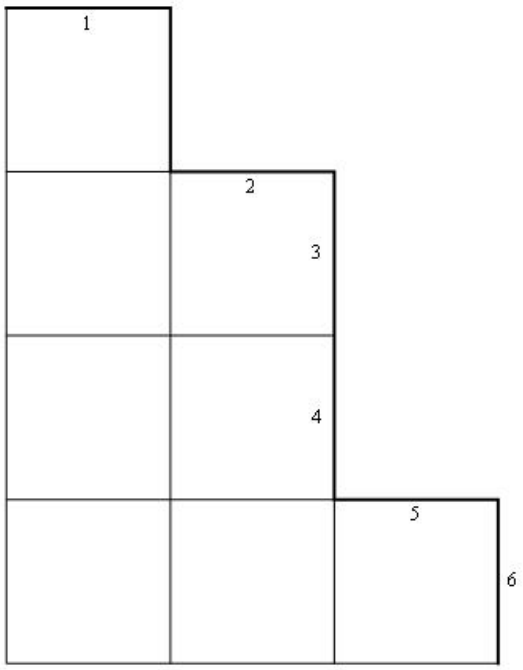

4.1. ábra. Core Reflector Boundary (PWR)

In a Monte Carlo code the irregular geometry can be implemented easily. It should be mentioned, that there are large regions, e. g. the top of the reactor, which are so complicated, that the corresponding albedo is fitted to the startup measurements.

A part of a PWR core-reflector boundary is shown in Fig. 4.1. Face pairs 1,2; 2,3; 4,5; and 5,6 may be coupled because the neutrons exiting near the joint corner may return through either face. The extent of coupling depends on the spatial distribution of the exiting currents along a given face. The face-face coupling may be also of importance in hexagonal fuel assemblies.

In connection with the reflector albedo, we mention the possibility of excluding the control rods (see Chapter 2) from the reactor calculation. The area of the control rod needs small discretization step, that slows down the calculation. When a suitable vicinity of the control rod is calculated separately and its response is calculated for example by a Monte Carlo code, we can determine the albedo and that albedo is usable to exclude the control rod region from the calculation.

4.4. Problems

1. What is a reasonable neutron spectrum to average cross-sections in the following energy ranges: high energies, slowing down, resonances, thermal energies?

2. How to determine the group cross-section for a mixture of two nuclei when one varies slowly, the other has a resonance in the energy range under consideration?

3. Estimate the error caused by the approximate spectrum used in group condensation!

4. Which core geometry assures the minimum leakage from among the following geometries: cubic, cylindrical, spherical?

5. With the geometry fixed, which boundary condition assures the maximum k_{eff}: white, black, albedo, periodical?

6. What is the benefit of surrounding the core by reflector? What are the ideal features of the reflector?

7. A burning poison is a material with high absorbtion cross-section in the thermal groups. What is the benefit of adding burning poison to the fuel?

8. During energy production, the fissionable material is consumed, the neutron absorbing fission products accumulate. How to maintain the critical state during the fuel cycle?

9. Where should we measure the neutron flux in the core? How to assure that the local power is everywhere under the prescribed limit?

10. A neutron impinges the core of a critical reactor. What will happen?

11. In which part of the core is applicable the asymptotic approximation? How would you determine by measurements the asymptotic part of the core?

12. The material composition above the core is not well known. How would you deal with the upper boundary of the core?

13. What kind of corrections should be introduced if the coupling between faces of fuel assemblies is not negligible? How can we estimate the improvement caused by the introduced correction?

5. fejezet

Neutron spectrum

The angular flux depends on the position, the energy, the angle of the neutron velocity, and the time. The term spectrum refers to the neutron distribution in the energy variable. Various reactors may have different spectra, which depends on the fuel and the moderator, see Chapter 2 for details. The neutron energy in a reactor usually varies between 10 MeV and 0 eV. In an ADS, the spallation source provides neutrons over 10 MeV. In PWRs and BWRs the spectrum is thermal, which means that the majority of the neutrons in the core has an energy close to the thermal range. In a fast breeder reactor, however, the majority of the neutrons has a high energy.

The usual treatment of the energy variable is the multigroup treatment, the number of energy groups may vary from one to a million. The extremely large group number is typically connected to the resonance region, where the cross-sections of the resonance nuclei may vary very fast. The spectrum is subdivided into four larger energy regions. The boundaries of the regions are not precisely determined, as they are connected to the features of the neutron-nucleus collision, and because the number of nuclei is very large, their behavior may be different.

In the fast region, the neutron energy falls into the $10\ MeV \leq E \leq 0.1\ MeV$ interval[1]. There the cross-sections are usually small and vary slowly with the energy. Consequently the neutron mean free path is large, and the coupling between fuel rods is provided mostly by fast neutrons. There is a difference between the fuel and coolant regions, the heavy elements in the fuel possess larger cross-sections than the coolant, which is usually water. In LWRs, the heterogeneity effect is small enough to permit using volume averaged cross-sections. Some 10-15% of the power originates from fast fission even in thermal reactors, the power distribution is smooth. Some heavy elements have resonance lines in the fast region but the Doppler broadening of the resonance line is proportional to the neutron temperature, i.e. with $\sqrt{E}$. Because of the Doppler broadening, the resonance lines usually overlap.

Elastic and inelastic scattering, and the associated slowing down features the lower part of the fast range, which sometimes is called slowing down region. The slowing down process determines the spectrum of the neutrons entering the next region, called resonance region.

The variation of cross-sections may reach several orders of magnitude in the resonance region. Instead of cross-sections resonance integrals are used in that range. The rapidly varying cross-sections cause problems not only in the generation of resonance integrals, see Section 5.3 in the present Chapter, but also in use in core calculations. Namely, in this area the number of energy groups may be in the order of hundred thousands. Between

[1]Some authors define the fast region as $10\ MeV \leq E \leq 5\ keV$, see [57]

resonances, the mean free path is relatively large but smaller than in the fission region. In a LWR, approximately 10-15 % of the reactor power is produced in the resonance region, a part of it during slowing down.

In the thermal range, the neutron energy is comparable to the kinetic energy of a nucleus therefore up-scattering is possible, furthermore the energy of the chemical binding is also close to the kinetic energy of the neutron. The limit between the resonance and the thermal region is loosely defined, usually some frequently encountered resonance lines of heavy isotopes are excluded from the thermal region. The upper limit of the thermal region is usually 0.625 eV or 1 eV, the lower limit is zero. The cross-sections vary smoothly, and larger than in the resonance region. Therefore the neutron mean free path is shorter, the neutron flux may vary faster in space. In LWRs, 70-80% of the energy is produced in the thermal range.

5.1. Fast neutrons

The maximum energy of neutrons emerging from fission is appr. 10 MeV. The neutron-nucleus collision results in nuclear reaction, the available nuclear reactions depend on the nucleus and the energy of the neutron. The first excited state of heavy nuclei is about $0.1MeV$, the light nuclei have higher excitation energies, the first niveau is about 1 MeV. Neutrons having more energy than the first excited state can lose part of their energy in inelastic collisions, thus in the range $10\ MeV - 0.1\ MeV$ the inelastic collisions may play an important role, but below that energy range the elastic scattering dominates. Since the fission cross-section is large only in the thermal energies, to sustain the chain reaction a portion of the neutrons must reach the thermal energy and in the slowing down of neutrons the elastic scattering is important.

In the energy range $E > 0.1MeV$ the total fission rate is about $\sim 10 - 25\%$ depending on the fuel type and the lattice. The accuracy of the calculated reaction rates depends on the approximations used in the calculation of the leakage, the scattering anisotropy, and the slowing down. In tight lattices, the void reactivity coefficient can be positive under specific conditions, therefore the fast energy range is important also from the point of view of safety. The fast neutrons have a non-negligible role also in the radiation damage of the reactor vessel.

The above mentioned aspects require a large number of energy groups in the flux calculation. In some codes the number of energy groups is 144 in the fast neutron range. The condensation of the energy groups to be used in spectral codes also requires attention. In some reactor types (such as PWRs), the fuel lattice is only slightly heterogeneous, and in the fast energy range constant flux can be applied in the cell homogenization. Flux ratios may be computed by cross-sections averaged by the flux ratios in an infinite homogeneous medium, that simplified procedure has only a slight effect on the k_{eff}.

In the cross-section calculation, the fission spectrum is applicable. It is taken into account that the various fissionable isotopes may have different fission spectrums. Furthermore, the spectrum of prompt neutrons and that of the delayed neutrons are different. The prompt neutron spectrum is usually approximated by Watt's analytical expression [165][p. 142]:

$$f_p(E) = C_1 \exp\left(-\frac{E}{C-2}\right) \sinh\left(\sqrt{C_3 E}\right), \tag{5.1}$$

where C_1, C_2, C_3 are fitted constants. For ^{235}U the constants are

$$C_1 = 0.453 \quad C_2 = 0.965 \quad C_3 = 2.29 \tag{5.2}$$

and E is in MeV units. A portion of the neutrons is released from the fission products after further nuclear reactions, see Section 7.1 in Chapter 7 for details. In the core design methods, the static calculation is the starting point, the static fission spectrum is a combination of the prompt spectrum f_p and the delayed spectra $f_i(E), i = 1, \ldots, 6$. Denote the fraction of the i-th delayed spectrum β_i, then the static spectrum is taken as

$$f_s(E) = (1 - \sum_{i=1}^{6} \beta_i) f_p(E) + \sum_{i=1}^{6} \beta_i f_i(E). \tag{5.3}$$

In static calculations that spectrum should be used as the fission spectrum $f(E)$ in the transport equation 3.132 and the diffusion equation (6.97).

5.2. Slowing down

The neutron spectrum can be determined from the neutron balance at energy E. In a large, homogeneous material the neutron balance is

$$\begin{aligned} \left(-D(E)B^2 + \Sigma_t(E)\right)\phi(E) = &\int_0^\infty \Sigma_{s0}(E' \to E)\phi(E')dE' \\ &+ \int_0^\infty \Sigma_{in}(E' \to E)\phi(E')dE' \\ &+ f(E)\int_0^\infty \nu\Sigma_f(E')\phi(E')dE'. \end{aligned} \tag{5.4}$$

Here we assumed isotropic scattering and no external source is present. The inelastic scattering is also present but we can treat it only by numerical methods, so we are going to neglect it[2]. We see from (5.4) that the spectrum depends on the cross-sections. Below we present a model for the determination of the slowing down kernel for the case when the scattering is elastic.

In the collision the energy E and the momentum $\mathbf{p}$ are conserved[166]. First we quote the general discussion of the collision. We consider the collision of two particles, their respective mass is m_1 and m_2, their respective speed is $\mathbf{v}_1$ and $\mathbf{v}_2$, their energy is $E_i = \mathbf{p}_i^2/(2m_i), i = 1, 2$. Their respective momentum after collision is $\mathbf{p}_i', i = 1, 2$ and energy $E_i', i = 1, 2$. We introduce the total mass

$$M_t = m_1 + m_2 \tag{5.5}$$

and the reduced mass m_r

$$m_r = \frac{m_1 m_2}{m_1 + m_2}, \tag{5.6}$$

the total momentum $\mathbf{P}$:

$$\mathbf{P} = \mathbf{p}_1 + \mathbf{p}_2, \tag{5.7}$$

the relative momentum $\mathbf{p}$:

$$\mathbf{p} = \frac{m_2\mathbf{p}_1 - m_1\mathbf{p}_2}{m_1 + m_2} = m_r(\mathbf{v}_1 - \mathbf{v}_2) \tag{5.8}$$

[2]Although in practical calculations (for example in a fast reactor) the inelastic scattering should be accounted for.

that is, the relative momentum equals the reduced mass multiplied by the relative velocity. The particle energy and momentum is expressed by the relative momentum $\mathbf{p}$ and total momentum $\mathbf{P}$ as

$$\mathbf{p}_1 = \frac{m_1}{M}\mathbf{P} - \mathbf{p}; \;\; \mathbf{p}_2 = \frac{m_2}{M}\mathbf{P} + \mathbf{p}, \tag{5.9}$$

the total energy expressed with $\mathbf{P}$ and $\mathbf{p}$ is

$$E = \frac{P^2}{2M} + \frac{p^2}{2m_r}. \tag{5.10}$$

In an elastic collision the total momentum

$$\mathbf{P} = \mathbf{P}' \tag{5.11}$$

remains unaltered and the absolute value of the relative momentum also remains unaltered:

$$|\mathbf{p}| = |\mathbf{p}'|. \tag{5.12}$$

That is, the collision only rotates the relative momenta $\mathbf{p}$. After the scattering in the center of mass coordinate system $|\mathbf{p}_1|$ and $|\mathbf{p}_2|$ do not change. It follows from (5.8) that in the center of mass coordinate system (CMS), the momentum of each mass before and after collision is the same, m_1 and m_2 move in opposite directions, the velocities of m_1 and m_2 are inversely proportional to the respective mass. Now we apply the kinematics of the elastic collision to the neutron-nucleus collision. The below given discussion follows [165].

Let a neutron of unit mass have velocity v_1 in the laboratory coordinate system (LCS), let the neutron collide with a nucleus of mass A. Since the kinetic energy of the nucleus due to the thermal motion is cca. 0.025 eV at room temperature, in the slowing down energy range the velocity of the nucleus may be neglected. The kinetic energy of the neutron is $E = v_n^2/2$ its momentum is $\mathbf{p} = \mathbf{v}_1$. The velocity v_c of the center of mass is parallel to $\mathbf{v}_1$ and its absolute value is

$$\mathbf{v}_c = \frac{\mathbf{v}_1}{A+1}. \tag{5.13}$$

We denote the scattering angle in the LCS by θ. The scattering measurements refer to the center of mass coordinate system (CMS), thus we need the scattering angle also in the LCS, that angle between the incident neutron velocity v_n' and exiting velocity v_n is Θ.

In the LCS the nucleus velocity before scattering is

$$-\mathbf{v}_c, \tag{5.14}$$

after scattering v_a, the neutron velocity after scattering is v_2. It follows from (5.11) and (5.12) that

$$v_n = v_1 - v_c = \frac{Av_1}{A+1} \tag{5.15}$$

and

$$v_a = v_c = \frac{v_1}{A+1}. \tag{5.16}$$

Since the transformation from the CMS to the LCS means adding the center of mass velocity, we have

$$\mathbf{v}_2 = \mathbf{v}_n + \mathbf{v}_c, \tag{5.17}$$

using (5.13) and (5.15) we get

$$\mathbf{v}_2^2 = |\mathbf{v}_n + \mathbf{v}_c|^2 = v_n^2 + v_c^2 + 2v_n v_c \cos\Theta = \frac{v_1^2\left(A^2 + 2A\cos\theta + 1\right)}{(A+1)^2}. \tag{5.18}$$

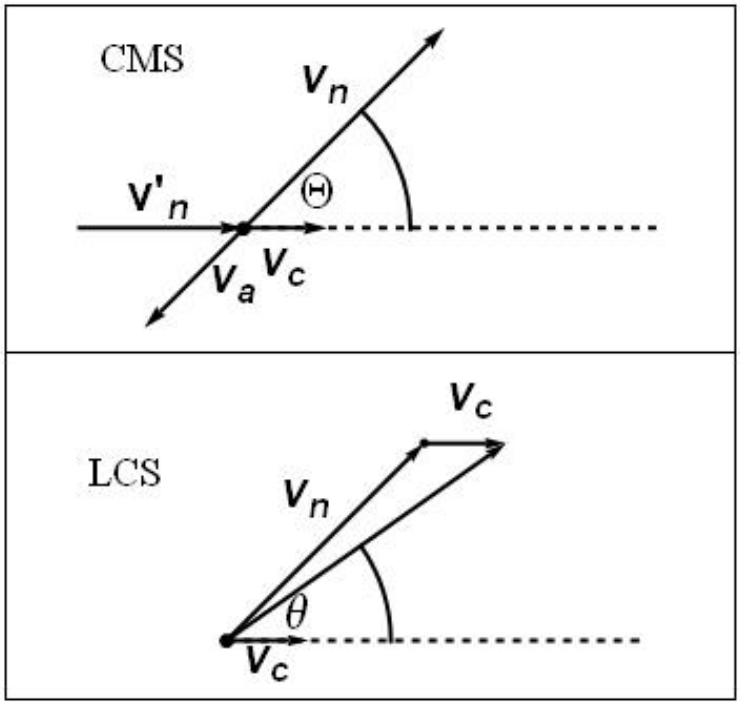

5.1. ábra. Slowing down by elastic collisions in LCS and CMS

We are interested in the neutron energy before E_1 and after E_2 collision, which is given by

$$\frac{E_2}{E_1} = \frac{v_2^2}{v_1^2} = \frac{1}{2}\left[(1+\alpha) + (1-\alpha)\cos\Theta\right], \tag{5.19}$$

where we have introduced

$$\alpha = \frac{(A-1)^2}{(A+1)^2}. \tag{5.20}$$

As $-1 \leq \cos\Theta \leq +1$, the neutron energy E_2 after collision falls into the interval

$$E_1 \geq E_2 \geq \alpha E_1. \tag{5.21}$$

Let the coordinate system be placed so that in the angular variable $\mathbf{\Omega}$ the φ variable be in the plane perpendicular to the neutron-nucleus axis and the Θ angle between the neutron-nucleus axis and the direction of the scattered neutron. When the scattering is isotropic, the scattering angle $\mathbf{\Omega}$ is distributed as

$$\frac{d\mathbf{\Omega}}{4\pi} = \frac{1}{2} d\cos\Theta. \tag{5.22}$$

Equation (5.17) is the key to connect Θ and θ. Comparing the x components, using (5.15) we find

$$\cos\theta = \frac{A\cos\Theta + 1}{\sqrt{(A^2 + 2A\cos\theta + 1)}}.$$

When the scattering is isotropic, the average scattering angle is

$$< \cos\theta >= \frac{1}{2}\int_{-1}^{+1} \sin\theta d\cos\Theta = \frac{2}{3A}, \tag{5.23}$$

suggesting that the scattering on small nuclei is rather un-isotropic than scattering on heavy nuclei.

The energy loss in elastic collisions is inversely proportional to the energy before collision. The average logarithmic energy decrement per collision is independent of the energy:

$$\xi = \int_{\alpha E_1}^{E_1} \ln\left(\frac{E_1}{E_2}\right) g(E_1, E_2), \tag{5.24}$$

where $g(E_1, E_2)$ the probability that the neutron suffering a collision at energy E_1 will have an energy in the interval $E_2, E_2 + dE_2$.

$$g(E_1, E_2) = \begin{cases} \frac{1}{E_1(1-\alpha)} & \alpha E_1 \leq E_2 \leq E_1 \\ 0 & \text{otherwise.} \end{cases} \tag{5.25}$$

The integral for isotropic scattering takes the form of

$$\xi = 1 + \frac{\alpha}{1-\alpha}\ln\alpha. \tag{5.26}$$

The neutron balance equation with isotropic scattering is

$$\left(D(E)B^2 + \Sigma_t(E)\right)\phi(E) = \int_E^{E/\alpha} \Sigma_s(E')\phi(E')\frac{dE'}{E'(1-\alpha)} + S(E). \tag{5.27}$$

The larger is ξ the less number of collisions is needed for the neutron to reach the thermal energy. The probability of absorption is $\Sigma_a/(\Sigma_s + \Sigma_a)$. The quality of a moderator is characterized by the (macroscopic) slowing down power and the (macroscopic) absorption cross-section. A good moderator has large slowing down power and small absorption cross-section. Another characteristics of the slowing down property is the moderating ratio:

$$\frac{\xi\Sigma_s}{\Sigma_a}. \tag{5.28}$$

The average number of collisions to thermalize a neutron of 2 MeV energy to 0.025 eV is

$$\frac{\ln\frac{2\cdot 10^6}{0.025}}{\xi} = \frac{18.2}{\xi}. \tag{5.29}$$

Table 5.1. gives examples[165][p. 148] for the slowing down properties of various materials.

Table 5.1 clearly shows the salient properties of heavy water and the large number of collisions needed for the neutron to slow down on a heavy nucleus.

The logarithmic energy loss suggests introducing a logarithmic energy scale. Following the tradition, we introduce the lethargy u by the definition

$$u = \ln\left(\frac{E_0}{E}\right), \tag{5.30}$$

where E_0 is an arbitrary reference energy, usually the highest energy in the reactor, usually $E_0 = 10\ MeV$ is chosen. Note, that in the new variable the neutron spectrum is slightly different:

$$\phi(u) = \phi(E)\left|\frac{dE}{du}\right| = \phi(E)E. \tag{5.31}$$

5.1. táblázat. Moderating properties of some nuclei

Moderator	H_2O	D_2O	^9Be	^{12}C	^{238}U
A	1	2	9	12	238
α	0	0.111	0.640	0.716	0.983
ξ	1.0	0.725	0.209	0.158	0.0084
$18.2/\xi$	18	25	87	115	2172
$\xi\Sigma_s$	1.3	0.08	0.15	0.061	0.04
$\xi\Sigma_s/\Sigma_a$	61	1538	125	190	0.16

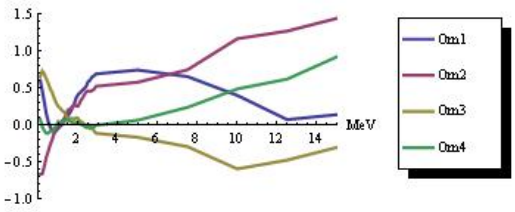

5.2. ábra. Energy dependence of $\omega_\ell, \ell = 1, \ldots, 4$ of deuterium

When the scattering is not isotropic in the CMC, instead of (5.22) the angular distribution of the scatted neutron is more general:

$$\frac{d\mathbf{\Omega}}{4\pi} = \chi(\cos\Theta) d\cos\Theta, \tag{5.32}$$

and the $\chi(\Theta)$ function is expanded into Legendre polynomials:

$$\chi(\cos\Theta) = \frac{1}{2}\sum_\ell \omega_\ell P_\ell(\mu), \tag{5.33}$$

where $\mu = \cos\Theta$. As an example, in Figure 5.2 the anisotropic components $\omega_\ell, \ell = 1, \ldots, 4$ are displayed as the function of the neutron energy E. The deuterium is important in the CANDU reactors, where the moderator is heavy water. The anisotropy influences the logarithmic energy decrement ξ, when the scattering is linearly anisotropic:

$$\xi = \int_{\alpha E}^{E} g(E' \to E) \ln\left(\frac{E'}{E}\right) dE' = \xi_0 - 3\bar{\mu}\left[\frac{\alpha\ln\alpha}{(1-\alpha)^2} + \frac{1+\alpha}{2(1-\alpha)}\right] \tag{5.34}$$

and the mean value of the scattering angle

$$\bar{\mu} = \frac{\omega_1}{3}. \tag{5.35}$$

In (5.34), ξ_0 is the logarithmic energy decrement for isotropic scattering (5.26). In the LCS, the mean value of the scattering angle is

$$\overline{\cos\theta} = \frac{1}{2}\int_{-1}^{+1} \frac{A\mu+1}{\sqrt{A^2+2A\mu+1}}\chi(\mu)d\mu = \frac{2}{3A} + \mu\left(1 - \frac{3}{5A^2}\right) \tag{5.36}$$

In general, $\bar{\mu} > 0$, consequently (5.34) shows that the anisotropy makes neutron slowing down less effective. That effect manifests at large neutron energies where the inelastic scattering gives a considerable contribution.

In the lethargy variable, the lethargy distribution of the scattered neutron in an isotropic scattering is written as

$$g(u_1,u_2)=\begin{cases}\frac{e^{u_1-u_2}}{1-\alpha} & u_1\le u_2\le u_1+\epsilon\\ 0 & u_2>u_1+\epsilon.\end{cases} \tag{5.37}$$

Here we introduced

$$\epsilon=-\ln\alpha. \tag{5.38}$$

In the lethargy variable the neutron balance takes the following form:

$$\left(D(u)B^2+\Sigma_t(u)\right)\phi(u)=\int_{u-\epsilon}^{u}\Sigma_s(u')\phi(u')\frac{e^(u'-u)}{1-\alpha}+S(u). \tag{5.39}$$

Note, that the leakage term has been written as $-D(u)B^2$ because the eigenvalues of the Laplace operator are negative in a finite volume.

5.2.1. Placzek transients

Relying on the above derived scattering kernel, we solve [165] the slowing down equations. To approach our goal gradually, first let us consider the no absorption case without leakage. We use the lethargy variable throughout the derivation. Our starting point is the neutron balance that now is

$$-\Sigma_s(u)\phi(u)+\int_{u-\epsilon}^{u}\Sigma_s(u')\phi(u')du'\frac{e^{u'-u}}{1-\alpha}du'+\delta(u)=0. \tag{5.40}$$

Note that the source is mono-energetic, it emits neutrons with lethargy $u=0$. The solution to (5.40) is singular at $u=0$, and it is convenient to use the scattering density $F_s(u)=\Sigma_s(u)\phi(u)$ as dependent variable. With the new dependent variable the balance is

$$F_s(u)-\int_{u-\epsilon}^{u}F_s(u')\frac{e^{u'-u}}{1-\alpha}du'=\delta(u). \tag{5.41}$$

The second term is the representation of the scattering operator $\mathcal{S}$ in the actually used model so now

$$(1-\mathcal{S})F_s(u)=\delta(u). \tag{5.42}$$

We get the solution by multiplying (5.42) by the inverse of $(1-\mathcal{S})$, where we immediately use the Neumann-series

$$F_s(u)=(1-\mathcal{S})^{-1}\delta(u)=\sum_{k=0}^{\infty}\mathcal{S}^k\delta(u). \tag{5.43}$$

The terms in the series have their respective physical meaning, $\mathcal{S}_k\delta(u)$ is the k-times collided flux. Note that the $k=0$ is the direct contribution from the flux, the first collided flux $\mathcal{S}\delta(u)$ is spread over the interval $0\le u\le\epsilon$, consequently is discontinuous at $u=\epsilon$. We get after direct calculation

$$\mathcal{S}\delta(u)=\int_{u-\epsilon}^{u}\delta(u)\frac{e^{u'-u}}{1-\alpha}du'=\frac{e^{-u}}{1-\alpha}. \tag{5.44}$$

After each collision the domain where $\mathcal{S}^k\delta(u)\neq 0$ increases by ϵ. The second order term is

$$\mathcal{S}^2\delta(u)=\int_{0}^{u}\mathcal{S}_1\delta(u')\frac{e^{u'-u}}{1-\alpha}du',\ \ 0\le u\le\epsilon \tag{5.45}$$

using (5.44), the result is

$$\mathcal{S}^2\delta(u) = \frac{1 - e^u - e^u u}{(1-\alpha)^2}. \tag{5.46}$$

In the interval $\epsilon \le u \le 2\epsilon$ the solution is

$$\begin{aligned} \mathcal{S}^2\delta(u) &= \int_\epsilon^{u-\epsilon} \frac{1-e^{-u'}}{1-\alpha}\frac{e^{u'-u}}{1-\alpha}du' \\ &= \frac{e^{-u}}{(1-\alpha)^2}\left(e^{u-\epsilon} - e^\epsilon + u - 2\epsilon\right). \end{aligned} \tag{5.47}$$

Observe that $\mathcal{S}\delta(u)$ is discontinuous at $u = \epsilon$, but $\mathcal{S}^2\delta(u)$ is continuous, although its derivative is discontinuous. The tendency continues, the domain of $\mathcal{S}^k\delta(u)$ is $(0, k\epsilon)$, it is continuous at $u = i\epsilon, i = 1, \ldots, k-1$ and its $k-1$-th derivative ($k \ge 1$) is also continuous. The behavior of the collision density $F_s(u)$ as well as the neutron flux $\Phi(u)$ is called Placzek transients. They appear at energies (lethargies) close to the source energy (lethargy). As the neutrons suffer more and more collisions, their distribution tends to an asymptotic value which is independent of the source energy.

Let us determine the number of neutrons per unit time, in unit volume, passing lethargy u during the slowing down process. Those neutrons collide at lethargy $u' < u$ and after the collision their lethargy u'' is smaller than u. Assuming isotropic scattering, we get

$$q(u) = \int_{u-\epsilon}^{u} F_s(u') \left[\int_u^{u'+\epsilon} \frac{e^{u'-u''}}{1-\alpha}du''\right] du'. \tag{5.48}$$

$q(u)$ is called slowing down density. At small lethargies, i.e. far from the source energy, the collision density is constant: $F_s(u) = c$, then

$$q(u) = c\xi.$$

If there is no absorption, every neutron passes lethargy u then $q(u) = 1$ and the asymptotic collision density is

$$\lim_{u\to\infty} F_s(u) = \frac{1}{\xi}. \tag{5.49}$$

Note that the slowing down density (5.48) does not involve $\mathcal{S}\delta(u)$, the contributions of the first collided neutrons so for $u < \epsilon$ (5.48) has to be corrected by the following additive term:

$$\int_u^\epsilon \frac{e^{-u'}}{1-\alpha}du'. \tag{5.50}$$

In the energy variable, the asymptotic flux is

$$\phi(E) = \frac{1}{\xi\Sigma_s(E)E}, \tag{5.51}$$

where we have used (5.31).

We introduce the notation $\psi_k(u)$ for the flux of neutrons having suffered k collisions, thus

$$\psi_0 = \delta(u); \quad \psi_1(u) = \mathcal{S}\delta(u); \quad \psi_2(u) = \mathcal{S}^2\delta(u), \ldots \tag{5.52}$$

and the neutron flux is

$$\phi(u) = \sum_{k=0}^{\infty} \psi_k(u). \tag{5.53}$$

$\psi_k(u)$ contributes only to $\Phi(u)$, $0 \le u \le k\epsilon$. The collision density is $F_s(u) = \Sigma_s(u)\phi(u)$ thus the collisions density can be give. Below we quote [165][p.153] the collision densities for $0 \le u \le 3\epsilon$.

$$F_s(u) = \frac{1}{1-\alpha}\exp\left(\frac{u\alpha}{1-\alpha}\right) \quad 0 \le u < \epsilon \tag{5.54}$$

$$F_s(u) = \frac{1}{1-\alpha}\exp\left(\frac{u\alpha}{1-\alpha}\right)(a_{11} + a_{12}(u-\epsilon))\,\epsilon \le u < 2\epsilon \tag{5.55}$$

$$F_s(u) = \frac{1}{1-\alpha}\exp\left(\frac{u\alpha}{1-\alpha}\right)\left(a_{21} + a_{22}(u-2\epsilon) + a_{23}(u-2\epsilon)^2\right)2\epsilon \le u < 3\epsilon. \tag{5.56}$$

Before we deal with the determination of the constant, give an alternative form of the slowing down equation (5.41). We separate the singular part[3] from the collision density:

$$F_s(u) = \delta(u) + \mathrm{F}_s(u) \tag{5.57}$$

and substituting this form of the slowing down density into (5.41), we get the following equation for the non-singular part of the collision density

$$\mathrm{F}_s(u) = \int_{u-\epsilon}^{u} \mathrm{F}_s(u')\frac{e^{u'-u}}{1-\alpha}du' + S_0(u), \tag{5.58}$$

where $S_0(u)$ differs from zero only on the interval $0 \le u \le \epsilon$ and there

$$S_0(u) = \frac{e^{-u}}{1-\alpha}. \tag{5.59}$$

Upon differentiation of equation (5.58) we get the following retarded differential equation:

$$\frac{d\mathrm{F}_s(u)}{du} = \frac{\alpha}{1-\alpha}\left[\mathrm{F}_s(u) - \mathrm{F}_s(u-\epsilon)\right]. \tag{5.60}$$

The point $U = \epsilon$ is excluded from the domain of (5.60) because there $S_0(u)$ is discontinuous. We get from (5.58) the initial condition

$$\lim_{u\to 0}\mathrm{F}_s(u) = \frac{1}{1-\alpha}. \tag{5.61}$$

Equation (5.60) can be solved recursively, firstly on the interval $0 < u < \epsilon$, secondly on the $\epsilon < u < 2\epsilon$ etc. On the left of the interval we recur to the integral equation and substituting $u = \epsilon$ in (5.58) we get

$$\begin{aligned}\lim_{u\to\epsilon}\mathrm{F}_s(u) &= \int_0^{\epsilon}\mathrm{F}_s(u')\frac{e^{u'-\epsilon}}{1-\alpha}du' \\ &= \frac{\alpha}{1-\alpha}\left[\exp\left(\frac{\epsilon}{1-\alpha}\right) - 1\right].\end{aligned} \tag{5.62}$$

The determination of the a_{ij} constants is left to the Reader as an exercise. The Placzek transients for four moderator types are shown in Fig. 5.3. The flux is shown in $\xi\Phi(u)$ units, the lethargy in ϵ unit for each scatterer nuclei.

[3]The notation $\mathrm{F}_s(u)$ differs only slightly from the $F_s(u)$ notation used for the collision density.

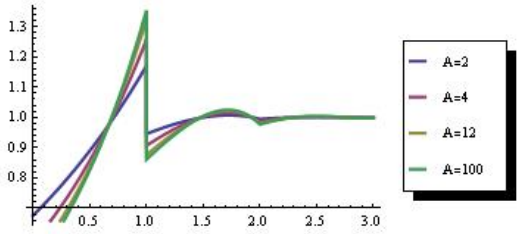

5.3. ábra. Placzek transients for four nuclei

The analysis of the slowing down process has led to the following conclusions:

1. The slowing down process has a transient energy (or lethargy) range, and an asymptotic range. The transient range in lethargy is a few times ϵ wide, after that comes the asymptotic range. The logarithmic energy decrement ξ is characteristic of the kinematics of the slowing down process. ξ depends on the mass number of the scatterer nucleus and the anisotropy of the scattering process. Further key parameters of the scattering are the $\overline{\cos\Theta}$, the mean value of the scattering angle and the slowing down density $q(u)$.

2. In the asymptotic range there is a simple relationship connecting the slowing down density and the neutron flux. This relationship can be used in the solution of the transport equation, the spectrum of the asymptotic flux varies as $1/E$ because $\Sigma_s(R)$ varies rather slowly with the energy. If the Placzek transients would not occur, we would have finished the discussion of slowing down. Unfortunately this can be done only for slowing down on hydrogen, there $\alpha = 0$ and the neutron may lose all its energy in a single collision. The slowing down on hydrogen can be solved analytically [2].

3. In the general case, we have to establish a relationship between the kinematics of the scattering and the flux. As we have seen, that relationship is exact in the asymptotic energy region and in hydrogen. Therefore we have to put up with approximate models in every other case. As we will see in the next two Sections, there are reasonable approximations both in the resonance region and in the thermal range.

4. The models to be introduced should depend on the mass of the scatterer nuclei. Not only the possible excitation energies of the scatterer, the anisotropy of the scattering process call for such a distinction but the fact that the slowing down on various nuclei is tractable independently offers seeking separate models for light nuclei.

5.2.2. Slowing down in the general case

In the general case[4], the neutron balance takes the form of

$$\Sigma_t(u)\Phi(u) = \int_{u-\epsilon}^{u} \Sigma_s(u')\Phi(u')\frac{e^{u'-u}}{1-\alpha}du' + Q(u). \tag{5.63}$$

In the energy range where $Q(u) = 0$, the neutrons slowing down at u but not slowing further at $u + du$ must be absorbed thus

$$\frac{dq(u)}{du} = -\Sigma_a(u)\Phi(u). \tag{5.64}$$

[4]The present Subsection follows [165].

If we have an easy to handle relationship between the flux, which is the key parameter in the neutron balance, and the slowing down density, which is a key parameter in the slowing down process, we are able to change the formalism for that variable which is more advantageous. The exact solution for the hydrogen moderator gives

$$q(u) = \xi \Sigma_t(u) \Phi(u), \tag{5.65}$$

and suggests seeking an approximate formula as

$$q(u) = \left(a\Sigma_a(u) + b\Sigma_s(u)\right) \Phi(u). \tag{5.66}$$

Substituting (5.66) into (5.64), we immediately obtain a simple differential equation for the slowing down density, its solution is:

$$q(u) = \exp\left[- \int_0^u \frac{\Sigma_a(u')}{a\Sigma_a(u') + b\Sigma_s(u')} du' \right], \tag{5.67}$$

but if we eliminate $q(u)$ using (5.66), we obtain a differential equation for the flux, its solution is

$$\Phi(u) = \frac{1}{a\Sigma_a(u) + b\Sigma_s(u)} \exp\left[- \int_0^u \frac{\Sigma_a(u')}{a\Sigma_a(u') + b\Sigma_s(u')} du' \right]. \tag{5.68}$$

For the neutron balance, it is important to estimate the fraction of neutrons that reach a given lethargy u, which is

$$p(0 \to u) = 1 - \int_0^u \Sigma_a(u') \Phi(u') du', \tag{5.69}$$

and p is called resonance escape probability for the absorption occurs mostly at the resonance lines of heavy nuclei. By direct calculation we get

$$p(0 \to u) = \exp\left[- \int_0^u \frac{\Sigma_a(u')}{a\Sigma_a(u') + b\Sigma_s(u')} du' \right]. \tag{5.70}$$

Comparing (5.70) and (5.67) we conclude that

$$p(0 \to u) = q(u). \tag{5.71}$$

Below we discuss three slowing down models. In order to get a relationship between the slowing down density and the flux, we return to the definition (5.48) of slowing down density but this time in a more general formalism. We are going to use the general form of the scattering law (5.37) and rewrite (5.48) as

$$q(u) = \int_{u-\epsilon}^{u} \Sigma_s(u') \Phi(u') \int_u^{u'+\epsilon} g(u' \to u'') du'' du'. \tag{5.72}$$

The $g(u' \to u'')$ scattering law has the following property:

$$g(u' \to u'') = g(u' - u''). \tag{5.73}$$

Now we expand the collision density around u in (5.72):

$$\begin{aligned} q(u) &= \int_{u-\epsilon}^{u} \left[\Sigma_s(u)\Phi(u) + \frac{d\Sigma_s(u)\Phi(u)}{du}(u' - u) + \dots \right] \int_u^{u'+\epsilon} g(u' \to u'') du'' du' \\ &= G_{10}(u)\Sigma_s(u)\Phi(u) + G_{20}(u)\frac{d\Sigma_s(u)\Phi(u)}{du} + \dots . \end{aligned} \tag{5.74}$$

Here we have introduced the following notation

$$G_{10}(u) = \int_{u-\epsilon}^{u} \int_{u}^{u'+\epsilon} g(u' - u'')du''du' \tag{5.75}$$

and

$$G_{20}(u) = \int_{u-\epsilon}^{u} (u' - u) \int_{u}^{u'+\epsilon} g(u' - u'')du'', \tag{5.76}$$

which expressions are the zeroth and first moments of the scattering kernel. From the approximation (5.8) we obtain the following relationship between the slowing down density and the flux:

$$q(u) + a\frac{dq(u)}{du} = b\Sigma_s(u)\Phi(u). \tag{5.77}$$

The left hand side is evaluated with the help of (5.74), the result is

$$\begin{aligned} q + a\frac{dq}{du} &= G_{10}\Sigma_s\Phi + G_{20}\frac{d\Sigma_s\Phi}{du} \\ &+ a\left[\frac{dG_{10}}{du}\Sigma_s\Phi + G_{10}\frac{d\Sigma_s\Phi}{du} + \frac{dG_{20}}{du}\frac{d\Sigma_s\Phi}{du} + G_{20}\frac{d^2\Sigma_s\Phi}{du^2}\right] + \dots \end{aligned} \tag{5.78}$$

We neglect the last two terms in the brackets, as in the expansion only first order derivatives have been retained. The result is

$$q + a\frac{dq}{du} = \left(G_{10} + a\frac{dG_{10}}{du}\right)\Sigma_s\Phi + (G_{20} + aG_{10})\frac{d\Sigma_s\Phi}{du}. \tag{5.79}$$

Remember, a and b are free constants, let

$$a(u) = -\frac{G_{20}(u)}{G_{10}(u)} \tag{5.80}$$

to simplify the right hand side of (5.78). With that choice of $a(u)$, we arrive at

$$q(u) + a(u)\frac{dq(u)}{du} = G_{10}(u)\Sigma_s(u)\Phi(u)\left(1 - \frac{da(u)}{du}\right). \tag{5.81}$$

It is possible to evaluate G_{10} and G_{20} from their definitions:

$$G_{10}(u) = -\int_{u-\epsilon}^{u} (u' - u)g(u' - u)du' = \xi(u) \tag{5.82}$$

and

$$G_{20}(u) = -\int_{u-\epsilon}^{u} \frac{(u' - u)^2}{2} g(u' - u)du'. \tag{5.83}$$

When in (5.81) da/du is small, we get

$$b \approx \xi(u). \tag{5.84}$$

Thus the free constants in the approximate relation (5.77) have been expressed by moments of the scattering law. The presented model is called Greuling-Goertzel slowing down model.

a is small for heavy scatterer nuclei therefore it can be neglected in (5.77):

$$q(u) = \xi(u)\Sigma_s(u)\Phi(u). \tag{5.85}$$

That simplified Greuling-Gortzel model has been proposed by Fermi, and is called Fermi slowing down model. The Fermi model is applicable for $A > 27$ nuclei.

Since the collision between a neutron and different nuclei are exclusive events, the slowing down density on different nuclei may be summed:

$$q(u) = \sum_i q_i(u), \tag{5.86}$$

here $q_i(u)$ is the slowing down density due to collision with nuclei of type i. We apply the Greuling-Gortzel model for the calculation of slowing down density on light nuclei, at the same time for $A > 27$, we may use the Fermi model, or for a resonance nuclei we use the Wigner model.

The Wigner slowing down model is applicable to determine the absorption rate in a resonance energy group.

Far from the source energies, the asymptotic flux gives remarkably good results for the space integral of the flux. Below we obtain the asymptotic solution when capture is not neglected. The derivation is due to Einstein [164][p. 300]. We consider the neutrons emitted from the source as white[5]. Those neutrons collide and either slow down or are absorbed. We retain the absorbed neutrons also as though the capture reaction were replaced by scattering. Then the total flux at $E < E_s$ will be

$$\Phi(E) = \frac{Q}{\xi \Sigma_t E}. \tag{5.87}$$

To remember that the absorbed neutrons are only hypothetically present, we assume them to be black. Actually, we are interested in the flux of white neutrons.

The probability that a neutron reaches an energy between E and $E + dE$ is equal to the number of neutrons $\Phi(E)\Sigma_t dE$ leaving that energy range divided by the total number of neutrons Q thus

$$\frac{\Phi(E)\Sigma_t dE}{Q} = \frac{dE}{\xi E}.$$

The probability that a neutron becomes black when being scattered out is Σ_a/Σ_t multiplied by the above given probability:

$$\frac{\Sigma_a}{\Sigma_t}\frac{dE}{\xi E}.$$

The probability of remaining white is

$$1 - \frac{\Sigma_a}{\Sigma_t}\frac{dE}{\xi E},$$

and finally the probability that a neutron remains white when slowing down to energy E is the product

$$p(E_s \to E) = \prod \left(1 - \frac{\Sigma_a dE}{\Sigma_t \xi E}\right) = \exp\left[-\int_E^{E_s} \frac{\Sigma_a(E')}{\Sigma_t(E')\xi}\frac{dE'}{E'}\right]. \tag{5.88}$$

In lethargy variable:

$$p(u_s \to u) = \exp\left[-\int_0^u \frac{\Sigma_a(u')}{\xi\Sigma_t(u')}du'\right]. \tag{5.89}$$

Comparing (5.89) to (5.66), we see that the Wigner approximation corresponds to

$$a = b = \xi. \tag{5.90}$$

[5]Actually we divide the neutrons into two disjoint groups, white and black.

5.3. Resonance region

The group averaging needs more care when the flux and the cross-sections vary fast within the boundaries of the energy group. In the present section we consider a given energy group g and the material under consideration has two components: moderator (subscript m) and fuel (subscript f). Group g is in the asymptotic energy range, say right after the end of the slowing down range. The moderator consists of light elements, so their cross-sections vary slowly with the energy E. The fuel, however, has at least one atom having resonance line in group g. We use the following notation for the group averaging:

$$< \Sigma\Phi >= \frac{\int_{E_g}^{E_{g-1}} \Sigma(E)\Phi(E)dE}{\int_{E_g}^{E_{g-1}} \Phi(E)dE}. \tag{5.91}$$

For slowly varying cross-sections $\Sigma(E)$

$$\begin{aligned} &\int_E^{E/\alpha} \frac{\Sigma(E')\Phi(E')}{(1-\alpha)E'}dE' = \int_E^{E/\alpha} \frac{\Sigma(E')}{(1-\alpha)E'}dE' \\ &\approx < \Sigma\Phi > \int_E^{E/\alpha} \frac{dE'}{(1-\alpha)E'^2} = \frac{1}{E} < \Sigma\Phi > . \end{aligned} \tag{5.92}$$

Below we investigate the group averaging when the cross-sections vary fast. We start with the neutron balance at energy E:

$$(\Sigma_{tf} + \Sigma_{tm})\Phi(E) = Q(E) \tag{5.93}$$

where

$$Q(E) = \int_E^{E/\alpha_f} \frac{\Sigma_{sf}(E')\Phi(E')}{(1-\alpha_f)E'}dE' + \int_E^{E/\alpha_m} \frac{\Sigma_{sm}(E')\Phi(E')}{(1-\alpha_m)E'}dE'. \tag{5.94}$$

Approximate methods are based on various approximate solutions to (5.93). We assume energy E to which the neutrons are scattered from a fuel atom to be beyond the resonance region of the fuel atom, and, the asymptotic $1/E$ spectrum is applicable hence the second term is

$$\int_{E_g}^{E_{g-1}} \frac{\Sigma_{sm}(E')\Phi(E')dE'}{(1-\alpha_m)E'} \approx \frac{1}{E} < \Sigma_{sm}\Phi > . \tag{5.95}$$

We assume that most scattered neutrons originate from the moderator: $\Sigma_{sf} << \Sigma_{sm}$ and there is no correlation between $\Sigma_{af}(E)$ and the arrival of scattered neutrons from $E' > E$.

In the first model, called narrow resonance, we assume the resonance line to be narrow compared to the energy range into which the neutrons are scattered. Therefore (5.93) reduces to

$$\left[\Sigma_{tf}(E) + \Sigma_{tm}(E)\right]\Phi(E) \approx \frac{1}{E}\left[< \Sigma_{sf}\Phi_0 > + < \Sigma_{sm}\Phi_0 >\right], \tag{5.96}$$

where Φ_0 is the asymptotic flux within the energy group. From (5.96) immediately follows that the flux varies as the reciprocal of the mixture cross-section, see Fig. 5.4. From (5.96) we immediately obtain

$$\Phi(E) \approx \frac{1}{E(\Sigma_{tf}(E) + \Sigma_{tm}(E))}. \tag{5.97}$$

The total cross-section of the moderator varies slowly compared to the total cross-section of the fuel over the energy group used to prepare group cross-sections, see (4.3). When leakage is taken into account, in (5.93) a term $D(E)B^2$ should be added to the left hand side, and

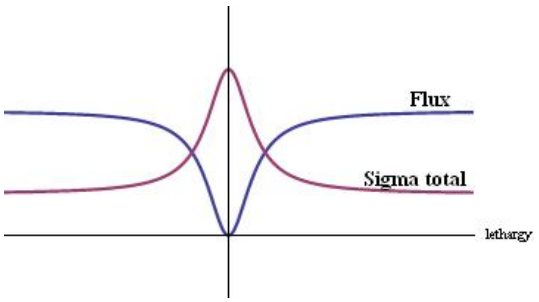

5.4. ábra. Energy dependence of the flux and the total cross-section

as a result, in (5.97) Σ_{tm} should be replaced by $\Sigma_{tm} + DB^2$. When the moderator-fuel ratio varies, the denominator varies between Σ_{tf} (pure fuel) and Σ_{tm} (pure moderator). The narrow resonance model predicts the flux to be maximally self-shielded for pure fuel, then

$$\Phi_0(E) \sim \frac{1}{E\Sigma_{tf}(E)}. \tag{5.98}$$

When the fuel is infinitely diluted, the flux will not be self-shielded, then

$$\Phi_0(E) \sim \frac{1}{E}. \tag{5.99}$$

Usually $\Sigma_{mt} >> \Sigma_{ft}$ because the moderator atoms prevail. Furthermore $\Sigma_{tm}(E) \sim const$ inside group g. Note that in the narrow resonance model the spectrum depends only on the energy dependence of the fuel cross-sections. This allows for creating application independent multigroup libraries.

Our second model is called wide resonance. In the model we assume the resonance line to be wide compared to the energy range into which the neutrons are scattered by the fuel atoms, furthermore, the fuel atom is taken as infinitely heavy, and only the moderator atoms slow the neutrons. Now the balance equation is

$$\int_E^{E/\alpha_m} \frac{\Sigma_{sm}(E')\Phi(E')dE'}{(1-\alpha)E'} \tag{5.100}$$

and now (5.93) is replaced by

$$\left[\Sigma_{tf}(E) + \Sigma_{tm}(E)\right]\Phi_0(E) = \Sigma_{sf}(E) + \frac{1}{E} < \Sigma_{sm}\Phi > . \tag{5.101}$$

Since $\Sigma_{af} >> \Sigma_{sf}$ and $\Sigma_{sf}(E)$ varies slowly, we may write

$$\Sigma_{tf}(E) = \Sigma_{af}(E) + \Sigma_{sf}(E) \approx \Sigma_{af}(E) + < \Sigma_{sf} > . \tag{5.102}$$

Henceforth in the wide resonance approximation the flux varies within group g as

$$\Phi(E) \sim \frac{1}{E(\Sigma_{af}(E) + \Sigma_{sm})}. \tag{5.103}$$

When the fuel nuclide density N_f and the moderator nuclide density N_m vary, the flux varies between the following limits:

$$\frac{1}{E\Sigma_{af}(E)} < \Phi(E) < \frac{1}{\Sigma_{sm}}, \tag{5.104}$$

the lower limit is in pure fuel, the upper in pure moderator.

The third model is called intermediate resonance model, and has been created because in a mixture of fuel isotopes neither of the aforementioned models may be applicable to each isotope. The intermediate resonance model was developed in order to treat entire range of resonances, and the energy distribution of neutrons scattered elastically by a fuel atom is assumed to be a linear combination of the distributions obtained in the narrow resonance and wide resonance model, respectively. Accordingly, the slowing down term is approximated as

$$\int_E^{E/\alpha_m} \frac{\Sigma_s(E')\Phi(E')dE'}{(1-\alpha)E'} \approx c\frac{1}{E} < \Sigma_{sm}\Phi > +(1-c)\Sigma_{sm}(E)\Phi(E). \tag{5.105}$$

The right hand side is the linear combination of the narrow resonance and the wide resonance models.

5.3.1. The subgroup method

Nikolaev and Hohlof[168] proposed a method for the calculation of the resonance cross-sections. The subgroup method is based on the following considerations. Let us consider the transport equation in a given group (c.f. Section 4.1 in Chapter 4) where one resonance line of a heavy atom is present. There the usual group constant preparation would not work because of two reasons. First, we can not find an *a priori* averaging spectrum, secondly, the cross-section variation with the lethargy within the group strongly influences the spectrum. The subgroup method assumes an internal spectrum form inside the group and derives the multigroup P_n equations (see Section 8.5 in Chapter 8) but the internal spectrum takes the resonance line into account.

In (4.3)-(4.6), we defined the group constants through averages with the scalar flux. At the same times we have seen that the solution of the transport equation (3.132) is the angular flux, so the correct averaging would use the angular flux, and the resulting group cross-sections would depend on $\mathbf{\Omega}$. For example, the averaged absorption cross-section would be

$$\Sigma_{ag}(\mathbf{r},\mathbf{\Omega}) = \frac{\int_{u_g}^{u_{g+1}} \Sigma_a(\mathbf{r},u,\mathbf{\Omega})\Phi(\mathbf{r},u,\mathbf{\Omega})du}{\int_{u_g}^{u_{g+1}} \Phi(\mathbf{r},u,\mathbf{\Omega})du}. \tag{5.106}$$

Another feature of the group constant set is that the homogenized group constants depend on the position even in a homogeneous material. As we see, the usage of the group constants is only a useful approximation. Below we use the correct group averaging in a given energy group where a resonance line resides within the group boundaries (u_g, u_{g+1}). We assume that the flux is separable into a slowly varying $\Psi(\mathbf{r},u,\mathbf{\Omega})$ and a resonance component $\phi_r(u,\mathbf{\Omega})$, the resonance line is assumed to be within the energy group, and the resonance component is space independent:

$$\Phi(\mathbf{r},u,\mathbf{\Omega}) \approx \Psi(\mathbf{r},u,\mathbf{\Omega})\phi_r(u,\mathbf{\Omega}). \tag{5.107}$$

The term Ψ varies slowly in that sense that it can be extracted from the integrand by using an appropriately selected lethargy value in the argument, for example

$$\begin{aligned}\Sigma_{xg} &= \frac{\int_{u_g}^{u_{g+1}} \Sigma_x(u)\Psi(\mathbf{r},u,\mathbf{\Omega})\phi_r(u,\mathbf{\Omega})du}{\int_{u_g}^{u_{g+1}} \Psi(\mathbf{r},u,\mathbf{\Omega})\phi_r(u,\mathbf{\Omega})du} \\ &= \frac{\Psi(\mathbf{r},\overline{u}_x,\mathbf{\Omega})}{\Psi(\mathbf{r},\overline{u},\mathbf{\Omega})} \frac{\int_{u_g}^{u_{g+1}} \Sigma_x(u)\Psi(\mathbf{r},u,\mathbf{\Omega})\phi_r(u,\mathbf{\Omega})du}{\int_{u_g}^{u_{g+1}} \Sigma_x(u)\phi_r(u,\mathbf{\Omega})du} \approx \Sigma_{xg}(\mathbf{\Omega}).\end{aligned} \tag{5.108}$$

This time we are using the static transport equation in the lethargy variable:

$$\begin{aligned}&\mathbf{\Omega}\boldsymbol{\nabla}\Phi(\mathbf{r},u,\mathbf{\Omega})+\Sigma_t(\mathbf{r},u)\Phi(\mathbf{r},u,\mathbf{\Omega})=\\&\int\int_{4\pi}\Sigma_s(\mathbf{r},u'\to u,\mathbf{\Omega}\mathbf{\Omega}')\Phi(\mathbf{r},u',\mathbf{\Omega}')d\mathbf{\Omega}'du'\\&+\frac{f(\mathbf{r},u)}{4\pi}\int_0^\infty\nu\Sigma_f(\mathbf{r},u')\int_{4\pi}\Phi(\mathbf{r},u',\mathbf{\Omega}')d\mathbf{\Omega}'du'+Q(\mathbf{r},u,\mathbf{\Omega}).\end{aligned}\tag{5.109}$$

When we seek the solution in the traditional P_n approximation in plane geometry, see Section 8.5 in Chapter 8:

$$\Phi(\mathbf{r},u,\mathbf{\Omega})=\frac{1}{4\pi}\sum_{l=0}^{L}\sum_{m=-l}^{+l}F_{n,m}(\mathbf{r},u)Y_{lm}(\mathbf{\Omega}).\tag{5.110}$$

Since the neutron density does not depend on φ, actually the neutron flux depends on x, the space variable, u-the lethargy; and μ the angular variable $\mathbf{\Omega}\mathbf{n}$ where n is the unit vector directed as $+x$. Thus (5.109) reduces to

$$\Phi(x,u,\mu)=\sum_{m=0}^{M}\frac{(2m+1)}{4\pi}F_m(x,u)P_m(\mu).\tag{5.111}$$

The scattering cross-section is also expanded in terms of Legendre polynomials:

$$\Sigma_s(u'\to u,\mu_0)\sum_{l=0}^{\infty}\frac{2l+1}{4\pi}\Sigma_{s,l}(u'\to u)P_l(\mu_0),\tag{5.112}$$

where $\mu_0=\mathbf{\Omega}\mathbf{\Omega}'$ is the scattering angle, and

$$\Sigma_{s,l}(u'\to u)=2\pi\int_{-1}^{+1}\Sigma_s(u'\to u)P_l(\mu_0).\tag{5.113}$$

Upon substituting (5.111)-(5.113) into (5.109) we obtain the following simplified form of (8.154):

$$\begin{aligned}&\frac{m}{(2m+1)}\frac{\partial F_{m-1}(x,u)}{\partial x}+\frac{m+1}{(2m+1)}\frac{\partial F_{m+1}(x,u)}{\partial x}+\Sigma_t(u)F_m(x,u)\\&=\int_0^u\Sigma_{s,m}(u'\to u)F_m(x,u')du'+\delta_{m0}S_0(x,u),\end{aligned}\tag{5.114}$$

where the source is assumed isotropic:

$$S_0=f(x,u)\int_0^\infty\nu\Sigma_f(u')F_0(x,u')du'+4\pi q_0(x,u).\tag{5.115}$$

Now our goal is to learn the resonance structure $\phi_r(u,\mu)$ in (5.107). In the P_n formalism, we seek the angular flux in the form of

$$F(x,u,\mu)=\sum_{m=0}^{\infty}\frac{(2m+1}{4\pi}\Psi_m(x,u)\phi_{r,m}(u)P_m(\mu),\tag{5.116}$$

where $\Psi_m(x,\mu)$ vary slowly with u, and the lethargy structure of the resonance is in the $\phi_{r,m}(u)$ terms. Now we integrate (5.114) over $(u_g u_{g+1})$ and obtain a set of equations for the Legendre components of the group fluxes

$$F_{gm}(x)=\int_{u_g}^{u_{g+1}}F_m(x,u)du.\tag{5.117}$$

The set of equations is:

$$\begin{aligned}&\frac{m}{2m+1}\frac{dF_{gm}(x)}{dx}+\frac{m+1}{2m+1}\frac{dF_{g,m+1}(x)}{dx}+\Sigma_{tg,m}F_{gm}(x)\\&=\sum_{g'=1}^{g}\Sigma_{sm,g'\to g}F_{mg'}(x)+\delta_{n,0}S_{0g}(x).\end{aligned}\tag{5.118}$$

Here no up-scattering is assumed, the group cross-sections are the same as in Section 8.5 in Chapter 8: the lethargy dependent cross-sections are weighted by the lethargy dependent flux in the energy group under consideration. But in a resonance group, the energy dependence is carried by the resonance structure $\phi_r(u)$ and the group cross-sections will be space independent.

Our goal is to determine the resonance structure $\phi_r(u)$. Let subdivide the spatial region, which is usually a fuel cell, into regions and we assume that in a spatial region the angular moments of the flux are well approximated by

$$F_m(x,u)=\phi_{rm}(u)e^{B_m(u)x}.\tag{5.119}$$

When (5.107) is a good approximation, $B_m(u)$ varies slowly. Observe that substituting (5.119) into (5.118), each term involving F_m will be a linear expression in ϕ_{rm} thus we obtain a set of linear equations for $\phi_{rm}(u)$. The coefficients in that equations involve angular moments of cross-sections, the $B_m(u), m=0,1,\dots$ functions. We neglect here the long technical details, the result is summarized as follows[170].

We introduce the following new variables to simplify the expressions. First of all, we integrate (5.119) over a homogeneous spatial zone, say (a,b). Let

$$V_m(u)=\frac{1}{B_m(u)}\left[e^{B_m(u)a}-e^{B_m(u)b}\right]\tag{5.120}$$

and the new dependent variable be

$$y_n(u)=\Sigma_t(u)\phi_{rm}(u)V_m(u).\tag{5.121}$$

Using the new variable in (5.118), we arrive at a recurrent system of linear equations for $y_n(u)$:

$$\begin{aligned}y_n(u)=I_n(u)&-\frac{n}{2n+1}\frac{B_{n-1}(u)}{\Sigma_t(u)}y_{n-1}(u)\\&-\frac{n+1}{2n+1}\frac{B_{n+1}(u)}{\Sigma_t(u)}y_{n+1}(u).\end{aligned}\tag{5.122}$$

The first $I_n(u)$ is

$$\begin{aligned}I_0(u)=&\int_0^u\frac{\Sigma_{s0}(u'\to u)}{\Sigma_t(u)}y_0(u')du'\\&+f(u)\int_0^\infty\frac{\nu\Sigma_f(u')}{\Sigma_t(u')}y_0(u')du'+\int_a^b S_0(x,u)dx,\end{aligned}\tag{5.123}$$

$I_n(u)$ of higher index is obtained in a recursive process not detailed here, see [170][Section 1.3].

At the end, we quote the final result for the resonance structure: the zeroth moment is given by

$$\begin{aligned}
\phi_{r0} &\approx \frac{I_0}{V_0}\left(\frac{1}{\Sigma_t(u)} + \frac{B_0B_1}{3}C_1(u)\right) \\
C_1(u) &= \left[\left(\frac{1}{\Sigma_t^3(u)} + \frac{a_1}{\Sigma_t^2(u)}\right) + \frac{B_0B_1}{3}\left(\frac{1}{\Sigma_t^5(u)} + \frac{a_1}{\Sigma_t^4(u)} + \frac{b_1}{\Sigma_t^2(u)} + D_1(u)\right)\right] \\
D_1(u) &= \frac{4}{15}B_1B_2\left(\frac{1}{\Sigma_t^5(u)} + \frac{a_1}{\Sigma_t^4(u)} + \frac{a_2}{\Sigma_t^3(u)} + \frac{b_1 + a_1a_2}{\Sigma_t^2(u)}\right).
\end{aligned} \tag{5.124}$$

Here

$$a_m = \frac{\sum_{k=0}^{m} a_k < \Sigma_{sm}/\Sigma_t^{m-k+1} >}{1 - < \Sigma_{sm}/\Sigma_t >} \tag{5.125}$$

where $< x >$ stands for the group average of x,

$$b_1 = \frac{< \Sigma_{s1}/\Sigma_t^4 > + a_1 < \Sigma_{s1}/\Sigma_t^3 >}{1 - < \Sigma_{s1}/\Sigma_t >}. \tag{5.126}$$

The first moment is

$$\begin{aligned}
\phi_{r1} &\approx -\frac{B_0I_0}{3V_1}\left[\left(\frac{1}{\Sigma_t^2(u)} + \frac{a_1}{\Sigma_t(u)}\right) + \frac{B_0B_1}{3}E_1 + \frac{4}{15}B_1B_2E_2\right] \\
E_1 &= \frac{1}{\Sigma_t^4(u)} + \frac{a_1}{\Sigma_t^3(u)} + \frac{b_1}{\Sigma_t(u)} \\
E_2 &= \frac{1}{\Sigma_t^4(u)} + \frac{a_1}{\Sigma_t^3(u)} + \frac{a_2}{\Sigma_t^2(u)} + \frac{b_1 + a_1a_2}{\Sigma_t}
\end{aligned} \tag{5.127}$$

As we see, the resonance structure depends mostly on the inverse of $\Sigma_t(u)$. The subgroup method determines the reaction rates in a given resonance group through integrals over the resonance group. The involved integrals are calculated by numerical integration, to this end the resonance group is subdivided into subgroups. To determine the group average of $1/\Sigma_t^n(u)$ consider the definition of group average:

$$< 1/\Sigma_t^n > = \frac{\int_{E_g}^{E_{g-1}} \frac{\Phi(E)dE}{\Sigma_t^n(E)}}{\int_{E_g}^{E_{g-1}} \Phi(E)dE},$$

since in the asymptotic range $\Phi(E) = 1/e$ and $du = -\Phi(E)dE$, in the lethargy variable

$$< 1/\Sigma_t^n > = \frac{\int_{u_{g-1}}^{u_g} \frac{du}{\Sigma_t^n(u)}}{u_g - u_{g-1}}. \tag{5.128}$$

Since the total cross-section varies rather fast in a resonance group, integrals of type (5.128) are replaced by the following Lebegue integral with $\Sigma_t(u)$ as measure:

$$< f(\Sigma_t) >_g = \int_{\Sigma_{tmin}}^{\Sigma_{tmax}} f(\Sigma_t)P_g(\Sigma_t)d\Sigma_t \tag{5.129}$$

where

$$P_g(\Sigma_t) = \frac{1}{\Delta u_g}\sum_k \left[\frac{du\,(\Sigma_t)}{d\Sigma_t}\right]_k, \tag{5.130}$$

where function $u(\Sigma_t)$ is the inverse of the function $\Sigma_t(u)$ and the summation runs over all the branches of the multi-valued function $u(\Sigma_t)$ which reside in group g. The meaning of the $P_g(\Sigma_t)$ function is the probability that the neutrons reside in one of the energy ranges in which the total cross-section value falls in the interval $(\Sigma_t, \Sigma_t + d\Sigma_t)$. We can calculate the integrals of type (5.129)by summation:

$$< f(\Sigma_t) >_g \approx \sum_{k=1}^{K} a_k f(\Sigma_{tk}). \tag{5.131}$$

The essence of the method is in the appropriate selection of weights a_k, number of subintervals K, values $f(\Sigma_{tk})$ so that $< f(\Sigma_t) >_g$ should be sufficiently accurate for a required family of functions $< f(\Sigma_t) >_g$.

As we have seen, we have three special models depending on the mass of the scatterer atom and the energy dependence of the cross-section. The slowing down processes on various atoms (or the slowing down in mixtures) can be considered as independent therefore if the nuclear density is

$$N = \sum_{i=1}^{I} N_i \tag{5.132}$$

then the slowing down density is decomposable as

$$q = \sum_{i=1}^{I} q_i, \tag{5.133}$$

and the determinantion of the slowing down density q_i we can use the model appropriate for the i-th atom type.

5.3.2. Resonance integral

An alternative method for the calculation of reaction rates in resonance groups is the application of the resonance integral and we express the reaction rates in a resonance group as a newly defined macroscopic cross-section, the resonance integral, multiplied by the so called fictive flux, which would be the flux if no resonance isotope were present. First we discuss the resonance absorption in a homogeneous region. The present Section follows [165].

The cross-section used to characterize the neutron-nucleus collision is determined by the energy level structure of the nucleus, see Section 3.3 in Chapter 3. If the neutron energy is near to the energy needed to excite a transition to a higher energy state of the compound nucleus the cross-section may considerable exceed (e.g. 10^6 *barn* instead of the normal few barn cross-section) the geometrical diameter of the nucleus. That situation is called resonance (absorption, capture, fission etc.). As we have seen in Chapter 5, a resonance cross-section rapidly varies with the energy (or lethargy).

When the neutron reaches the bottom of the slowing down range, the energy is close to the resonances of heavy nuclei. From the point of view of a self-sustaining chain reaction, it is essential to estimate the resonance escape probability p, see (5.88), that we repeat in the lethargy variable:

$$p(0 \to u) = \exp\left(- \int_0^u \frac{\Sigma_t(u')}{\xi \Sigma_t(u')} du' \right), \tag{5.134}$$

and recall that the above formula is accurate only in the narrow resonance approximation, and when the distance between consecutive resonance energies is large compared to the characteristic[6] ϵ value.

[6]Usually the ϵ belonging to an atom in the moderator.

As we have seen above, c.f. (5.132) and (5.133), the reaction rates on various nuclei can be calculated independently, including the slowing down. In the resonance region, we distinguish resonance nuclei, and we describe all the non-resonance nuclei by potential scattering. The potential scattering slowly varies with the lethargy, we consider it as constant. As to the resonance nucleus designated by subscript r, its absorption cross-section is dominant: $\Sigma_{tr} \approx \Sigma_{ar}$ In the chosen model, it is expedient to divide the total cross-section accordingly as

$$\Sigma_t(u) = \Sigma_p(u) + \Sigma_r(u) = \Sigma_p + \Sigma_a(u),$$

and subscript r may be dropped.

Depending on the lethargy u under consideration, we can distinguish two situations: at some lethargies $\Sigma_a(u) << \Sigma_p$ there (see Figure 5.4) the asymptotic flux is a good approximation:

$$\Psi_{fictional}(u) = \frac{1}{\xi\Sigma_p}. \tag{5.135}$$

In the resonance region $\Sigma_a(u) >> \Sigma_p$ this approximation is not applicable. There we rewrite equation (5.134) in the following form:

$$p(0 \to u) = \exp\left(\frac{-NI}{\xi\Sigma_p}\right) = \exp\frac{-NI}{\Psi_{fictional}(u)}, \tag{5.136}$$

where NI is a macroscopic cross-section, the product of a nuclide density N and a microscopic cross-section I. Comparing (5.136) and (5.134), we immediately see that

$$NI = \int_0^\infty \frac{\Sigma_p(u)\Sigma_a(u)}{\Sigma_t(u)}du. \tag{5.137}$$

The dimension of the resonance integral I is barn.

Note that p increases with increasing Σ_p in (5.134). Increasing Σ_p is obtained when the numbers of light nuclei are increased, i.e. when the resonance nuclei are diluted. Notwithstanding, the effective resonance integral I defined by (5.137) increases with increasing Σ_p. Taking the limit value

$$\lim_{\Sigma_p\to\infty} I = \int_0^\infty \frac{\frac{\Sigma_a}{N}}{\frac{\Sigma_t(u)}{\Sigma_p}}du = \int_0^\infty \sigma_a(u)du, \tag{5.138}$$

because

$$\lim_{\Sigma_p\to\infty} \frac{\Sigma_t}{\Sigma_p} = 1$$

and

$$\frac{\Sigma_a}{N} = \sigma_a.$$

We can evaluate the integral in (5.138) explicitly recalling the resonance formula for the capture cross-section:

$$\sigma_c(E) = \frac{\sigma_0}{1+x^2}\frac{\Gamma_\gamma}{\Gamma}, \tag{5.139}$$

where

$$x = \frac{E - E_r}{\Gamma/2} \tag{5.140}$$

and E_r is the resonance energy, Γ is the resonance width, Γ_γ is the width of the capture resonance line. Substituting (5.139) into (5.138) and carrying out the integration the result for the infinitely diluted resonance integral I_∞ is

$$I_\infty = \frac{\pi}{2}\sigma_0\frac{\Gamma_a}{E_r}. \tag{5.141}$$

The resonance integral for finite Σ_p can be evaluated explicitly when the potential scattering cross-section of the resonance nuclei can be neglected ($\sigma_{pr} << \sigma_{ar}$):

$$I(\sigma_p) = \frac{\sigma_p\Gamma_a}{2E_r}\int \frac{\frac{\sigma_0}{(1+x^2)}}{\sigma_p + \frac{\sigma_0}{(1+x^2)}}dx = I_\infty\frac{\sigma_p}{\sqrt{\sigma_p(\sigma_0+\sigma_p)}}, \tag{5.142}$$

here

$$\sigma_p = \frac{\Sigma_p}{N}. \tag{5.143}$$

In the integrals of the present Subsection the limits have been extended for $(-\infty, +\infty)$ because outside the resonance region the integrand tends to zero.

5.3.3. Resonance absorption in a lattice

The resonance absorption in a heterogeneous region differs from the resonance absorption in a homogenous region in that the fast neutrons are born in the fuel region, slow down in the moderator region and may be absorbed in another fuel region in the resonance energy range. Therefore the neutrons captured in a resonance line of the fuel can be subdivided into two disjoint set. In the first we encounter those neutrons having suffered their last collision in the fuel, in the second those collided last time in the moderator.

We discuss the narrow resonance case when the neutron captured in a resonance line collided last time at an energy far above the resonance line. At those energies potential scattering determines the fuel cross-sections, the flux varies slowly both in space and energy, the flux in the moderator is close to the flux in the fuel. At the resonance energies, see Fig. 5.4, the flux inside the rod is smaller than in the moderator.

First we deal with the energies above the resonance line. The first contribution is due to the neutrons last collided in the fuel. Estimate the number of neutrons absorbed on the resonance energy. A fraction of the neutrons emerging from the scattering density $\Sigma_{pf}\Phi V_f$ will be absorbed in the fuel. That fraction which does not leak out and is absorbed, i.e. let $P_0(\Sigma_t)$ stand for the escape probability from the fuel,

$$\int (1 - P_0(\Sigma_t))\frac{\Sigma_{af}}{\Sigma_{tf}}$$

henceforth the number of absorbed neutrons is

$$\Sigma_{pf}\Phi V_f \int (1 - P_0(\Sigma_t))\frac{\Sigma_{af}}{\Sigma_{tf}}, \tag{5.144}$$

where the integration runs over those lethargy values which may contribute to the absorption.

To estimate the contribution from the neutrons last collided in the moderator, we note that the scattering density is $\Sigma_{sm}\Phi$ where Σ_{sm} is the scattering cross-section of the moderator. In the estimation of the neutron fraction colliding in the fuel region, we use the Green's function

$$\int_{V_f} \Sigma_{af}(\mathbf{r}_2)\left[\int_{V_{mod}} \Sigma_{sm}(\mathbf{r}_1,\mathbf{r}_2)\mathcal{G}(\mathbf{r}_1,\mathbf{r}_2)d\mathbf{r}_1\right]d\mathbf{r}_2. \tag{5.145}$$

For the sake of comparison, the escape probability P_0 also can be expressed using the Green's function:

$$P_0(\Sigma_t) = \int_{V_m} \left[\int_{V_f} \frac{1}{V_f} \mathcal{G}(\mathbf{r}_2, \mathbf{r}_1) d\mathbf{r}_2 \right] \Sigma_{sm}(\mathbf{r}_1) d\mathbf{r}_1. \tag{5.146}$$

Although we explicitly indicated the space variables of the cross-sections, we assume the cross-sections to be constant in the fuel as well as in the moderator. Using the symmetry of the Green's function

$$\mathcal{G}(\mathbf{r}_1, \mathbf{r}_2) = \mathcal{G}(\mathbf{r}_2, \mathbf{r}_1)$$

the contribution, which we discuss, can be written as

$$\begin{aligned} &\int_{V_f} \Sigma_{af}(\mathbf{r}_f) \left[\int_{V_m} \Sigma_{sm}(\mathbf{r}_m) \Phi(\mathbf{r}_m) \mathcal{G}(\mathbf{r}_m, \mathbf{r}_f) d\mathbf{r}_m \right] d\mathbf{r}_f \\ &= \int_{V_f} \Sigma_{af}(\mathbf{r}_f) \left[\int_{V_m} \Sigma_{sm}(\mathbf{r}_m) \Phi(\mathbf{r}_m) \mathcal{G}(\mathbf{r}_f, \mathbf{r}_m) d\mathbf{r}_m \right] d\mathbf{r}_f = \Phi V \Sigma_{af} P_0(\Sigma_{tf}). \end{aligned} \tag{5.147}$$

Still we have to integrate (5.147) over the lethargy u (remember, the cross-sections are lethargy dependent) and add the contribution from the neutrons last collided in the fuel region (5.144), to get the total number of resonance absorptions in the fuel:

$$NI\Phi V \equiv \int \Sigma_{pf} \Phi V_f \int (1 - P_0(\Sigma_t)) \frac{\Sigma_{af}(u)}{\Sigma_{tf}(u)} du + \int \Phi V \Sigma_{af}(u) P_0(\Sigma_{tf}(u)) du. \tag{5.148}$$

Note that I is the resonance integral, we wanted to determine. The applicability of (5.148), however, strongly depends on the $P_0(\Sigma_t)$ expression, that depends on the Σ_t cross-section and the geometry of the fuel region. Wigner suggested the following approximation:

$$P_0(\Sigma_t) = \frac{1}{1 + \Sigma_t \ell}, \tag{5.149}$$

where ℓ is the average chord length in the rod. To determine ℓ, Wigner suggested the following thought of line.

Consider an infinite material, in which the flux Φ is constant in space. ΦV is the distance traveled by the neutrons in volume V under unit time. The number of neutron entering V through the boundary ∂V of V is $\partial V \Phi/4$, see Table 3.1. Let the average path covered by a neutron under unit time be ℓ, then the neutrons cover the distance of $\partial V \ell \Phi/4$ under unit time. Therefore

$$\ell = \frac{4V}{\partial V}. \tag{5.150}$$

Using Wigner's approximation in (5.148), we obtain

$$NI = \int \frac{\Sigma_{pf} + 1/\ell}{(\Sigma_{af} + \Sigma_{sf}) + 1/\ell} \Sigma_a(u) du. \tag{5.151}$$

Thus, the resonance absorbtion in a lattice can be calculated in the same way as in a homogeneous material, only the cross-sections need to be modified.

The accuracy of the resonance escape probability is essential for the design and economic operation of a nuclear reactor. It immediately effects the reactivity and through the reactivity the fuel cycle length, the refueling schedule. Therefore several approaches have been elaborated to determine the resonance escape probability.

The starting point of the approximate methods is equation (5.151), which means that it is possible to calculate the resonance integral of a heterogeneous system as the resonance

integral in an equivalent homogeneous system provided, the cross-sections in the equivalent homogeneous system have been modified in accordance with (5.151). In Ref.[143][p. 302], the following formulation is used.

5.1 Theorem (Equivalence theorem) *The calculation of the resonance absorption in a lattice can be reduced to the calculation of effective cross-sections of a homogeneous medium. The effective cross-section is modified by*

$$\frac{b}{\ell}, \tag{5.152}$$

where b is called Bell factor. The Bell factor is derived by the numerically determined $P_0(\Sigma_t)$ probability.

Note that the escape probability $P_0(\Sigma_t)$ depends on the geometry of the fuel rod, and also on the material properties of the fuel.

In a tight lattice, as in a water moderated reactor or in a fast reactor, there is a non-negligible probability that a fission neutron first collides in another fuel element. That probability is called Dancoff factor D. The correction for the Dancoff factor is used in various forms. In Ref.[143] we find the following correction:

$$\frac{b}{\ell}\frac{1-D}{(1-D)+bD}, \tag{5.153}$$

in [57][p. 167] the correction is written as

$$\frac{bD}{Nd_{rod}\,(1+(b-1)(1-D))} \tag{5.154}$$

where d_{rod} is the diameter of the fuel rod, b is the Bell factor.

Now it remains to determine b and D. In the S-WIMS code, Kowalska [57][p. 168] proposed the following approximation to the Bell factor for UO_2 fuel:

$$b = \frac{2.71x+1}{2.34x+1} \tag{5.155}$$

where

$$x = \frac{D}{Nd_{rod}\,(5+2\sigma_{s,ox})}, \tag{5.156}$$

where $\sigma_{s,ox}$ is the scattering cross-section of the oxygen.

A good approximation for the resonance escape probability p with the I resonance integral of ^{238}U and the average logarithmic decrement ξ is

$$p = \exp\left(-\frac{V_U N_U^{28} I}{V_m N_m (\xi\sigma)_m}\right). \tag{5.157}$$

We obtain a good approximation for the fast fission factor f by

$$f = \frac{N_U \sigma_{a25} V_U \bar{\Phi}_U}{N_U \sigma_{a25} V_U \bar{\Phi}_U + N_m \sigma_{am} V_m \bar{\Phi}_m} \tag{5.158}$$

where V_U, V_m are the volume of the uranium and moderator, respectively. $\bar{\Phi}_U, \bar{\Phi}_m$ are the average fluxes in the fuel and the moderator, respectively.

5.3.4. The Doppler effect

We have seen in Section 5.2 of Chapter 5, the scattering atom is not at rest, and its motion is taken into account through the effective cross-section (3.102). That effect is of outstanding importance in the resonance absorption since the energy loss of the neutron is usually large compared to the width of the resonance line therefore the resonance line only slightly contributes to the neutron balance. When the broadening caused by the temperature of the scatterer is taken into account, the effect of the resonance lines becomes more pronounced. That phenomenon renders an inherent negative feedback to the energy production by fission chain reaction.

Let m and M stand for the neutron mass and the mass of the resonant nucleus, respectively; $\mathbf{v}$ and $\mathbf{V}$ denote the neutron and resonant nucleus velocity. We assume the resonant nucleus to be in thermal equilibrium with its surroundings, thus the Boltzmann distribution determines the probability distribution of V:

$$P_3(\mathbf{V})d^3\mathbf{V} = \left(\frac{mA}{2\pi kT}\right)^{3/2} \exp\left(-\frac{mA\mathbf{V}^2}{2kT}\right) dV_x dV_y dV_z. \tag{5.159}$$

We fix the coordinate system so that the neutron flies along the z axis. The effective cross-section is

$$v\sigma_{eff}(v) = \int |\mathbf{v} - \mathbf{V}|\sigma(|\mathbf{v} - \mathbf{V}|)P_3(\mathbf{V})d^3\mathbf{V}, \tag{5.160}$$

substituting here (5.159), and integrating, we get for the effective absorption cross-section:

$$\sigma_{a,eff}(E) = \sigma_0 \frac{\Gamma_a}{\Gamma} \frac{\theta}{2\sqrt{\pi}} \int_{-\infty}^{\infty} \frac{\exp\left(-\theta(x-y)^2/4\right)}{1+y^2} dy. \tag{5.161}$$

Here

$$\theta = \frac{\Gamma}{\Delta}$$

and

$$\Delta = \left(\frac{4kTE_r}{A}\right)^{1/2}$$

is the Doppler width of the resonance line. In comparison with the Breit-Wigner formula, now the

$$\eta(\theta, x) = \frac{\theta}{2\sqrt{\pi}} \int_{-\infty}^{\infty} \frac{\exp\left(-\theta(x-y)^2/4\right)}{1+y^2} dy. \tag{5.162}$$

broadened lines have to be used and the corresponding resonance integral is

$$I(\sigma_p, T) = \frac{\sigma_p \Gamma_a}{2E_r} \int_{-\infty}^{+\infty} \frac{\sigma_0 \eta(\theta, x)}{\sigma_p + \sigma_0 \eta(\theta, x)} dx. \tag{5.163}$$

Below we summarize the main effects of the Doppler resonance line broadening:

1. When $T \to 0$, then $\Delta \to 0$ and $\theta \to \infty$ and

$$\lim_{T\to 0} \eta(\theta, x) = \frac{1}{1+x^2}, \tag{5.164}$$

there is no broadening.

2. The area under the broadened line equals the original area:

$$\int_{-\infty}^{+\infty} \eta(\theta, x)dx = \int_{-\infty}^{+\infty} \frac{dx}{1+x^2}. \tag{5.165}$$

As a consequence, the infinitely diluted resonance integral is independent of the temperature T.

3. The maximum of the cross-section of the broadened line is lower than σ_0, this is a consequence of the broadening.

4. The resonance integral is a monotonous function of the temperature. After differentiating (5.163), we obtain

$$\frac{\partial I(\sigma_p, T)}{\partial T} = \frac{\sigma_p \Gamma_a}{2E_r} \int_{-\infty}^{+\infty} \frac{\sigma_0 \sigma_p}{[\sigma_p + \sigma_0 \eta(\theta, x)]^2} \left[\frac{\partial \eta(\theta, x)}{\partial x}\right]^2 dx, \tag{5.166}$$

where we have used the following substitutions:

$$\frac{\partial \eta(\theta, x)}{\partial \theta} = -\frac{2}{\theta^3} \frac{\partial^2 \eta(\theta, x)}{\partial x^2}$$

and

$$\frac{\partial \theta}{\partial T} = -\frac{\theta}{2T}.$$

5.4. Thermalization

The process through which the neutrons become into thermal equilibrium with the host atoms is called thermalization. Neutrons thermalize through collisions with the host atoms. To set up a mathematical model for the thermalization, we have to know the features of the host atoms. The two extreme thermalization models are the neutron-atom collisions when the atom is free, as in a free gas; and when the atoms are arranged in a regular structure as in a crystal lattice. The latter model applies to a graphite moderator, the former for a gas cooled reactor. In the most frequently used PWR and BWR types the moderator is water, the main scatterer is the hydrogen, which is bound chemically. A chemically bound scatterer has kinetic and internal energy, the latter may manifest in rotational or translational vibration modes between the constituents of the compound. When a portion of the kinetic energy of the neutron in a collision is turned into internal energy, the collision is inelastic. A free atom can not participate in an inelastic collision.

The simplest thermalization model is the slowing down on free atoms because there the collision is elastic and the velocity distribution of the scatterer's speed is Maxwellian. That model is called Wigner-Wilkins thermalization model. The kinematics of the scattering is the same as the one we have used in the slowing down range, see Section 5.2 in Chapter 5. However, we have to take into consideration the following two characteristics of the thermalization:

1. In the description of slowing down, we have relied on the fact that the neutron energy decreases in a scattering. On the contrary, now the neutron energy is comparable to the kinetic energy of the scatterer therefore the neutron energy may increase.

2. The cross-sections are energy dependent, and usually the cross-sections are large in the thermal range. In a number of reactor types (e.g. BWR and PWR) the mean free path of the neutron may be smaller then the diameter of the fuel rod. That fact rules out simplifications that have been applicable in slowing down theory.

If we add that the absorption cross-section is also large in the thermal energy range and that excludes the diffusion approximation, we see the thermal energy range to be a real touch stone of the analysis.

Below we derive the scattering kernel in the Wigner-Wilkins model. The velocity $\mathbf{v}_c$ of the center of the neutron and scatterer system is

$$\mathbf{v}_c = \frac{\mathbf{v}' + A\mathbf{V}}{(A+1)^2} \tag{5.167}$$

where $\mathbf{V}$ stands for the velocity of the scatterer; and the neutron's velocity before the collision is

$$\mathbf{v}_n = \frac{A}{A+1}\mathbf{v}_r \tag{5.168}$$

where

$$\mathbf{v}_r = \mathbf{v}' - \mathbf{V} \tag{5.169}$$

is the relative velocity of the neutron. As before, in the CMCS the scattering alters only the direction of the neutron velocity. Denote θ and $\mathbf{v}_n^*$ the scattering angle, and the velocity of the neutron after scattering, respectively. Then

$$\mathbf{v}_n \mathbf{v}_n^* = v_n^2 \cos\theta.$$

Adding $\mathbf{v}_c$ to $\mathbf{v}_n^*$, we get the neutron speed $\mathbf{v}$ in the LCS, thus

$$\mathbf{v} = \mathbf{v}_n^* + \mathbf{v}_c, \tag{5.170}$$

and squaring both sides, we find the relationship

$$v^2 = v_n^2 + v_c^2 + 2v_n v_c \cos\theta_1 \tag{5.171}$$

where θ_1 is the angle between $\mathbf{v}_n^*$ and $\mathbf{v}_c$. Thus the neutron speed after scattering is limited as

$$v_{min}^2 = (v_n - v_c)^2 \le v \le (v_n + v_c)^2 = v_{max}^2. \tag{5.172}$$

Note that both θ and θ_1 is fixed from the point of view of the scattering, the only difference is in the direction of the z axis. Assume that the scattering is isotropic, then $\cos\theta$ and $\cos\theta_1$ are uniformly distributed in the $[-1,+1]$ interval. Differentiating (5.171) we arrive at:

$$vdv = v_n v_c d(\cos\theta_1) = \frac{v_{max}^2 - v_{min}^2}{4} d(\cos\theta_1). \tag{5.173}$$

Therefore the conditional probability of the neutron velocity after collision to fall into the interval $(v, v+dv)$ is

$$g(v' \to v|V,\mu) = \begin{cases} \frac{2vdv}{v_{max}^2 - v_{min}^2}, & v_{min} \le v \le v_{\max} \\ 0 & \text{otherwise.} \end{cases} \tag{5.174}$$

The condition fixes that the scatterer velocity V and the cosine of the angle between $\mathbf{v}'$ and $\mathbf{V}$ is μ.

A particle of velocity $\mathbf{v}'$ collides with a particle of velocity $\mathbf{V}$. After collision, the first particle's velocity is $\mathbf{v}$. Further notation: $v = |\mathbf{v}|, V = |\mathbf{V}|$.

$$\sigma_s(v' \to v) = \frac{\sigma_s}{2v'} \int_0^\infty 4\pi V^2 dV \int_{-1}^{+1} d\mu v_r g(v' \to v|V,\mu) P_3(V) \tag{5.175}$$

The result of the calculation is [165][Appendix 1]:

$$\sigma_s(E' \to E) = \frac{\sigma_s}{2E'}\eta^2 \left[erf\left(\eta\sqrt{\frac{E}{kT}} - \rho\sqrt{\frac{E'}{kT}}\right) \pm erf\left(\eta\sqrt{\frac{E}{kT}} + \rho\sqrt{\frac{E'}{kT}}\right)\right] + \frac{\sigma_s}{2E'}\eta^2 \left[erf\left(\eta\sqrt{\frac{E'}{kT}} - \rho\sqrt{\frac{E}{kT}}\right) \mp erf\left(\eta\sqrt{\frac{E'}{kT}} + \rho\sqrt{\frac{E}{kT}}\right)\right] \tag{5.176}$$

To obtain the scattering cross-section $\sigma_s(E')$, we have to integrate (5.176) over E, the result is

$$\sigma_s(E') = \frac{\sigma_s}{\beta\sqrt{\pi}}e^{-\beta^2} + \sigma_s\left(1 + \frac{1}{2\beta^2}\right) erf(\beta), \tag{5.177}$$

where we have introduced

$$\beta^2 = \frac{AE'}{kT}.$$

This concludes the derivation of the scattering cross-section at thermal energies. Remains the discussion of the internal energy of the scatterer. The appropriate models are in the subroutines of the thermalization programs. We shortly mention the Nelkin model for light water, where the water molecule is modeled by an oscillator with four eigenfrequencies. The Koppel-Young model that accounts for the rotational modes of the water molecule, too.

Below we mention that it is possible to transform the integral form of the balance equation into a differential equation, as in the Cadilhac model. The Cadilhac model is an engineering model which is used to speed up the calculation. The model is based on the functional relation between the slowing down density $q(E)$ and the flux, which is approximated by the following expression:

$$\frac{d\Phi(E)/M(E)}{dE} = g(E)q(E) - \frac{d}{dE}h(E)\frac{dq(E)}{dE}, \tag{5.178}$$

where $M(E)$ is the Maxwell spectrum:

$$M(E) = \frac{E}{T^2}e^{-E/T}. \tag{5.179}$$

Here T is the temperature. Functions $g(E)$ and $h(E)$ are adjusted to a given problem class, they are free parameters in the Cadilhac model. We present a few choices of the $g(E)$ and $h(E)$ functions.

- When
$$g(E) = (\xi\Sigma_s ETM(E)f(E))^{-1} \tag{5.180}$$
and
$$h(E) = 0 \tag{5.181}$$
is chosen, where $\Sigma_s, \xi\Sigma_s$ are the scattering and slowing down cross-section above the thermal energy range, respectively, we obtain the generalized heavy free gas model [TIC2][p. 183], in which $f(E)$ is a free parameter. When $f(E) \equiv 1$, we get the heavy free gas model.

- When
$$g(E) = (\xi\Sigma_s ETM(E))^{-1} \tag{5.182}$$

and

$$h(E) = \gamma \left(\xi \Sigma_s M(E)\right)^{-1} \tag{5.183}$$

are chosen, we obtain with $\gamma = 0$ again the heavy free gas model, otherwise free parameter γ is used to adjust results to the THERMOS calculations. When $\gamma = 1$, we obtain the so-called simplified Laletin model used in the UNIRASOS code.

- When the Wigner-Wilkins model is used, the Cadillac model is exact provided we introduce two free terms $f_1(E)$ and $f_2(E)$, the first one in the $g(E)$ parameter:

$$g(E) = \left(\Sigma_s E T M(E) f_1(E)\right)^{-1} \tag{5.184}$$

and the second one in the $h(E)$ parameter as

$$h(E) = \left(\Sigma_s M(E) f_2(E)\right)^{-1} \tag{5.185}$$

where we choose

$$f_1(E)^{-1} = \Sigma_s \left(\frac{1}{\Sigma_s(E)} - E \frac{d}{dE} \frac{1}{\Sigma_s(E)}\right) \tag{5.186}$$

and

$$f_2(E)^{-1} = \frac{\Sigma_s(E)}{\Sigma_s}. \tag{5.187}$$

In the LEOPARD code [57], slowing down on hydrogen is considered so $\xi = 1$.

- In the UNIRASOS code, the unphysical choices $f_1(E) = 1, f_2(E) = 0$ or $f_2(E) = 1/\gamma$ are also possible.

The above mentioned models have been studied in details, the assumptions have proved to be reasonable.

The equilibrium energy spectrum of the neutrons is the Maxwell spectrum with $A = 1$. In energy variable

$$M_T(E) = \frac{E}{E_T^2} e^{-E/E_T}, \tag{5.188}$$

where T is the equilibrium temperature. In the velocity variable,

$$M_T(v) = \left(\frac{m}{2\pi k T}\right)^{3/2} \exp\left(-\frac{m_n v^2}{2kT}\right) 4\pi v^2, \tag{5.189}$$

where m_n is the neutron mass. Note that $M_T(v)$ is the velocity spectrum, the flux spectrum is $M_T(v)v$. The scattering kernel satisfies the detailed balance:

$$M_T(E')\sigma_s(E' \to E) = M_T(E)\sigma_s(E \to E'). \tag{5.190}$$

Thermal equilibrium establishes only when no absorption is present. In the presence of absorption and leakage the balance equation takes the following form:

$$D(E)B^2 + \Sigma_t(E)\Phi(E) = q(E) \tag{5.191}$$

where $q(E)$ includes the elastic and inelastic scattering as well as the contribution from fission. As to the scattering, we divide the energy interval into two parts, the range $(0, E_m)$ is called thermal range and in the epithermal range (E_m, ∞) is selected so that slowing down theory be valid there. When there are resonance lines at low energies (this is the case with

plutonium isotopes) the resonance lines are placed into the thermal range, e.g. by choosing $E_m = 1.85eV$. Then the slowing down source is cut into two parts as

$$\int_0^\infty \Phi(E')\Sigma_s(E' \to E)dE' = \int_0^{E_m} \Phi(E')\Sigma_s(E' \to E)dE' + \int_{E_m}^\infty \psi(E')\Sigma_s(E' \to E)dE', \tag{5.192}$$

and in the second term the asymptotic slowing down can be used:

$$Q(E) = \int_{E_m}^\infty \psi(E')\Sigma_s(E' \to E)dE' = q(E_m)\left[\frac{1}{E_m} - \frac{\alpha}{E}\right] \tag{5.193}$$

with the restraint that $Q(E)$ may not be negative, the negative values are replaced by zeros. Thus the asymptotic slowing down equation is:

$$\left[D(E)B^2 + \Sigma_t(E)\right]\Phi(E) = Q(E) + \int_0^{E_m} \Phi(E')\Sigma_s(E' \to E)dE' \;\; 0 \le E \le E_m. \tag{5.194}$$

The leakage term is often merged with the absorption. That equation is solved by numerical methods.

We discuss the solution method used in the code THERMOS [171],[172]. We consider a cylindrical region, the unit cell of a reactor lattice, the cross-sections depend on the position. We study equation (5.194) in the following form:

$$\Sigma_t(\mathbf{r}, E)\Phi(\mathbf{r}, E) = \int_V T(\mathbf{r}' \to \mathbf{r})\left[Q(\mathbf{r}', E) + \int_0^{E_m} \Sigma_s(\mathbf{r}', E' \to E)\Phi(\mathbf{r}', E')dE'\right] d^3\mathbf{r}', \tag{5.195}$$

i.e. the scattering term has been separated into two parts: slowing down and migration, the neutrons having slowed down to energy E migrate from $\mathbf{r}'$ to $\mathbf{r}$, other neutrons slow down at position $\mathbf{r}'$. Isotropic scattering is assumed to avoid a too intricate formalism. The error of that approximation is reduced by the introduction of the transport correction. In THERMOS, $E_m = 0.625\ eV$ is the limit of the thermal range. The volume V is the unit cell (or Wigner-Seitz cell). It is assumed that the leakage out of V is zero, henceforth

$$\int_V T(\mathbf{r}' \to \mathbf{r})d^3\mathbf{r} = 1. \tag{5.196}$$

A consequence of that assumption is that all neutrons emerging from the source are absorbed in V:

$$\int_V \int_0^{E_m} \Sigma_a(\mathbf{r}, E)\Phi(\mathbf{r}, E)dEd^3\mathbf{r} = \int_V \int_0^{E_m} Q(\mathbf{r}, E)dEd^3\mathbf{r}. \tag{5.197}$$

In the energy transfer model the asymptotic $1/E$ spectrum is used. The spatial distribution of the epithermal flux is practically constant. All the cross-sections are assumed to by cylindrically symmetric, therefore the transport kernel $T(\mathbf{r}' \to \mathbf{r}, E)$ depends only on r', r, E. In the calculation velocity is used instead of the neutron energy E, the conversion is

$$E = 0.0253v^2 \;\; \Sigma_s(v' \to v) = 0.0506\Sigma_s(E' \to E). \tag{5.198}$$

For the discretization, we subdivide the velocity range into K groups and V is subdivided into S spatial intervals, each discretization is represented by the midpoints. The discretized form of (5.197) becomes:

$$\Sigma_{qk}N_{qk} = \sum_{p=1}^{S} T_{pqk}\left(Q_{pk} + \sum_{j=1}^{K} P_{pjk}N_{pj}\right), \tag{5.199}$$

where p, q are spatial indices, j, k refer to speeds, Σ_{qk} is the total cross-section in region q and velocity k, N_{qk} is the neutron density in region q and velocity k, Q_{pk} is the discretized source

$$Q_{pk} = Q(r_p, v_k)/v_k. \tag{5.200}$$

The transport matrix is

$$T_{pqk} = T(r_p \to r_q, v_k)/\Delta V_p, \tag{5.201}$$

the volume

$$\Delta V_p = 2\pi r_p \Delta r_p, \tag{5.202}$$

the scattering matrix is

$$P_{pjk} = \Sigma_s(r_p, v_j \to v_k) v_j \Delta v_j / v_k. \tag{5.203}$$

After discretization, the integral equation (5.197) has been transformed into a set of linear equations, the number of unknowns is Qk. In the solution the Gauss-Seidel iteration is used. The number of energy groups is max. 24, the number of energy groups is 16 in the original THERMOS code. Graphite, water, and heavy water has been used as moderator material.

5.5. Fermi age

Let us consider a large homogeneous region. In the previous Sections we have exploited the asymptotic slowing down spectrum but neglected the spatial distribution of the neutrons in the course of slowing down. The general approximate slowing down theory is based on a heuristic form of the slowing down density and flux, viz. (5.66). In the Wigner approximation that relationship is even simpler:

$$\Phi(\mathbf{r}, u) = \frac{q(\mathbf{r}, u)}{\xi \Sigma_t(u)}. \tag{5.204}$$

In an infinite region we established another relationship between the slowing down density and the neutron flux, (5.64). When besides the absorption also leakage is possible, (5.64) should be modified as follows:

$$\frac{\partial q(\mathbf{r}, u)}{\partial u} = -\Sigma_a(u)\Phi(\mathbf{r}, u) + D(u)\Delta\Phi(\mathbf{r}, u), \tag{5.205}$$

because the neutrons slowing down at lethargy u but not slowing further at lethargy $u + du$ must be either absorbed or leaked out. We express here the slowing down density from (5.204) and obtain the following differential equation for the slowing down density $q(qrr, u)$:

$$\frac{\partial q(\mathbf{r}, u)}{\partial u} = \frac{D(u)}{\xi \Sigma_t(u)} \Delta q(\mathbf{r}, u) - \frac{\Sigma_a(u)}{\xi \Sigma_t(u)} q(\mathbf{r}, u). \tag{5.206}$$

With the help of the resonance escape probability $p(0 \to u)$, see (5.134) the second term is eliminated in the following manner. We slightly modify the slowing down density as

$$q(\mathbf{r}, u) = \tilde{q}(\mathbf{r}, u) p(0 \to u), \tag{5.207}$$

and the introduced $\tilde{q}(\mathbf{r}, u)$ is the solution of

$$\frac{\partial \tilde{q}(\mathbf{r}, u)}{\partial u} = \frac{D(u)}{\xi \Sigma_t(u)} \Delta \tilde{q}(\mathbf{r}, u). \tag{5.208}$$

This equation is a diffusion (or heat conduction) type equation where the lethargy plays the role of time. To make the analogy complete, we introduce the $\tau(u)$ Fermi age:

$$\tau(u) = \int_0^u \frac{D(u')}{\xi\Sigma_t(u')} du'. \tag{5.209}$$

In the new variables, (5.206) takes the form of

$$\frac{\partial \tilde{q}(\mathbf{r}, u)}{\partial \tau} = \Delta \tilde{q}(\mathbf{r}, u), \tag{5.210}$$

called Fermi's age equation.

We seek the solution to (5.210) by separation, let $\tilde{q}(\mathbf{r}, u) = \Phi(\mathbf{r})T(\tau)$, where $\Phi(\mathbf{r})$ is an eigenfunction of the Laplace operator. Then

$$T(\tau) = e^{-B^2\tau}, \tag{5.211}$$

indicates the physical meaning of τ: the neutrons spread out during slowing down, the characteristic of the spread out is τ. That area should be added to L^2 defined in (6.81) as the square of the distance covered by the neutrons until absorption. Since $B^2\tau << 1$, the k_{eff} should be modified to take into account the neutron migration during slowing down:

$$k_{eff} = \frac{k_\infty e^{-B^2\tau}}{1 + L^2B^2} \approx \frac{k_\infty}{1 + (L^2 + \tau)B^2}. \tag{5.212}$$

The quantity

$$M^2 = L^2 + \tau \tag{5.213}$$

is called migration area. We only mention that for most moderators, $\tau >> L^2$ thus the majority of the neutron migration area attaches to the slowing down.

5.6. Validation and verification

We have surveyed several models that are used in the calculation of the neutron spectrum. The models rely on assumptions and it should be verified how good those models are. The models are used to calculate neutron flux or neutron density, non of them is measurable experimentally. The measurements are carried out on an experimental facility, it is possible to measure the activity of the fuel pellet in a zero reactor. The measurement gives the axial or radial flux distribution at a given position in the core. For details, see [64]

We often introduce additional parameters derived from the neutron spectrum, in order to verify the neutron spectrum obtained by the calculational model. It must be noted that the spectral parameters strongly depend on the detector cross-section library. The below given spectral parameters depend only on the cadmium cut-off energy.

ρ^{28} is the ratio of epithermal capture to the thermal capture in ^{238}U, δ^{25} is the ratio of the epithermal fission to the thermal fission, δ^{28} is the ratio of the epithermal fission in ^{238}U to the thermal fission, the modified conversion ratio, and the characterized variation of fissionable isotopes in the fuel. In practice, the end of the thermal energy region is the cut-off energy of cadmium E_{Cd}.

$$\rho^{28} = \frac{\int_{E_{Cd}}^{\infty} \Sigma_{c28}(E)\Phi(E)dE}{\int_0^{E_{Cd}} \Sigma_{c28}(E)\Phi(E)dE} \tag{5.214}$$

Parameter δ^{25} is the ratio of fast fission and total fission in ^{235}U:

$$\delta^{25} = \frac{\int_{E_{Cd}}^{\infty} \Sigma_{f25}(E)\Phi(E)dE}{\int_{0}^{E_{Cd}} \Sigma_{f25}(E)\Phi(E)dE} \tag{5.215}$$

The fast fission parameter δ^{28} is the ratio of fissions in ^{238}U to fissions in ^{235}U:

$$\delta^{28} = \frac{\int_{0}^{\infty} \Sigma_{f28}(E)\Phi(E)dE}{\int_{0}^{\infty} \Sigma_{f25}(E)\Phi(E)dE} \tag{5.216}$$

$$MCR = \frac{\int_{E_{Cd}}^{\infty} \Sigma_{x}(E)\Phi(E)dE}{\int_{0}^{E_{Cd}} \Sigma_{f25}(E)\Phi(E)dE} \tag{5.217}$$

$$CR = \frac{\int_{E_{Cd}}^{\infty} \Sigma_{f25}(E)\Phi(E)dE}{\int_{0}^{E_{Cd}} \Sigma_{f25}(E)\Phi(E)dE} \tag{5.218}$$

5.7. Problems

1. Suggest detector materials to measure the neutron flux in the following energy ranges: a, $E > 1MeV$; b, $1keV \leq E \leq 50keV$ c, $E < 1eV$. The cross-sections can be looked up at the IAEA home page.
2. What happens if the scattering is linearly anisotropic? Assuming that the scattering cross-section is almost symmetric, give the scattering theory using perturbation theory formalism.
3. Determine the a_{ij} constants in the Placzek transients.
4. Prove the slowing down formula (5.70).
5. What mechanism enters the resonance treatment in a lattice? Which situation is favorable for the neutron balance, the lumped fuel, or the fuel lattice?
6. What considerations apply in the lattice design (lattice pitch, fuel pin diameter, moderator material)?
7. Try to improve Wigner's formula (5.150)!
8. Which material is favorable for the thermalization, the liquid moderator or the solid, crystalline one?
9. Estimate how a focused a neutron beam spreads out during slowing down.
10. Estimate the period of time of thermal diffusion and the time, which is required for slowdown from the emitting energy to the thermal energy!
11. Solve the slowing down equations in approximation no absorption case without leakage. Use the Laplace-transformation! The neutron spectrum (source) is $f(E) = \delta(E)$.
12. Solve the slowing down equations in special case where the scattering and absorption cross sections are independent of the energy.
13. The polygonal cells are replaced to cylinder cells, how to determine the radius of cylinder cells? What condition must be replaced by a reflective boundary condition in the cylindrical cells?

6. fejezet

Diffusion Equation

6.1. Derivation of the diffusion equation

The simplest P_n approximation has proved extremely successful. It is generally used in physics, reactor physics is not an exception. The unfavorable mathematical properties of the transport operator $\mathcal{L}$ in equations (3.116) and (3.132) have made the transport theory to a terrain where approximate methods dominate. When using the diffusion theory, we relinquish the abrupt changes in the angular distribution and the higher angular moments in the scattering kernel, but we replace the wild, unmanageable transport operator with a tame, elliptic operator that offers the completeness of its eigenfunctions, which are smooth functions, and, a series of theorems preparing the ground for efficient applications.

We start with the derivation of the diffusion equation, immediately in multigroup formalism. We start out from equation (4.11) where the elastic scattering is assumed to be linearly anisotropic:

$$\Sigma_s(\mathbf{r}, g' \to g, \mathbf{\Omega}\mathbf{\Omega}') = \frac{1}{4\pi}\Sigma_{s0}(\mathbf{r}, g' \to g) + \frac{3}{4\pi}\Sigma_{s1}(\mathbf{r}, g' \to g)\mathbf{\Omega}\mathbf{\Omega}'. \tag{6.1}$$

Integrate (4.11) over the angular variable:

$$\begin{aligned} \frac{1}{v_g}\frac{\partial \Phi_g(\mathbf{r},t)}{\partial t} &= -\boldsymbol{\nabla}\mathbf{J}_g(\mathbf{r},t) - \Sigma_{tg}(\mathbf{r})\Phi_g(\mathbf{r},t) \\ &+ \sum_{g'=1}^{G}\Sigma_{s0}(\mathbf{r}, g' \to g)\Phi_{g'}(\mathbf{r},t) \\ &+ f_g\sum_{g'=1}^{G}\nu\Sigma_{fg'}(\mathbf{r})\Phi_{g',t}(\mathbf{r}) + Q_{0g,t}(\mathbf{r}). \end{aligned} \tag{6.2}$$

where

$$Q_{0g}(\mathbf{r},t) = \int_{4\pi} Q_g(\mathbf{r},\mathbf{\Omega},t)d\mathbf{\Omega}. \tag{6.3}$$

In equation (6.2), there are two dependent variables: the current vector $\mathbf{J}_g(\mathbf{r})$ and the scalar flux $\Phi_g(\mathbf{r})$.

To have a balance equation precise up to the first order spherical harmonics, we multiply (4.11) by $\mathbf{\Omega}$ and integrate:

$$\begin{aligned} \frac{1}{v_g}\frac{\partial \mathbf{J}_g(\mathbf{r},t)}{\partial t} &= -\frac{1}{3}\boldsymbol{\nabla}\Phi_g(\mathbf{r},t) - \int_{4\pi}\mathbf{\Omega}(\boldsymbol{\nabla}\mathbf{\Omega})\Phi_g(\mathbf{r},\mathbf{\Omega})d\mathbf{\Omega} - \Sigma_{tg}(\mathbf{r})\mathbf{J}_g(\mathbf{r},t) \\ &+ \frac{f_g}{4\pi}\sum_{g'=1}^{G}\nu\Sigma_{fg'}\mathbf{J}_{g'}(\mathbf{r},t) \\ &+ \sum_{g'=1}^{G}\Sigma_{s1,g'\to g}\mathbf{J}_g(\mathbf{r},t) + \mathbf{Q}_1(\mathbf{r},t). \end{aligned} \tag{6.4}$$

To obtain the traditional diffusion equation, we assume that

$$\sum_{g'=1}^{G}\Sigma_{s1,g'\to g}\mathbf{J}_g(\mathbf{r},t) \approx \Sigma_{s1,g}J_g(\mathbf{r},t) \tag{6.5}$$

and

$$\frac{1}{v_g}\frac{\partial J_g(\mathbf{r},t)}{\partial t} \approx 0. \tag{6.6}$$

With the above mentioned assumptions, (6.4) is a relationship between the neutron current $J_g(\mathbf{r},t)$ and the scalar flux $\Phi_g(\mathbf{r},t)$.

$$J_g(\mathbf{r},t) = -D_g\left[\boldsymbol{\nabla}\Phi_g(\mathbf{r})\right] \tag{6.7}$$

where

$$D_g = \frac{1}{3}\frac{1}{\Sigma_{tg} - \bar{\mu}\Sigma_{sg}} \equiv \frac{1}{3\Sigma_{g,tr}}, \tag{6.8}$$

where $\Sigma_{g,tr}$ is the transport cross-section. We also assume that the source is isotropic. Using (6.7) to eliminate the current in (6.2), we arrive at the well known diffusion equation:

$$\begin{aligned}\frac{1}{v_g}\frac{\partial\Phi_g(\mathbf{r},t)}{\partial t} &= \boldsymbol{\nabla}\left[D_g(\mathbf{r})\boldsymbol{\nabla}\Phi_g(\mathbf{r},t)\right] \\ &- \Sigma_{tg}(\mathbf{r},t)\Phi_g(\mathbf{r},t) \\ &+ \sum_{g'=1}^{G}\Sigma_{s0,g'\to g}(\mathbf{r})\Phi_{g'}(\mathbf{r},t) \\ &+ f_g\sum_{g'=1}^{G}\nu\Sigma_{fg'}(\mathbf{r})\Phi_{g'}(\mathbf{r},t) \\ &+ Q_0(\mathbf{r},t), \quad g = 1,\ldots,G.\end{aligned} \tag{6.9}$$

On the left hand side of the diffusion equation is the partial time derivative of the scalar flux, on the right hand side we find the leakage, the removal, the scattering, the fission terms and the external source. Thus in diffusion theory the reaction rates are represented by the following operators:

$$\mathcal{L}\Phi_g(\mathbf{r},t) = -\boldsymbol{\nabla}\left[D_g(\mathbf{r})\boldsymbol{\nabla}\Phi_g(\mathbf{r},t)\right] \tag{6.10}$$

$$\mathcal{R}\Phi_g(\mathbf{r},t) = \Sigma_{tg}(\mathbf{r},t)\Phi_g(\mathbf{r},t) \tag{6.11}$$

$$\mathcal{S}\Phi_g(\mathbf{r},t) = \sum_{g'=1}^{G}\Sigma_{s0,g'\to g}(\mathbf{r})\Phi_{g'}(\mathbf{r},t) \tag{6.12}$$

$$\mathcal{F}\Phi_g(\mathbf{r},t) = f_g\sum_{g'=1}^{G}\nu\Sigma_{fg'}(\mathbf{r})\Phi_{g'}(\mathbf{r},t). \tag{6.13}$$

Note, that in energy group representation the operators are replaced by matrices acting on the column vector of the group fluxes. The leakage operator $\mathcal{L}$ is represented by a diagonal matrix and two nabla ($\boldsymbol{\nabla}$) operators, thus the diffusion equation is a second order partial differential equation. Note that the gradient of the scalar flux in a given energy group gives no contribution to the current in other energy groups.

The removal operator ($\mathcal{R}$) is also diagonal but the structure of the scattering operator $\mathcal{S}$ depends on the scattering matrix, which is normally not diagonal. The structure of the fission operator $\mathcal{F}$ depends on the fission spectrum f_g but normally $\mathcal{F}$ is a matrix.

Equation (6.7) is called Fick's law. We encounter similar equations, where a current is related by the gradient of a scalar function in the statistical physics and chemistry. There the current is the result of collisions between the same kind of particles, whereas in reactor physics we neglect the neutron-neutron collisions, the Fick law is the result of neutron-host nucleus collisions.

The solution of the diffusion equation is subjected to boundary conditions. At material interfaces the normal component of the current

$$D_g \boldsymbol{\nabla} \mathbf{n} \Phi_g(\mathbf{r}), \tag{6.14}$$

and the flux $\Phi_g(\mathbf{r})$ must be continuous.

At an external boundary, three types of boundary conditions are used:

1. Dirichlet boundary value problem:

$$\Phi_g(\mathbf{r}_b) = f(\mathbf{r}_b), \tag{6.15}$$

   where $f(\mathbf{r}_b)$ is a given function.

2. Neumann boundary value problem:

$$\mathbf{n}\mathbf{J}_g(\mathbf{r}_b) = f(\mathbf{r}_b); \tag{6.16}$$

3. Mixed type boundary condition:

$$\alpha_g(\mathbf{r}_b)\Phi_g(\mathbf{r}_b) + \beta_g(\mathbf{r}_b)\mathbf{n}\mathbf{J}_b(\mathbf{r}_b) = h(\mathbf{r}_b), \tag{6.17}$$

   where $\alpha_g(\mathbf{r}_b), \beta_g(\mathbf{r}_b)$ and $h(\mathbf{r}_b)$ are given functions.

When $h_g(\mathbf{r}_b) = 0, \mathbf{r}_b \in \partial V$ and (6.9) contains no external source, the boundary value problem is called homogeneous, otherwise non-homogeneous. The boundary conditions allow for the following physical boundary conditions:

- given scalar flux along the boundary;
- given current along the boundary;
- given entering current along the boundary;
- given albedo along the boundary.

6.2. Mathematical properties of the diffusion equation

Diffusion theory is obviously an approximation to the transport theory. Such an approximation is justified, when it is easier to use and the approximations are acceptable in a number of usual situations. Most calculations of reactor physics must be based on numerical methods so in the present Section we survey those mathematical features of diffusion theory that make it applicable in theoretical (see Chapter 7) and practical (see Chapter 9) problems. Here we mention only two items:

- in diffusion theory, the eigenfunctions of the homogeneous eigenvalue problems form a complete function set, see Theorem 6.2;
- the involved operator is positive and makes it possible to work out effective numerical solution methods, see Theorem 6.1.

We collect the group fluxes into a single vector and define the diffusion operator $\mathcal{D}$ as follows. Write the diffusion equation (6.9) as

$$V\frac{\partial\underline{\Phi}}{\partial t}=\mathcal{D}\underline{\Phi}+\underline{Q} \tag{6.18}$$

where V is the diagonal matrix $V=diag(1/v_1,\ldots,1/v_G)$ and $\underline{\Phi}=(\Phi_1,\ldots,\Phi_G)$ are the group fluxes, $\underline{Q}=(Q_1\ldots,Q_G)$ the group sources. In explicit form, the diffusion operator is (c.f. (6.9)):

$$\begin{aligned}\mathcal{D}=&\boldsymbol{\nabla}\left[D_g(\mathbf{r})\boldsymbol{\nabla}\Phi_g(\mathbf{r},t)\right]\\&-\Sigma_{tg}(\mathbf{r},t)\Phi_g(\mathbf{r},t)\\&+\sum_{g'=1}^{G}\Sigma_{s0,g'\to g}(\mathbf{r})\Phi_{g'}(\mathbf{r},t)\\&+f_g\sum_{g'=1}^{G}\nu\Sigma_{fg'}(\mathbf{r})\Phi_{g'}(\mathbf{r},t),\end{aligned} \tag{6.19}$$

for $g=1,\ldots,G$ and $\mathbf{r}\in V$, supplemented with the following boundary condition

$$\alpha_g(\mathbf{r}_b)\Phi_g(\mathbf{r}_b)+\beta_g(\mathbf{r}_b)\mathbf{n}\mathbf{J}_b(\mathbf{r}_b)=0, \tag{6.20}$$

for $g=1,\ldots,G$ and $\mathbf{r}\in\partial V$. The action of the diffusion operator is defined over the G-tuples $\Phi=(\Phi_1(\mathbf{r}),\ldots,\Phi_g(\mathbf{r}))$ where the $\Phi_g(\mathbf{r})$ group fluxes are sufficiently smooth to apply the diffusion operator $\mathcal{D}$ on them[1].

Now we consider the following homogeneous, linear boundary value problem:

$$\mathcal{D}\underline{\Phi}(\mathbf{r})=\lambda\underline{\Phi}(\mathbf{r}),\quad \mathbf{r}\in V \tag{6.21}$$

and

$$\mathbf{A}(\mathbf{r}_b)\Phi(\mathbf{r}_b)+\mathbf{B}(\mathbf{r}_b)\frac{\partial\Phi(\mathbf{r}_b)}{\partial\mathbf{n}}=0,\quad \mathbf{r}_b\in\partial V, \tag{6.22}$$

where $\mathbf{A}(\mathbf{r}_b)>0,\mathbf{B}(\mathbf{r}_b)>0$. We call λ the eigenvalue of the $\mathcal{D}$ operator, the $\Phi(\mathbf{r})\neq 0\in V$ function-the eigenfunction of the $\mathcal{D}$ operator.

Below we quote theorems from the mathematical literature [151],[161], but to avoid unnecessary details like definitions of avoidable mathematical terms, we quote the theorems in a simplified form.

6.1 Theorem *The diffusion operator $\mathcal{D}$ possesses the following properties:*

1. *$\mathcal{D}$ is a positive operator: $(\mathcal{D}\underline{\Phi},\underline{\Phi})\geq 0$.*
2. *There is a fundamental solution $\Phi_0(\mathbf{r})>0,\mathbf{r}\in V$ and real eigenvalue λ_0.*

Below we construct the eigenfunctions of the Laplace operator that we intend to use in the boundary value problems in later Chapters. For this purpose, we need the following theorem.

[1]This can be achieved in two ways: either the cross-sections are smooth functions of $\mathbf{r}$ or at the discontinuity of the cross-section, i.e. at internal boundaries, boundary conditions assure the continuity of the group fluxes and group currents.

6.2 Theorem *The solutions of the eigenvalue problem*

$$\boldsymbol{\nabla}^2 F_i(\mathbf{r}) = \lambda_i F_i(\mathbf{r}), \quad \mathbf{r} \in V \tag{6.23}$$

with boundary condition

$$A(\mathbf{r}_b)F_i(\mathbf{r}_b) + B(\mathbf{r}_b)F_i(\mathbf{r}_b) = 0 \quad \mathbf{r} \in \partial V \tag{6.24}$$

form a complete function system in V.

See Valdimirov's book [161] for the proof. Thus any function obeying the boundary condition (6.24) is expressible as a linear combination of $F_i(\mathbf{r})$ functions. The following version of theorem 6.1 will be useful. We remark that the class of elliptic operators is wider than then the Laplace operator, see [161].

6.3 Theorem *Let operator $\mathcal{O}$ be an elliptical operator. The solutions to the eigenvalue problem*

$$\mathcal{O}\Psi(\mathbf{r}) = \lambda\Psi(\mathbf{r}), \quad \mathbf{r} \in V \tag{6.25}$$

with the homogeneous boundary condition

$$A(\mathbf{r}_b)\Psi(\mathbf{r}_b) + B(\mathbf{r}_b)\frac{\partial\Psi(\mathbf{r}_b)}{\partial\mathbf{n}} = 0 \tag{6.26}$$

where $A(\mathbf{r}_b)$ and $B(\mathbf{r}_b)$ are given functions, n is the outward normal at the boundary point $\mathbf{r}_b$, form a complete orthonormal system in V.

The theorem is applicable to the time independent form of the diffusion equation (6.9) because it is an elliptic differential equation.

The operators involved in the diffusion equation (6.9) are not self adjoint because the neutrons are born from fission, in the fast groups, and the thermal neutrons cause fission in the thermal group or groups. To discuss the adjoint diffusion equation, we have to analyze the diffusion operator $\mathcal{D}$ in equation (6.19). First we separate the operators associated with energy transport processes and write $\mathcal{D}$ as

$$\mathcal{D} = \mathcal{L} + \mathcal{S}_{en} \quad \text{where } \mathcal{S}_{en} = \mathcal{R} + \mathcal{S} + \mathcal{F} \tag{6.27}$$

where $\mathcal{S}_{en}$ comprises the energy transfer processes. First, we consider an infinite homogeneous material with a space independent source $Q_g, g = 1, \ldots, G$. Since $\mathcal{S}_{en}$ contains only multiplications by cross-sections, in this case S_{en} is a matrix $\boldsymbol{\Sigma}$ acting on the flux vector $\underline{\Phi}$ and we have to solve the following algebraic problem:

$$\boldsymbol{\Sigma}\underline{\Phi} = \underline{Q}, \tag{6.28}$$

and we know that for any $\underline{Q} > 0$ the fluxes are positive henceforth $\boldsymbol{\Sigma}^{-1}$ must be a positive matrix. The diagonal elements of $\boldsymbol{\Sigma}$ contain all processes removing neutrons. In the off-diagonal element, appear such removals as scattering or fission. Therefore the diagonal elements are of opposite sign than the off- diagonal elements, and the diagonal elements are larger than any off-diagonal element. Such a matrix is called M-matrix, and its mathematical properties have been studied [169]. These properties are exploited in numerical methods.

The Green's function is discussed in Appendix A, we have applied it to the transport equation throughout the preceding Chapters. Now we are going to apply it to the diffusion

equation remarking that the basic properties of the Green's $\mathcal{G}(\mathbf{r}, \mathbf{r}_0)$ function remain unaltered. Let $\mathcal{A}, \mathcal{B}$ denote linear operators, acting on distributions over a subdomain V of the Euclidean space $\mathbb{R}^n$. We consider the boundary value problem

$$\begin{aligned} \mathcal{A}\Phi(x) &= Q(x), \quad x \in V \qquad (6.29) \\ \mathcal{B}\Phi(x) &= 0, \quad x \in \partial V, \qquad (6.30) \end{aligned}$$

where ∂V is assumed a smooth surface[2]. Operator $\mathcal{A}$ is usually a second order partial differential operator, $\mathcal{B}$ is at most a first order differential operator.

The Green's function of problem (6.29)-(6.30) is the solution of the following boundary value problem:

$$\begin{aligned} \mathcal{A}\mathcal{G}(x, x_0) &= \delta(x - x_0), \quad x, x_0 \in V \qquad (6.31) \\ \mathcal{B}\mathcal{G}(x, x_0) &= 0, \quad x \in \partial V. \qquad (6.32) \end{aligned}$$

The Green's function has the following properties: :

- $\mathcal{G}(x, x_0) = \mathcal{G}(x_0, x)$ i.e. the Green's function is symmetric in its two arguments;
- The Green's function is bounded in V: $0 < \mathcal{G}(x, x_0) \leq K/|x - x_0|^2$;
- The Green's function is continuous in either variables ;
- $\mathcal{G}(x, x_0)$ has continuous first derivatives provided neither x nor x_0 lies on the boundary.

Using the properties of the Green's function, we find

$$\mathcal{A} \int_V \mathcal{G}(x, x_0) Q(x_0) dx_0 = \int_V \delta(x - x_0) Q(x_0) dx_0 = Q(x),$$

which proves that the solution of problem (6.29)-(6.30) is

$$\Phi(x) = \int_V \mathcal{G}(x, x_0) Q(x_0) dx_0. \qquad (6.33)$$

When $\mathcal{A}$ is a differential operator, it is often possible to find its eigenvalues and eigenfunctions:

$$\mathcal{A}\psi_k(x) = \lambda_k \psi_k(x), \quad k = 1, 2, \ldots \qquad (6.34)$$

and the eigenfunctions are orthonormal:

$$\int_V \psi_k(x) \psi_j(x) dx = \delta_{kj}, \qquad (6.35)$$

and, the Green's function is

$$\mathcal{G}(x, x_0) = \sum_{k=1}^{\infty} \frac{1}{\lambda_k} \psi_k^*(x_0) \psi_k(x), \quad x, x_0 \in V. \qquad (6.36)$$

When the differential equation (6.29)-(6.30) is difficult to solve, with the help of the Green's function the problem can be transformed into an integral equation. Consider the following frequently encountered problem:

$$\mathcal{A}\Phi(x) = \lambda \mathcal{B}\Phi(x), \quad x \in V. \qquad (6.37)$$

[2]We will apply the below presented results to regions of polygonal boundaries. There is a correct mathematical term, the *rectangular like* domain with which the contradiction is resolvable[179].

We consider the right hand side as a source and using the Green's function of operator $\mathcal{A}$ we arrive at the integral equation

$$\Phi(x) = \lambda \int_V \mathcal{G}_A(x, x_0)\mathcal{B}\Phi(x')dx'. \tag{6.38}$$

Finally, we note a useful property of the cross-section matrix in the diffusion equation (6.28). The elements of $\mathbf{\Sigma}$ are real therefore its eigenvalues as well as eigenvectors are either real or are in complex conjugated pairs. That property is also useful in numerical methods.

The adjoint static diffusion equation takes the following form:

$$(\mathcal{L}^+ + \mathcal{R}^+ + \frac{1}{k}\nu\mathcal{F}^+)\underline{\Phi}(\mathbf{r}) = 0, \tag{6.39}$$

where the superscript + refers to adjoint operator or matrix. That problem is involved in reactivity effect analysis, where importance weighted expressions are used and in perturbation theory, see Section 3.6.

Habetler and Martino approached the problem of fundamental solution differently. In multigroup diffusion theory [151] they write the neutron balance equation in a different form, this time to emphasize the energy transfer processes:

$$\frac{\partial\underline{\Phi}(\mathbf{r}, t)}{\partial t} = (\mathbf{L} + \mathbf{R} + \nu\mathbf{F})\underline{\Phi}(\mathbf{r}, t), \tag{6.40}$$

where $\underline{\Phi}(\mathbf{r}, t) = (\Phi_1(\mathbf{r}, t), \ldots, \Phi_G(\mathbf{r}, t))$ is the flux vector in the G energy group, $\mathbf{L} = diag(\mathcal{L}_1, \ldots, \mathcal{L}_G)$ is the diagonal leakage matrix, its elements are operators:

$$\mathcal{L}_j\Phi_j(\mathbf{r}) = \boldsymbol{\nabla}\left[D_j\boldsymbol{\nabla}\Phi_j(\mathbf{r})\right] \tag{6.41}$$

where D_j is the position dependent diffusion constant in energy group j and

$$\mathbf{D} = diag(D_1, D_2, \ldots, D_G), \tag{6.42}$$

matrix $\mathbf{R}$ replaces the removal operator, which is now

$$R_{ij} = \Sigma_{ti} + \Sigma_{si} - \Sigma_{s,j\to i}, \tag{6.43}$$

where $\Sigma_{s,j\to i}$ is the scattering cross-section from group j to group i and

$$\Sigma_{si} = \sum_{j=1}^{G} \Sigma_{i\to j}. \tag{6.44}$$

The following matrix $\mathbf{F}$ replaces the fission operator $\mathcal{F}$:

$$F_{ij} = \frac{\chi_i}{k}\nu\Sigma_{fj}, \;\; 1 \le i, j \le G. \tag{6.45}$$

Here χ_i is the fission spectrum in group i.

The solution of equation (6.40) refers to a regular, connected region V, which is the union of finite number of disjoint regions. The number of energy groups is G, each matrices $\mathbf{\Sigma}$ and $\mathbf{F}$ have G^2 elements, respectively, each $f_{ij}(\mathbf{r}) \ge 0$ in V, $a_{ij}(\mathbf{r}) \ge 0$, $a_{jj} \le 0$, each $D_j(\mathbf{r}) \ge 0$. We seek solutions having the following properties called $P1$:

- Each $\Phi_i(\mathbf{r})$ has bounded and continuous second-order derivatives in V;

- $\Phi_i(\mathbf{r})$ and the normal component of $D_i(\mathbf{r})\boldsymbol{\nabla}\Phi_i(\mathbf{r})$ are continuous across the interface between subregions;
- $\Phi_i(\mathbf{r})$ satisfies $\Phi_i(\mathbf{r})+\Gamma_i(\mathbf{r})\partial\Phi_j(\mathbf{r})/\partial n = 0$ (out-going partial current) on the boundary ∂V, where $\Gamma_i(\mathbf{r}) \geq 0$ for all i is the modified albedo in group i.

Habetler and Martino stipulate the following features of the operators:

- Each of the $\mathcal{L}_i$ operators is self-adjoint and has a Green's function $\mathcal{G}_i(\mathbf{r}, \mathbf{r}')$ and the Green's function possesses the properties 6.2:

$$\int_V G_i(\mathbf{r}, \mathbf{r}')D_i\Phi_i(\mathbf{r}')d^3\mathbf{r}' = -\Phi_i(\mathbf{r}), i = 1, \ldots, G; \tag{6.46}$$

  where $\Phi_i(\mathbf{r})$ has property $P1$.
- $\mathcal{G}_i(\mathbf{r}, \mathbf{r}')$ is continuous in $\mathbf{r}$ and $\mathbf{r}'$ in V.
- $\mathcal{G}_i(\mathbf{r}, \mathbf{r}')$ has continuous first derivatives provided $\mathbf{r} \neq \mathbf{r}'$ and neither $\mathbf{r}$ nor $\mathbf{r}'$ lies on a boundary or material interface.
- $\mathcal{G}_i(\mathbf{r}, \mathbf{r}')$ possesses properties P1 when $\mathbf{r}'$ is not on a material interface.
- There exists a number M such that

$$|\mathcal{G}_j(\mathbf{r}, \mathbf{r}') \leq \frac{M}{|\mathbf{r} - \mathbf{r}'|}; \quad \left|\frac{\partial\mathcal{G}_i}{\partial x}\right| + \left|\frac{\partial\mathcal{G}_i}{\partial y}\right| + \left|\frac{\partial\mathcal{G}_i}{\partial z}\right| \leq \frac{M}{|\mathbf{r} - \mathbf{r}'|^2}. \tag{6.47}$$

With the help of the introduced Green's function, the inverse of the leakage matrix can be given. It is a diagonal matrix, the entries being the Green's function of the leakage in the given energy group. The operator

$$\mathbf{L}^{-1} = -\delta_{jk}\int G_j(\mathbf{r}, \mathbf{r}')d^3\mathbf{r}'; 1 \leq j, k \leq G$$

is the inverse of $\mathcal{D}$ in the following sense:

$$\mathcal{D}^{-1}\mathcal{D}\Phi(\mathbf{r}) = \Phi(\mathbf{r}). \tag{6.48}$$

Since operator $\mathcal{D}^{-1}$ is self adjoint, it has a complete sequence of orthonormal eigenfunctions:

$$\mathcal{D}^{-1}F_j(\mathbf{r}) = \frac{1}{\alpha_j}F_j(\mathbf{r}), j = 1, 2, \ldots. \tag{6.49}$$

It can be shown [151] that eigenfunction F_1 possesses properties P1 thus has physical meaning, it is called fundamental solution. Finally, the following theorem claims the existence of a physically reasonable fundamental solution.

6.4 Theorem (Fundamental eigenfunction) *The time-independent eigenvalue problem [151] with no up-scattering*

$$\mathcal{F}(\mathcal{D} + \mathcal{L})^{-1}\Phi(\mathbf{r}) = \lambda_1\Phi(\mathbf{r}) \tag{6.50}$$

has a positive dominant eigenvalue λ_0, i.e. $\lambda_0 > |\lambda_k|$, $k \neq 0$ which is simple, $\Phi(\mathbf{r})$ corresponds to an eigenfunction $\Phi_0 = (\Phi_{01}(\mathbf{r}), \Phi_{02}(\mathbf{r}), \ldots, \Phi_{0,G}(\mathbf{r})) > 0$. The adjoint eigenfunction corresponding to λ_0 has all its components positive throughout V.

6.3. Derivation and limitations

In the derivation of the diffusion equation (6.9) we have made approximations. Now we assess them one by one. This is done to see the limitations of diffusion theory and to indicate possible improvements when diffusion theory proves to be inadequate.

The first assumption in the derivation is that we neglected the second, and higher moments of the angular flux. The first few terms in the expansion of the angular flux are:

$$\Phi_g(\mathbf{r},\mathbf{\Omega}) = \frac{1}{4\pi}\Phi_g(\mathbf{r}) + \frac{3}{4\pi}\sum_i J_{gi}(\mathbf{r})\Omega_i + \frac{5}{4\pi}\sum_i\sum_j L_{g,ij}(\mathbf{r})\Omega_i\Omega_j \tag{6.51}$$

where $\Phi_g(\mathbf{r})$ is the scalar flux, J_{gi} is the i-th component of the net current, and the usually neglected $L_{g,ij}$ is called the level. The scalar flux is obtained from the angular flux as

$$\Phi_g(\mathbf{r}) = \int 4\pi\Phi_g(\mathbf{r},\mathbf{\Omega})d\mathbf{\Omega}, \tag{6.52}$$

the components of the net currents are obtained as

$$J_{gi}(\mathbf{r}) = \int_{4\pi}\Phi_g(\mathbf{r},\mathbf{\Omega})\Omega_i d\mathbf{\Omega}, \tag{6.53}$$

and finally the levels $L_{g,ij}$ are

$$L_{g,ij}(\mathbf{r}) = \int_{4\pi}\Phi_g(\mathbf{r},\mathbf{\Omega})\Omega_i\Omega_j d\mathbf{\Omega}. \tag{6.54}$$

The diagonal level components are given by

$$L_{g,ii}(\mathbf{r}) = \Phi_g(\mathbf{r}) + \int_{4\pi}P_2(\mathbf{\Omega})\Phi_g(\mathbf{r},\mathbf{\Omega})d\mathbf{\Omega}, \tag{6.55}$$

and they play role in the boundary condition formulation in the spherical harmonics method [163], [162]. From equation (6.55) it is clear, that the level may not be neglected in a number of cases as the diagonal elements include the scalar flux.

The partial currents are given by (3.148) and (3.149) in diffusion theory. They must be positive by definition, that condition sets a limit to the gradient:

$$|\mathbf{\nabla}\Phi_g| \leq \frac{2\Phi_g}{D_g}. \tag{6.56}$$

It means the diffusion theory is applicable if the flux gradient is smaller than the above given limit. A limit for the gradient of the scalar flux is obtainable also from the integral form of the transport equation, see [164][p. 191-194]. Let us assume that in the source term of (3.177) only the scattering cross-section is present in a homogeneous material, and expand the space variable in $Q(\mathbf{r}')$ into a Taylor series around $\mathbf{r}' = \mathbf{r}$:

$$Q(\mathbf{r}') \approx \Sigma_{sg}\Phi_g(\mathbf{r}') \approx \Sigma_{sg}\left(\Phi_g(\mathbf{r}) + \mathbf{\Omega}(s'-s)\mathbf{\nabla}\Phi_g(\mathbf{r})\right) \tag{6.57}$$

where the scattering is assumed not to change the group index g. A new relationship between the net current and the flux gradient is obtained if we substitute (6.57) into the integral transport equation

$$\Phi_g(\boldsymbol{\omega},t) = \int_0^{s_0}\exp\left(-\Sigma_g(s',s)\right)Q_g(\mathbf{r}-s\mathbf{\Omega},\mathbf{\Omega},t-\frac{s'-s}{v})ds', \tag{6.58}$$

multiply both sides by $\mathbf{\Omega}$, and integrate over 4π for $\mathbf{\Omega}$. We obtain the following approximation for the diffusion coefficient:

$$D_g \approx \frac{1}{3}\frac{\Sigma_{sg}}{\Sigma_{tg}^2}. \tag{6.59}$$

When in (6.57) we retain the higher order terms, the net current–flux gradient relation would not be valid. Thus diffusion theory is applicable far from strong absorbers, far from material boundaries, in general where the scalar flux is closely isotropic and varies slowly with the position.

We neglected the time derivative of the current. When we retain the time derivative we obtain the following relation instead of Fick's law:

$$\frac{1}{\tau_g}\frac{\partial J_g(\mathbf{r},t)}{\partial t} = -J_g(\mathbf{r},t) + \sum_{g'=1}^{G}\frac{\Sigma_{s1,g'\to g}}{\Sigma_{tg}}J_{g'}(\mathbf{r},t). \tag{6.60}$$

Here $\tau_g = v_g\Sigma_{tg}$ is a relaxation time. The order of τ_g is $10^4 - 10^5$ s thus the correction is negligible for two reasons. Firstly, in time dependent problems the delayed neutrons play the determining role, see Chapter 7.1. Secondly, the modification is small although it alters the type of the diffusion equation, that now has transformed into the telegrapher's equation:

$$\begin{aligned}\frac{1}{v_g^2}\frac{\partial^2\Phi_g(\mathbf{r},t)}{\partial t^2} + \frac{1}{v_g}\frac{\partial\Phi_g(\mathbf{r},t)}{\partial t} = \boldsymbol{\nabla}\left[D_g(\mathbf{r})\boldsymbol{\nabla}\Phi_g(\mathbf{r},t)\right] \\ - \Sigma_{tg}(\mathbf{r},t)\Phi_g(\mathbf{r},t) \\ + \sum_{g'=1}^{G}\nu\Sigma_{s0,g'\to g}(\mathbf{r})\Phi_{g'}(\mathbf{r},t) \\ + f_g\sum_{g'=1}^{G}\nu\Sigma_{fg'}(\mathbf{r})\Phi_{g'}(\mathbf{r},t) \\ + Q_0(\mathbf{r},t).\end{aligned} \tag{6.61}$$

The essential difference between the telegrapher's equation and the diffusion equation is that in the diffusion equation any change in the external source immediately appears in the solution as though the action speed would be infinite. In the telegrapher's equation the action speed is finite, we speak of neutron waves propagating with a finite speed.

Note that if the scattering kernel in (6.60) is not diagonal, the current in group g is connected to the gradient of the scalar fluxes in other energy groups, in other words, the diffusion coefficient is a matrix in the energy groups. This approximation has appeared in the equivalent cross-section generation, among others in Section 9.1 of Chapter 9.

6.4. One group diffusion theory

We start with the static diffusion equation. Using the asymptotic theory, see Section 4.1 in Chapter 4, in a periodic structure of cells the leading term in the flux Φ_0 is the product of two functions:

$$\Phi_0(\mathbf{r},E,t) = u_0(\mathbf{r},E)\Phi(\mathbf{r},t) \tag{6.62}$$

where u_0 is periodic in $\mathbf{r}$. Now we use the diffusion approximation and discard the time dependence. When the cell is small, u_0 is constant in space and the energy and space dependence is separated. This observation makes it possible to integrate (6.62) over the energy E

and introduce the following spectrum averaged constants called one group constants:

$$D(\mathbf{r}) = \frac{\int_0^\infty D(\mathbf{r},E)u_0(\mathbf{r},E)dE}{\overline{u}_0} \tag{6.63}$$

$$\Sigma_a(\mathbf{r}) = \frac{\int_0^\infty \Sigma_a(\mathbf{r},E)u_0(\mathbf{r},E)dE}{\overline{u}_0} \tag{6.64}$$

$$\nu\Sigma_f(\mathbf{r}) = \frac{\int_0^\infty \nu\Sigma_f(\mathbf{r},E)u_0(\mathbf{r},E)dE}{\overline{u}_0} \tag{6.65}$$

$$\frac{1}{v(\mathbf{r})} = \frac{\int_0^\infty \frac{1}{v}u_0(\mathbf{r},E)dE}{\overline{u}_0} \tag{6.66}$$

$$Q(\mathbf{r}) = \frac{\int_0^\infty Q(\mathbf{r},E)u_0(\mathbf{r},E)dE}{\overline{u}_0} \tag{6.67}$$

where

$$\overline{u} = \int_0^\infty u_0(\mathbf{r},E)dE. \tag{6.68}$$

The result is that the cross-sections depend only on $\mathbf{r}$:

$$D(\mathbf{r})\boldsymbol{\nabla}^2\Phi(\mathbf{r}) - \Sigma_a(\mathbf{r})\Phi(\mathbf{r}) + \nu\Sigma_f(\mathbf{r})\Phi(\mathbf{r}) = Q(\mathbf{r}), \mathbf{r} \in V \tag{6.69}$$

with the boundary condition

$$A(\mathbf{r}_b)\Phi(\mathbf{r}_b) + B(\mathbf{r}_b)n\boldsymbol{\nabla}\Phi(\mathbf{r}_b) = 0, \quad \mathbf{r} \in \partial V. \tag{6.70}$$

The problem is amenable only to numerical solution methods discussed in Chapter 8. We organize the solution of the problem so that subdivide V into so many sub-volumes that cross-sections are practically constant in each sub-volume, and internal boundary conditions connect the sub-volumes. This requires the analysis of the one-group diffusion equation with constant coefficients:

$$D\boldsymbol{\nabla}^2\Phi(\mathbf{r}) + (\nu\Sigma_f - \Sigma_a)\Phi = Q(\mathbf{r}). \tag{6.71}$$

The solution can be given with the help of the Green's function:

$$\Phi(\mathbf{r}) = \int_V \mathcal{G}(\mathbf{r}-\mathbf{r}')Q(\mathbf{r}')d^3\mathbf{r}', \tag{6.72}$$

where

$$\boldsymbol{\nabla}^2\mathcal{G}(\mathbf{r}-\mathbf{r}') + (\nu\Sigma_f - \Sigma_t)\mathcal{G}(\mathbf{r}-\mathbf{r}') = \delta(\mathbf{r}'), \mathbf{r}, \mathbf{r}' \in V. \tag{6.73}$$

The Green's function is the key to the solution of (6.71).

The Green's function depends on the equation, e.g. in (6.73) the cross-sections may be constant or may depend on position; furthermore on the geometry of the region V. Some Green's functions are available in the literature, e.g. Polyanin's book [180] discusses several equation types. Below a short introduction is given to the determination of the Green's function. First we discuss the partial differential equations with constant coefficients. The general form of the equation is

$$P\left(\partial_{x_1}, \ldots, \partial_{x_n}\right)\mathcal{G}(x, x_0) = \delta(x - x_0) \tag{6.74}$$

where $x = (x_1, \ldots, x_n)$ and P is a polynomial of the partial differentials $\partial_{x_j}, j = 1, \ldots, n$ and δ is the n dimensional Dirac delta distribution. We apply the Fourier transform on (6.74), which leads to the substitution $\partial_{x_j} \to -ik_j, j = 1, \ldots, n$:

$$P(-ik_1, \ldots, -ik_n)\mathcal{F}\mathcal{G}(x, x_0) = 1, \tag{6.75}$$

where $\mathcal{F}$ is the operator of the Fourier transformation. The Green's function is obtained by the inverse Fourier transformation:

$$\mathcal{G}(x, x_0) = \mathcal{F}^{-1}\left(\frac{1}{P(-ik_1, \ldots, -ik_n)}\right). \tag{6.76}$$

This method immediately yields the Green's function of the infinite space (in arbitrary dimensions). When we need the Green's function of a finite domain, we need auxiliary technique, like the source image method. Further tricks are given in [55].

In the absence of an external source, the diffusion equation has nontrivial solution only when the cross-sections are dependent. The static solution belongs to the fundamental eigenvalue of the Laplace operator, this is the only positive eigenfunction in V. Let that eigenvalue be $-B_g^2$ where subscript g refers to 'geometry'. Thus if nontrivial solution exits, it must be the eigenfunction of the Laplace operator, and the cross-sections should satisfy

$$-B_g^2 D + (\nu\Sigma_f - \Sigma_a) = 0. \tag{6.77}$$

To ensure this, we introduce a free parameter by replacing $\nu \to \nu/k$, and the following choice of k guarantees the existence of a solution:

$$k = \frac{\nu\Sigma_f}{\Sigma_a + DB_g^2}, \tag{6.78}$$

or, dividing by Σ_a, we obtain

$$k = \frac{\frac{\nu\Sigma_f}{\Sigma_a}}{1 + \frac{D}{\Sigma_a}} = \frac{k_\infty}{1 + L^2 B_g^2}, \tag{6.79}$$

where

$$k_\infty = \frac{\nu\Sigma_f}{\Sigma_a} \tag{6.80}$$

is the infinite multiplication factor,

$$L^2 = \frac{D}{\Sigma_a} \tag{6.81}$$

is the square of the diffusion length. The k value by which the diffusion equation has a non-trivial solution is called effective multiplication factor and the notation k_{eff} is used for it[3].

The solution of the one-group diffusion equation is uniquely determined when one of the following is given along the boundary and it is not zero:

- scalar flux;
- entering partial current;

[3]In Section 5.5 of Chapter 5, it turns out that the migration of the neutrons during slowing down should be added to L^2.

- exiting partial current;
- net current;
- white boundary condition;
- black boundary condition;
- albedo boundary condition.

When the boundary condition is homogeneous, the solution contains a free normalization factor.

The boundary condition is fixed by a suitable material arrangement. The unreflected or bare reactor is obtained when the fissionable material is surrounded by vacuum. There at a distance, the so called extrapolation distance the scalar flux will be zero. The size of a given fissionable material with which $k_{eff} = 1$ establishes is called critical size, the mass of the fissionable material needed for the criticality is called the critical mass. The critical size and the critical mass depends on the cross-sections and the geometry. From a given material the critical mass is minimal for a sphere.

The term "diffusion" is used in several senses. Perhaps the best known is the reference to the particle diffusion through collisions, and the attached Fick's law (6.7) but there the wandering of the particle is a consequence of particle-particle collisions. In reactor physics, the neutron-neutron collisions are neglected, the neutron diffusion is realized by collisions with the host nuclei. One of the most important features of diffusion is its tendency to equalize differences in the neutron distribution, to smooth out rapid fluctuations. Its important mathematical feature is the linearity, in the absence of external sources the diffusion equation is linear in the flux $\Phi(\mathbf{r})$.

The integral form of the transport equation is applicable also in diffusion approximation, integrating the transport equation (3.132) over $\mathbf{\Omega}$ we get an integral equation for the scalar flux:

$$\Phi(\mathbf{r}, t) = \int_v \frac{\Sigma_s \Phi(\mathbf{r}', t - |\mathbf{r} - \mathbf{r}'|/v) e^{\Sigma_t |\mathbf{r} - \mathbf{r}'|}}{4\pi |\mathbf{r} - \mathbf{r}'|^2} d^3\mathbf{r}'. \tag{6.82}$$

The term

$$\frac{1}{4\pi |\mathbf{r} - \mathbf{r}'|^2}$$

is due to the assumed isotropic scattering, the scattered neutrons are equally distributed on the surface of the sphere of radius $|\mathbf{r} - \mathbf{r}'|$. The solution given by equation (6.82) to the diffusion equation corroborates the above mentioned properties of the diffusion equation.

In an infinite homogenous medium the stationary solution to the diffusion equation (6.9) can be given in closed for a couple of sources $Q(\mathbf{r})$. Let $Q(\mathbf{r})$ represent the source strength of a plane source, then

$$\Phi(x) = \frac{QL}{2D} e^{-|x|/L} \tag{6.83}$$

where x is the distance from the plane source,

$$L^2 = \frac{DN}{\Sigma_a}.$$

The flux of a line source is

$$\Phi(r) = \frac{Q}{2\pi D} K_0(r/L), \tag{6.84}$$

where K_0 is a modified Bessel function, see Appendix A.

Let the fissionable material (subscript c) in the core and the core is surrounded by a reflector (subscript r). The diffusion equation in the core is:

$$D_c \boldsymbol{\nabla}^2 \Phi_c(x) + \left(\frac{1}{k} \nu \Sigma_{fc} - \Sigma_{ac} \right) \Phi_c(x) = 0 \tag{6.85}$$

with the solution

$$\Phi_c(x) = a_c \sin(B_c x) + b_c \cos(B_c x) \tag{6.86}$$

where

$$B_c = \sqrt{\frac{\frac{1}{k} \nu \Sigma_{fc} - \Sigma_{ac}}{D_c}}. \tag{6.87}$$

The diffusion equation in the reflector is

$$D_r \boldsymbol{\nabla}^2 \Phi_r(x) - \Sigma_{ar} \Phi_r(x) = 0. \tag{6.88}$$

Its solution is

$$\Phi_r(x) = a_r e^{B_r x} + b_r e^{-B_r x}, \tag{6.89}$$

where

$$B_r = \sqrt{\Sigma_{ar}} D_r. \tag{6.90}$$

The solution is finite for any x when $a_r = 0$. Let the core-reflector boundary at x_b, where the flux and the current must be continuous thus we have the following internal boundary conditions:

$$\Phi_r(x_b) = \Phi_c(x_b) \tag{6.91}$$

and

$$D_r \frac{d\Phi_r(x_b)}{dx_b} = D_c \frac{d\Phi_c(x_b)}{dx_b}. \tag{6.92}$$

We place the origin of the coordinate system at the middle of the core, so that the material distribution is symmetric. Then the flux in the core must be positive and even function of x therefore $a_c = 0$. The remaining two constants, b_c and b_r have to be determined from (6.91) and (6.92):

$$b_r e^{-B_r x_b} = b_c \cos(B_c x_b) \tag{6.93}$$

$$b_r \left[D_r B_r e^{-B_r x_b} \right] = b_c \left[D_c B_c \sin(B_c x_b) \right]. \tag{6.94}$$

Upon dividing (6.94) by (6.93), we get the solvability condition:

$$D_r B_r = D_c B_c \tan(B_c x_b), \tag{6.95}$$

which is a transcendent equation to determine k in B_c in terms of x_b. That value of k is the critical eigenvalue k_{eff} making the reflected reactor critical. In other words, when the size of the core is fixed, the k_{eff} is determined by (6.95). On the other hand, when we seek the size of the core just making the reflected reactor critical, we have to find x_b such that $k_{eff} = 1$ be fulfilled.

When the core is unreflected, the criticality condition is

$$x_b B_c = \frac{\pi}{2}, \tag{6.96}$$

and we can compare the critical size of the reflected reactor with the critical size of the bare reactor. The difference is called reflector saving. The reflector saving depends on the

reflector thickness H_r, after $H_r = 2B_r$ the reflector saving reaches its asymptotic value, addig more reflector results in practically no saving. The physical reason of reflector saving is that a fraction of the neutrons leaking out from the core will be scattered back to the core.

The neutron flux is determined from (6.71), where the cross-sections may depend on $\mathbf{r}$. Some solution methods are discussed in Chapter 8. Here we mention only that in reactor physics the scalar flux $\Phi(\mathbf{r})$ usually varies slowly therefore the numerical methods based on low order polynomial applications are used. When the material composition is strongly heterogeneous, or anisotropic, more sophisticated methods may be needed.

6.5. Few group diffusion theory

Below we discuss the eigenvalues and eigenfunctions of the diffusion operator in a homogeneous V. When the material parameters depend on position, we can subdivide the volume into sub-volumes where the material parameters are constant, and we see the sub-volumes by boundary conditions along the joint boundaries.

The static diffusion equation in a homogeneous volume takes the following form:

$$\begin{aligned} 0 =& \boldsymbol{\nabla}\left[D_g \boldsymbol{\nabla}\Phi_g(\mathbf{r})\right] - \Sigma_{tg}\Phi_g(\mathbf{r},t) \\ &+ \frac{1}{k}\sum_{g'=1}^{G} \nu\Sigma_{s0,g'\to g}\Phi_{g'}(\mathbf{r},t) + f_g \sum_{g'=1}^{G} \nu\Sigma_{fg'}\Phi_{g'}(\mathbf{r},t), \end{aligned} \tag{6.97}$$

where k is a given number such that the considered V is subcritical. We introduce the diagonal matrix formed from the diffusion constants:

$$\mathbf{D} = diag(D_1, \ldots, D_G), \tag{6.98}$$

and the energy transfer matrix S:

$$S_{gg'} = -\Sigma_{tg}\delta_{gg'} + \nu\Sigma_{s0,g'\to g} + \frac{1}{k} f_g \nu\Sigma_{fg'}, \tag{6.99}$$

for $1 \le g, g' \le G$, and the diffusion equation now takes the following simple form:

$$\mathbf{D}\boldsymbol{\nabla}^2\underline{\Phi}(\mathbf{r}) + \mathbf{S}\underline{\Phi}(\mathbf{r}) = 0, \mathbf{r} \in V. \tag{6.100}$$

Firstly, we solve the eigenvalue problem of matrix $\mathbf{D}^{-1}\mathbf{S}$:

$$\mathbf{D}^{-1}\mathbf{S}\underline{t}_i = \lambda_i^2 \underline{t}_i, \quad i = 1, \ldots, G. \tag{6.101}$$

Secondly, we create an eigenfunction of the Laplace operator associated with the eigenvalue $-\lambda_i^2$ and meeting one of the prescribed homogeneous boundary conditions ($\alpha_g(\mathbf{r}_b)$ and $\beta_g(\mathbf{r}_b)$ are given functions)

$$\alpha_g(\mathbf{r}_b)\Phi_g(\mathbf{r}_b) + \beta_g(\mathbf{r}_b)\Phi_g(\mathbf{r}_b) = 0, \quad \mathbf{r}_b \in \partial V; \quad g = 1, \ldots, G. \tag{6.102}$$

The eigenvalues of the cross-section matrix $\mathbf{S}$ may be positive and negative as well. The required function is

$$\underline{\Phi}(\mathbf{r}) = \sum_{k=1}^{G} \underline{t}_k \int_0^{2\pi} w_k(\theta) e^{i\lambda_k \mathbf{e}(\theta)\mathbf{r}} d\theta, \tag{6.103}$$

where

$$\mathbf{e}(\theta) = (\cos(\theta), \sin(\theta)), \tag{6.104}$$

and the weight function $w_k(\theta)$ should be chosen so that (6.102) is met. In (6.103), the exponential function decomposes either into trigonometric functions or hyperbolic functions depending on the sign of the eigenvalue λ_k^2.

Note that the analytical solution (6.102) to the multigroup diffusion equation (6.97) satisfies the diffusion equation at every point $\mathbf{r} \in V$ and by a suitable choice of the weight functions $w_k(\theta)$ is able to accommodate any reasonable boundary condition. Consequently, it allows for arbitrarily accurate solution in a volume composed of sub-volumes with position independent material compositions. In a practical calculation, it suffices to use a second order approximation on a face, or, to use values of the flux, current or other physical quantity as boundary condition at three boundary points.

The flux is a physical quantity, we check if the solution is physically reasonable. The matrix $\mathbf{S}$ is non-singular, diagonally dominant, its diagonal elements are negative, the off-diagonal elements are positive. Its eigenvalues should be positive in V. Consider an infinite region with constant cross-sections and a constant source, then in the balance equation (6.97) the leakage term is zero, the cross-sections are constant thus the equation takes the following form:

$$\mathbf{S}\underline{\Phi} = \underline{Q}. \tag{6.105}$$

When the source elements are positive, the flux Φ should be positive hence the inverse of $\mathbf{S}$ should also be positive. When $\underline{Q} = 0$, there may exist a nontrivial solution when the determinant of $\mathbf{S}$ is zero. That condition fixes the free factor k in (6.99), that will be the infinite multiplication factor of the material having the cross-section matrix $\mathbf{S}$. The eigenvalues of matrix $\mathbf{S}$ determine possible material bucklings. The fundamental eigenvalue belongs to a positive eigenvector, the term associated with it in the solution of the diffusion equation gives a major contribution to the volume integrated flux. The other terms which are associated with non-positive eigenvectors give major contributions to the flux at the boundary and play dominant role in the boundary conditions. As an illustration, consider a two-group ($G = 2$) diffusion equation in slab geometry. The solution is

$$\underline{\Phi}(x) = e^{((B_1 x))}\underline{t}_1 + e^{(B_2 x)}\underline{t}_2 \tag{6.106}$$

where

$$\underline{t}_1 = \begin{pmatrix} 1 \\ \frac{D_2 B_1^2 + \Sigma_2 - \frac{f_2}{k}\nu\Sigma_{f2}}{\Sigma_{1\to 2} + \frac{f_2}{k}\nu\Sigma_{f1}} \end{pmatrix} \tag{6.107}$$

and

$$\underline{t}_2 = \begin{pmatrix} 1 \\ \frac{\Sigma_{2\to 1} + \frac{f_1}{k}\nu\Sigma_{f2}}{\Sigma_2 - \frac{f_2}{k}\nu\Sigma_{f2} - D_1 B_2^2} \end{pmatrix} \tag{6.108}$$

furthermore

$$B_1^2 = \frac{1}{2}\left[\beta_1 + \beta_2 + \sqrt{(\beta_1 - \beta_2)^2 + \frac{4\delta_1\delta_2}{D_1 D_2}}\right] \tag{6.109}$$

$$B_2^2 = \frac{1}{2}\left[\beta_1 + \beta_2 - \sqrt{(\beta_1 - \beta_2)^2 + \frac{4\delta_1\delta_2}{D_1 D_2}}\right] \tag{6.110}$$

where

$$\beta_i = \frac{\Sigma_i - \frac{f_i}{k}\nu\Sigma_{fi}}{D_i}, i = 1, 2;$$

$$\delta_i = \Sigma_{i\to i'} + \frac{f_{i'}}{k}\nu\Sigma_{fi}, i' \neq i.$$

The contributions to the average flux are:

$$\overline{\underline{\Phi}}_{B_1} = \frac{1}{2L}\int_{-L}^{+L} \underline{\Phi}(x)dx = \frac{\sinh(B_1 L)}{2LB_1}\underline{t}_1 \tag{6.111}$$

and

$$\overline{\underline{\Phi}}_{B_2} = \frac{1}{2L}\int_{-L}^{+L} \underline{\Phi}(x)dx = \frac{\sinh(B_2 L)}{2LB_2}\underline{t}_1 \tag{6.112}$$

We get explicit formulas by writing out explicitly equations (6.97) under the following assumptions. Fission takes place only in the thermal group, all the fission neutrons are born in the fast group. Only down scattering is assumed from the fast group to the thermal group. All the cross-sections are constant in space.

$$D_1\boldsymbol{\nabla}^2\Phi_1(\mathbf{r}) - (\Sigma_{a1} + \Sigma_{r1})\,\Phi_1(\mathbf{r}) + \nu\Sigma_{f2}\Phi_2(\mathbf{r}) = 0 \tag{6.113}$$

$$D_2\boldsymbol{\nabla}^2\Phi_2(\mathbf{r}) - \Sigma_{a2}\Phi_2(\mathbf{r}) + \Sigma_{r1}\Phi_1(\mathbf{r}) = 0 \tag{6.114}$$

In cylindrical geometry, the general form of the solution is

$$\Phi_1(r) = aJ_0(B_2 r) + bY_0(B_2 r) + cI_0(B_1 r) + dK_0(B_1 r) \tag{6.115}$$

$$\Phi_2 = at_{22}J_0(B_2 r) + bt_{22}Y_0(B_2 r) + ct_{12}I_0(B_1 r) + dt_{12}K_0(B_1 r) \tag{6.116}$$

where $t_1 = (t_{11}, t_{12})$, $t_2 = (t_{21}, t_{22})$ are given by (6.15) and (6.16), respectively[4].

Finally, in two energy groups, the k_∞ is

$$k_\infty = (1 + L_1^2 B_g^2)(1 + L_2^2 B_g^2) \tag{6.117}$$

where B_g is the geometrical buckling and the square of the diffusion length is

$$L_1^2 = \frac{DE_1}{\Sigma_{a1} + \Sigma_{r1}} \tag{6.118}$$

$$L_2^2 = \frac{D_2}{\Sigma_{a2}}, \tag{6.119}$$

with self explaining notation for the cross-sections.

After that short detour, investigate the criticality problem. Theorem 6.2 assures the eigenfunctions of the Laplace operator to form a complete orthonormal system in V. Theorem 6.1 assures the existence of a fundamental solution to the diffusion equation on any reasonable volume V. The static diffusion equation (6.97) has a non-identically zero solution only when the determinant of the matrix multiplying the fluxes is zero. That condition is an equation for the free parameter k, the number of roots equals the number of energy groups. Since the fission term in the balance equation must be real and positive, only one root remains, that root is called the effective multiplication factor, k_{eff}.

The eigenvectors of matrix $\mathbf{S}$ play an important role in the boundary condition. The solution proportional to the fundamental eigenvalue varies slowly with the position, consequently gives a major contribution to the volume averaged reaction rates. The other eigenvalues vary rapidly with the position, their contributions to the volume averaged reaction rates are smaller but they play a determining role in the boundary condition. Thus the spectrum of the boundary condition may induce spatial transients in V but the transients amplitude rapidly

[4]The Bessel functions in the solution appear because in a spherically symmetric geometry we have to integrate (6.103) over all directions.

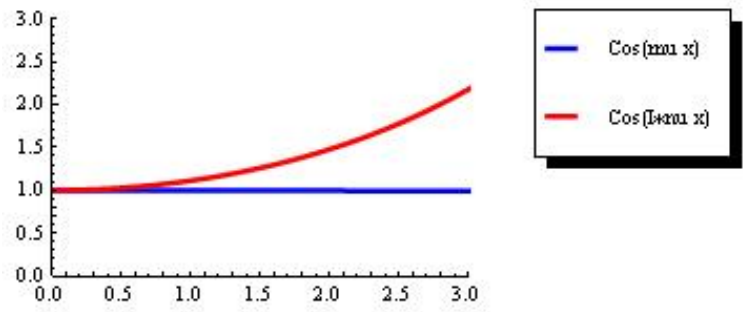

6.1. ábra. The fundamental mode (blue line) and the transient (red)

decreases with the distance from the boundary. As an illustration, we show a two energy group case from an IAEA PWR benchmark. The cross sections are $D_1 = 1.5$; $D2 = 0.4$; $\Sigma_{s1\to 2} = 0.02$; $\Sigma_{a1} = 0.01$; $\Sigma_{a2} = 0.08$; $\Sigma_{s2\to 1} = 0$; $\nu\Sigma_{f1} = 0$; $\nu\Sigma_{f2} = 0.135$ and all the fission source appears in the first energy group. The fundamental eigenvector is $\underline{t}_1 = (0.970774, 0.239994)$ with eigenvalue $B_1^2 = -0.00224972$; the transient eigenvector is $\underline{t}_2 = (0.406558, -0.913625)$ with eigenvalue $B_2^2 = 0.22225$. The space dependent part of the solution is $e^{B_i x}$ shown in Fig. 6.1. The figure clearly shows that the term involving the first root of (6.109) grows to three times larger than does the term involving the second root of (6.110).

6.6. RMs in diffusion theory

It is especially easy to determine the response matrices (RM) in a homogeneous volume in diffusion theory because we have the analytical solution (6.103). Before setting out to determine the response matrix, we recall that in diffusion theory the partial currents and the flux and net currents are interrelated, see (3.148) and (3.149). Let us write the relationship between entering and exiting currents as

$$\underline{J}_+ = \mathbf{R}\underline{J}_- \tag{6.120}$$

where

$$\underline{J}_\pm = (J_{1\pm}, \ldots, J_{G\pm}) \tag{6.121}$$

Using the relationships (3.148) and (3.149) we find the following relation between group fluxes and net currents on the boundary:

$$\underline{J}_n = \frac{1}{2}(\mathbf{R} - E)(\mathbf{R} + E)^{-1}\underline{\Phi}. \tag{6.122}$$

The structure of the response matrix is obtained from (6.103). We replace $w_k(\theta)$ by $c_k w_k(\theta)$ and require the new $w_k(\theta)$ to be normalized as

$$\int_0^{2\pi} w_k(\theta)d\theta = 1$$

for every k. Furthermore, we collect the column vectors $\underline{t}_k$ into matrix $\mathbf{T}$, then (6.103) takes the following concise form:

$$\Phi_g(\mathbf{r}) = \sum_{k=1}^{G} T_{kg} f_k(\mathbf{r}) c_k \tag{6.123}$$

where

$$f_k(\mathbf{r}) = \int_0^{2\pi} w_k(\theta) e^{i\lambda_k \mathbf{e}(\theta)\mathbf{r}} d\theta. \tag{6.124}$$

Using matrix notation, we rewrite (6.123) as

$$\underline{\Phi}(\mathbf{r}) = \mathbf{T} < f_k(\mathbf{r}) > \underline{c}. \tag{6.125}$$

Note that $\mathbf{r}$ dependence is encountered only in the diagonal matrix $< f_k(\mathbf{r}) >$, that fact facilitates the construction of various response matrices. The partial current, the net current, the average flux and average net current along a face are all formed from the scalar flux $\Phi(\mathbf{r})$ by operations acting solely on the space variable. Therefore the structure of equation (6.125) will be preserved.

We introduce operators forming the above mentioned physical quantities:

$$\underline{J}_- = \mathbf{A}_{in} \underline{\Phi}(\mathbf{r}) = \mathbf{T} < \mathcal{A}_{in} f_k(\mathbf{r}) > \underline{c} \tag{6.126}$$

$$\underline{J}_+ = \mathbf{A}_{out} \underline{\Phi}(\mathbf{r}) = \mathbf{T} < \mathcal{A}_{out} f_k(\mathbf{r}) > \underline{c} \tag{6.127}$$

$$\underline{J}_n = \mathbf{A}_{net} \underline{\Phi}(\mathbf{r}) = \mathbf{T} < \mathcal{A}_{net} f_k(\mathbf{r}) > \underline{c} \tag{6.128}$$

$$\underline{\Phi}_{av} = \mathbf{A}_{\Phi av} \underline{\Phi}(\mathbf{r}) = \mathbf{T} < \mathcal{A}_{\Phi av} f_k(\mathbf{r}) > \underline{c}, \tag{6.129}$$

and the operators $\mathcal{A}$ contain the operations acting on the scalar flux.

The response matrix that forms the net current from the entering currents is combined from (6.126) and (6.128) so that we express from (6.126) the constants c_k and substitute them into (6.128):

$$\underline{J}_n = \left(\mathbf{T} < \mathcal{A}_{out} f_k(\mathbf{r}) >< \mathcal{A}_{out} f_k(\mathbf{r}) >^{-1} \mathbf{T}^{-1} \right) \underline{J}_-. \tag{6.130}$$

The concrete forms of the $\mathcal{A}$ operators depend on the representation. The boundary condition may be fixed at specific point(s) of the boundary, usually at face centers or at Gaussian points to determine the face integrals precisely, but face average may be rendered to face centers, or the average, the first- and second moments along faces also may be used as boundary condition.

The general response matrix of a homogeneous region is similar to a diagonal matrix because when $\mathcal{A}$ is a response matrix then

$$\mathbf{T}^{-1} \mathcal{A} \mathbf{T} \tag{6.131}$$

is a diagonal matrix. This structure makes it easy to make response matrices corresponding to the special form preserved by a homogeneous material, c.f. Section 4.2 in Chapter 4. This observation also facilitates making such response matrices which preserve the shape of the face wise input and the output as discussed in Section 8.4 of Chapter 8. We have given the analytic solution in (6.125), where we encounter free parameters in the diagonal matrix

6.1. táblázat. Symmetry components of partial current moments

Subspace	m=0	m=1	m=2
1	$I_1+I_2+I_3+I_4$	0	$K_1+K_2+K_3+K_4$
2	0	$L_1+L_2+L_3+L_4$	0
3	$I_1-I_2+I_3-I_4$	0	$K_1-K_2+K_3-K_4$
4	0	$L_1-L_2+L_3-L_4$	0
5a	I_1-I_3	L_1-L_3	K_1-K_3
5b	I_2-I_4	L_2-L_4	K_2-K_4

$< f_k(\mathbf{r}) >$, viz. in the weight function. Below we discuss the selection of the weight function for a square node assuming we wish to retain three points or moments per face.

Assume that the boundary condition is described by second order functions at each face. Then the partial currents have three components: a constant, a linear and a quadratic, in notation $J_\pm = (J^0_\pm, J^1_\pm, J^2_\pm)$. Thus the boundary condition is given by $3n_F$ components, where n_F is the number of faces. We may exploit, however, the technique introduced in Section 3.6 of Chapter 1, then the face-wise forms are preserved although the constant, linear, and quadratic terms are mixed. We use the pattern 3.260 in a square shaped node, but now we have to account of three components and the response matrix looks like

$$\begin{pmatrix} J^0_+ \\ J^1_+ \\ J^2_+ \end{pmatrix} = \begin{pmatrix} T_{00} & T_{01} & T_{02} \\ T_{10} & T_{11} & T_{12} \\ T_{20} & T_{21} & T_{22} \end{pmatrix} \begin{pmatrix} J^0_- \\ J^1_- \\ J^2_- \end{pmatrix}. \tag{6.132}$$

Here T_{ij} has the following meaning. When the given entering current pattern is of order j then its contribution to the i-th order exiting current is T_{ij}. Since the pattern fixes the face-wise partial currents, T_{ij} is independent of the face index.

The preserved boundary patterns are connected to the transformation properties of the partial currents, and for example the constant partial currents at the four faces remain invariant under reflections but the linear terms change sign, the similar terms are not trivial [176]. The amplitudes at the four faces can be read out from the second column of Table 6.1. The pattern of the partial currents at the four faces of the square shaped cell is labeled here by the index of the invariant subspace, given in the first column of Table 6.1. We also read out which moments are mixed by the response matrix of a homogeneous square cell: the moments within a given line. We see from line 2, that averages and second moments induce each other.

Below we derive the most important response matrices for a homogeneous region.

1. *Slab geometry.* We describe the homogeneous material $-h \le x \le +h$ interval by one group cross-sections Σ and D, the flux is given by

$$\Phi(x) = a\cos(Bx) + b\sin(Bx) \tag{6.133}$$

where

$$B = \sqrt{\frac{\Sigma}{D}}. \tag{6.134}$$

Let $F_L = \Phi(-h)$ and $F_R = \Phi(+h)$. Since

$$\frac{F_L+F_R}{2} = a\cos(Bh); \quad \frac{F_R-F_L}{2} = b\sin(Bh) \tag{6.135}$$

furthermore the boundary currents are $J_L = DB(-a\sin(Bh) + b\cos(Bh))$ $J_R = DB(a\sin(Bh) - b\cos(Bh))$ we find

$$\frac{J_R - J_L}{2} = a\sin(Bh); \quad \frac{J_R + J_L}{2} = b\cos(Bh), \tag{6.136}$$

the boundary currents are expressed by the boundary fluxes as

$$J_R - J_L = \tan(Bh)F_L + F_R; \quad J_R + J_L = \cot(Bh)(F_R - F_L). \tag{6.137}$$

or

$$J_R = \frac{\tan(Bh) - \cot(Bh)}{2}F_L + \frac{\tan(Bh) + \cot(Bh)}{2}F_R \tag{6.138}$$

$$J_L = -\frac{\cot(Bh) + \tan(Bh)}{2}F_L + \frac{\cot(Bh) - \tan(Bh)}{2}F_R \tag{6.139}$$

therefore the response matrix is

$$\begin{pmatrix} J_L \\ J_R \end{pmatrix} = \mathbf{R}\begin{pmatrix} F_L \\ F_R \end{pmatrix} \tag{6.140}$$

where

$$\mathbf{R} = \begin{pmatrix} -\frac{\cot(Bh)+\tan(Bh)}{2} & \frac{\cot(Bh)-\tan(Bh)}{2} \\ \frac{\tan(Bh)-\cot(Bh)}{2} & \frac{\tan(Bh)+\cot(Bh)}{2} \end{pmatrix}. \tag{6.141}$$

2. *Square geometry.* In two- and three dimensional geometry, the boundary of the volume V is more complex and the derivation of the response matrix is more complicated. To simplify the calculations, we choose the analytical solution in accordance with the geometry. In (6.124), we choose $w_k(\theta) = \delta(\theta - \theta_i)$ for $\theta_i = i\pi/4, i = 1, \ldots, 4$ and identify the four faces of the square with $(i-1)\pi/4 \leq \theta \leq i\pi/4$ for $i = 1, \ldots, 4$. With that choice, we have

$$f_k(\mathbf{r}) = \sum_{j=1}^{4} w_{kj} e^{i\lambda_k \mathbf{e}_j \mathbf{r}}, \tag{6.142}$$

and a possible choice of the $\mathbf{e}_j$ directions is:

$$\mathbf{e}_1 = (1,0), \mathbf{e}_2 = (0,1), \mathbf{e}_3 = (-1,0), e_{\mathbf{4}} = (0,-1). \tag{6.143}$$

We select the corresponding w_{kj} weight so that the calculation be simple, for example $(1,1,1,1), (1,-1,1,-1), (1,0,-1,0), (0,1,0,-1)$ and any four tuple can be expressed with those vectors, the result is

$$\begin{aligned} f_k(x,y) = {} & A_{k1}(\cos(\lambda_k x) + \cos(\lambda_k y)) \\ & + A_{k2}(\cos(\lambda_k x) - \cos(\lambda_k y)) \\ & + A_{k3}\sin(\lambda_k x) \\ & + A_{k4}\sin(\lambda_k y). \end{aligned} \tag{6.144}$$

and the flux is expressed as

$$\begin{aligned} \Phi_g(x,y) = \sum_{k=1}^{G} T_{kg}\big(& A_{k1}\cos(\lambda_k x) + \cos(\lambda_k y) \\ & + A_{k2}(\cos(\lambda_k x) - \cos(\lambda_k y)) \\ & + A_{k3}\sin(\lambda_k x) \\ & + A_{k4}\sin(\lambda_k y)\big). \end{aligned} \tag{6.145}$$

The advantage of using the functions (6.144) is that A_{k1} gives equal contributions to the four sides of the square as the decomposition (6.144) is the application of the decomposition (3.261) for diffusion theory. Accordingly, after a long but straightforward calculation we get the following relationship between the face averaged fluxes $\underline{\varphi}_g$ and face averaged net currents $\underline{J}_g$:

$$\underline{J}_g = \sum_{g'=1}^{G} \mathfrak{R}_{gg'} \varphi_{g'} \tag{6.146}$$

where $\mathfrak{R}_{gg'}$ is a 4×4 matrix possessing the following structure: its elements are cyclic: $R_{ij} = R_{|i-j|}$ and

$$R_0 = R_{k_1} + R_{k_2} + R_{k_3} \tag{6.147}$$

$$R_1 = R_{k_1} - R_{k_2} \tag{6.148}$$

$$R_2 = R_{k_1} + R_{k_2} - R_{k_3} \tag{6.149}$$

where R_{k_i} is the response matrix calculated from the flux proportional to A_{k_i} in (6.145).

Here we give the sketch of the calculation of the response matrix elements. First, we have to determine the face averaged fluxes at the faces of the square. Let the corner points be $(-a/2, -a/2), (+a/2, -a/2), (+a/2, +a/2), (-a/2, +a/2)$. We read out the four components of the space dependent flux from the four terms in (6.145). The average flux over the face $(-a/2, -a/2)$ is

$$F_1 = \frac{1}{a} \int_{-a/2}^{+a/2} \left[\cos(\lambda_k x) + \cos(\lambda_k a/2)\right] dx = a \cos\frac{\lambda_k a}{2} + \frac{2 \sin\frac{\lambda_k a}{2}}{\lambda_k}. \tag{6.150}$$

The average net current is

$$C_1 = -\int_{-a/2}^{+a/2} D_g \left.\frac{\partial \cos(\lambda_k x) + \cos(\lambda_k y)}{\partial y}\right|_{y=-a/2} = D_g \int_{-a/2}^{+a/2} \lambda_k \sin\lambda_k y dy. \tag{6.151}$$

The integrals over the four sides give identical results. The four components in (6.145) are linearly independent thus the further steps of the calculations are identical for the four functions and we obtain the response matrices from (6.129) and (6.130).

The calculation is feasible also in three dimensions. Let volume V be a hexagonal pile, its faces are numbered so that faces $1, \ldots, 6$ are six rectangle, face No. $7, 8$ is the top, and bottom hexagon, respectively. The partial current vectors have 8 components numbered in accordance with the face numbering, thus J_+^7 is the exiting currents at the top of the hexagonal pile. We separate the six radial partial currents $J_\pm^r \equiv J_\pm^i, i = 1, \ldots, 6$ and the two axial currents $J_\pm^a \equiv J_\pm^i, i = 7, 8$ and with that notation the response matrix equation takes the following form:

$$\begin{pmatrix} J_+^r \\ J_+^a \end{pmatrix} = \begin{pmatrix} \mathbf{M}_{rr} & \mathbf{M}_{ra} \\ \mathbf{M}_{ar}^+ & \mathbf{M}_{aa} \end{pmatrix} \tag{6.152}$$

where

$$\mathbf{M}_{rr} = \begin{pmatrix} T & R_1 & R_2 & R_3 & R_2 & R_1 \\ R_1 & T & R_1 & R_2 & R_3 & R_2 \\ R_2 & R_1 & T & R_1 & R_2 & R_3 \\ R_3 & R_2 & R_1 & T & R_1 & R_2 \\ R_2 & R_3 & R_2 & R_1 & T & R_1 \\ R_1 & R_2 & R_3 & R_2 & R_1 & T \end{pmatrix} \tag{6.153}$$

and

$$\mathbf{M}_{ra} = \begin{pmatrix} A & A \\ A & A \\ A & A \\ A & A \\ A & A \\ A & A \end{pmatrix} \tag{6.154}$$

$$\mathbf{R}_{ar} = \begin{pmatrix} E & E & E & E & E & E \\ E & E & E & E & E & E \end{pmatrix} \tag{6.155}$$

$$\mathbf{R}_{aa} = \begin{pmatrix} C & B \\ B & C \end{pmatrix}. \tag{6.156}$$

6.7. Time dependence in diffusion theory

Most of the time dependent processes require either a more detailed description of the fission process, those technics are discusses in Chapter 7. Here we deal with a special problem: the solution of the time dependent diffusion equation in an infinite, homogeneous medium with a source periodic in time. These considerations allow us to express the general solution of the time dependent diffusion equation in terms of the eigenfunctions of the Laplace operator. Throughout the present Section, we deal with the following one group form of the time dependent diffusion equation:

$$\frac{1}{v}\frac{\partial\Phi(\mathbf{r},t)}{\partial t} = D\boldsymbol{\nabla}^2\Phi(\mathbf{r},t) - \Sigma_a\Phi(\mathbf{r},t) + Q(\mathbf{r},t), \quad \mathbf{r}\in V. \tag{6.157}$$

We expand the solution in terms of the eigenfunctions of the Laplace operator as

$$\boldsymbol{\nabla}^2\Psi_n(\mathbf{r}) = -B_n^2\Psi_n(\mathbf{r}), \quad n = 1, 2, \ldots \tag{6.158}$$

as the functions $\Psi_n(\mathbf{r})$ form a complete system in V to expand an arbitrary function with the same homogeneous boundary condition on the boundary ∂V.

First, investigate the neutron distribution in a source free medium if the initial neutron distribution $\psi_0(\mathbf{r})$ is given at $t = 0$. Then the flux at time t is

$$\Phi(\mathbf{r},t) = \psi_0(\mathbf{r})e^{-(vDB^2+v\Sigma_a)t}. \tag{6.159}$$

Now if we choose $\psi_0(\mathbf{r}) = \Psi_n(\mathbf{r})$ then in the case $Q(\mathbf{r},t) = 0$ in (6.157), we obtain the general time dependent solution to (6.157) as

$$\Phi(\mathbf{r},t) = \sum_n c_n e^{-(vDB_n^2+v\Sigma_a)t}\Psi_n(\mathbf{r}) \tag{6.160}$$

The constants c_n are determined by the initial condition $\psi_0(\mathbf{r})$ which always can be expressed by the eigenfunctions $\Psi_n(\mathbf{r})$. Rewrite (6.160) as

$$\Phi(\mathbf{r},t) = \sum_n c_n(t)\Psi_n(\mathbf{r}), \tag{6.161}$$

where the time dependent constant decrease exponentially with time. There are two exponents, each one corresponds to a physical process in which the neutron number decreases in V. The first one is leakage, the second one is absorption. Note that the exponent of

the leakage term the eigenvalue B_n of the Laplacian is encountered and the eigenvalues $B_n, n = 1, 2, \ldots$ can be numbered so that they increase with n, then the higher modes decrease faster, after a long time the lowest eigenvalue remains, see (3.143) in Chapter 3, Section 3.3 for the transport equation and because the $\Psi_n(\mathbf{r})$ functions vary more rapidly with increasing n, we observe again the equalizing property of the diffusion equation.

When the source is not zero in (6.157), we expand the source in an analogous manner:

$$Q(\mathbf{r}, t) = \sum_m q_m(t)\Psi_m(\mathbf{r}) \tag{6.162}$$

where

$$q_m(t) = \int_V Q(\mathbf{r}, t)\Psi_m(\mathbf{r})d^3\mathbf{r}. \tag{6.163}$$

Since the Ψ_m eigenfunctions are orthogonal when we seek the solution in the form of (6.161), the coefficients are the solutions of

$$\frac{1}{v}\frac{dc_n(t)}{dt} = -(DB_n^2 + \Sigma_a)c_n(t) + q_n(t), \tag{6.164}$$

with the solution

$$c_n(t) = e^{-v(DB_n^2 + Sigma_a)t}c_n(0) - \int_0^t e^{-v(DB_n^2 + Sigma_a)(t-t')}q_n(t')dt'. \tag{6.165}$$

We see from the solution that only the source components of low indices dominate after long time, again showing the smoothing feature of diffusion.

When the source is constant in time, (6.157) makes it possible to measure the diffusion length

$$\sqrt{\frac{D}{\Sigma_a}}$$

by measuring the spatial distribution of the neutron flux in a suitable, simple geometry.

Now we investigate, in a homogeneous media, the flux created by a localized thermal source of periodically varying strength. This time instead of (6.157) we study

$$\frac{1}{v}\frac{\partial\Phi(\mathbf{r}, t)}{\partial t} = D\boldsymbol{\nabla}^2\Phi(\mathbf{r}, t) - \Sigma_a\Phi(\mathbf{r}, t) + Q(\mathbf{r})e^{i\omega t}, \quad \mathbf{r} \in V. \tag{6.166}$$

We seek the solution in the form

$$\Phi(\mathbf{r}, t) = \phi(\mathbf{r})e^{i\omega t}.$$

The space dependent part is the solution of

$$\frac{i\omega}{v}\phi(\mathbf{r}) = D\boldsymbol{\nabla}^2\phi(\mathbf{r}) - \Sigma_a\phi(\mathbf{r}), \tag{6.167}$$

the solution if which are waves, in spherical geometry ϕ repends only on the radius r:

$$\phi(r) = c\frac{e^{\pm\mu r}}{r} \tag{6.168}$$

where

$$\mu^2 = \frac{\Sigma_a}{D} + \frac{i\omega}{Dv}. \tag{6.169}$$

Following Ref. [164][p. 213], we introduce an intermediate parameter

$$\rho^2 = \left[\left(\frac{\Sigma_a}{D} \right)^2 + \left(\frac{\omega}{Dv} \right)^2 \right]^{1/2} \tag{6.170}$$

and express the space and time dependent flux as

$$\Phi(r,t) \sim \frac{1}{r} e^{\pm r/a} e^{i(\omega t) - 2\pi r/l_w}, \tag{6.171}$$

where a is the attenuation distance

$$a = \sqrt{\frac{2}{\frac{\Sigma_a}{D}} + \rho^2}, \tag{6.172}$$

and l_w is the wave length

$$l_w = 2\pi \sqrt{\frac{2}{\rho^2 - \frac{\Sigma_a}{D}}}. \tag{6.173}$$

The wave propagation velocity v_w is given as

$$v_w = \omega \sqrt{\frac{2}{\rho^2 - \frac{\Sigma_a}{D}}}. \tag{6.174}$$

The propagation velocity increases with the frequency, thus the neutron waves disperse even in a homogeneous material. In the extreme cases when in ρ one of the two additive terms dominates, the velocity formula (6.174) becomes simple:

$$v_w = \sqrt{2Dv\omega} \tag{6.175}$$

when

$$\frac{\omega}{Dv} >> \frac{\Sigma_a}{D}$$

and

$$v_w = 2\sqrt{\frac{\Sigma_a}{D}} Dv \tag{6.176}$$

when

$$\frac{\omega}{Dv} << \frac{\Sigma_a}{D}.$$

The order of v_w is appr. $10^4 cm/sec$ in graphite.

The wavelength, velocity, and attenuation lengths are easily measurable. This is a convenient way to measure the diffusion coefficient D.

The time dependent processes will also be discussed in Sections 7.1, 7.3 of Chapter 7.

6.8. Problems

1. Solve the diffusion equation in the following homogeneous material: a) $D = 1.0$ cm, $\Sigma_a = 0.6$ $1/cm$, $\nu\Sigma_f = 0.2$ 1/cm. b)$D_1 = 1$ cm, $D_2 = 0.6$ cm, $\Sigma_1 = 0.1$ 1/cm, $\Sigma_{a2} = 0.08$ cm, Σ_{c2}=0.06 1/cm, the number of secondary neutrons is $\nu = 2.4$, they appear in group 1.

2. What is the critical size of the materials in Problem 1? What k_{eff} makes them critical?

3. What is the solution of the one-group diffusion equation in a homogeneous slab cell with the boundary condition $\Phi(0) = 1, J(0) = 0$?

4. Show that the diffusion equation takes the same form after the $x \to x + a$ translation!

5. Solve the diffusion equation in a two-region infinite cylinder!

6. Solve the unreflected diffusion equation in a two-region slab!

7. Solve the diffusion equation in a two-region cylinder if the second region is non-multiplying material!

8. Calculate $R_{ki}, i = 1, 2, 3, 4$ in (6.147)!

9. Show that in the previous problem $R_{k4} = R_{k3}$!

10. Determine matrices T, R_i, A, B, C, D, E in equations (6.152)-(6.156)! Use the following directions for the buckling vectors $B_i = (\cos\alpha_i, \sin\alpha_i)$ where $\alpha_i = (i-1)\pi/3$!

11. Calculate the partial neutron current J^+ and J^- at direction for the surface normal vector $\mathbf{N} = \left(1/2, \sqrt{3}/2, 0\right)$! Use the approximated vector flux:

$$\Psi(r, E, \mathbf{\Omega}) = \frac{1}{4\pi}\Phi(r, E) + \frac{3}{4\pi}\mathbf{\Omega}\mathbf{J}(r, E).$$

12. What is the radius and height ratio in critical cylinder, if the critical mass is minimal?

13. What is the critical radius of pure ^{235}U material which density is 18.8 g/cm^3? The non-zero microscopical cross sections are $\sigma_f = 1.6$ barn, $\sigma_s = 4$ barn and every fission produces average 2.5 neutrons. Use the diffusion approximation and the scattering is isotropic.

14. Solve the diffusion equation in homogeneous, isotropic neutron source with radius R, if the source emits 1 neutron/sec! The group constants are same in the internal and external spheres.

15. Provide an estimate of the neutron current in the diffusion and the neutron transport framework!

16. Determine the albedo of a finite (t thickness) reflector in one dimensional slab geometry! Investigate the $t \to \infty$ limit, too.

7. fejezet

Solution Methods

The solution method varies with the problem under consideration. In the present Chapter, we select a few typical problems: the solution of the kinetic equation, selected problems of the power distribution limits and the problem of setting up a calculational model for core design problem resolutions.

7.1. Kinetics

The present Section is dedicated to specific time dependent models. As we have seen in Chapter 1, the transport equation (3.116) accounts also of the time dependent problems, now we revise (3.116) for possible corrections.

In (3.116) each term describes a reactions rates. The neutron-nucleus reaction has the following phases:

- a collision between the neutron and the nucleus. The neutron velocity is in the order of $10^5\ cm/s$, the diameter of the nucleus is in the order of $10^{-12}\ cm$ thus the collision takes place in appr. $10^{-17}/s$;
- in the second phase the binding energy of the neutron as well as its kinetic energy is redistributed among the nucleons in a large number of collisions. That phenomenon is partly collective motion partly individual interaction between the nucleons.
- As a result of the interaction series between the nucleons, a group of nucleons may leave the range of the attractive nuclear forces and new reaction product(s) may appear.

From the above rather qualitative model it is seen that the nuclear reactions are rather fast, compared to any macroscopic phenomena, like neutron balance in the core, the process can be regarded as instantaneous.

In (3.116), we assumed the collision to be local, the scattered neutron or the fission product appear at the same position $\mathbf{r}$ where the neutron-nucleon collision took place. On the other hand, we have seen that the atoms move, their velocities follow the Maxwell distribution. As long as the reaction time of a nuclear reaction is not greater then the distance traveled by the atom during the neutron-nucleus reaction, the assumption on the neutron-nucleus reaction being local is acceptable.

Unfortunately, a fraction of the neutrons is not released in the above described prompt process. A part of the neutrons emerging from fission is prompt, but other neutrons appear after a cascade of nuclear reactions. Those neutrons are emitted instantaneously which appear not later than $10^{-8}\ sec$ after the fission event. Others are called delayed neutrons. As the excitation energy gained at the neutron capture is distributed between the fission fragments, which release their excitation energies in a sequence of nuclear reactions. These fission fragments are called delayed neutron precursors or precursors. The members of the cascade emitting delayed neutrons are called daughter nuclei. Consider the following example [173]. The ^{87}Br is a fission product, the β decay into the ground state is forbidden thus two transition routes are possible, both by β^- decay, the first one into the excited state of ^{87}Kr the other one into a lower energy state of ^{87}Kr, which is a daughter nucleus. ^{87}Kr emits a neutron and decays into the stable ^{86}Kr.

The delayed neutrons are arranged into six delayed neutron groups. A delayed neutron group has a decay constant and a relative abundance. For ^{235}U the delayed neutron group parameters are given, after [173][p. 6] in Table 7.1. We only mention here that the data depend on the fissionable isotope. The abundances are normalized so that

$$\sum_{i=1}^{6} a_i = 1$$

7.1. táblázat. Delayed neutron group decay constants λ_i and abundances a_i

Group No.	λ_i $[s^{-1}]$	a_i
1	0.0127	0.038
2	0.0317	0.213
3	0.115	0.188
4	0.311	0.407
5	1.40	0.128
6	3.87	0.026

where

$$\sum_{i=1}^{6} \beta_i = \beta; \quad \beta_i = a_i \beta.$$

but the delayed neutron fraction β, the mean number neutrons per fission and the delayed neutron factors of the delayed neutron groups depend also on the neutron spectrum, see [174].

The above given observations rearrange the structure of the time dependent transport equation, and make the transport formalism more intricate. Below we give the complete form of the transport equation with the delayed neutron groups by reassessing each term in the (3.116):

1. The leakage term does not change:

$$\mathcal{L}\Phi(\boldsymbol{\omega}, t) = -\boldsymbol{\nabla}\boldsymbol{\Omega}\Phi(\boldsymbol{\omega}, t). \tag{7.1}$$

2. The removal term does not change:

$$\mathcal{R}\Phi(\boldsymbol{\omega}, t) = \Sigma_t(\boldsymbol{\omega}, t)\Phi(\boldsymbol{\omega}, t) \tag{7.2}$$

3. In the fission term we have to take into account that the number of secondary neutrons varies with the delayed neutron groups:

$$\mathcal{F}\Phi(\boldsymbol{\omega}, t) = \sum_{j=1}^{6} f_{0j}(E) \int \Phi(\boldsymbol{\omega}' t)\nu_j(\boldsymbol{\omega}', t)\Sigma_f(\boldsymbol{\omega}', t)(1-\beta_j), dE'. \tag{7.3}$$

Here $f_{0j}(E)$ is the fission spectrum in the delayed neutron group j and from the decay of the precursors a new source appears:

$$\sum_{j=1}^{6} \lambda_j f_j(E) C_j(\mathbf{r}, t), \tag{7.4}$$

$f_j(E)$ standing for the spectrum of the emerging neutrons.

4. The scattering operator does not change:

$$\mathcal{S}\Phi(\boldsymbol{\omega}, t) = \int \Sigma_s(\mathbf{r}, E', \boldsymbol{\Omega}' \to E, \boldsymbol{\Omega})\Phi(\mathbf{r}, E', \boldsymbol{\Omega}')dE'd\boldsymbol{\Omega}'. \tag{7.5}$$

5. The external source does not change $Q(\boldsymbol{\omega}, t)$.

We have to complement the set of equations because the precursor densities also vary, they are formed in fission and they diminish by decay, the balance equation is:

$$\frac{\partial C_i(\mathbf{r},t)}{\partial t} = \sum_{j=1}^{N_f}\sum_{j=1}^{6}\int \beta_{ij}\nu_j\Phi(\mathbf{r},E',\mathbf{\Omega}',t)\Sigma_f(\mathbf{r},E',\mathbf{\Omega}',t)dE'd\mathbf{\Omega}' - \lambda_i C_i(\mathbf{r},t). \tag{7.6}$$

Here we allowed the possibility of more than one kind of fuel isotope being present in the core, their number is N_f, subscript j is associated with the fissionable isotopes in (7.6). The formalism has been presented only to show how intricate the problem is in its entirety.

To find the explicit relationship with the notation of Chapter 3, we introduce the following notation.

$$\mathcal{L}_0 = -\mathbf{\Omega}\boldsymbol{\nabla} - \Sigma_t + \int \Sigma_s(\mathbf{r},E'\to E,\mathbf{\Omega}\mathbf{\Omega}')d\mathbf{\Omega}'dE' \tag{7.7}$$

which is the removal operator plus the scattering term in the transport operator. We separate the prompt fission term from the delayed contributions:

$$\mathcal{M}_0 = \sum_{j=1}^{N_f}\frac{f_{0j}(E)}{4\pi}\int \nu_j(E')(1-\beta_j)\Sigma_{fj}(\mathbf{r},E')d\mathbf{\Omega}dE' \tag{7.8}$$

where subscript j labels the fissionable isotopes, the average number of secondary neutrons is ν_j the delayed neutron fraction is β_j. f_{0j} is the prompt yield of fissionable isotope j. The delayed fission operator for delayed neutron group i is

$$\mathcal{M}_i = \sum_{j=1}^{N_f}\frac{f_i(E)}{4\pi}\int \beta_{ij}\nu_j(E')\Sigma_{fj}(\mathbf{r},E')d\mathbf{\Omega}dE' \tag{7.9}$$

Here f_i is the fission spectrum in delayed neutron group i. The angular distribution of the fission neutrons is assumed isotropic. With the introduced operators the neutron and precursor balance becomes

$$\frac{\partial\Phi}{\partial t} = (\mathcal{L}+\mathcal{M}_0)\Phi + \sum_{i=1}^{6}\lambda_i f_i C_i \tag{7.10}$$

$$\frac{\partial C_i f_i}{\partial t} = \mathcal{M}_i\Phi - \lambda_i f_i C_i. \tag{7.11}$$

The last equation has been multiplied by f_i, c.f. (7.6). In a stationary reactor

$$(\mathcal{L}+\mathcal{M})\Phi_0(\mathbf{r},E,\mathbf{\Omega}) = 0 \tag{7.12}$$

holds, where

$$\mathcal{M} = \sum_{j=1}^{N_f}\frac{f_j(E)}{4\pi}\int \nu_j(E')\Sigma_{fj}(\mathbf{r},E')d\mathbf{\Omega}dE' \tag{7.13}$$

and the fission spectrum is defined for isotope j as

$$f_j(E) = (1-\beta_j)f_{0j}(E) + \sum_{i=1}^{6}\beta_{ij}f_j(E), \tag{7.14}$$

see equation (5.3). Equation (7.12) is linear in Φ_0 thus nontrivial solution exists if the involved $(\mathcal{L}+\mathcal{M})$ operator has a non empty null space. To this end, we introduce the k_{eff} is we did in Chapter 3. The only difference is that now we have to include the equation (7.6) for the precursor densities, which is only a formal difference.

7.2. Reactor kinetics

Consider equations (7.10)-(7.11) that we now rewrite in matrix form. We introduce the unknown vector $\underline{\psi}(t)$:

$$\underline{\psi} = \begin{pmatrix} \Phi(\mathbf{r}, E, \mathbf{\Omega}, t) \\ C_1(\mathbf{r}, t) f_1(E) \\ \vdots \\ C_6(\mathbf{r}, t) f_6(E) \end{pmatrix} \tag{7.15}$$

and the kinetic matrix

$$\mathbf{K} = \begin{pmatrix} \mathcal{L}+\mathcal{M} & \lambda_1 & \lambda_2 & \cdots & \lambda_6 \\ \mathcal{M}_1 & -\lambda_1 & 0 & \cdots & 0 \\ \mathcal{M}_2 & 0 & -\lambda_2 & \cdots & 0 \\ \vdots & 0 & \cdots & \ddots & 0 \\ \mathcal{M}_6 & 0 & 0 & \cdots & -\lambda_6 \end{pmatrix}, \tag{7.16}$$

and equations (7.10)-(7.11) are written in the new terms as

$$\frac{\partial \underline{\psi}}{\partial t} = \mathbf{K}\underline{\psi}. \tag{7.17}$$

If it is possible to determine the eigenvectors [173][Section 2]

$$\mathbf{K}\underline{\phi}_n = \omega_n \underline{\phi}_n, \quad n = 1, 2, \ldots, 7 \tag{7.18}$$

then

$$\underline{\psi}(t) = \sum_{n=0}^{\infty} (\underline{\phi}_n^+, \underline{\psi}(0)) \phi_n e^{i\omega t}. \tag{7.19}$$

We choose the initial condition

$$\Psi(\mathbf{r}, E, \mathbf{\Omega}, 0) = \delta(\mathbf{r} - \mathbf{r}_0)\delta(E - E_0)\delta(\mathbf{\Omega} - \mathbf{\Omega}_0), \tag{7.20}$$

i.e. a single neutron is present at $t = 0$ at $\mathbf{r}_0$, its energy is E_0 and it flies along direction $\mathbf{\Omega}_0$. When the initial state is stationary,

$$\underline{\psi}(t) = \sum_{n=0}^{\infty} \Phi_n^+(\mathbf{r}_0, E_0, \mathbf{\Omega}_0) \Phi_n(\mathbf{r}, E, \mathbf{\Omega}) e^{\omega_n t}. \tag{7.21}$$

We have seen in Chapter 3 that the real parts of the eigenvalues ω_n are all real and smaller than the fundamental eigenvalue which is zero therefore the higher modes disappear with the time.

To make the kinetic equations (7.10)- (7.11) more transparent, first we transform them and then introduce simplifications. The usual procedure [173], [165], [175] is to separate the angular flux into a time dependent amplitude $P(t)$ and a shape function $\phi(\mathbf{r}, E, \mathbf{\Omega}, t)$:

$$\Phi(\mathbf{r}, E, \mathbf{\Omega}, t) = P(t)\phi(\mathbf{r}, E, t). \tag{7.22}$$

We substitute (7.22) into (7.10)- (7.11) to arrive at

$$P(t)\frac{\partial \phi}{\partial t} + \phi \frac{dP}{dt} = P(t)(\mathcal{L}+\mathcal{M})\phi + \sum_{i=1}^{6} \lambda_i f_i C_i + Q \tag{7.23}$$

$$\frac{\partial f_i C_i}{\partial t} = P(t)\mathcal{M}_i(t)\phi - \lambda_i f_i C_i. \tag{7.24}$$

where the involved operators are given by (7.1),(7.9), and (7.13). We assume a static reference solution $\Phi_0(\mathbf{r}, E, \mathbf{\Omega})$ for the same reactor with $S = 0$ is given. The reference solution refers to a hypothetic reactor which is so close to the reactor under consideration that the differences can be considered as perturbations. We also assume that the adjoint fluxes $\Phi^+_{0n}, n = 1, 2, \ldots$ of the reference reactors are known. Form the scalar product of the terms in (7.23), (7.24) and the fundamental mode Φ^+_{00}. In the result, we use the scalar product notation:

$$(\Phi^+_{00}, \phi)\frac{dP}{dt} + P\frac{d}{dt}(\Phi^+_{00}, \phi) = P(\Phi^+_{00}, (\mathcal{L} + \mathcal{M})\phi) \tag{7.25}$$

$$+ \sum_{i=1}^{6} \lambda_i(\Phi^+_{00}, f_i C_i) + (\Phi^+_{00}, Q) \tag{7.26}$$

$$\frac{d}{dt}(\Phi^+_{00}, f_i C_i) = P(\Phi^+_{00}, M_i(t)\phi) - \lambda_i(\Phi^+_{00}, f_i C_i). \tag{7.27}$$

Note that in the approximation form (7.22) the normalization of $P(t)$ has not been fixed so we follow the normalization suggested by Henry [175]:

$$\frac{d(\Phi^+_{00}, \phi)}{dt} = \frac{d}{dt}\int_V \int\int \Phi^+_{00}(\mathbf{r}, E, \mathbf{\Omega})\phi(\mathbf{r}, E, \mathbf{\Omega}, t) d\mathbf{\Omega} dE d^3\mathbf{r} = 0. \tag{7.28}$$

$\Phi^+_{00}((\mathbf{r}, E, \mathbf{\Omega})$ is the importance of the neutrons in the reference solution, in (7.28) the total importance of the neutron in the state $\phi(\mathbf{r}, E, \mathbf{\Omega}, t)$ remains constant in time, and the shape function $P(t)$ should be chosen accordingly. Note that at the same time $\phi(\mathbf{r}, E, \mathbf{\Omega}, t)$ may change locally with t. This condition is fulfilled when the amplitude function is the ratio of the distribution Φ and of the distribution ϕ:

$$P(t) = \frac{(\Phi^+_{00}, \Phi)}{(\Phi^+_{00}, \phi)}. \tag{7.29}$$

When normalization of ϕ is such that the denominator be unity, the physical meaning of the amplitude $P(t)$ is the value of the total importance in the actual reactor at time t and not the total number of neutrons.

Now we return to the main kinetics equations (7.25) - (7.27), which serve for the determination the kinetics of the neutron field. With the chosen normalization of $P(t)$, the second term on the left hand side of (7.25) is zero. The reference reactor is assumed to be critical, whereas the real reactor under consideration is not. The difference is caused by the time dependent difference in the cross-sections. We write the cross-sections in the actual reactor as

$$\mathcal{L}(t) + \mathcal{M}(t) = \mathcal{L}_0 + \mathcal{M}_0 + \delta(\mathcal{L}_0(t) + \mathcal{M}_0(t)) \tag{7.30}$$

where subscript 0 refers to the static reference reactor. Substituting (7.30) into (7.25), using that

$$(\Phi^+_{00}, (\mathcal{L}_0 + \mathcal{M}_0)\phi) = 0$$

the following simple form is obtained for the kinetic equations:

$$\frac{dP}{dt} = \frac{\rho(t) - \beta_{eff}}{\Lambda} P(t) + \sum_{i=1}^{6} \lambda_i C_{i,eff}(t) + Q_{eff}(t) \tag{7.31}$$

$$\frac{dC_{i,eff}}{dt} = \frac{\beta_i}{\Lambda} P(t) - \lambda_i C_{i,eff}(t), \tag{7.32}$$

where we have introduced the following definitions: $\rho(t)$ is the reactivity extended to time dependent processes. Remember, the original definition in Chapter 3 had no time dependence. The time dependent reactivity is defined as

$$\rho(t) = \frac{1}{F}\left(\Phi_{00}^{+}, \delta(\mathcal{L}_0(t) + \mathcal{M}_0(t)), \phi\right). \tag{7.33}$$

β_{eff} is the effective delayed neutron fraction in the i-th delayed neutron group:

$$\beta_{eff,i} = \frac{1}{F}\left(\Phi_{00}^{+}, \delta\mathcal{M}_i(t), \phi\right) \tag{7.34}$$

and

$$\beta_{eff} = \sum_{i=1}^{6} \beta_{eff,i}. \tag{7.35}$$

The mean generation time Λ is

$$\Lambda = \frac{1}{F}\left(\Phi_{00}^{+}, \phi\right), \tag{7.36}$$

the normalization factor:

$$F = \left(\Phi_{00}^{+}, \mathcal{M}(t)\phi\right). \tag{7.37}$$

The effective source

$$Q_{eff} = \frac{1}{F\Lambda}\left(\Phi_{00}^{+}, Q\right), \tag{7.38}$$

and the effective delayed neutron precursor densities:

$$C_{i,eff} = \frac{1}{F\Lambda}\left(\Phi_{00}^{+}, f_i C_i\right) \tag{7.39}$$

We add the following comments to equations (7.31)-(7.32). As we have made no neglect, no approximation has been introduced in the derivation hence (7.31)-(7.32) are as good as the original equations (7.10)-(7.11). On the other hand the derived equations include the unknown shape function $\phi(\mathbf{r}, E, \mathbf{\Omega}, t)$ which, in turn, can be determined only from the kinetic equations. Our effort is justified by the fact that the new formalism (7.31)-(7.32) makes it easy to implement various practical approximations.

Note that the normalization factor F cancels out in equations (7.31) -(7.32). At the same time, F does not cancel out in equations (7.33)-(7.35).

The reactivity (7.33) only approximately can be interpreted as the reactivity determined from the static eigenvalue problem. This is because in kinetics we consider a reactor, whose parameters vary with time. It should be emphasized here, that various definitions of reactivity can be given depending on the ϕ function used in (7.33). Following [173], we mention two of them.

1. The simplest approximation is to separate the static neutron field from the time dependent solution and to write the time dependent solution as

$$\Phi(\mathbf{r}, E, \mathbf{\Omega}, t) \approx \frac{P(t)}{P_0}\Phi_0(\mathbf{r}, E, \mathbf{\Omega}). \tag{7.40}$$

   Then $P(t)/P(0)$ is the instantaneous (relative) power. This approximation is adequate when the power shape changes slowly.

2. Another possibility is to solve the static eigenvalue problem at various time moments, and calculate $\rho(t)$ from the static eigenvalue k_{eff} at t, the shape function is chosen conveniently as the solution of the static eigenvalue problem at t. The reactivity determined by that method is called static reactivity.

In the next Section, we discuss the solution of the kinetic equation in diffusion approximation.

7.3. Approximate solution of the time dependent diffusion equation

In Chapter 6 we studied the diffusion approximation to the transport equation. There we have neglected the delayed neutron effect. For the sake of simplicity, now we study the neutron kinetics in one energy group diffusion approximation. The equation for the delayed neutron precursors remains the same, in the equation for the neutron flux we have to modify the leakage and the production terms. In a homogeneous material, the one energy group diffusion approximation of the kinetics equations are

$$\frac{1}{v}\frac{\partial\Phi(\mathbf{r},t)}{\partial t} = D\Delta\Phi(\mathbf{r},t) - \Sigma_a\Phi(\mathbf{r},t) + \nu\Sigma_f(1-\beta)\Phi(\mathbf{r},t) + \sum_{i=1}^{6}\lambda_i C_i(\mathbf{r},t) Q(\mathbf{r},t) \quad (7.41)$$

$$\frac{\partial C_i(\mathbf{r},t)}{\partial t} = \beta_i\nu\Sigma_f\Phi(\mathbf{r},t) - \lambda_i C_i(\mathbf{r},t). \quad (7.42)$$

We seek the solution by the Fourier method, the dependent variables take the forms

$$\Phi(\mathbf{r},t) = \sum_n \Phi_n(\mathbf{r})\phi_n(t) \quad (7.43)$$

$$C_i(\mathbf{r},t) = \sum_n \Phi_n(\mathbf{r})C_{in}(t), \quad (7.44)$$

where the functions $\Phi_n(\mathbf{r})$ form a complete function set. For that purpose we choose the eigenfunctions of the Laplace operator supplemented with a suitable homogeneous boundary condition at the boundary ∂V of volume V:

$$\Delta\Phi_n(\mathbf{r}) = -B_n^2\Phi_n(\mathbf{r}). \quad (7.45)$$

If there is an external source, we expand it also in terms of the chosen basis:

$$Q(\mathbf{r},t) = \sum_n \Phi_n(\mathbf{r})Q_n. \quad (7.46)$$

After substituting (7.42)-(7.46) into (7.41)-(7.42), we multiply the resulting equation with the elements of the eigenfunctions of the Laplacian, we get the following equations:

$$\frac{d\phi_n(t)}{dt} = \frac{\rho_n - \beta}{\Lambda}\phi_n(t) + Q_n(t) + \sum_{i=1}^{6}\lambda_i C_{in}(t) \quad (7.47)$$

and

$$\frac{dC_{in}(t)}{dt} = \frac{\beta_i}{\Lambda}\phi_n(t) - \lambda_i C_{in}(t). \quad (7.48)$$

Here, we have introduced a number of new variables having physical meanings to make the result more transparent. First of all, we introduced the quantity ρ_n which is analogue to the reactivity but is applied to the n-th eigenfunction of the Laplace operator. The homogeneous equation

$$D\Delta\Phi_n(\mathbf{r}) - \Sigma_a\Phi_n(\mathbf{r}) + \frac{\nu}{k_n}\Sigma_f\Phi_n(\mathbf{r}) = 0 \quad (7.49)$$

has nontrivial solution only when

$$k_n = \frac{\nu\Sigma_f}{DB_n^2 + \Sigma_a}, \quad (7.50)$$

and the associated reactivity is defined as

$$\rho_n = 1 - \frac{1}{k_n}. \tag{7.51}$$

The generation time associated with mode n is defined as

$$\Lambda = \frac{\ell_n}{k_n} = \frac{1}{\nu\Sigma_f v} \tag{7.52}$$

where ℓ_n the prompt neutron life time given by

$$\ell_n = \frac{1}{v\left(DB_n^2 + \Sigma_a\right)}. \tag{7.53}$$

In the reactor operation, it is essential to measure the reactivity. To this end, let us consider the fundamental mode $n = 1$. Then $k_1 = k_{eff}$ and $\rho_1 = \rho$ defined from the static eigenvalue k_{eff}. Assume that

$$\phi_1(t) = \phi_0 e^{\omega t} \quad \text{and } C_i(t) = C_{i0} e^{\omega t}. \tag{7.54}$$

Substituting (7.54) into (7.47)-(7.48), we obtain a linear equation set having nontrivial solution only when

$$\frac{\rho_1}{\beta} = \frac{\Lambda}{\beta}\omega + \sum_{i=1}^{6} \frac{\beta_i/\beta}{\lambda_i + \omega}, \tag{7.55}$$

and then the amplitudes are related as

$$C_{i0} = \frac{\beta_i}{\Lambda} \frac{\phi_0}{\lambda_i + \omega}. \tag{7.56}$$

Equation (7.55) relates ω to the reactivity ρ, and is called inhour equation.

In a reactor, when the reactivity is given, the possible relaxation times are the roots of (7.55). The $\rho_1(\omega)$ curve possesses the following structure:

- the curve is discontinuous at $\omega = \lambda_i, i = 1, \ldots, 6$ and there its sign are also changes;
- any $\rho_1 = constant$ line intersects the curve at seven points, the intersections give the possible exponents in (7.54);
- six roots are always negative, the seventh root is positive only when $\rho_1 > 0$.

We cut the plot of $\rho(\omega)$ into four parts using the constants in Table 7.1, and show it in Fig. 7.1. In practice, not the exponential ω is used but the T_{2x} the time under which the neutron population is doubled. Its connection with ω is

$$\omega = \frac{\ln 2}{T_{2x}}. \tag{7.57}$$

In (7.54), the reactivity is obtained in β units. The reactivity expressed in β units is called dollar. In subcritical/supercritical state the reactivity is negative/positive, respectively. The reactivity expressed in dollar has safety implications as T_{2x} decreases below 1 *sec.* The reactor state when $\rho > 1$ dollar is called reactor excursion.

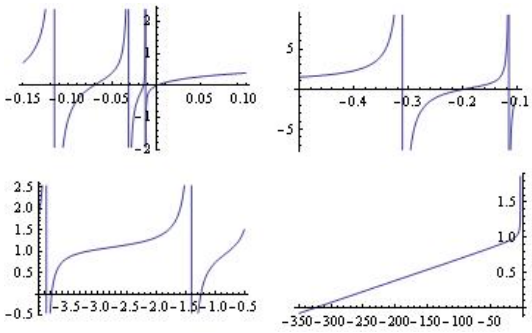

7.1. ábra. The $\rho(\omega)$ curve

T_{2x} (sec)	ρ/β
0.01	1.1510
0.10	0.9796
1.00	0.7908
10.00	0.3991
100.00	0.0988

7.2. táblázat. Doubling time vs. reactivity

7.4. Reactivity measurement

One of the most important tasks in reactor operation and control is to measure the reactivity. In the solution of that task the results of kinetics are applied. As we have seen in the preceding Sections, the reactivity determines the time dependence of the neutron flux, hence it is possible to base the reactivity control on the measurement of the flux as function of time. Using (7.55), we find the relationship between the reactivity and the doubling time. Usually a reactor is operated at $\rho \approx 0$ but in a planned transient the reactivity may differ from zero, see Table 7.2. As we see, the time available for reactivity control would be rather small in the positive reactivity range. The core of a power reactor is large, see Chapter 2 for details, any change in the technology processes has its time constant. The neutron balance can be changed in two ways. The first one is the insertion of control rods, the second one is changing the boron concentration. The latter is a slow process, the former is faster: the operator (or the automatic control) sends a signal to the control rod drive to drop the control rods. Low reactivity changes are smoothly handled by the automatic reactivity control, small changes in technological parameters are automatically compensated by the control rod motion, see the Section 2.4 in Chapter 2. In the reactor control, the feedback effects play the determining role.

When the doubling time is too small, in spite of the negative feedback, the power level may reach a level when the coolant pressure grows fast due to mass boiling. In the reactor technique, the $\rho \leq 1\$$ is considered as transient, the $\rho > 1\$$ situations are reactor excursions because of the short interaction time. The control system has a simple algorithm that compares the consecutive detector signals and estimates the reactivity. When the control rod characteristics is known, the control rod movement needed to compensate the reactivity can be estimated.

7.5. Control rod characteristics

We introduce two simple models to assess the influence of the control rod insertion on the reactivity. Both models serve as demonstration, in the design or operation more precise models are used.

To demonstrate the effect of the control rod, we consider[143][Chapter XXIX] a homogeneous cylindrical reactor of radius R and height H. For the sake of simplicity, we assume that R and H include the corresponding extrapolation distance therefore

$$\Phi(H, r) = \Phi(0, r) = 0, \quad \text{for } 0 \leq r \leq R, \tag{7.58}$$

and

$$\Phi(z, R) = 0, \quad \text{for } 0 \leq z \leq Z. \tag{7.59}$$

In our simplified control rod model, the rod is inserted at the center of the core, i.e. at $r = 0$, the rod is a black absorber in the thermal group and transparent in the epithermal group. The radius of the control rod is a and it is fully inserted, the control rod fills the region $0 \leq r \leq a,\ 0 \leq z \leq Z$. The neutron flux $\Phi(r, z)$ is described in two energy groups.

The corresponding analytical solution is given by (6.115) and (6.116). When the rod is inserted, the k_∞ of the core reduces by δk_∞. When the rod is inserted, a new critical state establishes. The new critical state is determined by four equations, from which the free amplitudes a, b, c and d of the flux are determined. Those equations are:

- the fast flux is zero at the boundary of the cylinder, at $r = R$.
- the thermal flux is zero at $r = R$.
- $d\Phi/dr = 0$ at $r = a$ for the fast flux.
- at $r = a$ the black boundary condition $\Phi_2(a) - \Gamma\Phi'(a) = 0$ holds in the thermal group, where Γ is the black albedo.

After a long and tedious calculation, one obtains[143][p. 458] the following reactivity change for a LWR:

$$\delta k_\infty = 7.5 \frac{L_2^2}{R^2} \frac{1}{0.116 + \Gamma/a \frac{L_1^2}{M^2} \ln\left(\frac{L_1 L_2}{Ma} + \frac{L_2^2}{M^2 \ln \frac{R}{aj}}\right)} \tag{7.60}$$

where

$$M^2 = L_1^2 + L_2^2 \tag{7.61}$$

and $j = 2.405$ the first zero of the Bessel function $J_0(r)$. Formula (7.60) shows that the reactivity decrement is larger with larger control rod radius a, and smaller with the core radius R.

In the second model [165][Section 7.4], we investigate the impact of the control rod axial position on the reactivity decrement. From the definition (3.164) of the reactivity one can immediately see that the reactivity perturbation is given by (3.224):

$$\delta\rho = -\frac{(\Phi^+, [\delta\mathcal{D}]\,\Phi)}{(\Phi^+, \mathcal{F}\Phi)} \tag{7.62}$$

where k_{eff} is the eigenvalue before the rod insertion. The rod insertion does not change the fission operator so it is not included in the nominator, and the denominator is a constant. To calculate the flux, we use the $\Phi(\mathbf{r}) = \Phi(x, y, z)$ flux in one group approximation, and assume

that the x, y dependent part is separable in an amplitude $A(x, y)$. To meet the boundary conditions at the top of the core $z = H$ and at the end of the inserted rod at $z = 0$, we write the flux in the form of

$$\Phi(x, y, z) = \sin\left(\frac{\pi z}{H}\right) A(x, y). \tag{7.63}$$

The destruction operator changes only because of the rod insertion therefore

$$\delta\mathcal{D}(\mathbf{r}) = \begin{cases} -\Sigma_{ar} & \text{if } \mathbf{r} \in V_{rod} \\ 0 & \text{otherwise.} \end{cases} \tag{7.64}$$

Now we can readily evaluate (7.62), the reactivity changes only with z:

$$\delta\rho(z) = c \int_z^H \sin^2(\pi z'/H)\, dz' = \frac{H - z}{2} + \frac{H}{4\pi} \sin(2\pi z/H. \tag{7.65}$$

The curve $\rho(z)$ is called control rod characteristics. Its realistic determination in a production code is based on a reactor calculational model, usually in a global reactor code with suitable parametrized library.

7.6. Deterministic reactivity measurement

The point kinetics model may serve as a solid basis for elaborating measuring methods of the reactivity. The starting point is the inhour equation (7.55) relating T_{2x} with ρ/β. When the reactivity is negative the number of neutrons decreases exponentially with time, when positive, increases exponentially. In the former case the low neutron level, in the latter the manifesting feed-back effect may cause problems. The mentioned circumstances limit the measurable reactivity range to $0.2 - 0.3$ dollar.

In the small positive reactivity range, the measurement of the T_{2x} is applicable and we evaluate the reactivity from the inhour equation (7.55). Following [165], the summary of the measurement is as follows:

- We let the power increasing and record the detector counts as function of time. Thus we measure the $\phi(t)$.
- The $\phi(t)$ function is the sum of exponentials. It is known that after sufficiently long time the fundamental mode becomes dominant. By the method of fitting exponentials to $\phi(t)$, we determine the ω_0 or T_{2x} of the fundamental mode.
- We substitute ω_0 or T_{2x} into the inhour equation (7.55) and determine ρ/β.

When ρ is needed, we have to determine β_{eff} as well.

In the $\rho < 0$ range, the pulsed neutron source method is applicable. It follows from the inhour equation that the neutron density of a one-moment source exponentially decreases with time, and, there are seven roots ω_i of the $\phi(t)$ curve. When the one-moment source is repeated periodically, we can select the repetition time T so that a given time constant be dominant asymptotically. Let the first pulse appear at $t = 0$, then the flux in the time window $(t, t + dt)$ the number of neutrons is

$$\sum_{j=0}^{6} \phi_j e^{i\omega_j t} dt \tag{7.66}$$

After infinitely many pulses the neutron distribution is

$$\phi(t)dt = \sum_{n=-\infty}^{0} \sum_{j=0}^{6} \phi_j e^{\omega_j (t+nT)} dt = \sum_{j=0}^{6} \frac{\phi_j}{1 - e^{\omega_j T}} e^{\omega_j t} dt. \tag{7.67}$$

As one can see in Fig. 7.1,

$$-\omega_6 >> \lambda_i, \quad i = 1, 2, \ldots, 6, \tag{7.68}$$

and using that in (7.55), we obtain

$$\omega_6 \approx -\frac{\beta}{\Lambda} \left(1 - \frac{\rho}{\beta}\right). \tag{7.69}$$

When $\rho = 0$ we use the notation $\omega_6 = \omega_{6kr} \approx -\beta/\Lambda$. Using the new variable in (7.69) we express the reactivity by ω_6 and ω_{6kr} as

$$-\frac{\rho}{\beta} = \frac{\omega_6 - \omega_{6kr}}{\omega_{6kr}}. \tag{7.70}$$

Now we choose T so that

$$|\omega_6 T| >> 1, \quad |\omega_j T| << 1, \quad j = 0, 1, \ldots, 5. \tag{7.71}$$

With that choice, the term $j = 6$ diminishes by the arrival of the next impulse but the $j < 6$ terms vary just a little and the following approximation becomes applicable:

$$\phi(t)dt \approx \phi_6 e^{\omega_6 t} dt + \sum_{j=0}^{5} \frac{\phi_j}{-\omega_j T} e^{\omega_j t} dt \approx \phi_6 e^{\omega_6 t} dt + b dt. \tag{7.72}$$

The curve recorded by the time analyzer is the sum of an exponential function plus a background bdt, and ω_6 is obtained by a fitting. Repeating the procedure at other control rod positions, we are able to extrapolate to the critical control rod position and using (7.70), we get also the reactivity. That reactivity measurement method is called Simmons-King method.

The Sjöstrand method avoids using the extrapolation of ω_6 to the critical state thus the reactivity can be evaluated from a single measurement. The two terms in (7.72) distinguish clearly, the background is constant, the other term decreases rapidly. The former is associated with the delayed neutrons, the latter to the prompt neutrons. The area after the respective curve is

$$A_p = \int_0^T \phi_6 e^{\omega_6 t} dt = \phi_6 \frac{e^{\omega_6 T} - 1}{\omega_6} \tag{7.73}$$

for the prompt term, and

$$A_d = bT \tag{7.74}$$

from the delayed term. The reactivity is the ratio of the two areas:

$$-\frac{\rho}{\beta} = \frac{A_p}{A_d}. \tag{7.75}$$

Assume that the source provides S neutrons into the reactor in each pulse. Then, after long time the number of neutrons in the reactor will be

$$S + Sk_{eff} + Sk_{eff}^2 + \cdots = \frac{S}{1 - k_{eff}}. \tag{7.76}$$

That number is the sum of the prompt and delayed neutrons. That number is proportional to $A_p + A_d$. Consider now the neutron numbers due to the prompt neutrons only, the number of those neutrons is

$$\frac{S}{1-(1-\beta)k_{eff}}, \tag{7.77}$$

that number is proportional to A_p. Form their ratio:

$$\frac{A_p + A_d}{A_p} = \frac{1-(1-\beta)k_{eff}}{1-k_{eff}} = 1 + \frac{\beta}{\rho}, \tag{7.78}$$

as stated.

7.7. Problems

1. We put a source in the subcritical reactor at $t = 0$ which emits 10^6 neutron/sec. The reactivity is -1 \$. Determine and plot the flux in the first 3 minutes!

2. We make the reactor supercritical with $\rho = 0.6$ \$ at $t = 0$, and put a source into the reactor for instance. The source power is 32000 neutron/sec. The generation time is 25 μs. Determine and plot the flux in the first 3 minutes!

3. Determine the time dependent neutron flux in the critical reactor with constant neutron source! At $t < 0$ the reactor was subcritical, at $t = 0$ moment it became critical. What is the asymptotic flux?

4. In a reactor the reactivity changes between -0.1 \$ and +0.1 \$ following the sinus function with the period $T = 1$ s. How does the flux and the average flux in this reactor? The generation time is 25 μs.

5. Repeat the previous problem but using a square function instead of sinus function.

6. In the subcritical reactor there is a time dependent (external) neutron source with 10^6 neutron/sec. After stabilization of the asymptotic flux, at $t = 0$ moment the external source is pulled out from the reactor. The reactivity is $\rho = -1$, the generation time is 25 μs. Plot and determine numerically the neutron flux!

7. Clear exponential flux is formed in the supercritical reactor ($\rho = 0.2\$, \Lambda = 25\mu$s). At $t = 0$, we reset the reactor into critical state. Determine how changes of the neutron flux $\phi(t)$ and the concentration of delayed-neutron daughter nuclides $C_i(t)$! What is the main difference between the time dependence of $\phi(t)$ and $C_i(t)$?

8. The position of a control rod changes as a low amplitude sinus function around the critical state in a reactor, consequently the reactivity changes similarly. Calculate the neutron flux variation as function of the angular frequency (ω) of the excitation. Analyze in details the special case when $\omega \gg \lambda_i$!

8. fejezet

Numerical Methods

In the preceding Chapters the neutron flux, slowing down density or the other physical quantities have been identified as the solution of an equation. In Chapter 6 that equation is a second order differential equation for the neutron flux, in Subsection 3.6.1 an integral equation for the collision density. Unfortunately those equations can be solved mostly by numerical methods.

An exact solution means that the function satisfying the given equation and given boundary condition serves as a recipe to determine the physical quantity (flux, slowing down density, reaction rate etc.) with arbitrary precision. But what is the recipe? It is an infinite sequence of algebraic operations. For what do we use the solution of the problem? Usually one has to decide which one of the rival theories gives results closer to the reality. But in physics, the reality means measured values which are burdened with inevitable uncertainties.

This means that for practical purposes it suffices to derive a solution of limited accuracy. We do not give up the quest for arbitrarily accurate solution, those approximate solutions are preferred which are capable of providing us with results of a required accuracy. Numerical techniques penetrate natural sciences. Today the Monte Carlo numerical simulation method is the most popular, but there was a time when mechanical models, later electrical models were built to study the actual intriguing phenomena.

An approximate solution may be based either on physical or mathematical considerations. Physical considerations are built on ranking the involved phenomena and a physical model is elaborated that accurately reflects the few most important phenomena. Usually it is known in advance that the solution contains a large (or low) frequency component, if it varies slowly or abruptly and so on. That kind of a priori knowledge can readily be implemented in the basis functions that we use to express the solution.

Mathematical considerations rely on an approximation to the solution expanded in an infinite basis set which is truncated so that the solution be satisfactory. In the rest of the present Chapter, methods will be discussed that are based on mathematical and physical considerations. First, we bring up some general principles, later we discuss three particular methods. The finite element method deserves the reader's attention because it is universal, the nodal method is favored by one of the authors, the finite difference method is the most known.

Most of the authors' experience comes from nuclear physics where special requirements have been established. In an eigenvalue problem, the minimal accuracy of the eigenvalue is 0.0001, the averaged accuracy of the solution over parts of the volume should be in the range of 0.001. The number of unknowns in a problem varies from 18 000 on. The allotted time depends on the application type, on-line calculations should run in a short time, off-line calculations should be completed in a few seconds because of the large number of variations to be analyzed.

The engineering and physical problems fall into one of the following three categories:

1. The solution is sought in a volume V whose characteristic size (such as diameter) is large compared to the characteristic distance (such as relaxation length or mean free path) of the involved process and the material properties and the solution vary slowly with the distance. This is the case with elliptic equations in large homogeneous volumes. A good approach is to subdivide V into subvolumes and approximate the solution in each subvolume by low order polynomials and suitable boundary conditions provide smooth solution at the joint boundary of two adjacent subvolumes.

2. The solution is sought in a volume V whose material properties change rapidly and the solution is expected to vary rapidly. This is the case with hyperbolic equations. In that case one has to select the basis functions so that at least some of them should be

able to exhibit that kind of behavior. That kind of problems are encountered in fluid and gas dynamics when the processes are fast.

3. The worst situation is when V is large, the material properties may exhibit sudden variations along a given direction but along other directions slow variations appear. This is the case with plasma physics and some of the streaming problems. This is one of the most problematic areas of the numerical modeling.

When analyzing a problem, the above considerations should be taken into account in the selection of the basis functions, the iteration process, and finally the analyst should know if the phenomenon to be studied is suitable for being modeled by the chosen method or not. The number of independent coordinates of the angular flux $\Phi(\mathbf{r}, E, \mathbf{\Omega})$ is seven, the problem is multidimensional even in such approximate models as the S_n or diffusion model. The material distribution in a reactor core is complex. Although the core may consist of several homogeneous regions, the material parameters like the temperature, isotope composition may vary with the location. Therefore the analyst's first tasks to find a discretization of the volume V in which the solution of the given problem is sought. The second task is to find a suitable basis on each sub-volume and to expand the solution locally in terms of those basis functions. The third step is to find the expansion coefficients on each subvolume.

We assume that using the above considerations, we have chosen a set of basis functions $f_n(x),\ n = 1, \ldots, \infty$. It is assumed that any possible solution can be expressed as a linear combination of the basis functions, i.e. the basis functions are complete. We seek the solution $\Phi(x)$ of a boundary value problem

$$\mathbf{A}\Phi(x) = 0, \quad x \in V, \tag{8.1}$$

$$\mathbf{B}\Phi(x) = 0, \quad x \in \partial V. \tag{8.2}$$

Here operators $\mathbf{A}$, $\mathbf{B}$ may contain material properties of volume V and the boundary ∂V. The independent variable x embodies all the physical variables of the problem: space coordinates, time, energy etc. Thus the restrictions $x \in V, x \in \partial V$ apply only tho the spatial variables in x. We assume that the admissible solutions, as well as the functions considered in the sequel, are square integrable functions on V, and the following scalar product is defined among them:

$$(\Phi_1(x), \Phi_2(x)) \equiv \int\limits_V \Phi_1(x)\Phi_2(x)\, dx.$$

We write problem (8.1)–(8.2) into the symbolic form

$$\mathbf{A}\Phi(x) = 0, \quad x \in V. \tag{8.3}$$

Since the chosen basis is complete, we can expand the solution as

$$\Phi(x) = \sum_{n=1}^{\infty} c_n f_n(x), \tag{8.4}$$

where the $f_n(x)$ functions are orthonormal but not necessarily complete. The $f_n(x)$ functions are called coordinates as we express the solution by them. Instead of solving directly (8.1), we may seek an approximate solution $\Phi_N(x)$ which has the property

$$(\mathbf{A}\Phi_N(x), f_n(x)) = 0, \quad n = 1, \ldots, N. \tag{8.5}$$

When $N = \infty$, $\Phi_N(x)$ must be the exact solution. Clearly, the solution contains the following error:

$$\delta\Phi(x) = \sum_{n=N+1}^{\infty} c_n f_n(x). \tag{8.6}$$

An important token of the mastery of a numerical approximation is the appropriate ordering of the basis functions to achieve a fast decrease of c_n with increasing n. We call $\Phi_N(x)$ the weak solution of (8.3).

Let us note that above we have used the basis functions in two roles: first in the expansion, second in the weighting (8.5). Those two function sets can be separated and instead of (8.5) we may demand

$$(\mathbf{A}\Phi_N(x), w_m(x)) = 0, \quad m = 1, \ldots, M, \tag{8.7}$$

where $w_m(x)$ is a weight function. When $M = N$, and the weight functions are appropriately chosen, the coefficients in the expansion can be determined. When $w_m(x) = f_m(x)$, i.e. the weight functions are the basis functions themselves, we obtain the Galerkin method. Then *"One may hope for a sufficiently accurate solution even if the number of coordinates is small,"*[41][p. 157].

In the weak form, we transform the operator into a matrix, the solution into a vector, and the original mathematical problem into the solution of a linear equation. Substituting (8.4) into (8.1) and forming a dot product with $f_{n'}(x)$, we arrive at the following linear equation:

$$\sum_{n=1}^{N} (f_{n'}(x); \mathbf{A}f_n(x))c_n = 0, n' = 1, \ldots, N; \tag{8.8}$$

if we introduce

$$\mathbf{A}_{nn'} = (f_{n'}(x); \mathbf{A}f_n(x)) \tag{8.9}$$

and

$$\mathbf{c} = col(c_1, \ldots, c_N), \tag{8.10}$$

equation (8.1) can be written as

$$\mathbf{Ac} = 0. \tag{8.11}$$

Nontrivial solution exists only when $det(\mathbf{A}) = 0$, a condition to determine the critical state, see Section 3.3 in Chapter 3.

Often the eigenfunctions of operator $\mathbf{A}$ may be used as basis, or, when $\mathbf{A} = \mathbf{A_1} + \mathbf{A_2}$ then eigenfunctions of $\mathbf{A_1}$ or $\mathbf{A_2}$ may also often be used as basis.

When the basis functions are labeled according to their physical importance, the error of $\Phi_N(x)$ decreases rapidly with increasing N. In reactor physics, the neutron balance is of primary importance, and the flux usually varies slowly with the space coordinate hence low ranking polynomials of the spatial variable offer a reasonable choice. Equation (8.5) is called the weak form of (8.1). At this point it should be emphasized that the neutron physics problems radically differ from the thermal hydraulics problem. The former may be described by an elliptic operator, as in the widely used diffusion approximation, whereas the thermal hydraulics problem attaches to an hyperbolic operator. As a consequence, the neutron physics problem have a smooth solution, in contrast with the thermal hydraulics problem where the solutions may be discontinuous [42]. This is the reason that numerical methods for thermal hydraulics is discussed separately.

In reactor physics, we encounter the following types of problems:

- eigenvalue problem;

- source problem;
- boundary value problem.

Below we estimate the number of unknowns. It is possible to formulate the problem in various ways, let us consider the unknowns as group fluxes at given points of the reactor core. In the full core flux calculation by fuel rods, the number of unknowns is $N_g * N_{fuel} * N_{layer}$ where N_g is the number of energy groups, usually $2 \leq N_g \leq 6$, N_{fuel} is the number of fuel elements $N_{fuel} = N_{ass} * N_{pin}$ where N_{ass} is the number of fuel assemblies in the core, and N_{pin} is the number of fuel rods per assembly, $40 \leq N_{ass} \leq 400$, $20 \leq N_{pin} \leq 126$. N_{layer} is the number of axial layers, $10 \leq N_{layer} \leq 20$. From the given numbers the lower limit of the unknowns is 1600 the upper limit is 2×10^7.

In the memory of a computer, a number is represented on a finite number of bits. The result of a multiplication $a * b$ would require as many bits as the total number of bits used to represent a and b from which the lower bits are lost, this is the round-off error which sets a limit to the complexity of the computations feasible on a computer. When solving a linear equation with N unknowns at least N^2 multiplications are needed thus in a large problem exclusively an iterative solution is possible.

An efficient numerical method has the following components:

- A set $\mathcal{S} \in V$, the solution will be determined at points $s \in \mathcal{S}$;
- An efficient interpolation scheme to reconstruct $\Phi(x)$ from $\Phi(s)$, $s \in \mathcal{S}$;
- A transformation of equation (8.1) to an equation from which $\Phi(s)$, $s \in \mathcal{S}$ can be determined.

Throughout the following three subsections three numerical methods will be discussed. It is a common feature of the methods that by increasing the number of points in $\mathcal{S}$, the accuracy of the solution increases.

To understand the iterative methods let us consider the solution of a linear problem:

$$\mathbf{A}\mathbf{x} = \mathbf{b} \tag{8.12}$$

where $\mathbf{A}$ is a given $N \times N$ matrix, $\mathbf{b}$ is a given vector of N element. Let us partition $\mathbf{A}$ as

$$\mathbf{A} = \mathbf{L} + \mathbf{D} + \mathbf{U} \tag{8.13}$$

where $\mathbf{L}$ is a lower triangular, $\mathbf{D}$ is diagonal and $\mathbf{U}$ is upper triangular matrix. Rearranging (8.13) as

$$(\mathbf{D} + \mathbf{L})\mathbf{x} = \mathbf{b} - \mathbf{U}\mathbf{x} \tag{8.14}$$

we obtain the following iteration:

$$\mathbf{x}_{k+1} = \mathbf{D}^{-1}\mathbf{b} - \mathbf{D}^{-1}(\mathbf{L}\mathbf{x}_{k+1} + \mathbf{U}\mathbf{x}_k), k = 0, 1, 2, \ldots \tag{8.15}$$

which is the well known Gauss-Seidel iteration.

In an eigenvalue problem, the power method is applicable, as we have used it in Section 3.3 of Chapter 3. When operator (or matrix) $\mathbf{A}$ is applied repeatedly on a given vector $\mathbf{b}$ which is not orthogonal to the fundamental eigenfunction (eigenvector) of $\mathbf{A}$ the iteration $\mathbf{x}_k = \mathbf{A}^{\mathbf{k}}\mathbf{b} = \mathbf{A}\mathbf{x}_{\mathbf{k-1}}$ tends to the fundamental eigenvector as $k \to \infty$. Thus the ratio of the first two eigenvalues determine the convergence rate.

8.1. Acceleration

A large numerical problem needs acceleration. There are two major approaches to acceleration: when the power iteration with the matrix of equation

$$\mathbf{A}(k)\mathbf{x}_i = a\mathbf{x}_{i+1}, \tag{8.16}$$

is too slow, we may use that the eigenvalue of $f(\mathbf{A})$ is $f(\lambda)$ provided eigenvalue of $\mathbf{A}$ is λ. The convergence rate depends on the ratio λ_1/λ_2 where λ_1 is the dominant eigenvalue[1]. The iteration process becomes faster if we chose a function $f(\mathbf{A})$ such that $f(\lambda_1)/f(\lambda_2) > \lambda_1/\lambda_2$. To reduce the computational works, only such $f(\mathbf{A})$ functions are considered which are low order polynomials. The well known Cayley-Hamilton theorem [43] claims that any matrix function reduces to a polynomial whose degree equals the order of matrix A. The simplest variant of the method is the successive overrelaxation (SOR) method. In an iteration step (8.15), we replace the old guess $\mathbf{x}_k$ by the improved guess $\mathbf{x}_{k+1}$. But if the change $\mathbf{x}_k \to \mathbf{x}_{k+1}$ improves the convergence why do we not make a larger step? We introduce the overrelaxation parameter ω and modify (8.15) as

$$\mathbf{D}\mathbf{x}_{k+1} = \omega\left(\mathbf{L}\mathbf{x}_{k+1} + \mathbf{U}\mathbf{x}_k + \mathbf{b}\right) + (1-\omega)\mathbf{D}\mathbf{x}_k. \tag{8.17}$$

Now remains only to estimate the optimal overrelaxation parameter. According to [43][p. 111], the most rapid convergence is obtained when

$$\omega = \frac{2}{1 - \rho\left((\mathbf{D}-\mathbf{L})^{-1}\mathbf{U}\right)}, \tag{8.18}$$

where $\rho(\mathbf{X})$ is the spectral radius of matrix $\mathbf{X}$.

The second: using the last few iterates, we give a prediction for the next iterate. The following acceleration technique has been elaborated by Cs. J. Hegedűs [44].

In the iteration, there are two levels: the inner and the outer iteration. The inner iteration determines the eigenvalue $\mathbf{x}$ at a given value of k. The outer iteration improves the estimation of k. The iteration is based on Arnoldi's method [44]. The choice has been made to implement

- an algorithm that converges fast;
- simple to be implemented as it uses only matrix vector multiplication;
- an estimate of the error;
- a method without estimation of the spectrum of the matrix $\mathbf{A}(k)$.

The method is exhaustively described in [45]. The main steps of the method are:

- an initial guess $\mathbf{x}_0$ is chosen;
- We determine the h_{ij} elements of a Hessenberg (upper triangular) matrix $\mathbf{H}$ by the recursion:

$$h_{i+1,i}\mathbf{x}_{i+1} = \mathbf{A}\mathbf{x}_i - \sum_{j=1}^{i} h_{ji}\mathbf{x}_j, \tag{8.19}$$

where

$$h_{ji} = \mathbf{x}_j^{+}\mathbf{A}\mathbf{x}_i, \tag{8.20}$$

and superscript + stands for the transposed vector.

[1] We assume that we seek the eigenfunction associated with the dominant eigenvalue.

- The next step is the solution of the reduced eigenvalue problem

$$\mathbf{Hv} = \lambda \mathbf{v}, \tag{8.21}$$

where $\mathbf{H} = \{h_{ij}\}$ and we seek the maximal positive eigenvalue and the associated eigenvector.

We quote here without proof seven theorems underlying the method.

8.1 Theorem

$$|\lambda_{max}(\mathbf{A}) - \lambda_{\mathbf{max}}(\mathbf{H})| \leq |v_k h_{k+1,k}|\, s^{-1}(\lambda), \tag{8.22}$$

where v_k is the kth element of vector $\mathbf{v}$, $\|\mathbf{w}\|_2 = 1$, $\mathbf{w}$ is the left eigenvector of $\mathbf{H}$: $\mathbf{w}^+\mathbf{H} = \lambda_{max}\mathbf{w}^+$, $s(\lambda) = |\mathbf{w}^+\mathbf{v}|$ is the sensitivity of the eigenvalue. $\mathbf{H}$ is a square matrix of order k. Relation (8.22) *indicates the accuracy of the eigenvalue estimate.*

8.2 Theorem *In the subspace spanned out by the vectors $\mathbf{x}_1, \ldots, \mathbf{x}_k$ the solution of the eigenvalue problem* (8.16) *is*

$$\tilde{\mathbf{x}}_1 = \sum_{j=1}^{k} v_j \mathbf{x}_j, \tag{8.23}$$

where $\|\mathbf{v}\|_2 = 1$, $\|\mathbf{x}\|_2 = 1$, $j = 1, 2, \ldots, k$. Here $\tilde{\mathbf{x}}_1$ is the last estimate of the dominant eigenvector of $\mathbf{A}$.

8.3 Theorem *The angle between vectors $\mathbf{x}$ and $\tilde{\mathbf{x}}_1$ is given by*

$$\sphericalangle(x, \tilde{\mathbf{x}}_1) \leq |v_k h_{k+1,k}|^{1/2} s^{-1/2}(\lambda). \tag{8.24}$$

That estimate is used to measure the deviation of the last estimate from the exact solution.

8.4 Theorem *When the method is restarted from the $\tilde{\mathbf{x}}_1$ vector then*

$$\tilde{h}_{11} = \lambda, \quad \tilde{h}_{21} = v_k h_{k+1,k}, \quad \tilde{\mathbf{x}}_2 = \mathbf{x}_{k+1}. \tag{8.25}$$

That restart measure is meant to avoid large round-off errors because of the recalculation of the starting vectors. That is important at the start of a new internal iteration sweep.

8.5 Theorem *Vector $\tilde{\mathbf{x}}_1$ is the optimal choice in the subspace spanned out by $\mathrm{x}_1 \ldots, \mathbf{x}_k$. The Rayleigh ratio*

$$\max_{z_1,\ldots,z_k} \left(\sum_{j=1}^{k} z_j \mathbf{x}_j^+ A \sum_{j=1}^{k} z_j \mathbf{x}_j \right) = \lambda \tag{8.26}$$

is maximal when $z_j = u_j$, $j = 1, \ldots, k$.

8.6 Theorem *The function space spanned out by $\mathbf{x}_1, \mathbf{x}_2, \ldots, \mathbf{x}_k$ is the same as the function space spanned out by $\mathbf{x}_1, \mathbf{A}\mathbf{x}_1 \ldots, \mathbf{A}\mathbf{x}_k$.*

The above theorem shows the Arnoldi method to be optimal thus it is faster than the power iteration or the acceleration based on Chebishev polynomials.

8.7 Theorem *It is possible to obtain the Hessenberg matrix $\mathbf{H}$ by applying the Gram-Schmidt orthogonalization to the Krylov base.*

The outer iteration starts with $k = 1$, in equation (8.16). In the internal iteration we watch the change of the angle variation of the extrapolated vector $\tilde{\mathbf{x}}_1$ compared to the initial guess. When the difference exceeds 0.15 radian but the last change is less then 1.15 radian then a new k_{new} value is calculated from the condition that the dominant eigenvalue of $\lambda A(k_{new}) = 1$. When we have at least three consecutive estimations of k, the new estimate for k is obtained from a weighted least square fit. The algorithm also makes an estimation from the overall balance equation (4.11) or (6.2), where parameter k serves the solvability of the linear equation. To this end in (4.11) number $\nu \to \nu/k$ is substituted, where k is the last estimate of k in the outer iteration.

8.2. Finite difference

The finite difference method (FDM) provides a scheme to determine $\Phi(s), s \in \mathcal{S}$, where $\mathcal{S}$ is a set of discrete points in V. The location of elements of $\mathcal{S}$ adhere to a discretization scheme, actually $\mathcal{S}$ is a net, the solution will be determined at specific points of the net. FDM is the lowest order FEM, the discretization points may be either the midpoints of the elements (mesh centered scheme) or at the midpoints of the faces separating neighboring elements (face centered scheme). The method presented here is only one of the available FDMs, it is widely applied in reactor physics to solve first and second order partial differential equations. Here we consider the following problem:

$$D\nabla^2\Phi(x,y) + \Sigma\Phi(x,y) = Q(x,y), \tag{8.27}$$

where D, Σ are material parameters [165], assumed to be constant in a subvolume. The presented discussion was chosen for its simplicity, FDM is capable of using non-uniform meshes, too.

Just as with the zeroth order FEM, see Fig. 8.1, V is subdivided into subvolumes. Now we construct a solution scheme with one unknown at the center of each subvolume. Between two adjacent centers the solution is approximated by a linear interpolation. We follow the notation traditional in the FDM literature: the central subvolume has index 0, the neighbors are indexed as $1, \ldots, n_F$ where n_F is the number of faces of a subvolume. Let the flux, the solution of the BVP to be solved, Φ_i be at the center of subvolume i. The interpolation should result in continuous boundary flux and current. That condition is satisfied [43] if the boundary flux Φ_{bi} at the joint boundary of subvolumes 0 and i is

$$\Phi_{bi} = \frac{D_0\Phi_1 + D_i\Phi_i}{D_0 + D_i} \tag{8.28}$$

and the net current is

$$J_{bi} = -\frac{D_0 D_i}{h(D_0 + D_i)}\left(\Phi_0 - \Phi_i\right). \tag{8.29}$$

The integral of a linear function over a symmetric subvolume equals the value at the center multiplied by the volume of the subvolume. We derive an equation in which only fluxes at the subvolume centers occur. Such an equation is obtained when integrating the diffusion equation over subvolume with subscript 0. Reaction rates include only Φ_0, the boundary net current $(\Phi_0 - \Phi_i)$, thus we obtain the finite difference form of the diffusion equation as

$$F\sum_{i=1}^{n_F} -\frac{D_{0g}D_{ig}}{h(D_{0g} + D_{ig})}\left(\Phi_{0g} - \Phi_{ig}\right) + V\Sigma_{0g}\Phi_{0g} = Q_{0g}, \tag{8.30}$$

where V is the volume of the congruent subvolumes, F is the area of a face, faces are assumed congruent. In the FDM, the averaged solution in subvolume V_k equals Φ_k, the solution at the subvolume centre. From (8.30) it is clear that if we write the FD scheme with one big matrix $\mathbf{A}$ multiplying a big vector $\mathbf{x}$ composed of the fluxes at the centers of the subvolumes, $\mathbf{A}$ has a block structure: the number of non-zero elements in row i equals the number of neighbors[2]. It is an advantage, since in a large system we need not to store the large number of zeros in $\mathbf{A}$, and that structure allows for effective matrix operations [43].

When face i is an external boundary, $\Phi_{k'}$, the solution in the adjacent subvolume is undefined. But on an external boundary there is a boundary condition that is formulated, in general, as a linear expression of the solution and gradient on the boundary. The boundary condition is satisfied if a hypothetical neighbor subvolume is assumed, in which the solution is such that the boundary condition is satisfied.

The error of the FDM is proportional [43] to $1/h$, where h is the characteristic distance between adjacent subvolumes. The accuracy is satisfactory when the characteristic relaxation distance of the problem (such as diffusion length)is comparable to the mesh size h.

As a result, the FDM yields a set of linear equations for Φ_k, and the number of equations equals the number of unknowns. It can be shown [43] that the equations are solvable. FDM is applicable to source and eigenvalue problems as well.

An important problem in connection with FDM is the handling of numerical errors. In electromagnetic problems, or in streaming problems, divergence, curl, gradient may be involved. For example, if the problem is rotation free, the numerical error may lead to appearance of rotation, therefore special care is needed in a number of streaming problems. Interested Readers should consult with [47], [48].

8.3. Finite elements

We present the finite element method (FEM) on the example of the multigroup diffusion equation. The diffusion equation in the energy group g is written as

$$-D_g \boldsymbol{\nabla}^2 \Phi_g(\mathbf{r}) + \Sigma_{tg} \Phi_g(\mathbf{r}) = Q_g(\mathbf{r}), \quad g = 1, \ldots, G; \tag{8.31}$$

where the source term Q_g includes all the contributions (scattering and fission) from the other energy groups. We assume the flux to be square integrable in the volume V: $\Phi_g(\mathbf{r}) \in \mathbb{L}_2(V)$, furthermore $\boldsymbol{\nabla}\Phi_g(\mathbf{r}) \in \mathbb{L}_2(V)$. The boundary condition prescribed at the boundary ∂V is either the flux equal to zero or the current equal to zero. We formulate that condition in the following manner. Let

$$\partial V = \partial V_1 \cup \partial V_2 \tag{8.32}$$

and when $\mathbf{r} \in \partial V_1$ then $\Phi(\mathbf{r}) = 0$ and when $\mathbf{r} \in V_2$ then $n\boldsymbol{\nabla}\Phi_g(\mathbf{r}) = 0$. Formally we are dealing with a source problem:

$$\mathcal{A}_g \Phi_g(\mathbf{r}) = Q_g(\mathbf{r}), \tag{8.33}$$

where $\mathcal{A}$ stands for the operations on the right hand side of (8.31) and we seek the solution in the weak form, i.e. we express

$$\Phi_g(\mathbf{r}) = \sum_{i=1}^{N} \alpha_i^g f_i(\mathbf{r}) \tag{8.34}$$

[2]At an external boundary, usually no new non-zero element shows up.

where f_i is a local low ranking polynomial. More precisely, we subdivide V into subvolumes V_i:

$$V = \cup_{\ell=1}^{L} V_\ell, \quad V_\ell \cap V_{\ell'} = \emptyset \quad \ell \neq \ell' \tag{8.35}$$

and on each subvolume we apply expansion (8.34). We may derive a set of equations for the unknown coefficients α_i in two ways. The first one is the variational formalism, the second one is simply using the weak solution condition to equation (8.33). We follow the latter way, let us define the scalar product as

$$(f(\mathbf{r}); \mathcal{A}\Phi_g(\mathbf{r})) = \int_V \left(-D_g \boldsymbol{\nabla}\Phi_g(\mathbf{r})\boldsymbol{\nabla} f(\mathbf{r}) + \Sigma_{tg}\Phi_g(\mathbf{r}) f(\mathbf{r})\right) d^3\mathbf{r} \tag{8.36}$$

for any function $f(\mathbf{r})$ that can be represented in the form of (8.34). As to the source term, the scalar product is

$$(f(\mathbf{r}), Q_g(\mathbf{r})) = \int_V Q_g(\mathbf{r}) f(\mathbf{r}) d^3\mathbf{r}. \tag{8.37}$$

We obtain the following system of equations by substituting (8.34) into (8.31) and multiplying the resulting equation by $f_j(\mathbf{r})$ and integrating over V:

$$\sum_{j=1}^{G} A_{ij}^g \alpha_j^g = q_i^g, \quad i = 1, \ldots, N \tag{8.38}$$

and

$$A_{ij}^g = (f_i(\mathbf{r}); \mathcal{A} f_j(\mathbf{r})), i, j = 1, \ldots, N; \tag{8.39}$$

$$q_i^g = (f(\mathbf{r}, \mathbf{v}, t)_i(\mathbf{r}); Q_g(\mathbf{r})), i = 1, \ldots, G. \tag{8.40}$$

Equation (8.38) is valid whatever is the discretization moreover the matrix is always symmetric:

$$A_{ij}^g = A_{ji}^g. \tag{8.41}$$

In a large volume the solution may behave differently thus we utilize the advantage offered by the discretization. Firstly, we may define different basis functions over each of the different subvolumes, which is called element in the FEM. Secondly, the shape of the elements also may vary provided we find an affine map from every element into a reference element, say into the unit cube $V_0 = [0,1] \times [0,1] \times [0,1]$. Before addressing such practical problems as accuracy and effectiveness, we assess the following general features of the FEM. Let h stand for the maximal diameter of an element in the discretization and define the norm in the function space $\mathbb{L}_2$ as

$$||\Phi||_p^2 = \sum_{|\alpha|<p} \int_V \left(\mathcal{D}^\alpha \Phi\right)^2 d^3\mathbf{r}, \tag{8.42}$$

here

$$\alpha = (\alpha_1, \alpha_2, \alpha_3), \quad |\alpha| = \alpha_1 + \alpha_2 + \alpha_3, \tag{8.43}$$

and the operator of the partial derivation is

$$\mathcal{D}^\alpha = \frac{\partial^{\alpha_1+\alpha_2+\alpha_3}}{\partial x^{\alpha_1} \partial y^{\alpha_2} \partial_z^{\alpha_3}}. \tag{8.44}$$

Using the above introduced notation, it can be shown [49] that the FEM provides an arbitrary accurate solution in the following sense. The convergence rate of the approximate solution, i.e. the difference between the exact solution Φ and the approximate solution Φ_ℓ is

$$||\Phi_g - \Phi_{g\ell}|| \leq C h^{k-\ell} ||\Phi_g||_k; \quad \text{for } \ll \geq 2 - k. \tag{8.45}$$

Here k is the lowest degree of the monomial not present in the space of the approximating polynomials

$$k = \min_{x^i y^j z^k} \notin \mathbb{P}(R_\ell) \tag{8.46}$$

where $\mathbb{P}(R_\ell)$ is the space of approximating polynomials and R_ℓ is the given discretization.

(8.45) offers the following methods for increasing the accuracy of the FEM: either we refine the discretization or a given discretization use a higher order approximation. Thus we have to adjoin one more index to the matrix (8.39), viz. the number ℓ of the elements within the discretization and

$$A^g_{ij} = \sum_{\ell=1}^{L} A^{g\ell}_{ij},$$

where in subvolume V_ℓ the matrix elements have three contributions from the x, y and z components of the leakage term, and one contribution from the removal. Each term includes two types of multiplicative factors, one from the material properties of element ℓ as well as the geometry of the element $h^\ell_x h^\ell_y h^\ell_z$ and a term involving integrals of the polynomials over the element $S^x_{i\ell j\ell}, S^y_{i\ell j\ell}, S^z_{i\ell j\ell}$ furthermore $M_{i\ell j\ell}$:

$$\begin{aligned} A^{g\ell}_{ij} = {} & D^\ell_g \frac{h^\ell_y h^\ell_z}{h^\ell_x} S^x_{i\ell j\ell} + D^\ell_g \frac{h^\ell_x h^\ell_z}{h^\ell_y} S^y_{i\ell j\ell} \\ & + D^\ell_g \frac{h^\ell_x h^\ell_y}{h^\ell_z} S^z_{i\ell j\ell} + \Sigma^\ell_{tg} h^\ell_x h^\ell_y h^\ell_z M_{i\ell j\ell}. \end{aligned} \tag{8.47}$$

The integrals are calculated on the reference cube, let the basis function set on the reference cube be $R_i(x, y, z)$ then

$$S^x_{ij} = \int \frac{\partial R_i}{\partial x} \frac{\partial R_j}{\partial x} dxdydz \tag{8.48}$$

$$S^y_{ij} = \int \frac{\partial R_i}{\partial y} \frac{\partial R_j}{\partial y} dxdydz \tag{8.49}$$

$$S^z_{ij} = \int \frac{\partial R_i}{\partial z} \frac{\partial R_j}{\partial z} dxdydz \tag{8.50}$$

the three stiffness matrices and the mass matrix

$$M_{ij} = \int P_i P_j dxdydz. \tag{8.51}$$

The stiffness and mass matrices strongly influence the convergence of the FEM iterations.

The next step is to build up the basis functions from the solution values at specific points of the elements. Let $\mathfrak{S}$ be the set of points where the solution is assumed known. Then the basis functions are interpolating functions built on given values of the solution at points $s \in \mathfrak{S}$. We need N basis functions, that requires N points where the solution is known. There is a large variety of FEMs, below we discuss a particular case, where V is a planar region subdivided into triangular elements. We identify the a subvolume by its corner points $P_1 = (x_1, y_1)$, $P_2 = (x_2, y_2)$ and $P_3 = (x_3, y_3)$. The first step is that we have to express the coordinates of a running point $P = (x, y) \in V_k$. This is done (see Fig. 8.1) as follows.

$$\begin{pmatrix} 1 \\ x \\ y \end{pmatrix} = \begin{pmatrix} 1 & 1 & 1 \\ x_1 & x_2 & x_3 \\ y_1 & y_2 & y_3 \end{pmatrix} \begin{pmatrix} u_1 \\ u_2 \\ u_3 \end{pmatrix}, \tag{8.52}$$

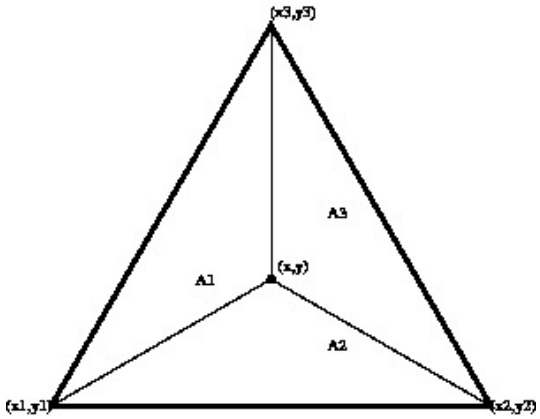

8.1. ábra. Coordinates in a triangular element

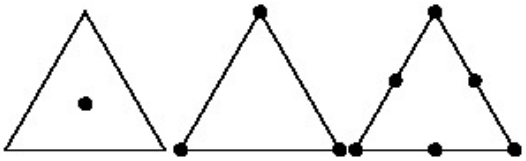

8.2. ábra. Coordinates where the solution is determined in a triangular element

where $u_i = A_i/A$, the areas A_i, $i = 1, 2, 3$ are shown in Fig. 8.1 and $A = A_1 + A_2 + A_3$. The interpolation goes by n-th order polynomials with m free coefficients:

$$p^{(n)}(x, y) = \sum_{l=1}^{m} a_l x^i y^j, \tag{8.53}$$

where the summation goes over the at most nth order polynomials of the form $x^i y^j, i+j = l$, $m = (n + 1)(n + 2)/2$. The a_l coefficients are collected into a vector of m elements: $\mathbf{a} = (a_1, \ldots, a_n)$ and are expressed with the solution values $\mathbf{P} = (\Phi(P_1), \ldots, \Phi(P_m))$ at m points in V_k, the positions of the P points are shown in Fig. 8.2. When $n = 0, m = 1$ the interpolation point is at the center of the element, when $n = 1, m = 3$, the interpolation points are selected at the corners of the triangular element, when $n = 2, m = 6$, the interpolation points are at the midpoints of the boundary line segments, and at the corner points. Formally the coefficients in vector $\mathbf{a}$ and the solution values in vector $\mathbf{P}$ are connected by a non-singular matrix $\mathbf{B}$:

$$\mathbf{P} = \mathbf{B}\mathbf{a}, \tag{8.54}$$

where $\mathbf{B}$ is an $n \times n$ matrix with elements of the m powers in (8.53) at the m positions indicated in Fig. 8.2. Since $\mathbf{B}$ is not singular, the coefficients of the expansion (8.53) can be expressed by the values of the unknown functions as

$$\mathbf{a} = \mathbf{B}^{-1}\mathbf{P}. \tag{8.55}$$

Formally we may write (8.53) as a scalar product:

$$p^{(n)}(x, y) = \mathbf{b}^{+}(x, y)\mathbf{a}, \tag{8.56}$$

where $\mathbf{b}(x,y) = (f_1(x,y), \ldots, f_m(x,y))$ is an m-tuple with the m polynomials $x^i y^j$, hence in subvolume V_k the FEM uses the approximation

$$\Phi(x,y) = \mathbf{b}^+(x,y)\mathbf{B}^{-1}\mathbf{P}, \tag{8.57}$$

which is actually an interpolation scheme because $\mathbf{P}$ has been formed from values of the solution at specific points. The next step is the derivation of an equation for the $\mathbf{P}$ vector. This is done using the weak form (8.36) of the equation to be solved. In (8.36) we need the following $m \times m$ matrix:

$$\mathbf{M} = \int_{V_k} \mathbf{b}\mathbf{A}\mathbf{b}^+ \, dx\, dy, \tag{8.58}$$

whose i, j element is

$$\int_{V_k} f_i(x,y)\mathbf{A}f_j(x,y) \, dx\, dy, \tag{8.59}$$

and (8.36) amounts to

$$\mathbf{M}\mathbf{B}^{-1}\mathbf{P} = 0, \tag{8.60}$$

which make just the m equations for the unknown values $(\Phi(P_1), \ldots, \Phi(P_m))$ of the solution at the m prefixed points. It can be shown that the matrix is not singular [49].

Once the solution in a given element is known, we need a procedure for the entire volume V. From the approximations used in an element, a large variety of interpolating functions can be constructed. For a survey, see [49]. Common feature of the various methods is that the polynomial approximations fall into two categories:

- in the Lagrange family the interpolating functions are continuous functions along the joint boundary of adjacent nodes;
- in the Hermite family the normal gradients (or the normal component of the current) are continuous at the joint boundary.

In most commercial codes either possibility is offered for the user. The FEM approximates the solution over V by element-wise polynomials

$$\Big\{ f_{n,1}(x,y), f_{n,2}(x,y), \ldots, f_{n,K}(x,y) \Big\}, \tag{8.61}$$

where V is subdivided into K elements, and nth order approximation is used on each element. The components $f_{n,k}(x,y)$, $k = 1, \ldots, K$ are extended over the entire V so that

$$f_{n,k}(x,y) = \begin{cases} p^{(n)}(x,y) & \text{for } (x,y) \in V_k, \\ 0 & \text{otherwise.} \end{cases} \tag{8.62}$$

8.4. Nodal methods

In a PWR, the typical relaxation distance in the thermal energy group is 1 *cm*. The height of the reactor core is app. 250 *cm*, the radius of the core is also about 250 *cm*. When we use FDM, in a discretization leading to acceptable accuracy the mesh size must be close to the relaxation distance hence at least $2.5^3 10^6$ meshes are needed. To solve sets of linear equations with around 10^7 unknowns on routine base would need not only a numerically stable but also a fast algorithm. In the 1970s, two views existed. The first one trusted in the capabilities of the acceleration technique and would rely on the FDM, the other sought novel numerical methods that cut the computation time considerable shorter.

One of the possible new technics, the FEM, has been discussed in the previous Subsection. The main idea of the FEM can be summarized as follows. We subdivide volume V into elements $V_i, i = 1, 2 \ldots$ which are of $10 - 20$ mean free path in diameter. The solution is V_i is determined by a low ranking polynomial from the solution values at specific points. With the interpolation polynomial in the hand, we determine the reaction rates in V_i, including the boundary currents. The FEM has proved appr. 20 times faster than the FDM [50].

Another technique, called nodal method, aimed at determining only volume integrated reaction rates in V_i, that is called this time a node, but the method was careful to give a good representation of the boundary currents to connect the solution at node boundaries seamlessly.

In the first nodal codes, the flux was approximated by low ranking polynomials. Later A. F. Henry et al. integrated the diffusion equation over two independent spatial variables, and got an ODE in one variable and the exact solution could be given. That method had two problems. Firstly, the integrated leakage terms, the cross-leakage had to be approximated as a polynomial and an additional iteration along the spatial directions was needed. By 1980, it came clear that the 3D diffusion equation can be solved and the solution can be used in the nodal method. After that, only one limitation remained: the accuracy of the boundary condition but practice has proven that in large fuel assemblies, like a PWR or VVER-1000 assembly, it suffices to approximate the boundary current by a second order polynomial on a face of the fuel assembly.

8.4.1. Nodal diffusion theory

We write the multigroup diffusion equation into the following form:

$$\mathbf{D}\boldsymbol{\nabla}^2\boldsymbol{\Phi}(\mathbf{r}) + \boldsymbol{\Sigma}\boldsymbol{\Phi}(\mathbf{r}) = 0 \tag{8.63}$$

where $\mathbf{D}$ is the diagonal matrix formed from the group diffusion coefficients, $\boldsymbol{\Sigma}$ is the cross-section matrix involving the group transfer processes (e.g. scattering, fission). A formal solution of (8.63) is

$$\boldsymbol{\Phi}(\mathbf{r}) = \sum_{k=1}^{G} \mathbf{t}_k \int_{4\pi} w_k(\boldsymbol{\alpha}) e^{i(\lambda_k \boldsymbol{\alpha})\mathbf{r}} d\boldsymbol{\alpha}, \tag{8.64}$$

where

$$\mathbf{D}^{-1}\boldsymbol{\Sigma}\mathbf{t}_k = \lambda_k^2 \mathbf{t}_k, \tag{8.65}$$

i.e. $\mathbf{t}_k$ and λ_k^2 are the eigenvectors and eigenvalues of matrix $\mathbf{D}^{-1}\boldsymbol{\Sigma}$.

In (8.64) $w_k(\boldsymbol{\alpha})$ is a positive weight function depending on the unit vector $\boldsymbol{\alpha}$. Substituting (8.64) into (8.63) and using (8.65), we can check that (8.64) is a solution with arbitrary $w(\boldsymbol{\alpha})$ indeed. The presented solution is too complicated for practical calculations, thus we simplify it. The boundary condition is sufficiently accurate for the nodal calculations when the current is given in three points for we are able to determine the average, first and second moments along a face of the subvolume under consideration. To this end, we subdivide the unit sphere into n_F disjoint segments corresponding to the n_F faces of the node, and in each segment we choose the weight function to differ from zero only in three directions. Let the mentioned directions be $\boldsymbol{\alpha}_{nk}, n = 1, n_F; m = 0, 1, 2$ then the analytical solution takes the form of

$$\boldsymbol{\Phi}(\mathbf{r}) = \sum_{n=1}^{n_F} \sum_{m=0}^{2} \sum_{k=1}^{G} \mathbf{t}_k w_{knm} e^{i(\lambda_k \boldsymbol{\alpha}_{nk})\mathbf{r}}, \tag{8.66}$$

where the unknown w_{knm} weights are to be determined from the moments of the boundary condition at the n_F faces of the node. Eventually, we determine the w_{knm} constants from the

boundary conditions. When we use partial currents as boundary condition, the algorithm proceeds in the following way:

1. in the node under consideration, we collect the entering current moments at the n_F boundaries. Here we use the condition that the entering current at a given face is the exiting current of the neighboring node;
2. from the known entering currents we determine $w_{knm}, k = 1, \ldots, G; n = 1, \ldots, n_F; m = 0, \ldots, 2$ using (8.66);
3. from the flux we determine the moments of the exiting currents at the n_F boundaries;
4. from the flux we determine the reaction rates in the node under consideration.

Note that all the energy groups are treated simultaneously, there is no separated internal iteration for the nodes and external iteration for the energy groups. Furthermore, the above described iteration suits for calculating the responses of the node, see Section 6.6 in Chapter 6. This is why the result depends in a relaxed way on the diameter of the node, we have to account of the effect of the approximate boundary condition.

8.4.2. Nodal transport theory

We present two transport theory formalisms. The first one is based on the even-odd decomposition of the angular flux, the second one is a particular application of the response matrix method.

The even-odd parity transport equation

As R. Stammler remarked, there is no general algorithm for the P_n approximation, thus to reach a prefixed accuracy we have to resort to another approximation. In Section 8.6 we discuss the S_n method, now we deal with the even-odd parity representation of the angular flux. We have seen in Section 6.5 of Chapter 6 that if the P_1 decomposition of the angular flux is not satisfactory, we need the level besides the scalar flux. This requirement has led to the even-odd parity decomposition of the angular flux. We introduce the even and odd angular fluxes as

$$\Psi_+(\mathbf{r}, E, \mathbf{\Omega}) = \frac{1}{2}\left(\Phi(\mathbf{r}, E, \mathbf{\Omega}) + \Phi(\mathbf{r}, E, -\mathbf{\Omega})\right) \tag{8.67}$$

and

$$\Psi_-(\mathbf{r}, E, \mathbf{\Omega}) = \frac{1}{2}\left(\Phi(\mathbf{r}, E, \mathbf{\Omega}) - \Phi(\mathbf{r}, E, -\mathbf{\Omega})\right), \tag{8.68}$$

respectively. Assume that the source is isotropic, then

$$Q(\mathbf{r}, E, \mathbf{\Omega}) = \frac{1}{4\pi} Q_0(\mathbf{r}, E), \tag{8.69}$$

where we have assumed isotropic source. We repeat the transport equation (3.132) in the following simplified form:

$$\mathbf{\Omega}\boldsymbol{\nabla}\Phi(\mathbf{r}, E, \mathbf{\Omega}) + \Sigma(\mathbf{r}, E)\Phi(\mathbf{r}, E, \mathbf{\Omega}) = Q(\mathbf{r}, E), \tag{8.70}$$

and for the argument $-\mathbf{\Omega}$:

$$-\mathbf{\Omega}\boldsymbol{\nabla}\Phi(\mathbf{r}, E, -\mathbf{\Omega}) + \Sigma(\mathbf{r}, E)\Phi(\mathbf{r}, E, -\mathbf{\Omega}) = Q(\mathbf{r}, E), \tag{8.71}$$

adding (8.70) and (8.71), we find the following equation for the even parity angular flux:

$$\mathbf{\Omega}\boldsymbol{\nabla}\Psi_-(\mathbf{r},E,\mathbf{\Omega})+\Sigma(\mathbf{r},E)\Psi_+(\mathbf{r},E,\mathbf{\Omega})=Q(\mathbf{r},E), \tag{8.72}$$

subtracting (8.71) from (8.69), we obtain

$$\mathbf{\Omega}\boldsymbol{\nabla}\Psi_+(\mathbf{r},E,\mathbf{\Omega})+\Sigma(\mathbf{r},E)\Psi_-(\mathbf{r},E,\mathbf{\Omega})=0. \tag{8.73}$$

As we see, the even and odd parity fluxes form a coupled equation set. To eliminate the odd term, we use the following relationship between Ψ_+ and Ψ_- that we obtained from (8.73):

$$\Psi_-(\mathbf{r},E,\mathbf{\Omega})=\frac{[-\mathbf{\Omega}\boldsymbol{\nabla}\Psi_+(\mathbf{r},E,\mathbf{\Omega})]}{\Sigma(\mathbf{r},E)}. \tag{8.74}$$

Before proceeding with the derivation, we note two relationships. The scalar flux is expressed with the even parity component as:

$$\Phi(\mathbf{r},E)=\int_{4\pi}\Psi_+(\mathbf{r},E,\mathbf{\Omega})d\mathbf{\Omega}, \tag{8.75}$$

and the net current with the odd component as

$$\mathbf{J}(\mathbf{r},E)=\int_{4\pi}\mathbf{\Omega}\Phi(\mathbf{r},E,\mathbf{\Omega})d\mathbf{\Omega}=\int_{4\pi}\mathbf{\Omega}\Psi_-(\mathbf{r},E,\mathbf{\Omega})d\mathbf{\Omega}, \tag{8.76}$$

using here (8.74), we find the following relationship between the net current and even parity angular flux:

$$\mathbf{J}(\mathbf{r},E)=\frac{1}{\Sigma(\mathbf{r},E)}\int_{4\pi}\mathbf{\Omega}(\mathbf{\Omega}\boldsymbol{\nabla})\Psi_+(\mathbf{r},E,\mathbf{\Omega})d\mathbf{\Omega}. \tag{8.77}$$

The vacuum boundary conditions for the even and odd parity fluxes are [51]:

$$\Psi_+(\mathbf{r}_b,E,\mathbf{\Omega})=\pm\Psi_-(\mathbf{r}_b,E,\mathbf{\Omega}), \tag{8.78}$$

where the $+$ and $-$ sign holds for $\mathbf{n\Omega}>0$ and $\mathbf{n\Omega}<0$, respectively.

(8.76) indicates that the odd parity angular flux is a generalization of the neutron current, similarly (8.75) shows that the even parity angular flux is a generalization of the scalar flux. (8.74) is a relationship between the even and odd parity angular fluxes. Below we present the theory [52] of a variational method to find the even and odd parity angular fluxes. Fundamentals of the variational method have been given in Section 3.6 in Chapter 3. In order to simplify the derivation, the continuous energy variable is considered in multigroup approximation see Section 4.1 in Chapter 4. Then equations (8.72) and (8.73) express the neutron balance in group g, which is purely formal, and because we are always dealing with the balance in group g the group index may be discarded. The source term Q provides the connection between the energy groups automatically.

First we have to find variables q of the variational formalism such that they result the transport equation (or one of its approximations) as Euler-Lagrange equation. In the even-odd parity formalism q has two components because the solution is determined by Ψ_+ and Ψ_-. The second, and far from trivial step, is to find function L in (3.230) so that the Euler-Lagrange equations (3.233) give just equations (8.72) and (8.73). Before giving the L function, we exploit the physical approach to a boundary value problem, viz. volume V is subdivided into subvolumes and the cross-sections are assumed to be constant in a subvolume.

We prescribe continuity conditions at the interface between adjacent subvolumes. Now the L function is a sum over the subvolumes:

$$L[\Psi_+, \Psi_i] = \sum_{i=1}^{I} L_i[\Psi_{i+}, \Psi_{i-}]. \tag{8.79}$$

The equations to determine the even-odd parity fluxes are:

$$\mathbf{\Omega\nabla}\frac{\mathbf{\Omega}}{\Sigma_g}\mathbf{\Omega\nabla}\Psi_{g-}(\mathbf{r},\mathbf{\Omega}) + \Sigma_g\Psi_{g+}(\mathbf{r},\mathbf{\Omega}) = Q_g \tag{8.80}$$

$$\mathbf{\Omega\nabla}\Psi_{g+}(\mathbf{r},\mathbf{\Omega}) + \Sigma(\mathbf{r},E)\Psi_{g-}(\mathbf{r},\mathbf{\Omega}) = 0. \tag{8.81}$$

Note, that in the source term the isotropic slowing down contributions from the other energy groups is included. In that case the formalism is the same in every energy group, the source term automatically couples the energy groups. From now on we speak of the calculation in a given energy group and the group index is suppressed. The VARIANT algorithm uses the following L_i function in subvolume V_i:

$$\begin{aligned} L_i[\Psi_+, \Psi_-] = &\int_{V_i}\left\{\int_{4\pi}\left[\frac{(\mathbf{\Omega\nabla}\Psi_{i+})^2}{\Sigma_i} + \Sigma_i\Psi_{i+}^2\right]d\mathbf{\Omega} - \Sigma_{si}\Phi_i^2 - 2\Phi_i Q_i\right\}d^3\mathbf{r} \\ &+ 2\int_{\partial V_i}\int \mathbf{\Omega}\mathbf{n}_i\Psi_{i+}\Psi_{i-}d\mathbf{\Omega}dS_i. \end{aligned} \tag{8.82}$$

Note, that in the functional we find the scalar flux Φ_i, the even-odd parity fluxes Φ_{i+}, Φ_{i-}. n_i is the outward normal vector at the boundary ∂V_i, dS_i is the infinitesimal surface element on ∂V_i, Σ_{si} is the scattering cross-section in V_i.

We endeavor to work out a linear equation set to minimize $L[\Psi_+, \Psi_i]$. First, we show that the condition $\delta L[\Psi_+, \Psi_i] = 0$ is equivalent to equations (8.72) and (8.73). To this end we consider the change of L when $\Psi_+ \to \Psi_+ + \delta\Psi_+$ and $\Psi_- \to \Psi_- + \delta\Psi_-$. Keeping the first order terms in equation (3.231), we obtain

$$\begin{aligned} \delta L[\Psi_+, \Psi_-] = &\int_{V_i}\int_{4\pi}\left[\frac{\mathbf{\Omega\nabla}\delta\Psi_+\mathbf{\Omega\nabla}\Psi_+}{\Sigma}\Psi_+\delta\Psi_+\right]d\mathbf{\Omega} - \delta\Phi(\Sigma_s\Phi + Q) \\ &+ 2\int_{\partial V}\int_{4\pi}\mathbf{\Omega}\mathbf{n}(\Psi_-\delta\Psi_+\Psi_+\delta\Psi_-). \end{aligned} \tag{8.83}$$

Here we introduced

$$\delta\Phi = \int_{4\pi}\delta\Psi_+ d\mathbf{\Omega}, \tag{8.84}$$

and $\delta\Phi = \delta\Phi(r)$ in V_i. We transform the first integral into a divergence using the identity

$$\mathbf{\nabla}\left[\mathbf{\Omega}\delta\Psi_+\frac{\mathbf{\Omega\nabla}\Psi_+}{\Sigma}\right] = \frac{\mathbf{\Omega\nabla}\delta\Psi_+}{\Sigma}\mathbf{\Omega\nabla}\Psi_+ + \delta\Psi_+\mathbf{\Omega\nabla}\left(\frac{\mathbf{\Omega\nabla}\Psi_+}{\Sigma}\right), \tag{8.85}$$

and use the divergence theorem

$$\int_V\int_{4\pi}\mathbf{\Omega\nabla}(\delta\Psi_+\mathbf{\Omega\nabla}\Psi_+)d\mathbf{\Omega}d^3\mathbf{r} = \oint\int_{4\pi}\mathbf{\Omega}\mathbf{n}\delta\Psi_+\mathbf{\Omega\nabla}\Psi_+ d\mathbf{\Omega}dS. \tag{8.86}$$

The resulting equation is

$$\begin{aligned}\delta L[\Psi_+,\Psi_-] &= 2\int_{V_i}\int_{4\pi}\delta\Psi_+ \\ &\left(-\mathbf{\Omega\nabla}\frac{\mathbf{\Omega\nabla}\Psi_+}{\Sigma}+\Sigma\Psi_+-\Sigma_s\Phi_Q\right)d\mathbf{\Omega}d^3\mathbf{r} \\ +2\int_{\partial_V}\int_{4\pi}\mathbf{\Omega n}\delta\Psi_+&\left(\frac{\mathbf{\Omega\nabla}\Psi_+}{\Sigma}+\Psi_-\right)dS+2\int_{\partial V}\int_{4\pi}\mathbf{\Omega n}\Psi_+ d\mathbf{\Omega}dS.\end{aligned} \tag{8.87}$$

The first variation is stationary when the coefficients of $\delta\Psi_+, \delta\Psi_-$ vanish in (8.87), these conditions are just equations (8.72) and (8.73).

At an internal interface, the two adjacent subvolumes contribute to the surface integrals in (8.87), but note that the normal vectors have opposite signs. The two surface integrals in (8.87) cancel only if the even parity flux is continuous (the second integral) and if the odd parity flux is continuous (first integral).

The next step is to select a basis, to expand the even and odd angular fluxes in terms of that basis, and to determine the expansion coefficients from the variational principle. The trial functions should depend on space and angle in a given energy group, that makes the procedure more complicated. Following [52], we choose the basis functions as

$$\Psi_+(\mathbf{r},\mathbf{\Omega}) = \sum_{i,j} p_{ij}U_{ij}(\mathbf{r},\mathbf{\Omega}) \tag{8.88}$$

where

$$U_{ij}(\mathbf{r},\mathbf{\Omega}) = f_i(\mathbf{r})g_j(\mathbf{\Omega}) \tag{8.89}$$

and the U_{ij} basis is orthonormal:

$$\int_V U_{ij}(\mathbf{r},\mathbf{\Omega})U_{i'j'}(\mathbf{r},\mathbf{\Omega})d^3\mathbf{r} = \delta_{ii'}\delta jj' \tag{8.90}$$

for every j, j'. Furthermore the odd components are expanded as

$$\Psi_-(\mathbf{r},\mathbf{\Omega}) = \sum_{i,j,b} q_{ijb}V_{ijb}(\mathbf{r},\mathbf{\Omega}), \tag{8.91}$$

here

$$V_{ijb}(\mathbf{r},\mathbf{\Omega}) = h_{jb}(\mathbf{r})k_{jb}(\mathbf{\Omega}); \tag{8.92}$$

functions $k_{jb}(\mathbf{\Omega})$ are odd-order spherical harmonics, and

$$\int_b h_{jb}(\mathbf{r})h_{j'b}(\mathbf{r})dS_b = \delta_{jj'} \tag{8.93}$$

for any internal boundary b in V. The source term is also decomposed in terms of $f_i(\mathbf{r})$:

$$Q(\mathbf{r}) = \sum_i s_i f_i(\mathbf{r}). \tag{8.94}$$

In (8.87) we also encounter the scalar flux, which is decomposed as

$$\Phi(\mathbf{r}) \approx \sum_i \sum_j p_{ij}\delta_{1j}. \tag{8.95}$$

The V_{ijb} functions are orthogonal in the following sense:

$$\int_b V_{ijb}(\mathbf{r},\mathbf{\Omega})V_{i'j'b}(\mathbf{r},\mathbf{\Omega})dS = \delta ii'\delta_{jj'} \tag{8.96}$$

for any internal interface b in V.

After substituting (8.88), (8.91), and (8.94), (8.95), and using the orthogonality relations (8.90), (8.93), (8.96), we get the following expression:

$$L[p,q] = p^T Ap - 2q^T s + 2\sum_{b\in V} p^T Mq \tag{8.97}$$

where integrals of the basis functions are collected in A and M. This expression is stationary in p if

$$p = A^{-1}s + A^{-1}Mq. \tag{8.98}$$

(8.98) relates the even parity fluxes (more precisely, its coefficients) p on the subvolume interfaces to the source moments s within the subvolume to the odd parity flux moments q on the subvolume interfaces. The variations of q result the continuity at the internal interfaces:

$$p_b = M_b^T p, \text{ for every } b \in V. \tag{8.99}$$

The end of the variational method is a set of linear equations that can be solved by the methods discussed in Chapter 8.

The response matrix iteration in transport theory

Below we deal with the problem of determining the angular flux in a periodic lattice in transport theory frame using the response matrix technique [53], [54]. In the theory, we exploit the geometrical symmetry of the cell and we assume that the material distribution in the cell does not break the symmetry of the geometry. This assumption entails that the cell must be small compared to the gradient of the flux, otherwise power and temperature gradient would appear in the cell. We also assume that it suffices to use the linear transport equation, the feedbacks may be neglected.

We assume furthermore that the cell and its immediate surroundings are part of a large lattice, which is critical, hence, the cell or the cell plus its surroundings are subcritical. Then, if there is no entering current on the boundary of the region under investigation, the only solution to the static transport equation is identically zero. Under the stipulated condition we seek the solution to the transport equation in multigroup approximation, with given entering currents along the cell boundary. First let us consider the angular flux in a single symmetric cell, $\mathbf{r} \in V$, and assume the geometry of the cell to be a square. The square is invariant under specific reflections and rotations, it has eight symmetries [55] that form the group C_{4v}. Let the entering current $I_i(\mathbf{r}_b), \mathbf{r}_b \in \partial V$ transform under the elements of the C_{4v} group in the following manner:

$$\mathcal{P}_h I_i(\mathbf{r}_b) = I_i(\mathbf{P}_h^{-1}\mathbf{r}_b) \tag{8.100}$$

where h is an element of the C_{4v} group, $\mathcal{P}_h$ is the operator describing the action of symmetry h on a function, and $\mathbf{P}_h$ is a matrix [56] describing the action of h on the space coordinate $\mathbf{r}$. Any function is decomposable into irreducible components labeled by α, k, $k = 1,\ldots,\ell_\alpha$, where ℓ_α is called the dimension of the irreducible subspace α. The group elements transform elements of a given irreducible subspace among each other. The irreducible subspaces can be looked up in the so called character tables [183].

Below we summarize the properties of the irreducible components.

1. Any function can be decomposed into irreducible components of a given finite group.

2. The irreducible components of a function $f(\mathbf{r})$ is determined by the formula:

$$f_i^\alpha(\mathbf{r}) = \sum_{h\in H} D_{ij}^\alpha(h) f(h\mathbf{r}). \tag{8.101}$$

3. The irreducible components are orthogonal:

$$\int_V f_i^\alpha(\mathbf{r}) f_j^\beta(\mathbf{r}) d^3\mathbf{r} = 0, \quad \text{if } i \neq j, \alpha \neq \beta. \tag{8.102}$$

4. There is an irreducible representation (irrep), the unit representation, which is invariant under the elements of the group H.

Let $\mathcal{O}$ be an operator that commutes with the elements of the group H. Then $\mathcal{O}f^{\alpha,k}$ belongs to the same irrep as $f_k^\alpha(\mathbf{r})$. The following physical quantities belong to the same irrep: scalar flux, normal component of the net current, exiting and incident current, angular current.

In a subcritical V, the angular flux in V belongs to the same irrep as does the boundary value prescribed on the boundary. It is always possible to obtain the square V from a subset $V_0 \subset V$ of the square by applying the symmetries of the square on V_0. For example, by the two orthogonal diagonals, we subdivide the square into four congruent triangles. It suffices to know the solution over one of the triangles V_0, applying $h \in H$, we are able to reconstruct the solution over the entire square. The area of V is eight times the area of V_0 for a square cell. A similar statement holds for the boundary ∂V, which is the union of eight half faces. The formalism simplifies when we speak of only four faces exploiting that the even and odd functions automatically take care of the "side halving".

Assume that the boundary condition transforms as irrep α, k does. Then, it suffices to give the solution $\psi(\mathbf{r})$ of the transport equation on $\mathbf{r} \in V_0$, as the solution on V is given as $\mathcal{P}_h\psi(\mathbf{r}) = \psi(\mathbf{P}_h\mathbf{r}), h \in H$. It can be shown that the reconstruction is completely determined by one of the following four four-tuples:

$$\mathbf{e}_1 = (1,1,1,1); \;\; \mathbf{e}_2 = (1,-1,1,-1); \;\; \mathbf{e}_3 = (1,0,-1,0); \;\; \mathbf{e}_4 = (0,1,0,-1). \tag{8.103}$$

Consequently, the boundary condition is completely determined by giving the index i of the $\mathbf{e}_i$ vector according to which the boundary value transforms under the symmetries of the square, and the boundary value over the boundary of the square. Furthermore, the general case, including the non-symmetric one, is a linear combination of the symmetric cases. Similarly, it suffices to give the solution over one of the triangles and give the vector according to the solution transforms in V.

Let the boundary condition be $I_{ig}(\mathbf{r}_b)\mathbf{e}_i$ in energy group g. We write the solution of the transport equation in energy group g' as $\psi_{igg'}(\mathbf{r})$. Four model-boundary value problems will describe the neutron distribution in V: $\psi_{igg'}(\mathbf{r}, \mathbf{\Omega}), i = 1, 4$.

As to the model boundary conditions, there are four possible boundary conditions along

the four sides: $N_{ig}(\mathbf{r}_b), i = 1, 4$. Since

$$\begin{pmatrix} N_{1g} \\ N_{2g} \\ N_{3g} \\ N_{4g} \end{pmatrix} = \frac{N_{1g}+N_{2g}+N_{3g}+N_{4g}}{4} \begin{pmatrix} 1 \\ 1 \\ 1 \\ 1 \end{pmatrix} + \frac{N_{1g}-N_{2g}+N_{3g}-N_{4g}}{4} \begin{pmatrix} 1 \\ -1 \\ 1 \\ -1 \end{pmatrix} + \frac{N_{1g}-N_{3g}}{2} \begin{pmatrix} 1 \\ 0 \\ -1 \\ 0 \end{pmatrix} + \frac{N_{2g}-N_{4g}}{2} \begin{pmatrix} 0 \\ 1 \\ 0 \\ -1 \end{pmatrix} \tag{8.104}$$

and the irreps of the boundary conditions are

$$I_{1g} = \frac{N_{1g}+N_{2g}+N_{3g}+N_{4g}}{4} \tag{8.105}$$

$$I_{2g} = \frac{N_{1g}-N_{2g}+N_{3g}-N_{4g}}{4} \tag{8.106}$$

$$I_{3g} = \frac{N_{1g}-N_{3g}}{2} \tag{8.107}$$

$$I_{4g} = \frac{N_{2g}-N_{4g}}{2}. \tag{8.108}$$

and the angular flux $\Phi_g(\mathbf{r}, \mathbf{\Omega})$ in V is given by

$$\Phi_g(\mathbf{r}, \mathbf{\Omega}) = \sum_{i=1}^{4} \sum_{g'=1}^{G} I_{ig'} \psi_{igg'}(\mathbf{r}, \mathbf{\Omega}). \tag{8.109}$$

Here we present a simplified derivation. Actually, the basis functions $\psi_{igg'}(\mathbf{r}, \mathbf{\Omega})$ depend on the independent variables $\mathbf{r}$ and $\mathbf{\Omega}$, and their irreducible components are direct products of functions depending on $\mathbf{r}$ or $\mathbf{\Omega}$. Such a discussion is rather long, see [55].

We need two quantities determined on the cell boundary: the face averaged flux and the face averaged normal component of the net current. The notation for the former is

$$F_{i,g} = \int_{\partial V_i} \int_{4\pi} \Phi_g(\mathbf{r}, \mathbf{\Omega}) d\mathbf{\Omega} dS, \quad i = 1, \ldots, 4, \tag{8.110}$$

the latter

$$C_{i,g} = \int_{\partial V_i} \int_{4\pi} \mathbf{\Omega}\mathbf{n} \Phi_g(\mathbf{r}, \mathbf{\Omega}) d\mathbf{\Omega} dS; \quad i = 1, \ldots, 4. \tag{8.111}$$

The angular flux $\Phi_g(\mathbf{r}, \mathbf{\Omega})$ is linear in the irreps $I_{ig'}$, see (8.109), therefore the irreps of the boundary fluxes and currents are also linear in the irreps $I_{ig'}$. In view of this, we may write

$$F_{ig} = \sum_{g'=1}^{G} R^i_{gg'} I_{ig}, i = 1, \ldots, 4; \tag{8.112}$$

because the irreps are linearly independent. Analogously, the irreps of the current are given by

$$C_{ig} = \sum_{g'=1}^{G} T^i_{gg'} I_{ig}, i = 1, \ldots, 4. \tag{8.113}$$

To simplify the notation, we collect the four irreps into one vector and write

$$\mathbf{C}_g = \sum_{g'=1}^{G} \mathrm{T}_{gg'} \mathbf{I}_{g'} \tag{8.114}$$

where

$$T_{gg'} = diag(T^1_{gg'}, T^2_{gg'}, T^3_{gg'}, T^4_{gg'}). \tag{8.115}$$

We are able to express the irreps in a given cell with the help the values at the four faces of the cell, using (8.105)-(8.108):

$$F_{ig} = \sum_{i'=1}^{4} I_{i'g} e_{i'in}, \tag{8.116}$$

where vectors $\mathbf{e}_i$ are given in (8.103). Analogously, the four boundary currents at the four cell faces are given as

$$C_{ig} = \sum_{g'=1}^{G} \sum_{i'=1}^{4} T^{i'}_{gg'} I_{i'g}. \tag{8.117}$$

Now we are able to include also the interface connection between adjacent cells. To this end, we have to fix the node numbering, see Fig. 8.3. The node index is added as a left superscript, e.g. ${}^0\mathbf{I}_1$ stands for the symmetric boundary value in cell No. 0. Our goal is to derive an equation for the symmetric $\mathbf{I}_1$ amplitudes in the boundary condition see (8.100).

Now we return to the numerical method for solving the static transport equation in multigroup formalism:

$$\boldsymbol{\Omega}\boldsymbol{\nabla}\Phi_g(\mathbf{r},\boldsymbol{\Omega}) + \Sigma_g\Phi_g(\mathbf{r},\boldsymbol{\Omega}) = \sum_{g'=1}^{G} \Sigma_s(g' \to g, \boldsymbol{\Omega}' \to \boldsymbol{\Omega}) + \frac{f_g}{4\pi} \sum_{g'=1}^{G} \nu\Sigma_{fg'} \int_{4\pi} \Phi_{g'}(\mathbf{r},\boldsymbol{\Omega}')d\boldsymbol{\Omega}';$$
$$g = 1, \ldots, G. \tag{8.118}$$

For the sake of simplicity we assume isotropic scattering:

$$\Sigma_s(g' \to g, \boldsymbol{\Omega}' \to \boldsymbol{\Omega}) \to \Sigma_s(g' \to g).$$

We apply the variational method to a volume V composed of $N >> 1$ identical cells. The solution on V is written as $\Psi_g, g = 1, \ldots, G$ and it is the function making stationary the functional

$$L[\Psi_g] = \int_V \int_{4\pi} (\boldsymbol{\Omega}\boldsymbol{\nabla}\Psi_g)^2 + \Sigma_g\Psi_g^2 - 2Q_g\Psi_g d^3\mathbf{r}d\boldsymbol{\Omega} + \int_{\partial V} \int_{4\pi} \boldsymbol{\Omega}\mathbf{n}\Psi^2 dSd\boldsymbol{\Omega}, \tag{8.119}$$

here Q_g is the sum of sources in energy group g. The variation of functional L is

$$\delta L = \int_V \int_{4\pi} (\boldsymbol{\Omega}\boldsymbol{\nabla}\Psi + \Sigma_g\Psi_g - Q_g)\, \delta\Psi_g d^3\mathbf{r}d\boldsymbol{\Omega} + \int_{\partial V} \int_{4\pi} \boldsymbol{\Omega}\mathbf{n}\Psi_g\delta\Psi_g, \tag{8.120}$$

which vanishes for arbitrary $\delta\Psi$ when Ψ_g is the solution of (8.118) inside V and $\mathbf{n}\boldsymbol{\Omega}\Psi$ is continuous on the boundaries. We are going to minimize the functional (8.119) for the approximate solution by a suitable choice of the free parameters. In doing so, we decompose the integrals into sums of integrals over individual cells:

$$L[\Psi_g] = \sum_{n=1}^{N} L_n[\Psi_{n,g}] \tag{8.121}$$

and in cell n

$$L_n[\Psi_{n,g}] = \int_{V_n} (\mathbf{\Omega}\boldsymbol{\nabla}\Psi_{ng})^2 + \Sigma_g \Psi_{ng}^2 - 2Q_g\Psi_{ng} d^3\mathbf{r} + \int_{\partial V_n}\int_{4\pi} \mathbf{\Omega}\mathbf{n}\Psi_{ng}^2(\mathbf{r}_b,\mathbf{\Omega})dSd\mathbf{\Omega}. \quad (8.122)$$

In the evaluation of the surface integral we have to remember that a given internal cell boundary we get two contributions from the two adjacent cells and the direction of the normal $\mathbf{n}$ is opposite on the two sides therefore the last terms are

$$\int_{\partial V_n}\int_{4\pi} \mathbf{\Omega}\mathbf{n}(\Psi_{ng}(\mathbf{r}_b,\mathbf{\Omega}) - \Psi_{n'g}(\mathbf{r}_b,\mathbf{\Omega}))\delta\Psi_g dSd\mathbf{\Omega} \quad (8.123)$$

minimal when at the boundary points $\mathbf{r}_b$ the angular flux multiplied by $\mathbf{\Omega}\mathbf{n}$ is continuous.

The first step in setting up an approximate method is to choose the basis functions in terms of which the approximate solution is expressed. Here we rely on the symmetry of the boundary condition. The boundary conditions at the boundary of a square cell fall into four categories, transforming according to one of the four vectors given in (8.103). If this is not the case the boundary condition is decomposable into such components by means of (8.104). When the cell is small, we may discard the space dependence on a side. In general, we may need a polynomial approximation along a given face. To this end, we introduce the local coordinate $-a \leq \xi \leq +a$ and we expand the position dependent scalar flux along face i as

$$\Phi_i(\xi) = \sum_{m=0}^{M} b_m P_m(\xi). \quad (8.124)$$

Unfortunately the symmetry properties of the polynomials differ, for example the symmetries of polynomials even in ξ differ from the properties of the odd polynomials [3]. For the sake of simplicity, we assume the angular flux is constant along a face of the cell.

It is known that the angular flux at the boundary determines the solution, see theorem 3.1 in Chapter 1, thus by an appropriate decomposition of the angular flux on the boundary, the corresponding solutions of the transport equations form a complete system. That observation is the basis of the below given approximate solution[53],[54].

Since the symmetry of the boundary condition at the cell boundary determines the symmetry of the solution to the transport equation inside a cell, the trial functions are classified according to the symmetry of the boundary condition. The residuum of the variation depends on the continuity of the angular moments at the internal boundaries, see (8.123), so we choose the normal component of the net current as boundary condition. We classify the boundary currents according to their transformation rule among the four faces, we distinguish four classes. To cut the discussion short, we assume that face averaged boundary conditions are used. Then, the normal components of the net currents at the cell boundary are proportional to $\mathbf{e}_1, \mathbf{e}_2, \mathbf{e}_3$ and $\mathbf{e}_4$. The angular flux inside the cell is uniquely determined by the boundary net currents, so we use the following maps, see Table 8.1. Note that linear combinations of boundary currents or fluxes have the same symmetry as the boundary current or flux. The linear transformation here amounts to a multiplication by matrix $E_{gg'}, F_{gg'}$, and $H_{gg'}$, respectively. Note that the first irrep I_{1g}, is the average of the net currents at the four faces.

Since there is no essential difference between the third and fourth irreps, the transformation operator is the same for them (Schur's lemma), see [55]. Our approximation neglects that higher angular moments may appear at the boundary and the spatial shape of the

[3] Odd angular moments also transform differently from the even angular moments, see Ref. [55] for the details.

Irrep	BC	Ang. flux.
1	$\mathbf{e}_1 \mathrm{I}^i_{1g}$	$\sum_{g'=1}^{G} E_{gg'} \mathrm{I}^i_{1g'}$
2	$\mathbf{e}_2 \mathrm{I}^i_{2g}$	$\sum_{g'=1}^{G} F_{gg'} \mathrm{I}^i_{2g'}$
3	$\mathbf{e}_3 \mathrm{I}^i_{3g}$	$\sum_{g'=1}^{G} H_{gg'} \mathrm{I}^i_{3g'}$
4	$\mathbf{e}_4 \mathrm{I}^i_{4g}$	$\sum_{g'=1}^{G} H_{gg'} \mathrm{I}^i_{4g'}$

8.1. táblázat. Angular flux and boundary net currents in cell No. i

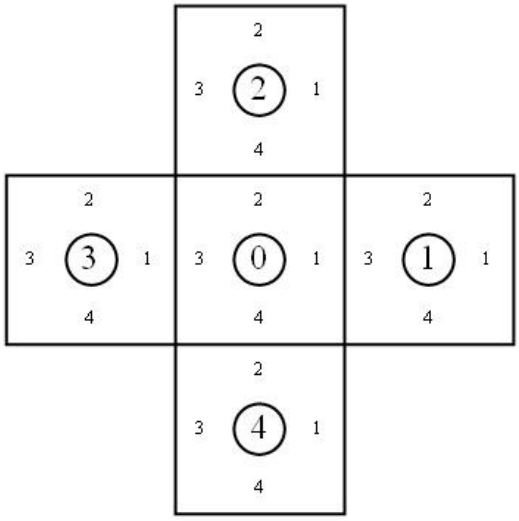

8.3. ábra. Cell and face numbering in the square lattice

current may vary along a face. In the following discussion, only the scalar flux will be used, thus the operators E, F and H are meant to give the scalar flux.

Now we show that the average flux in a cell satisfies a diffusion-like equation. First we need a systematic node numbering in the volume filled out by identical cells, see Figure 8.3. At the joint boundary of adjacent cells the fluxes determined in the two cells should be the same, but the net currents have different signs because the normal directions differ in the cells. The symmetric component (or irrep) in the central cell is

$$\mathrm{I}^0_{1g} = \frac{1}{4}\left(J^0_{1g} + J^0_{2g} + J^0_{3g} + J^0_{4g}\right) \tag{8.125}$$

and the continuity conditions are at the cell boundaries:

$$J^0_{1g} = -J^1_{3g}; \;\; J^0_{2g} = -J^2_{4g}; \;\; J^0_{3g} = -J^3_{1g}; \;\; J^0_{4g} = -J^4_{2g}; \;\; . \tag{8.126}$$

The net current at boundary k of cell m can be expressed by the irreps as

$$J^m_{kg} = \mathrm{I}^m_{1g} e_{1k} + \mathrm{I}^m_{2g} e_{2k} + \mathrm{I}^m_{3g} e_{3k} + \mathrm{I}^m_{4g} e_{4k}, \;\; k = 1, \ldots, 4. \tag{8.127}$$

Substituting (8.127) into the right hand side of (8.126), we get the following relationship between the irreps of the neighboring cells:

$$\mathrm{I}^0_{1g} = -\frac{1}{4}\sum_{k=1}^{4} \mathrm{I}^k_{1g} e_{1k} + \mathrm{I}^k_{2g} e_{2k} + \mathrm{I}^k_{3g} e_{3k} + \mathrm{I}^k_{4g} e_{4k}. \tag{8.128}$$

Now we write down the continuity of the boundary fluxes. We obtain the boundary fluxes from Table 8.1 on either side of (8.125). A further simplification is introduced, we assume that matrices H are the same for each cell, whereas matrices E may distinguished by a superscript:

$$E_g^0 \mathrm{I}_{1g}^0 = -\frac{1}{4} \sum_{k=1}^{4} E_g^k \mathrm{I}_1 e_{1k} + F_g^k \mathrm{I}_{2g} e_{2k} + H_g^k (\mathrm{I}_{3g}^k e_{3k} + \mathrm{I}_{4g}^k e_{4k}). \tag{8.129}$$

Multiply (8.125) by H_g^k and dropping the k superscript in H_g^k we get

$$(E_g^0 + H_g)\mathrm{I}_{1g}^0 = -\frac{1}{4} \sum_{k=1}^{4} (E_g^k - H_g)\mathrm{I}_{1g}^k + (H_g - F_g^k)\mathrm{I}_{2g} e_{2k}, \tag{8.130}$$

which is a difference equations for the irreducible normal components on the boundaries of the cells. In the difference scheme, only the neighboring cells are involved. Note that the symmetric irrep occurs with all the $k = 0, 1, \ldots, 4$ subscripts. Laletin simplified the above expression by introducing

$$\Phi_k = (E_g^k - H_g) I_{1g}^k \tag{8.131}$$

and

$$\Lambda_1 \Phi_0 = \frac{1}{a^2} \left(\sum_{k=1}^{4} \Phi_k - \Phi_0 \right), \tag{8.132}$$

and arrives at the following equation:

$$\Lambda_1 \Phi_0 - \kappa_0^2 \Phi_0 + \frac{1}{a^2} (H_g - F_g^k) \mathrm{I}_{2g}^k . e_{2k} = 0 \tag{8.133}$$

When we integrate the neutron balance over a cell, we get a relationship between the volume averaged flux and the symmetric current irrep:

$$\frac{1}{S} I_{1g}^k + \frac{1}{V} \bar{\Sigma} \bar{\Phi} = 0, \tag{8.134}$$

indicating that the symmetric current at the boundary is proportional to the average flux.

8.5. P_n method

In the transport equation, we encounter angular dependence in the scattering operator and the angular flux. Neutron scattering is invariant with respect to rotations around the line connecting the neutron and the nucleus. Therefore it is natural to employ a numerical method in which we expand every $\mathbf{\Omega}$ dependent function in terms of the eigenfunctions of the rotation transformation. First, let us see those functions.

8.5.1. Spherical harmonics

We study the transformation properties of the angular variable $\mathbf{\Omega}$ under rotations. Obviously there are three independent rotations around the x, y and z axes. We use the coordinates of $\mathbf{\Omega}$ as explained in Chapter 3. Rotations around the coordinate axes are given by the following operators:

$$\mathcal{L}_x = -i \left(y \partial_z - z \partial_y \right), \tag{8.135}$$

$$\mathcal{L}_y = -i\left(z\partial_x - x\partial_z\right), \tag{8.136}$$

$$\mathcal{L}_z = -i\left(x\partial_y - y\partial_x\right). \tag{8.137}$$

Instead of seeking eigenfunctions of the operators $\mathcal{L}_x, \mathcal{L}_y$, and $\mathcal{L}_z$ it suffices to find the eigenfunctions of two operators. Let us introduce

$$\mathcal{L}^2 = \mathcal{L}_x^2 + \mathcal{L}_y^2 + \mathcal{L}_z^2 \tag{8.138}$$

which commutes with $\mathcal{L}_x, \mathcal{L}_y, \mathcal{L}_z$:

$$\mathcal{L}^2\mathcal{L}_z - \mathcal{L}_z\mathcal{L}^2 = \left[\mathcal{L}^2\mathcal{L}_z\right] = 0 \tag{8.139}$$

and

$$\left[\mathcal{L}^2\mathcal{L}_y - \mathcal{L}_y\mathcal{L}^2\right] = \left[\mathcal{L}^2\mathcal{L}_x - \mathcal{L}_x\mathcal{L}^2\right] = 0. \tag{8.140}$$

The eigenfunctions $f_{\ell m}(\mathbf{\Omega})$ of the rotation operators can be labeled by two integers ℓ, m. The operator $\mathcal{L}_z$ leaves invariant $f_{\ell m}(\mathbf{\Omega})$:

$$\mathcal{L}_z f_{\ell m} = m f_{\ell m}, m = 0, 1, 2, \ldots \tag{8.141}$$

its eigenvalues are integers. The eigenvalues of $\mathcal{L}^2$ are

$$\mathcal{L}^2 f_{\ell m} = (\ell+1)\ell f_{\ell m}. \tag{8.142}$$

The $\mathbf{\Omega}$ vector is given as function of angles θ and φ, and the eigenfunctions are given as function of θ and φ:

$$Y_{\ell m}(\theta,\varphi) = \left[\frac{(\ell-m)!}{(\ell+m)!}\right]^{1/2} P_\ell^m\left(\frac{2\ell+1}{4\pi}\frac{(\ell-|m|)!}{(\ell+|m|)!}\cos\theta\right)e^{im\varphi}. \tag{8.143}$$

Here $P_\ell^m(x)$ is the associated Legendre polynomial. When ℓ, m are integers, and $0 \le m \le \ell$ the $P_\ell^m(x)$ function is non-singular on $[-1, 1]$. We obtain the associated Legendre polynomials from the Legendre polynomials by the formula

$$P_\ell^m(x) = (-1)^m(1-x^2)^{m/2}\frac{d^m}{dx^m}P_\ell(x). \tag{8.144}$$

The spherical harmonics obey the following addition property and allow us to express a polynomial of the dot products in terms of spherical harmonics:

$$P_\ell(\mathbf{\Omega}\cdot\mathbf{\Omega}') = \sum_{m=-\ell}^{+\ell}\frac{4\pi}{2\ell+1}Y_{\ell m}^*(\mathbf{\Omega})Y_{\ell m}(\mathbf{\Omega}'). \tag{8.145}$$

The Legendre polynomials $P_n(x)$ are the solutions of the Legendre differential equation

$$\frac{d}{dx}\left[(1-x^2)\frac{dP_n(x)}{dx}\right] + n(n+1)P_n(x) = 0, \quad |x| < 1. \tag{8.146}$$

They are obtained recursively from

$$P_0(x) = 1; \quad P_1(x) = x \tag{8.147}$$

using the rule

$$(n+1)P_{n+1}(x) = (2n+1)xP_n(x) - nP_{n-1}(x). \tag{8.148}$$

The spherical harmonics are orthogonal:

$$\int_{4\pi} Y_{\ell m}^*(\mathbf{\Omega})Y_{\ell' m'}(\mathbf{\Omega})d\mathbf{\Omega} = \delta_{\ell\ell'}\delta_{mm'}. \tag{8.149}$$

Using (8.149), we can expand any function of $\mathbf{\Omega}$ as a linear combination of spherical harmonics.

8.5.2. The P_n equations

Using the orthogonality and completeness of the spherical harmonics, we expand the angular flux as

$$\Phi(\mathbf{r}, E, \mathbf{\Omega}) = \sum_{\ell=0}^{\infty} \sum_{m=-\ell}^{+\ell} \left(\frac{2\ell+1}{4\pi} \right)^{1/2} \phi_{\ell m}(\mathbf{r}, E) Y_{\ell m}(\mathbf{\Omega}). \tag{8.150}$$

The integral in the scattering operator involves the scattering cross-section with $\mathbf{\Omega}\mathbf{\Omega}'$ in its argument. Using (8.145), we expand it in terms of spherical harmonics as

$$\begin{aligned} \Sigma_s(E' \to E, \mathbf{\Omega}'\mathbf{\Omega}) &= \sum_{\ell=0}^{L} \sum_{m=-\ell}^{+\ell} \Sigma_\ell(E' \to E) P_\ell(\mathbf{\Omega}'\mathbf{\Omega}) \\ &= \sum_{\ell=0}^{L} \sum_{m=-\ell}^{+\ell} \Sigma_\ell(E' \to E) Y^*_{\ell m}(\mathbf{\Omega}') Y_{\ell m}(\mathbf{\Omega}). \end{aligned} \tag{8.151}$$

Using the orthogonality (8.149), the scattering term in the transport equation (3.116) becomes

$$\begin{aligned} &\int_0^\infty \int_{4\pi} \Sigma_s(E' \to E, \mathbf{\Omega}'\mathbf{\Omega}) \Phi(\mathbf{r}, E', \mathbf{\Omega}') d\mathbf{\Omega}' dE \\ &= \sum_{\ell=0}^{L} \sum_{m=-\ell}^{+\ell} Y_{\ell m}(\mathbf{\Omega}) \int_0^\infty \Sigma_\ell(E' \to E) \phi_{\ell m}(\mathbf{r}, E') dE'. \end{aligned} \tag{8.152}$$

In the other terms in (3.116), (8.150) is used directly, except the leakage term which becomes

$$\int_{4\pi} Y_{\ell' m'}(\mathbf{\Omega}) Y_{\ell m}(\mathbf{\Omega}) \tag{8.153}$$

and complicates the P_n equations. The result is

$$\begin{aligned} &\left[\frac{(\ell+2+m)(\ell+1+n)}{(2\ell+3)^2} \right]^{1/2} \left[-\frac{1}{2} \frac{\partial \phi_{\ell+1,m+1}}{\partial x} - \frac{i}{2} \frac{\partial \phi_{\ell+1,m+1}}{\partial y} \right] \\ &+ \left[\frac{(\ell+1-m)(\ell+2-m)}{(2\ell+3)^2} \right]^{1/2} \left[\frac{1}{2} \frac{\partial \phi_{\ell+1,m-1}}{\partial x} - \frac{i}{2} \frac{\partial \phi_{\ell+1,m-1}}{\partial y} \right] \\ &+ \left[\frac{(\ell-m-1)(\ell-m)}{(2\ell+1)^2} \right]^{1/2} \left[\frac{1}{2} \frac{\partial \phi_{\ell-1,m+1}}{\partial x} - \frac{i}{2} \frac{\partial \phi_{\ell-1,m+1}}{\partial y} \right] \\ &+ \left[\frac{(\ell+m)(\ell+m-1)}{(2\ell-1)^2} \right]^{1/2} \left[-\frac{1}{2} \frac{\partial \phi_{\ell-1,m-1}}{\partial x} + \frac{i}{2} \frac{\partial \phi_{\ell-1,m-1}}{\partial y} \right] \\ &+ \left[\frac{(\ell+1+m)(\ell+1-m)}{(2\ell+3)^2} \right]^{1/2} \frac{\partial \phi_{\ell+1,m}}{\partial z} \\ &+ \left[\frac{(\ell+m)(\ell-m)}{(2\ell-1)^2} \right]^{1/2} \frac{\partial \phi_{\ell-1,m}}{\partial z} + \Sigma_t \phi_{ellm} \\ &= \int_0^\infty \Sigma_\ell(E' \to E) \phi_{\ell m}(\mathbf{r}, E') dE' + Q_{\ell m}. \end{aligned} \tag{8.154}$$

The derivative of the component ℓ, m contains derivatives of ℓ_1 and $\ell+1$ in the first subscript, and $m+1$ and $m-1$ in the second subscript. Moreover, partial derivatives of all the space coordinates are involved. This is why there does not exist a general P_n code.

Each equation for a $\phi_{\ell m}$ contains a contribution from its own $\phi_{\ell m}$ exclusively through the scattering operator whereas the first four terms in equation (8.154), which couples the different components, belong to the leakage operator. Therefore when the flux is constant in space, the $\phi_{\ell m}$ components develop independently in energy, and in time dependent problems, in time. There are two processes changing the direction of the neutron speed: scattering and fission. Fission is usually assumed to be isotropic so it can be disregarded in that respect. The ℓ-th Legendre moment of the scattering cross-section in (8.154) occurs only in the equation for $\phi_{\ell m}$ with the same ℓ.

Equation (8.154) is actually an infinite set of equations. The set is usually terminated (closure) by assuming that

$$\frac{\partial \phi_{L+1,m\pm1}}{\partial x} = \frac{\partial \phi_{L+1,m\pm1}}{\partial y} = \frac{\partial \phi_{L+1,\pm1}}{\partial z} = 0 \tag{8.155}$$

for some L. The finite set of equations obtained in this way is called the P_L approximation. The P_1 approximation is called diffusion theory and we have discussed it in Chapter 6.

As to the internal boundary conditions, we have seen that at internal boundaries the angular flux in the direction of the interface may be discontinuous. Thus the continuity of the components of all $\phi_{\ell m}$ may not be prescribed.

The scalar flux and the normal component of the current should always be continuous. N. I. Laletin proposed[57][p. 439] to derive the current not as the gradient of the scalar flux but from the second angular moments of the angular flux:

$$J_i(E,\mathbf{r}) = -\frac{1}{3\Sigma_{tr}} \sum_{j=1}^{3} \frac{\partial}{\partial x_j} L_{ij}(E,\mathbf{r}),\ i = 1,2,3, \tag{8.156}$$

where

$$L_{ij}(E,\mathbf{r}) = 3 \int_{4\pi} \Omega_i \Omega_j \Phi(\mathbf{r},E,\mathbf{\Omega}) d\mathbf{\Omega} \tag{8.157}$$

is the level tensor, the diagonal terms are

$$L_{ii}(\mathbf{r},E) = \Phi(\mathbf{r},E) + 2\Phi_{2i}(\mathbf{r},E) \tag{8.158}$$

and

$$\Phi_{2i}(\mathbf{r},E) = \int_{4\pi} P_2(\Omega_i) \Phi(\mathbf{r},E,\mathbf{\Omega}) d\mathbf{\Omega} \tag{8.159}$$

is the level, the second angular moment of the angular flux.

We can not discuss here the problem of boundary condition in more detail. We only mention here that exploiting the analytical solution derived by Case [147] we are able to get an analytical solution. We expand the angular dependent parts of the solution in terms of spherical harmonics, more precisely, because of the plane geometry, into Legendre polynomials of μ. Case's method derives the analytical solution to the transport equation in the form of sums of a space dependent function $e^{x/\kappa}$ multiplied by an angle dependent function $M_\kappa(\mu)$. Below we explicitly express the solution as

$$\Phi(x,\mu) = \sum_{n=0}^{N} \frac{2n+1}{4\pi} P_n(\mu) \psi_n(x). \tag{8.160}$$

We get equations for $\psi_n(x)$. Then after substituting (8.160) into

$$\mu \frac{\partial \Phi(x,\mu)}{\partial x} + \Phi(x,\mu) = \frac{c}{2} \int_{-1}^{+1} \Phi(x,\mu') d\mu' + Q(x,\mu) \tag{8.161}$$

we multiply by $P_n(\mu)$ and integrate over μ, using the orthogonality

$$\int_{-1}^{+1} P_n(\mu)P_m(\mu)d\mu = \delta_{nm}\frac{2}{2n+1} \tag{8.162}$$

and recursion relation

$$\xi P_n(\xi) = \frac{n}{2n+1}P_{n-1}(\xi) + \frac{n+1}{2n+1}P_{n+1}(\xi). \tag{8.163}$$

In this way we obtain the following recursion rule for the space dependent part of the solution:

$$(n+1)\psi'_{n+1}(x) + n\psi_{n-1}(x) + (2n+1)(1-c\delta_{n0})\psi_n(x) = 0, \tag{8.164}$$

for $n = 0, 1, \ldots, N$; primes denote differentiation with respect to x. We assume

$$\psi'_{N+1} = 0$$

to close the set of equations (8.164). Equations (8.164) are linear in ψ_i. Thus a nontrivial solution exists only when the determinant is zero. Using

$$\psi_n(x) = g_n e^{x/\kappa} \tag{8.165}$$

form, we get the following homogeneous equation set for g_n:

$$\kappa[(2n+1) - c\delta_{0n}]g_n + [(n+1)g_{n+1} + np_{n-1}] = 0 \tag{8.166}$$

The determinant of that equation set is an N-th order polynomial in κ. The zeros of the determinant depend on c.

Now we are able to investigate the limit of the solution at infinity. To this end, consider the upper half space. The zeros κ of the determinant occur in positive-negative pairs. When the flux vanishes at $x = \infty$, those coefficients in the $\psi_n(x)$ functions which include $\exp \kappa x$ must vanish.

When the plane is finite, let us consider its free surface at $x = 0$. The exact boundary condition would be

$$\Phi(0, \mu) = 0 \tag{8.167}$$

for $\mu > 0$. In the P_n approximation we have only a solution of finitely many degrees of freedom, when N is odd, we can satisfy $(N+1)/2$ conditions. As Davison's noted [58][p. 129] the boundary condition can be reduced to $(N+1)/2$ conditions in one of the following three ways:

- We choose $(N+1)/2$ positive directions and satisfy the boundary condition at these points;
- We choose $(N+1)/2$ orthogonal functions defined on $[0, 1]$ and choose $\Phi(0, \mu)$ to be orthogonal to them;
- We replace the vacuum in $x < 0$ by a completely black material, and the boundary condition is the continuity of the angular moments (apart from the angle parallel to the boundary).

Mark showed that the latter condition is equivalent to the first one provided we have chosen the directions μ_j as the roots of

$$P_{N+1}(\mu_j) = 0. \tag{8.168}$$

These are called Mark boundary condition.

The second method can be realized by noting that the odd Legendre functions form a complete set. In the roles of the boundary condition, the total number of incoming neutrons is the most important as it influences the neutron balance in the volume under consideration. Condition (8.168) amounts to

$$\int_0^1 \Phi(0,\mu)\mu d\mu = 0. \tag{8.169}$$

Therefore Marshak proposed the boundary conditions

$$\int_0^1 \Phi(0,\mu)P_{2j-1}(\mu)d\mu = 0, \quad j = 1,2,\ldots,(N+1)/2, \tag{8.170}$$

that assures (8.168).

The fact that the angular flux at a material interface may be discontinuous in the direction parallel to the interface suggests two decompositions into P_n components, one for each range separated by the direction of the interface. That approximation is called DP_n method or double P_n method.

Let us expand the angular flux as

$$\Phi(x,\mu) = \sum_{\ell=0}^{\infty} \frac{2\ell+1}{4\pi}\left[\varphi_\ell^+(x)P_\ell^+(\mu) + \varphi_\ell^-(x)P_\ell^-(\mu)\right], \tag{8.171}$$

where

$$P_\ell^+(\mu) = \begin{cases} P_\ell(2\mu-1), & 0 \le \mu \le 1 \\ 0, & -1 \le \mu < 0 \end{cases} \tag{8.172}$$

$$P_\ell^-(\mu) = \begin{cases} 0, & 0 \le \mu \le 1 \\ P_\ell(2\mu+1), & -1 \le \mu < 0 \end{cases} \tag{8.173}$$

The space-dependent components are determined as

$$\varphi_\ell^+(x) = \int_0^1 \Phi(x,\mu)P_\ell^+(\mu)d\mu \tag{8.174}$$

and

$$\varphi_\ell^-(x) = \int_{-1}^0 \Phi(x,\mu)P_\ell^-(\mu)d\mu. \tag{8.175}$$

After substituting the above expansion into the transport equation and making use of the orthogonality, we obtain the DP_n equations:

$$2\ell\frac{d\varphi_{\ell-1}^\pm}{dx} \pm (2\ell+1)\frac{d\varphi_{\ell+1}^\pm}{dx} + 2(2\ell+1)\Sigma_t\varphi_\ell^\pm(x) = \Sigma_s(\varphi_0^+ + \varphi_0^-) + 2Q_0\delta_{\ell 0}. \tag{8.176}$$

The B_n method separates the space dependent part of the angular flux with the help of the eigenfunctions of the Laplace operator in the given geometry. Far from boundaries the space-dependence of the neutron flux is separable:

$$\Phi(\mathbf{r},E,\mathbf{\Omega}) = F_1(\mathbf{r})F_2(E,\mathbf{\Omega}). \tag{8.177}$$

Assuming the space-dependence of the flux and the source term in the form of

$$F_1(\mathbf{r}) = e^{i\mathbf{B}\mathbf{r}}, \tag{8.178}$$

we obtain an equation for the $F_2(E,\mathbf{\Omega})$ function:

$$(\mathbf{\Omega}B+\Sigma_t)F_2(E,\mathbf{\Omega})=\int_0^\infty\int_{4\pi}\Sigma_s(E'\to E,\mathbf{\Omega}'\mathbf{\Omega})F_2(E',\mathbf{\Omega}')dE'd\mathbf{\Omega}'+Q(E,\mathbf{\Omega}). \quad (8.179)$$

(8.179) is solved for $F_2(E,\mathbf{\Omega})$ so that the angular dependence is expanded into low order only in the scattering kernel, whereas in $F_2(E,\mathbf{\Omega})$ a better approximation is used. The neutron spectrum obtained by the B_1 method is superior to the P_1 solution.

8.6. S_n method

There is a general S_n method in contrast to the P_n method, where the system of equations for different n is different and there is no general P_n algorithm. We discuss the approximate solution methods starting out from the multigroup, static form of the transport equation:

$$\begin{aligned}&\mathbf{\Omega}\boldsymbol{\nabla}\Phi_g(\mathbf{r},\mathbf{\Omega})+\Sigma_{tg}\Phi_g(\mathbf{r},\mathbf{\Omega})=\\&\sum_{g'=1}^{G}\Sigma_s(\mathbf{r};g',\mathbf{\Omega}'\to g,\mathbf{\Omega})\Phi_{g'}(\mathbf{r},\mathbf{\Omega}')\\&+\frac{1}{k}\frac{f_g}{4\pi}\sum_{g'=1}^{G}\Sigma_{fg'}(\mathbf{r})\int_{4\pi}\Phi_{g'}(\mathbf{r},\mathbf{\Omega}')d\mathbf{\Omega}',\end{aligned} \quad (8.180)$$

where we have assumed that the angular distribution of the neutrons emerging from fission is isotropic. The fission spectrum f_g might depend on position because the densities of the fissionable isotopes may vary with the position and have different fission spectra. We neglect that, although in the burnup calculation, see Section 9.4 in Chapter 9, it will be taken into account. We have not yet specified the scattering model yet. In Section 8.5 we discussed the P_n approximation, there the scattering kernel has been expanded in a finite set of Legendre polynomials. Using that expansion, the scattering term is written as

$$\begin{aligned}&\sum_{g'=1}^{G}\Sigma_s(\mathbf{r};g',\mathbf{\Omega}'\to g,\mathbf{\Omega})\Phi_{g'}(\mathbf{r},\mathbf{\Omega}')=\\&\sum_{g'=1}^{G}\sum_{l=0}^{L}\sum_{m=-l}^{+l}Y_{lm}(\mathbf{\Omega})\Sigma_s(\mathbf{r};l,g'\to g)\int_{4\pi}Y_{lm}^*(\mathbf{\Omega}')\Phi_{g'}(\mathbf{\Omega}')d\mathbf{\Omega}'.\end{aligned} \quad (8.181)$$

Details can be found in Section 8.5. Now we will consider the angular variable. In Section 8.5, we have seen that all $\mathbf{\Omega}$ dependent term can be expanded in a suitable basis: the spherical functions $Y_{\ell m}$. In the present Section we consider an alternative method of angular discretization. The idea is to replace the continuous $\mathbf{\Omega}$ variable with a finite number of discrete directions $\mathbf{\Omega}_m, m=1,\ldots,M$. Before going into details let us study the structure of equation (8.180). When we seek the solution in the energy group g, the fluxes in the other groups may be considered as known functions and as a given source. Thus the solution procedure breaks up into a sequence of steps. In a given step we find the flux in a particular group, and in the next group that solution gives a contribution to the source. The nature of the fission source does not differ from the scattering source; it is just an energy integrated component in the source. Note however, that in the source we find angle-integrated expressions of the angular flux, and we have to consider this when designing the angle discretization. In the

actual group g, we have to solve the equation given below:

$$\mathbf{\Omega}\boldsymbol{\nabla}\Phi_g(\mathbf{r},\mathbf{\Omega})+\Sigma_{tg}\Phi_g(\mathbf{r},\mathbf{\Omega})=\sum_{l=0}^{L}\sum_{m=-l}^{+l}Y_{lm}(\mathbf{\Omega})\Sigma_s(\mathbf{r};l,g'\to g)\int_{4\pi}Y^*_{lm}(\mathbf{\Omega}')\Phi_{g'}(\mathbf{\Omega}')d\mathbf{\Omega}'+Q(\mathbf{r},\mathbf{\Omega}). \tag{8.182}$$

This is the basic form of the transport problem to be solved by the discrete ordinate method. The first step is to choose a set of discrete directions $\mathbf{\Omega}_m, m=1,2,\ldots,M$ called rays. Since in equation (8.182) we need to integrate, we allocate a weight w_m to $\mathbf{\Omega}_m$ in order to calculate integrals over angle. Dropping the group index, in each group we have to evaluate equation (8.182) at each of the $\mathbf{\Omega}_m$ discrete directions:

$$\mathbf{\Omega}_m\boldsymbol{\nabla}\Phi(\mathbf{r},\mathbf{\Omega}_m)+\Sigma_t\Phi(\mathbf{r},\mathbf{\Omega}_m)=\sum_{\ell=0}^{L}\sum_{n=-\ell}^{+\ell}Y_{\ell n}(\mathbf{\Omega}_m)\Sigma_{sl}\int_{4\pi}Y^*_{\ell n}(\mathbf{\Omega}')\Phi(\mathbf{r},\mathbf{\Omega}')d\mathbf{\Omega}' \tag{8.183}$$
$$+Q(\mathbf{r},\mathbf{\Omega}_m),\quad m=1,2,\ldots,M.$$

The weights are used in the calculation of an integral in the manner given below. To find the angular moment $\varphi_{\ell n}$ of the angular flux $\Phi(\mathbf{r},\mathbf{\Omega})$ we have to calculate the integral

$$\varphi_{\ell n}(\mathbf{r})\equiv\int Y^*_{\ell n}(\mathbf{\Omega})\Phi(\mathbf{r},\mathbf{\Omega})d\mathbf{\Omega}\cong\sum_{m=1}^{M}w_mY^*_{\ell m}(\mathbf{\Omega}_m)\Phi(\mathbf{r},\mathbf{\Omega}_m), \tag{8.184}$$

which has been approximated above by a weighted sum.

We also discretize the space variable, the discretization depending on the geometry. On the discretized mesh (8.184) is solved by a suitable numerical method (finite difference, finite element, or nodal). The structure of the discretized equations is

$$\mathbf{R}\underline{F}=\mathbf{S}\underline{F}+\underline{Q} \tag{8.185}$$

where $\mathbf{R}$ is the discretized operator (i.e. matrix) on the left-hand side of (8.182), matrix $\mathbf{S}$ is the scattering term and $\underline{Q}$ is the source term. $\underline{F}$ is the discretized angular flux at the discretized angular and spatial points, and the length of vector $\underline{F}$ equals the number of angular directions multiplied by the number of space points.

Equation (8.185) is solved by iterative methods, see Section 8.1.

8.6.1. Directions and weights

Assume no advance knowledge of the solution is available. Then the selection of $\mathbf{\Omega}_m$ should be based on general considerations. We characterize a ray $\mathbf{\Omega}_m$ by the direction cosines (μ_x,μ_y,μ_z), with respect to the coordinate axes x,y,z, respectively. It is reasonable to choose the direction cosines from the same set $\alpha_1,\ldots,\alpha_m$. We show that the specification of one direction cosine α_1 uniquely determines all direction cosines provided trivial invariance principles are satisfied.

If the geometry is general, the three axes x,y,z are equivalent because we may label them arbitrarily. Similarly, along a given axis the positive and negative directions are equivalent. Therefore the angular-direction set should be invariant under any rotation by integer multiples of 90^o. Therefore each octant of the unit sphere hosting the directions should be equivalent. Rotations and reflections leave the unit sphere invariant and map the coordinates

of the direction cosines into each other. Therefore the admissible μ_x, μ_y, μ_z should be taken from the same set, i.e $\mu_i = \alpha_1, \ldots, \alpha_M, i = x, y, z$. Furthermore, because the unit sphere is symmetric with respect to reflection, the ordered set $\alpha_1, \ldots, \alpha_M$ where $\alpha_1 < \alpha_2 < \cdots < \alpha_M$ should be symmetric with respect to $\alpha = 0$. The independent elements of the set are $\alpha_1, \ldots, \alpha_{M/2}$. Invariance requires the discrete $\mathbf{\Omega}_m$ vectors to lie on loci of constant μ_x, μ_y or μ_z (i.e. on latitudes).

The direction cosines are unit vectors so they satisfy the

$$\mu_x^2 + \mu_y^2 + \mu_z^2 = 1$$

relation. Each one of the coordinates must be equal to one element of the ordered set $\alpha_1, \ldots, \alpha_M$. Let those elements be

$$(\alpha_{xi}, \alpha_{yj}, \alpha_{zk}).$$

Because they lie on the unit sphere, the indices must satisfy

$$xi + yj + zk = M/2 + 2. \tag{8.186}$$

Consider the direction $\mathbf{\Omega}_1 = (\alpha_{xi}, \alpha_{yj}, \alpha_{zk})$ and move to the next point $\mathbf{\Omega}_2$ along the increasing μ_y latitude. In this way we arrive at $\mu_{xi}, \mu_{y,j+1}$ and the third coordinate of the neighboring point must be $\mu_{z,k-1}$ (because if one coordinate increases the other must decrease when passing to a neighboring point while the third latitude is held constant). Hence the neighboring point is $\mathbf{\Omega}_2 = (\mu_{xi}, \mu_{y,j+1}, \mu_{z,k-1})$. Using that $\mathbf{\Omega}_1$ and $\mathbf{\Omega}_2$ are unit vectors, we find

$$\mu_{xi}^2 + \mu_{yj}^2 + \mu_{zk}^2 = 1 = \mu_{xi}^2 + \mu_{y,j+1}^2 + \mu_{z,k-1}^2$$

or

$$\mu_{yj}^2 - \mu_{y,j+1}^2 = \mu_{z,k-1}^2 - \mu_{z,k}^2 \tag{8.187}$$

where j, k are arbitrary. The directions cosines are taken from the same set. Therefore the α_i numbers are such that

$$\alpha_i^2 = \alpha_{i-1}^2 + c, \quad \text{for all } i, \tag{8.188}$$

and

$$\alpha_i^2 = \alpha_1^2 + c(i-1). \tag{8.189}$$

If we have M direction cosines along each axis, there are $M/2$ points for $\alpha_i > 0$ and there is a point having coordinates $(\alpha_1, \alpha_1, \alpha_{M/2})$ therefore

$$c = \frac{2(1 - 3\alpha_1^2)}{M - 2}. \tag{8.190}$$

Henceforth α_1 determines all the $\alpha_i, i = 2, \ldots, M/2$. When $\alpha_1 > 1/\sqrt{3}$, the points tend to cluster close to $\alpha = 0$, whereas when α is small, the points cluster around the poles.

As to the space variable, when the geometry is known, the directions can be chosen accordingly. This is the case in plane or spherical geometry. When one angle coordinate determines the position of a point on the unit sphere, the integration in (8.184) simplifies. In plane geometry the integration over φ reduces to a multiplication by 2π because of rotational invariance. Hence

$$\int_{4\pi} P_l(\mathbf{\Omega})\Phi(\mathbf{\Omega})d\mathbf{\Omega} = 2\pi \int_{-1}^{+1} P_l(\mu)\Phi(\mu)d\mu \cong \sum_{m=1}^{M} w_m P_l(\mu_m)\Phi(\mu_m). \tag{8.191}$$

The weights should be chosen so that they are projection invariant. This is assured by the appropriate choice of the directions as discussed above. In addition also the approximate integrals should have small error. The M point Gaussian-quadrature set integrates exactly a polynomial of degree $2M-1$ and is projection invariant. Also it gives positive scalar flux when the angular flux is everywhere positive. The net current must be zero when the angular flux is constant. Therefore the weights should obey

$$\sum_{m=1}^{M} w_m \mathbf{\Omega}_m = 0, \tag{8.192}$$

or by components

$$\sum_{m=1}^{M} w_m \mu_{xm} = \sum_{m=1}^{M} w_m \mu_{ym} = \sum_{m=1}^{M} w_m \mu_{zm} = 0 \tag{8.193}$$

for odd M. Based on the P_1 approximation, from the discretized in angle angular flux the following relations are obtained:

$$\sum_{m=1}^{M} w_m \mu_{xm}^2 = \sum_{m=1}^{M} w_m \mu_{ym}^2 = \sum_{m=1}^{M} w_m \mu_{zm}^2 = \frac{1}{3}. \tag{8.194}$$

In general, the even-moment conditions fix the relation

$$\sum_{m=1}^{M} w_m \mu_{xm}^n = \frac{1}{n+1}. \tag{8.195}$$

The arrangement of directions in one octant and the weights must be invariant under 120^o rotations of the octant. A 120^o rotation brings one axis into another. This indicates that when the order of approximation is increased from M to $M+1$, $M/2$ new directions must be added in each octant. If the number of directions per octant is M, the number of directions in the eight octants is

$$M(M+2), \text{ in 3D}; \quad \frac{1}{2}M(M+2), \text{ in 2D}; \quad M \text{ in 1D}. \tag{8.196}$$

8.6.2. Boundary conditions

The zero-entering angular flux or free surface boundary condition is

$$\Phi_g(\mathbf{r}_b, \mathbf{\Omega}_m) = 0, \;\; \mathbf{\Omega}_m \mathbf{n}(\mathbf{r}_b) < 0. \tag{8.197}$$

In plane geometry using Gaussian quadrature this boundary condition is equivalent to the Mark boundary condition; see 8.5. Hence, the P_n-S_n equivalence in slab geometry holds only when the Mark boundary condition is used in the P_n method. Note that (8.197) can be achieved by surrounding V by a completely absorbing medium.

Reflective boundary condition is realized by specular reflection. In rectangular coordinate the boundary at $\mathbf{r}_b = (x_b, y_b)$:

$$\Phi(x_b, y, \mathbf{\Omega}_{mx}, \mathbf{\Omega}_{my}) = \Phi(x_b, y, -\mathbf{\Omega}_{mx}, \mathbf{\Omega}_{my}) \tag{8.198}$$

and

$$\Phi(x, y_b, \mathbf{\Omega}_{mx}, \mathbf{\Omega}_{my}) = \Phi(x, y_b, \mathbf{\Omega}_{mx}, -\mathbf{\Omega}_{my}). \tag{8.199}$$

In the case of white reflection first the exiting current is calculated:

$$J_+(\mathbf{r}_b) = \sum_{m=1}^{M} w_m \mathbf{\Omega}_m \mathbf{n}(\mathbf{r}_b)\Phi(\mathbf{r}_b, \mathbf{\Omega}_m);\ \text{for } \mathbf{\Omega}_m \mathbf{n}(\mathbf{r}_b) < 0 \tag{8.200}$$

and the re-entrant current must be the same

$$J_-(\mathbf{r}_b) = \sum_{m=1}^{M} w_m \mathbf{\Omega}_m \mathbf{n}(\mathbf{r}_b)\Phi(\mathbf{r}_b, \mathbf{\Omega}_m);\ \text{for } \mathbf{\Omega}_m \mathbf{n}(\mathbf{r}_b) > 0 = J_+(\mathbf{r}_b). \tag{8.201}$$

In the P_1 approximation on the boundary, the angular flux is linear in $\mathbf{\Omega}$ and independent of subscript m thus it is readily determined from (8.201).

The albedo boundary condition can be simplified. The general albedo matrix is too complicated for practical calculations; therefore the following simplifications are introduced:

$$\Phi(\mathbf{r}_b, \mathbf{\Omega}) = \frac{\Gamma \sum_{m=1}^{M} w_m \mathbf{\Omega}_m \mathbf{n}(\mathbf{r}_b)\Phi(\mathbf{r}_b, \mathbf{\Omega}') + \frac{j_{ext}}{4\pi}}{\sum_{m=1}^{M} w_m \mathbf{\Omega}_m \mathbf{n}(\mathbf{r}_b)} \tag{8.202}$$

where $\mathbf{\Omega}' = -\mathbf{\Omega}\mathbf{n}(\mathbf{r}_b)$.

Below we demonstrate the equivalence of the S_n equations with Gaussian quadrature in (8.191) to the P_{n-1} equations with Mark boundary conditions. The proof follows the line given in Ref. [59]. We restrict the discussion to plane geometry. Then the angular variable reduces to μ, the cosine of the angle between $\mathbf{\Omega}$ and the x axis. Also, instead of the spherical harmonics we may use the Legendre polynomials $P_l(\mu)$. The angular flux $\Phi(x, \mu)$, the discrete ordinate moments of the angular flux are given by

$$\tilde{\varphi}(x) = 2\pi \sum_{m=1}^{M} w_m P_l(\mu_m)\Phi(x, \mu_m), \tag{8.203}$$

the spherical harmonics moments for the angular flux are

$$\varphi_l(x) = 2\pi \int_{-1}^{+1} P_l(\mu)\Phi(x, \mu)d\mu. \tag{8.204}$$

The angular discrete ordinates moments for the source $Q(x, \mu)$ are:

$$\tilde{q}_l(x) = 2\pi \sum_{m=1}^{N} w_m P_l(\mu_m)Q(x, \mu_m). \tag{8.205}$$

and the spherical harmonics moments are

$$q_l(x) = 2\pi \int_{-1}^{+1} P_l(\mu)Q(x, \mu)d\mu. \tag{8.206}$$

The transport equation in the discrete ordinate formalism is

$$\mu_m \frac{d\varphi_m}{dx} + \Sigma_t \varphi_m(x) = \sum_{l'=1}^{L} \frac{2l'+1}{4\pi} \Sigma_{sl'} \widetilde{\varphi}_{l'}(x) P_{l'}(\mu_m) + q_m. \tag{8.207}$$

Multiply (8.207) by $2\pi P_l(\mu_m)$ and sum over m to find

$$\begin{aligned} 2\pi \sum_{m=1}^{N} w_m P_l(\mu_m)\mu_m \frac{d\varphi_m}{dx} + 2\pi\Sigma_t \sum_{m=1}^{N} w_m P_l(\mu_m)\varphi(x,\mu_m) \\ = 2\pi \sum_{l'=0}^{L} \frac{2l'+1}{4\pi}\Sigma_{sl'}\varphi_{l'}(x) \sum_{m=1}^{N} w_m P_l(\mu_m)P_{l'}(\mu_m) \\ + 2\pi \sum_{m=1}^{N} w_m P_l(\mu_m) q(x,\mu_m). \end{aligned} \tag{8.208}$$

Using the definition for $\varphi_l(x)$ and the identity

$$\mu P_l(\mu = \frac{l+1}{2l+1}P_{l+1}(\mu) + \frac{l}{2L+1}P_{l-1}(\mu), \tag{8.209}$$

we find the following form for (8.208):

$$\begin{aligned} \frac{l+1}{2l+1}\frac{d\widetilde{\varphi}_{l+1}}{dx} + \frac{l}{2l+1}\frac{d\widetilde{\varphi}_{l-1}}{dx} + \Sigma_t\widetilde{\varphi}_l(x) \\ = 2\pi \sum_{l'=0}^{L} \frac{2l'+1}{4\pi}\Sigma_{sl'}\widetilde{\varphi}_{l'}(x) \sum_{m=1}^{M} w_m P_l(\mu_m) + \widetilde{q}_l. \end{aligned} \tag{8.210}$$

Equation (8.210) holds for $l = 0, 1, \ldots, N-1$. The N point Gaussian quadrature is exact for $2N-1$ order polynomials. Thus if the order of anisotropy is not greater than L

$$\sum_{m=1}^{N} w_m P_l(\mu_m)P_l(\mu_m) = \int_{-1}^{+1} P_l(\mu)P_{l'}(\mu)d\mu = \frac{2}{2l+1}\delta_{ll'}. \tag{8.211}$$

Now remembering that in the P_n method

$$\frac{d\widetilde{\varphi}_N}{dx} = 0.$$

To achieve this condition, we have to choose the discrete directions μ_m in the S_n method so that the P_N components obey

$$\widetilde{\varphi}(x) = 2\pi \sum_{m=1}^{N} w_m P_N(\mu_m)\varphi(x,\mu_m) = 0. \tag{8.212}$$

In other words, the μ_m directions be the roots of $P_N(\mu)$, which is just the definition of the Gaussian quadrature. When we define $\varphi(x,\mu), \mu \neq \mu_m$ as

$$\varphi(x,\mu) = \sum_{l=0}^{N} \frac{2l+1}{4\pi}\widetilde{\varphi}_l(x)P_l(\mu), \tag{8.213}$$

we obtain the P_n solution using an S_n calculation.

8.6.3. FD and nodal schemes

In the investigation of the space variable, we simplify the angle-dependent portion of the problem by assuming isotropic scattering but space-dependent cross-sections.

$$\mathbf{\Omega}_m \boldsymbol{\nabla} \Phi(\mathbf{r}, \mathbf{\Omega}_m) + \Sigma_t(\mathbf{r})\Phi(\mathbf{r}, \mathbf{\Omega}_m) = \frac{\Sigma_s(\mathbf{r})}{4\pi} \sum_{n=1}^{M} w_n \Phi(\mathbf{r}, \mathbf{\Omega}_n) + Q(\mathbf{r}, \mathbf{\Omega}_m), \tag{8.214}$$

for the discrete directions $\mathbf{\Omega}_m, m = 1, \ldots, M$. First we consider a simple, one- dimensional case. Then (8.183) in plane geometry can be written as

$$\mu \frac{\partial \Phi(x,\mu)}{\partial x} + \Sigma_t \Phi(x,\mu) = \frac{1}{2}\Sigma_s(x) \int_{-1}^{+1} \Phi(x,\mu') + Q(x,\mu). \tag{8.215}$$

The discrete ordinates equations are for $m = 1, 2, \ldots, M$

$$\mu_m \frac{d}{dx}\Phi(x,\mu_m) + \Sigma_t(x)\Phi(x,\mu_m) = \frac{1}{2}\sum_{n=1}^{M} w_n \Phi(x,\mu_n) + Q(x,\mu_m). \tag{8.216}$$

We solve (8.216) by the finite-difference method and introduce a spatial mesh $x_1, x_2, \ldots, x_I$ which are the midpoints of I intervals. The cross-sections are assumed constant in a given interval, the boundary between intervals i and $i+1$ is denoted by $x_{i+1/2}$. A discretized equation is obtained by integrating (8.216) over $x_{i-1/2} \le x \le x_{i+1/2}$. We assume that

$$\int_{x_{i-1/2}}^{x_{i+1/2}} \Phi(x)\Sigma(x)dx \simeq \Phi(x_i)\Sigma(x_i)(x_{i+1/2} - x_{i-1/2}). \tag{8.217}$$

Now the differential equation (8.216) turns into the following difference equation:

$$\begin{aligned} \mu_m \left[\frac{\Phi(x_{i+1/2},\mu_m) - \Phi(x_{i-1/2},\mu_m)}{x_{i+1/2} - x_{i-1/2}} + \right] &+ \Sigma_t(x_i)\Phi(x_i,\mu_m) \\ &+ \frac{1}{2}\Sigma_s(x_i)\sum_{n=1}^{M} w_n \Phi(x_i,\mu_n) + Q(x_i,\mu_m). \end{aligned} \tag{8.218}$$

The number of unknowns equals the number of $\Phi(x_i,\mu_m)$ + the number of $\Phi(x_{i\pm1/2},\mu_m)$ quantities which equals $(2I+1)M$. Equations (8.218) are linear, the number of equations being $I * M$. To make the problem tractable, we have to reduce the number of unknowns to the number of equations. If the flux is linear over the interval $x_{i-1/2} \le x \le x_{i+1/2}$ we have

$$\Phi(x_i, m) = \frac{\Phi(x_{i+1/2}, m) + \Phi(x_{i-1/2}, m)}{2}, \tag{8.219}$$

and equation (8.218) reduces to

$$\mu_m F_i + \Sigma_t(x_i)F_i = q_i, \tag{8.220}$$

where

$$F_i = \frac{\Phi(x_{i+1/2}, m) - \Phi(x_{i-1/2}, m)}{\Delta x_i} \tag{8.221}$$

and

$$q_i = \frac{1}{2}\Sigma_s(x_i)\sum_{n=1}^{M} w_n \Phi(x_i, n) + Q(x_i, m). \tag{8.222}$$

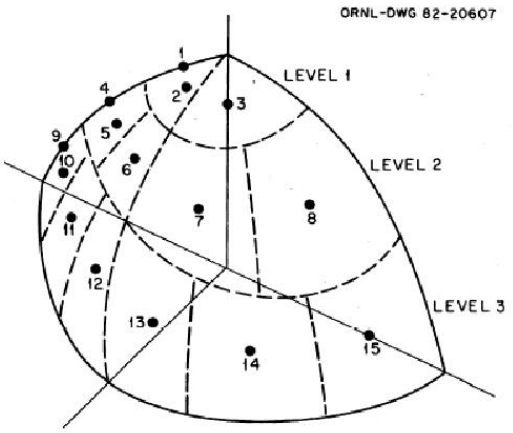

8.4. ábra. Discrete directions in the S_N method

(8.219) is the one-dimensional version of the so-called diamond difference scheme.

Now we have $(I+1)M$ unknowns, but we have to eliminate further M unknowns to make the problem solvable. This is done by fixing the boundary conditions at the external boundary of the leftmost and rightmost intervals. Then the problem is uniquely determined when the $M/2$ entering angular fluxes are fixed at the boundary. Other boundary conditions can also be implemented, such as the vacuum boundary condition, specifying angular fluxes in the entering directions, the reflecting, or albedo boundary conditions.

The solution methods for the resulting set of equations are discussed in Section 8.1 of the present Chapter.

Now we pass on to a 2D formulation of the S_n method. For simplicity's sake isotropic scattering is assumed, with the discretized geometry shown in Fig. 8.4. We consider a node labeled by indices i, j. Its volume is V_{ij} characterized by $x_{i-1/2} \le x \le x_{i+1/2}$ and $y_{j-1/2} \le y \le y_{j+1/2}$. The scattering cross-section is Σ_s^{ij}, the external source is Q^{ij}.

We collect the contributions to the neutron-balance equation. Neutrons leave V_{ij} through the boundaries $A_{i+1/2}, A_{i-1/2}$ and boundaries $B_{j+1/2}, B_{j-1/2}$. The loss across the four boundaries is

$$\mu_m w_m \left(A_{i+1/2} \varphi_m^{i+1/2,j} - A_{i-1/2,j} \varphi_m^{i-1/2,j} \right) + \eta_m w_m \left(B_{i,j+1/2} \varphi_m^{i,j+1/2} - B_{i,j-1/2} \varphi_m^{ij,-1/2} \right), \tag{8.223}$$

where the discrete direction is $\mathbf{\Omega}_m = (\mu_m, \eta_m)$, the weight w_m is $w_m = \Delta\mathbf{\Omega}$, the width of the discrete directions.

The removal term is

$$\Sigma_t^{i,j} \varphi_m^{ij} w_m, \tag{8.224}$$

the scattering source plus the contribution from the external source are

$$q_m^{ij} = \left[\frac{\Sigma_s^{ij}}{4\pi}\sum_{n=1}^{M} w_n \varphi_n^{ij}\right] V_{ij} w_m + Q_m^{ij} V_{ij}. \tag{8.225}$$

The neutrons also exit the phase space point $V_{ij}\Delta\mathbf{\Omega}_m$ by leaving $\Delta\mathbf{\Omega}_m$. That loss is proportional to the surface through which the neutrons leave and to the angular flux at the boundaries of the angular interval $\mathbf{\Omega}_{m\pm1/2}$. It can be written as

$$\left(A_{i+1/2,j} - A_{i-1/2,j}\right)\left(c_{m+1/2}\varphi_{m+1/2}^{ij} - c_{m-1/2}\varphi_{m-1/2}^{ij}\right) \tag{8.226}$$

and

$$\left(B_{i,j+1/2} - B_{i,j-1/2}\right)\left(d_{m+1/2}\varphi_{m+1/2}^{ij} - d_{m-1/2}\varphi_{m-1/2}^{ij}\right) \tag{8.227}$$

where the factors $c_{m\pm1/2}$ and $d_{m\pm1/2}$ have to be fixed. Now we are able to write down the neutron balance for phase space point $V_{i,j}\Delta\mathbf{\Omega}_m$:

$$\begin{aligned}
&\mu_m\left(A_{i+1/2}\varphi_m^{i+1/2,j} - A_{i-1/2,j}\varphi_m^{i-1/2,j}\right)\\
&+\eta_m\left(B_{i,j+1/2}\varphi_m^{i,j+1/2} - B_{i,j-1/2}\varphi_m^{i,j-1/2}\right)\\
&+\left(A_{i+1/2,j} - A_{i-1/2,j}\right)\left(\frac{c_{m+1/2}}{w_m}\varphi_{m+1/2}^{ij} - \frac{c_{m-1/2}}{w_m}\varphi_{m-1/2}^{ij}\right)\\
&+\Sigma_t^{i,j}\varphi_m^{ij}.
\end{aligned} \tag{8.228}$$

Now we return to the evaluation of $c_{m\pm1/2}$ and $d_{m\pm1/2}$. Consider a case where the external source Q is constant, the Σ_a is also constant. If the flux is constant as well, say Φ_0, which is the case if the leakage from V_{ij} is zero, then the balance equation reads as

$$\begin{aligned}
&\mu_m\left(A_{i+1/2}\Phi_0 - A_{i-1/2,j}\Phi_0\right)\\
&+\eta_m\left(B_{i,j+1/2}\Phi_0 - B_{i,j-1/2}\Phi_0\right)\\
&+\left(A_{i+1/2,j} - A_{i-1/2,j}\right)\left(\frac{c_{m+1/2}}{w_m}\Phi_0 - \frac{c_{m-1/2}}{w_m}\Phi_0\right)\\
&+\Sigma_t\Phi_0 V_{ij} = \frac{Q_0}{4\pi}V_{ij}.
\end{aligned} \tag{8.229}$$

In this situation the neutrons emitted from the source, balance out the absorptions, thus

$$\Sigma_t\Phi_0 = \frac{Q_0}{4\pi}.$$

Let the $x = \textit{constant}$ lines parallel to the y axis then the second term cancels in (8.229), and we are left with

$$c_{m+1/2} - c_{m-1/2} = -\mu_m w_m. \tag{8.230}$$

A similar equation for $d_{m\pm1/2}$ is obtained analogously. In a general geometry the evaluation of $c_{m\pm1/2}$ and $d_{m\pm1/2}$ is more complicated as $\mathbf{\Omega}_m$ may depend on both μ and η. When necessary, one may consult with the user's manual of the code to be applied [60],[61].

8.6.4. The ray effect

Every approximate model endeavors to replace a complex problem by a simpler one. The price to be paid for this is the limited applicability of the simpler model. The S_n method replaces the continuous directions in which the neutrons may fly by a set of discrete rays. This approximation causes no problem when the volume under consideration is filled with similar materials. Then the sources are more or less evenly distributed as in a usual core calculation.

When the user abandons standard structures and moves on to more exotic ones he/she may be surprised that his/her usually well behaving method performs poorly. If one has only a few discrete directions in an S_n code, and the sources are unevenly distributed, the neutrons may never enter portions of the volume and give a completely false result, or, possibly an unexpectedly large error. When the neutrons may move in any direction, the flux they create is constant on the surface of a sphere. If the neutrons move only in a few directions, their flux will be anomalously low in some directions.

The first question is how to explore the error and how to improve the accuracy. Benchmarking is a possible solution. There are well-defined problems with known solutions. Solving the problem by an S_n program, we can compare the approximate solution with the reference and find out the accuracy of the procedure. There are simple problems with exact solutions [62]. There are more realistic problems collected [63], and reactor-specific benchmarks [64].

To mitigate the error caused by using discrete directions, one can increase the number of directions. This would reduce the error and increase the running time of the algorithm. The $S_n \to P_{n-1}$ conversion also may reduce the error, but the higher order P_n algorithm may need a lot of work when n is large.

8.7. Collision probability method

The previous Sections discussed approximate solutions based on the expansion of the angular flux in terms of a complete set of function. In the P_n method, the complete function set was the spherical harmonics. That approximation has proved successful because low-order spherical functions have led to quite good approximate solutions. As we have seen see in Chapter 6, the diffusion theory is the most widely applied numerical approximation in reactor physics. We mention the S_n method as a contrast, in the sense that to obtain reasonable results $n = 8$ is the minimal value to be used. We have left the question of spatial discretization open, to be discussed along with the numerical methods. It has been a common feature of the methods we have discussed that the resulting set of equations in either approximate method has led to a set of differential equations. Starting from the integral form of the transport equation, it is possible to get an approximate solution without differentiation appearing in the approximate equations.

To launch our analysis, we quote the following integral equation for the scalar flux (see Section 3.6 in Chapter 3):

$$\Phi(\mathbf{r}) = \int_V \frac{e^{-d(\mathbf{r},\mathbf{r}')}}{4\pi|\mathbf{r}-\mathbf{r}'|^2} Q(\mathbf{r}')d^3\mathbf{r}', \tag{8.231}$$

where $d(\mathbf{r},\mathbf{r}')$ is the optical thickness between points $\mathbf{r},\mathbf{r}' \in V$ and Q is the source. In Section 3.6 of Chapter 3, we have seen that the integral transport equation can be used to get an integral equation for the angular flux.

The idea of the collision probability is to subdivide V into disjoint $V_1, \ldots, V_N$ regions and to use in each region the flux weighted cross-sections and the average flux to evaluate the integral in (8.231). Thus we introduce

$$\Phi_i = \frac{1}{V_i} \int_{V_i} \Phi(\mathbf{r}) d^3\mathbf{r} \tag{8.232}$$

$$\Sigma_{ti} = \frac{\int_{V_i} \Sigma_t(\mathbf{r}) \Phi(\mathbf{r}) d^3\mathbf{r}}{\int_{V_i} \Phi(\mathbf{r}) d^3\mathbf{r}} \tag{8.233}$$

$$Q_i = \frac{1}{V_i} \int_{V_i} Q(\mathbf{r}) d^3\mathbf{r}. \tag{8.234}$$

Now we multiply (8.231) by $\Sigma_t(\mathbf{r})$ and integrate over V, using (8.232)-(8.234), to get

$$\Sigma_{ti} \Phi_i V_i = \sum_{i'=1}^{N} P_{ii'} \left(\Sigma_{sj} \Phi_j + Q_j \right) V_{i'} \tag{8.235}$$

where

$$P_{ii'} = \frac{\int_{V_i} \Sigma_{ti}(\mathbf{r}) \int_{V_{i'}} \frac{e^{-d(\mathbf{r},\mathbf{r}')}}{4\pi|\mathbf{r}-\mathbf{r}'|^2} (\mathbf{r}') d^3\mathbf{r}'}{Q} \int_{V_{i'}} Q(\mathbf{r}') d^3\mathbf{r}' \tag{8.236}$$

is the probability of a neutron being born in region i' and suffering its first collision in region i.

Equation (8.235) is a system of linear equations for the scalar fluxes Φ_i.

To throw light on the P_{ij} probability, we study a simplified case. We have seen in Chapter 3 that the probability that a neutron leaving point i in the direction of point j does not collide before reaching j is $e^{-d(i,j)}$. But our P_{ij} is the similar probability only averaged over regions i and j. Let regions i and j be two infinite parallel lines, say L_i and L_j, separated by a distance $d(i,j)$. A particular neutron path may be labeled by the angle θ between the neutron path and line i. Let $P(L_i, L_j, \theta)$ give the probability that a neutron travels from L_i to L_j without a collision. Then

$$P(L_i, L_j, \theta) = e^{-d(i,j)/\sin\theta}.$$

Assuming that the paths labeled by various θ values are equally probable, the average probability is

$$P(L_i, L_j) = \frac{\int_0^\pi \sin\theta P(i,j,\theta) d\theta}{\int_0^\pi \sin\theta d\theta} = \frac{1}{2} \int_0^\pi \sin\theta e^{-d(i,j)/\sin\theta} d\theta. \tag{8.237}$$

The desired probability is given by a so called Bickley function, see Appendix A:

$$P(L_i, L_j) = K i_2(d) \tag{8.238}$$

since the distance between lines L_i and L_j is constant. Note that we have established a correspondence between two quantities. On the one hand, (8.237) is the P_{ij} between points i and j in a planar geometry assuming the neutrons are emitted isotropically. On the other hand, we get a similar expression (8.238) for the collision probability between lines L_i and L_j, but the non-collision probability e^{-d} is replaced by a Bickley function, the planar attenuation factor. Note that (8.238) has only one parameter: d the distance in mean-free path between points i and j in (8.237).

The following considerations originate from Carlvik[65]. In a general two-dimensional geometry, the average probability that a neutron uniformly and isotropically emitted from V_j suffers its first collision in the volume V_i can be given as the sequence of the following two, independent events:

- the neutron does not collide in V_j; the probability of that event is p_1;
- the neutron collides in V_i; the probability of that event is p_2.

Let the length of the line segment drawn in the motion direction ϕ of the neutron be a and let the neutron be born at position x on that line. Furthermore, let the distance between the volumes V_j and V_j be τ_1. Then, in accordance with our analysis above, p_1 and p_2 are expressible by the Bickley functions as

$$p_1 = Ki_2(a - x + \tau)$$

and

$$p_2 = 1 - Ki_2(\tau_2)$$

where τ_2 is the length of the line segment in the volume V_i. Since p_1 and p_2 are probabilities of independent events, their probabilities have to be multiplied. Thus for the given direction we get

$$P_{ij}(x, y, \phi) = Ki_2(\Sigma_j(a - x) + \tau_1) - Ki_2(\Sigma_j(a - x) + \tau_2),$$

where τ_1, τ_2 and a depend on ϕ.

The probability obtained in this way should be averaged first over the birthplace x of the neutron and secondly over the flying direction ϕ. The result of the first step is

$$P_{ij}(\phi) = \frac{\int_0^a P(x, y, \phi)dx}{\int_0^a dx}, \tag{8.239}$$

the final result being

$$\begin{aligned} P_{ij} = &\frac{1}{2\pi V_j \Sigma_j} \\ &\int \left[Ki_3(\tau_2) - Ki_3(\tau_3 + \tau_2) - Ki_3(\tau_2 + \tau_1) + Ki_3(\tau_2\tau_1 + \tau_3)\right] dyd\phi. \end{aligned} \tag{8.240}$$

Here τ_3 is the length of the line segment directed along the neutron velocity, in volume V_i. The resulting expression should be corrected for the self collision probability P_{ii}:

$$P_{ii} = 1 - \frac{1}{2\pi V_i \Sigma_i} \int \int \left[Ki_3(0) - Ki_3(\tau_3)\right] dyd\phi.$$

Now we have determined every probability needed in (8.235) to find the fluxes. The probabilities satisfy the reciprocity relation

$$V_j \Sigma_{tj} P_{ij} = V_i \Sigma_{ti} P_{ji}. \tag{8.241}$$

The collision probability method requires a large amount of computational effort. The evaluation of the Bickley functions and the large number of collision probabilities require determining the length of the line segments of a given direction falling into each subvolume. In annular geometry, the calculation can be simplified.

8.8. Problems

1. A subcritical system can be used as neutron multiplier. What is the relationship between the multiplication factor and the reactivity of the subcritical system?

2. How to measure the criticality of a strongly supercritical system?

3. When neutron multiplying systems are close enough to be coupled by neutron leakage they are called coupled systems. Analyze the criticality of a coupled system!

4. Find the time dependent flux in a subcritical system with external source!

5. What is the symmetry of the spherical sector $r = 1, 0 \leq \theta, \phi \leq \pi/2$?

6. Show that if $\alpha_i, \alpha_j, \alpha_k$ are directions in the S_n method, then $i + j + k = N/2 + 2$!

7. Show that in the S_N method for each higher order of approximation $N/2$ new discrete directions are added per octant!

8. Show that the number of discrete directions for a general N is $N(N + 2)$ in 3D, $N(N + 2)/2$ in 2D, and N in 1D!

9. It is well-known that the P_1 approximation is equivalent to the diffusion model, which is based on Fick's law. How the Fick's law is amended, if higher-order ($l = 2$) approximation is used in the P_l method?

10. What are the limitations of the S_n method?

11. Show that an octant of the unit sphere is invariant under 120° rotation!

12. Show that when increasing the number of directions from M to $M + 1$, $M/2$ new directions must be added per octant!

9. fejezet

Model Making

The present Chapter is devoted to the hierarchy of the reactor calculation. We start with the cell calculation, the approximations used in the unit cell calculations. The subsequent section deals with the fuel assembly problem, the next one with the calculation of the entire reactor. Then we deal with the determination of the albedo at the core-reflector interface, the burnup, the effects of the fission products, including xenon and samarium poisoning, as well as the xenon transients.

The calculational models are built on the theory that we have discussed in Chapter 4, utilize the approximate solution methods presented in Chapter 6. The topic of the present Chapter is the solution of characteristic complex problems in reactor calculation with the help of the theory and the approximations at our disposal.

9.1. Cell calculation

The conclusions we can draw from the asymptotic theory are summarized as follows:

- the solution of the neutron transport equation in a periodic structure, the lattice, has a component which is a periodic. The lattice is obtained by the repetition of a unit cell. The angular fluxes $u_0(\mathbf{r}, E, \mathbf{\Omega}), u_1(\mathbf{r}, E, \mathbf{\Omega})$ determined for the unit cell are applied in the derivation of group constants in the equation for the macroflux.
- The unit cell calculation means the solution of an eigenvalue problem with appropriate boundary conditions, the eigenvalue is the k_∞, the eigenfunction is the angular flux in the unit cell.
- The number of energy groups should be large enough to reflect the main features of the flux otherwise the homogenized and group condensed constants lead to false criticality, and false power distributions.

The task of cell calculation is to find the periodic cell fluxes. The cell has three homogeneous regions: the fuel, the clad and the moderator. Usually the regions are small compared to the mean free path of neutrons. The shape of the fuel and clad regions is a circular cylinder, the outer boundary of the cell depending on the lattice geometry may be a square or a hexagon. The calculation is usually carried out for a cylindrical cell, the square or hexagon is replaced by a disk of equal area, its equivalent radius R is determined from the lattice pitch d as

$$R = \frac{d}{\sqrt{\pi}} \quad R = \frac{d}{(2\pi/\sqrt{3})^2}, \tag{9.1}$$

for square and hexagonal lattices, respectively. As to $u_0(\mathbf{r}, E, \Omega)$, at the outer boundary, a boundary condition is prescribed. Frequently used boundary conditions include

- white boundary condition (albedo equal to one);
- zero current;
- reflective boundary condition when the neutron reflects from the boundary.

As will be mentioned in Chapter 7, different numerical method is used at different parts of the energy spectrum. In the thermal part of the spectrum, see Section 7.5 the mean free path is small, usually the integral transport equation is used. The cell is subdivided into radial regions and collision probability method is used, see THERMOS. In the resonance region, see Section 7.4, the applied model depends on the resonances. We distinguish resolved and

unresolved resonances, narrow resonance model, or the free gas models. In the epithermal region, the slowing down theory based on the slowing down density, supplemented by B_1 or P_1 methods can be used, see Chapter 6 Section 6.2.

A frequently used method for calculating the group fluxes is the collision probability method, see Section 8.7 in Chapter 6. We have discussed various approaches to determine the neutron flux in a periodic, finite or infinite, lattice composed either from identical or different cells. The presented theories may seem not to reconcile but for the practice they convey the same message. The flux in a lattice has the following structure:

$$\Phi(\mathbf{r}, E) = \Phi_{as}(\mathbf{r}, E) + a\Phi_{tr}(\mathbf{r}, E) \tag{9.2}$$

where Φ_{as} is the asymptotic flux, which establishes inside a large volume built from one cell type, Φ_{tr} is a transient flux. The transient flux may be different at lattice non-uniformity, like near a control rod, reflector, or in the vicinity of a different cell type. In various theories the precise meanings of either term may vary, see [5] for a survey. Let us average (9.2) over E and $\mathbf{r}$, the result is

$$\tilde{\Phi} = \tilde{\Phi}_{as} + a\tilde{\Phi}_{tr}, \tag{9.3}$$

and, because the leakage can be neglected in the asymptotic term, the following expression is a good approximation for the asymptotic term

$$\Phi_{as} = \frac{\bar{Q}}{\bar{\Sigma}}, \tag{9.4}$$

here $\bar{Q}, \bar{\Sigma}$ is the space and energy averaged neutron source and removal cross-section, respectively. The average cross-section of reaction type x may be written as

$$\bar{\Sigma}_x = \bar{\Sigma}_{as,x} R_x(\bar{\Phi}_{as}/\bar{\Phi}), \tag{9.5}$$

and the R_x correction factor is

$$R_x(\bar{\Phi}_{as}/\bar{\Phi}) = \frac{\bar{\Phi}_{as}}{\bar{\Phi}} + \frac{\Sigma_{tr,x}}{\Sigma_{as,x}}\left[1 - \frac{\bar{\Phi}_{as}}{\bar{\Phi}}\right] \tag{9.6}$$

indicating that neutron spectrum variations may induce a cross-section variation which is linear in $\bar{\Phi}_{as}/\bar{\Phi}$ called spectral index. That observation suggests including spectrum variation in the list of parameters which influence the actual cross-section. That idea of M. Lehmann [57][p. 308] has been implemented in reactor codes, the method is called spectral index parametrization. The asymptotic-transient decomposition is applicable in cell- and global reactor calculations as well.

At epithermal energies the heterogeneity is less pronounced than at thermal energies because of the larger mean free path. The neutrons that emerge from fission are located in the fuel region at the central part of the unit cell and a few collisions are needed for the flux to spread out over the entire cell.

At high energies, the neutron spatial distribution is concentrated to the fuel region. Fission, however, is initiated mostly by thermal neutrons thus the thermal neutron calculation should precede the epithermal heterogeneity calculation. The flux distribution below the fission energies rapidly flattens out in the cell. This suggests that slowing down calculations can be made by volume weighting.

In the resonance energy region, the resonance lines of heavy elements and some nuclei in the structural elements may cause complications. In the energy range, where the resonance peaks the flux decreases. That phenomenon is confined to a narrow energy region. If the

cross-sections are large, the flux strongly depends on the position. The spatial distribution of resonance elements determines where the flux decreases. Therefore the reaction rates in the resonance region should be determined in a fine energy resolution. In the epithermal calculation the usual number of energy groups is a few times of ten, this is insufficient to the sufficiently accurate flux calculations in the resonance energy region. Paramount resonance absorption occurs in the energy range $E < 200eV$. Here the resonance shielding must be determined precisely, the flux depression below its value in the absence of resonance nuclei must be known precisely, and the difference in some cases may be as small as a few percent. For this reason, most resonance shielding calculations focus on large resonances, for example ^{235}U,$^{239}\,Pu$ at $0.29\,eV$, ^{240}Pu at $1.06eV$.

In resonance shielding calculations the flux $\Phi_k(u)$ per unit lethargy in region k is expressed by the product

$$\Phi_k(u) = f_k(u)\Phi(u), \tag{9.7}$$

where $f_k(u)$ is the shielding function that changes fast near the resonance energy; $\Phi(u)$- the flux decay function which accounts for the resonance absorption in the lattice cell.

Denote Φ_0 and q_0 the flux and slowing down density, respectively for a resonance line. Thus

$$\frac{\Phi_0}{q_0} = \frac{\Phi(u)}{q(u)}, \tag{9.8}$$

where $q(u)$ is integrated over the entire cell. Since the decrease of the slowing down density is due to absorption, we have

$$-dq = \sum_i \sum_k N_{ik} V_k \sigma_{ia}(u)\Phi_k(u)du, \tag{9.9}$$

where N_{ik} is the nuclide density of isotope i in region k of volume V_k, σ_{ia} is the microscopic absorption cross-section of isotope i, $\Phi_k(u)$-the flux in region k. Using (9.8), we can solve the differential equation (9.9):

$$\frac{q(u)}{q_0} = \frac{\Phi(u)}{\Phi_0} = \exp\left[-\frac{\Phi_0}{q_0}\sum_i \sum_k N_{ik} V_k I^a_{eff,ik}(u)\right] \tag{9.10}$$

where

$$I^a_{eff,ik}(u) = \int_{u_0}^{u} \sigma_{ia}(u) f_k(u) du. \tag{9.11}$$

Here u_0 is a lethargy above the resonance lethargy region and we used the initial condition

$$\Phi(u_0) = \Phi_0;\; q(u_0) = q_0. \tag{9.12}$$

The resonance shielding determines the region dependent shielding function $f_k(u)$. Expression (9.10) is exact if the weight of the absorber is infinite and the moderator is hydrogen [144].

The resonance shielding function is usually determined for individual resonances. The narrow resonance approximation assumes the resonance line to be narrow and the resonance lines do not interfere. In that approximation

$$f(u) = \frac{\Sigma_{Pi} + \Sigma_{other}}{\Sigma_t(u)}, \tag{9.13}$$

where Σ_{Pi} is the potential scattering cross-section of resonance absorber i, Σ_{other} is the scattering cross-section of all other nuclei, Σ_t is the total cross-section.

Various numerical methods are applied in the cell calculation. In the epithermal range the slowing down density and flux based calculations appeared first in the MUFT code. P_n and B_n method, as well as collision probability calculations (WIMS, PIJ) are also applicable. The formalism varies from the integral transport equation, see Section 4.3 in Chapter 4, to the integro differential transport equation, see Section 4.2 in Chapter 4.

In the resonance region, two approximations are frequently used: the resonance integral formalism, and the subgroup method, see Section 7.4 in Chapter 7.

9.2. Assembly calculation

The objective of the assembly calculation is twofold. On the one hand, to provide the global reactor calculation with assembly homogenized cross-sections, or response matrices. That we call first type assembly calculation. On the other hand, to reconstruct the intra assembly distribution from the results of the global calculation, that we call second type assembly calculation.

The applied technique includes the collision probability methods applied in the WIMS, and PIJ codes, the response matrix method is used in the KARATE, SHM, and VARIANT codes. Here we deal with the less known Surface Harmonic Method [57][pp. 407-453] method.

The applied methods vary in describing the material, the mathematical model and the accepted approximations. The fuel assembly has an internal structure, it is built up from either homogenized or heterogeneous cells. The number of cells is in the order of 100, when the cell is subdivided into three regions, this is a rather frequent case, the total number of regions may exceed 300.

The mathematical model and the accepted approximation depend on the goal of the assembly calculation. The three major goals are:

1. providing the global calculation with assembly parameters (first type). Those parameters are usually few group diffusion theory parameters, response matrices, or collision probabilities.

2. determination of the intra assembly power or flux distribution (second type) from the assembly powers determined from the global calculation (remember, disadvantage factors k_q, k_k, k_z are needed for the safe operation and the in-core measurement processing also needs calculated date, see Chapter 10.

3. studying effects caused by the heterogeneous structure of the assembly (e.g. water gap, control rod, burnable poison).

The number of the energy groups in the assembly calculation is 4-8, depending on the reactor type. The global reactor calculation (finite element method, nodal method) needs diffusion theory parameters but collision probabilities also may be used.

The methodology of the assembly calculation depends on the optical thicknessλ of the assembly. When the assembly thickness exceeds 10λ, more computational effort is needed.

9.3. Full core calculation

The stating point is that the solution of the transport equation is unique if the entering current distribution is known along the boundary. The transport equation (3.116) is linear without thermal feedback, and then we can normalize the flux arbitrarily. It is usual that in the full core calculation the thermal power of the reactor is given as input and the total

fission power of the reactor is normalized accordingly. The criticality in the global reactor calculation is set by one of the following considerations:

- in core design calculations the criticality regulating parameter is the k_{eff} eigenvalue;
- in fuel cycle calculations, the regulating parameter is either the control rod position H or the boron concentration c_B. As the fuel burns, the reactivity is regulated by H and c_B so that the operational conditions are met. Since $k_{eff} = k_{eff}(c_B, H)$, the calculation is essentially the same for either regulation type. The difference is only in the estimation of the next guess of the parameter value. To this the $k_{eff}(H)$ and $k_{eff}(c_B)$ curves, or the reactivity coefficients

  $$\frac{\partial \rho}{\partial c_B}, \quad \text{or} \quad \frac{\partial \rho}{\partial H}$$

  are required.
- on-line calculations receive the actual core parameters (H, c_B, T_{in}) and the coolant flow rate G, and the goal is to find power ratios for given assembly pairs (one is metered, the other is not) to check the reactor parameters subjected to limitations.
- in a simulator, the emphasis is on the realistic time development of the data displayed on the control room panel, in real time. In a simulator session various transients play the main roles, the reactivity development should be followed with reasonable accuracy, there the reactivity coefficients are heavily utilized.

In the core calculation the reactivity is determined in the following iteration.

- Step 1. The initial (H, c_B, T_{in}) are given. To determine the fluxes and powers, an iteration is set up. First, the thermal hydraulics parameters $(T_f, T_m, \rho_{mod}, X)$, i.e. the fuel temperature, the moderator temperature, the moderator density, and the void fraction are determined. The few group diffusion equation is solved for a reasonable accuracy.
- Step 2. From Step 1, we get a power distribution, that serves as input to the thermal hydraulics module, and the $(T_f, T_m, \rho_{mod}, X)$ are recalculated for a reasonable accuracy. Step 2 closes one step of the neutronics-thermal hydraulics feedback iteration.
- Step 3. At the end of the feedback iteration, the selected control parameters are modified according to the reactivity coefficients, to approach the criticality. Note that in this step several components play, since the reactivity depends among others on T_f, T_m, X.
- Step 4. We return to Step 1, using the fresh control parameters (H, c_B, T_{in}), and repeat the iteration until convergence.
- Step 5. When converged, the algorithm determines all the required outputs that may include:
  - assembly-wise power distribution;
  - fuel rod-wise power distribution is obtained by repeating a type 2 assembly calculation;
  - isotope composition. The isotopes entering into the parameter set of the parametrized cross-section library are obtained immediately. Additional isotope compositions need auxiliary calculations.

The above steps concern the routine core calculations. There are situations when transient calculations are needed, including:

- operational transients initiated by technological processes (xenon and samarium poisoning, shut down, start up, main circulating pump transients etc.);
- accident situations, when the calculational model is used to study the consequences of postulated accidents;
- severe accident situations, where the calculational model is used to estimate the released radioactivity and the exposure of the staff;
- calculations needed in the safety analysis studies.

In the operational calculations, the analyst has to choose the appropriate model for each component in the calculational scheme. Within a given model (say we have chosen the finite element model) there are further options (e.g. the order of the approximation, the output) to be determined. Here it is difficult to give a general description or preferences. Experience and practice may orient the analyst in that respect. Once the solution is known, we can determine the exiting current.

9.4. Burnup calculations

In a steam boiler, the fuel burns and the coal turns to ash and gases. In a nuclear power plant the fuel is a fissionable material from which a part of the fissionable material turns to nuclear ash. That process is called burnup, the ash is called spent fuel. The present Subsection deals with details and modelling of the burnup process.

The amount of heat liberated in the reactor core is a fraction of the energy liberated in the fission nuclear reaction, see Table 1.1 that gives the distribution of fission energy [2, p. 71]. The instantaneously released energy is about 174 MeV. Since the nuclide transmutations depend on the number of fissions, the power of the reactor is a parameter in the burnup equations. The number of fission reactions also depends on the position thus the speed of burnup depends on the position of the fuel assembly in the core, the position of the fuel rod in the assembly, and, it depends on the spatial region to be considered inside the fuel rod. As a consequence of fission, a fissionable nucleus is replaced by fission products. Some fission products are strong absorbers thus fission reduces the reactivity.

The nuclide transmutations of the fissionable materials are discussed usually separately from the fission products because the fission products are usually light, non-fissionable elements. Opposite to that, some non-fissionable fuel isotopes capture neutrons and after further nuclear reactions may turn to fissionable isotopes. As a consequence, the possible nuclear reactions increase the number of nuclei involved, so we speak of nuclear chains, referring to the sequences of nuclei associated with the capture and fission reactions. Two units of burnup are in use. The first one is the fraction of fuel atoms that undergone fission, it is called FIMA from fissions per initial metal atom, and is given in percent. The second one is the actual energy liberated per unit fuel mass, its usual unit is MWd/t, where the liberated energy is measured in the ratio of released energy as the product of power in mega watt units, times the duration of the energy production in days. The mass is measured in metric tons. Thus $365MWd/t$ is the burnup level if a reactor operates for 365 days at 1 MW power over 365 days provided the core contained at the start 1 metric ton fresh fuel.

9.4.1. Fuel chains

Usually the fresh fuel contains uranium isotopes although there are reactors operating on mixed uranium-plutonium fuel. The thorium as fuel is brings in a new transition line because the ^{230}Th thorium isotope may lead to ^{231}Pa, ^{232}Pa,^{233}Pa and ^{233}U production. Those isotopes can be handled by the procedures described in Section 9.4.4.

The traditional notation leaves out the first digit of the atomic number of the nucleus under consideration and complements it with the last digit of the mass number. Thus N_{25} is the atomic density of ^{235}U because uranium has 92 protons, the last digit is kept, and we supplement it by the last digit (5) of the mass number (235).

The atomic density of ^{235}U decreases with the time:

$$\frac{dN_{25}}{dt} = -N_{25}(t)\sum_g \sigma_{ag}^{25}\Phi_g(t). \tag{9.14}$$

Integrating (9.14) we find that the solution is

$$N_{25}(t) = N_{25}(0)e^{-(\sum_g \sigma_{ag}^{25}\int_0^t \Phi_g(t')dt')}. \tag{9.15}$$

Equation (9.15) shows that the amount of spent fuel depends on the neutron spectrum and the thermal power of the reactor. We introduce the spectrum averaged cross-section as:

$$\sigma_a^{25} = \frac{\sum_g \sigma_{ag}\Phi_g}{\sum_g \Phi_g} \tag{9.16}$$

and the total flux

$$\Phi = \sum_g \Phi_g. \tag{9.17}$$

In the following equations we use group condensed cross sections and total flux. Equation (9.15) in the new variables becomes

$$\frac{dN_{25}}{dt} = -N_{25}(t)\sigma_a^{25}\Phi(t). \tag{9.18}$$

We introduce the notation

$$F(t) = \int_0^t \Phi(t')dt', \tag{9.19}$$

which is used as the measure of the irradiation. $F(t)$ is called fluence its unit is neutron per square centimeter. The number of ^{235}U nuclei monotonously decreases with time.

The next chain originates from the isotope ^{238}U which after capturing a neutron undergoes a beta decay into ^{239}Np that also undergoes a beta decay and forms ^{239}Pu. Thus that chain has four members, each equation has the same structure: the change in the atomic density, which is the first derivative with respect to the time, equals the difference between the production and decay rates. The ^{238}U atomic density decreases due to absorption:

$$\frac{dN_{28}}{dt} = -N_{28}(t)\sigma_a^{28}. \tag{9.20}$$

The ^{239}U decays thus the balance is:

$$\frac{dN_{29}}{dt} = \sigma_c^{28}\Phi(t)N_{28} - \lambda_{29}N_{29}(t). \tag{9.21}$$

^{239}Np is produced as the result of the decay:

$$\frac{dN_{39}}{dt} = \lambda_{29}N_{29}(t) - \lambda_{39}N_{39}(t). \tag{9.22}$$

After a beta decay, the ^{239}Pa becomes ^{239}Pu:

$$\frac{dN_{49}}{dt} = \lambda_{39}N_{39}(t) - \sigma_a^{49}\Phi(t)N_{49}(t). \tag{9.23}$$

Since $\lambda_{29} = 4.910^{-4}\ \ 1/sec$ and $\lambda_{39} = 3.610^{-6}\ \ 1/sec$, and the absorption cross-sections of ^{239}U and ^{239}Np are negligible, the mentioned isotopes may be left out.

The solution of (9.20) is also given in terms of the fluence F:

$$N_{28}(F) = N_{28}(0)e^{-(\sigma_a^{28}F)}. \tag{9.24}$$

When $\Phi \sim 10^{13}\ \ 1/cm^2/sec\ N_{28} \sim constant$. The plutonium isotopes are obtained from the following equations.

The half lives of the radionuclides ^{239}U and ^{239}Np are much shorter than the half life of their parent radionuclide ^{238}U. In that situation the production of ^{239}U and ^{239}Np is approximately constant. The quantity of radionuclides ^{239}U and ^{239}Np build up until their atomic densities decaying per unit time becomes equal to the number being produced per unit time; the quantity of radionuclides ^{239}U and ^{239}Np then reache a constant, equilibrium value. Since we may assume that their initial concentration is zero, full equilibrium usually takes several half-lives of radionuclide ^{239}U and ^{239}Np to establish. Such a situation is called secular equilibrium. The balance of the plutonium isotope is simple, as ^{239}Pu is formed from ^{239}U by capture, the other plutonium isotopes are formed only by capture from plutonium isotopes. Note that using the chain rule for the derivatives, we can eliminate the flux from equations (9.19)

$$\frac{dN(t)}{dt} = \frac{dN(F)}{dF}\frac{dF}{dt} = \frac{dN(F)}{dF}\Phi. \tag{9.25}$$

and arrive at the following equations:

$$\frac{dN_{49}}{dF} = \sigma_c^{28}N_{28}(F) - \sigma_a^{49}N_{49}(F) \tag{9.26}$$

$$\frac{dN_{40}}{dF} = \sigma_c^{49}N_{49}(F) - \sigma_a^{40}N_{40}(F) \tag{9.27}$$

$$\frac{dN_{41}}{dF} = \sigma_c^{40}N_{40}(F) - \sigma_a^{41}N_{41}(F). \tag{9.28}$$

The solutions are for small fluence values ($f << 1$):

$$N_{49}(F) = \sigma_c^{28}N_{28}F \tag{9.29}$$

$$N_{40}(F) = \sigma_c^{28}\sigma_c^{49}N_{28}\frac{F^2}{2} \tag{9.30}$$

$$N_{41}(F) = \sigma_c^{28}\sigma_c^{49}\sigma_c^{40}N_{28}\frac{F^3}{6}. \tag{9.31}$$

For small fluence values, the atomic densities of ^{241}Pu, ^{241}Pu, and ^{241}Pu vary as F, F^2 and F^3.

The conversion factor C also connects to the atomic densities of plutonium isotopes. The conversion factor is

$$C = \frac{\text{mass of plutonium produced}}{\text{mass of } ^{235}U \text{ isotope used}}. \tag{9.32}$$

The conversion factor strongly depends on the reactor type because the neutron spectrum and the initial enrichment of the fuel may differ. Usual values are $0.6 \leq C < 1$ but in fast reactors $C > 1$ is possible. If $C > 1$ the reactor is called breader.

9.4.2. Xenon poisoning

Two fission products have extremely large absorption cross-sections, ^{135}Xe and ^{147}Sm. Here we discuss the xenon problem, and the next Subsubsection is reserved for the samarium problem.

The fission reaction rate is $\Sigma_f\Phi$, the atomic density of a given fission product P is written as $Y_P\Sigma_f\Phi$, where Y_P is the yield of fission product P. The yields of fission products of ^{235}U caused by slow neutrons is shown in Fig. 3.5. Note that the maximal yield is less than 10%, the curve is almost symmetric, the maximum yields are not at the fission products of equal mass. The yield of tellurium is $y_{Te} = 0.064$, the half life of ^{135}Te is $19.2sec$, emitting a β^- particle it decays into ^{136}I which undergoes another β^- decay with half life $6.58h$ and produces ^{135}Xe. The thermal absorption cross section of xenon 135 is $\sigma_a = 3.1\ \ 10^6$ barn. As in connection with the plutonium isotopes we have seen, we may leave out the short life time tellurium. The balances of the ^{135}I and ^{135}Xe are:

$$\frac{dN_I}{dt} = Y_I\Sigma_f\Phi - \lambda_I N_I, \tag{9.33}$$

$$\frac{dN_{Xe}}{dt} = Y_{Xe}\Sigma_f\Phi + \lambda_I N_I - \lambda_{Xe}N_{Xe} - \sigma_{Xe}N_{Xe}\Phi. \tag{9.34}$$

The equilibrium (when $dN_i/dt = 0$) iodine and xenon concentrations are

$$N_I(\infty) = \frac{Y_I\Sigma_f\Phi}{\lambda_I} \tag{9.35}$$

and

$$N_{Xe}(\infty) = \frac{(Y_I + Y_{Xe})\Sigma_f\Phi}{(\lambda_{Xe} + \sigma_{Xe}\Phi)}. \tag{9.36}$$

$$N_{Xe}(t) = N_{Xe}(\infty)e^{-\lambda_{Xe}t} + \frac{\lambda_I}{\lambda_{Xe} - \lambda_I}N_I(\infty)\left(e^{-\lambda_I t} - e^{-\lambda_{Xe}t}\right). \tag{9.37}$$

The xenon poisoning may have two consequences. The first one is that after reactor shut down, the xenon concentration increases, the other one is the appearance of spatial oscillations in large reactor cores.

In large reactors spatial oscillation of the xenon concentration may occur [143][Chapter XXVIII], that may lead not only to an increase in the local and axial power peaking factors but also to instability. Assume that for some reason the neutron flux suddenly increases at a given point of the reactor core. According to equations (9.33) and (9.34) N_{Xe} decreases at that point, that leads to a reactivity increase. The increased reactivity also results in larger flux. That qualitative consideration shows that positive feedback is possible thus we have to analyze the stability in details.

Let the initial position is a stationary core state, where we describe the neutron flux in one energy group diffusion theory:

$$M^2\boldsymbol{\nabla}^2\Phi_0 + (k-1)\Phi_0 - \alpha X_0\Phi_0 = 0, \tag{9.38}$$

where k is the multiplication factor when $N_{Xe} = 0$ and α is the reactivity reduction due to unit xenon concentration, M^2 is the neutron migration area. In equilibrium the iodine and xenon concentrations satisfy

$$Y_I \Sigma_f \Phi_0 - \lambda_I N_{I0} = 0 \tag{9.39}$$

$$Y_{Xe} \Sigma_f \Phi_0 + \lambda_I N_{I0} - \lambda_{Xe} N_{Xe0} - \sigma_{Xe} N_{Xe0} \Phi_0 = 0. \tag{9.40}$$

In the perturbed state, we have

$$\Phi = \Phi_0 + \delta\Phi; \quad N_I = N_{I0} + \delta N_I; \quad N_{Xe} = N_{Xe0} + \delta N_{Xe}. \tag{9.41}$$

In the perturbed state, the flux obeys the time dependent diffusion equation that now we write as

$$\Lambda \frac{\partial \Phi}{\partial t} = M^2 \Phi + (k-1)\Phi - \alpha X \Phi. \tag{9.42}$$

Note, that this equation is nonlinear because of the $X\Phi$ term. Substituting here (9.41) and using the stationary relations (9.39) and (9.40) we get the following equations for the perturbations:

$$\lambda \frac{\partial \delta\Phi}{\partial t} = M^2 \boldsymbol{\nabla}^2 \delta\Phi + (k-1)\delta\Phi - \alpha \delta N_{Xe} \Phi_0 - \alpha N_{Xe0} \delta\Phi \tag{9.43}$$

$$\frac{\partial \delta N_I}{\partial t} = Y_I \Sigma_f \delta\Phi - \lambda_I \delta N_I \tag{9.44}$$

$$\frac{\partial N_{Xe}}{\partial t} = Y_{Xe} \Sigma_f \delta\Phi + \lambda_I \delta N_I - \lambda_{Xe} \delta N_{Xe} - \sigma_{Xe} \delta N_{Xe} \Phi_0 - \sigma_{Xe} N_{Xe0} \delta\Phi. \tag{9.45}$$

The stability of equations (9.43)-(9.45) should be studied by the means of stability analysis, see Section 6.7 in Chapter 6. The analysis would require a time and space dependent code. To remain within the analytical calculation, we eliminate the time dependence by assuming that the time dependence takes the form $\exp(\omega t)$. Then we have to study the following equations:

$$\lambda\omega\delta\Phi = M^2 \boldsymbol{\nabla}^2 \delta\Phi + (k-1)\delta\Phi - \alpha \delta N_{Xe} \Phi_0 - \alpha N_{Xe0} \delta\Phi \tag{9.46}$$

$$\omega \delta N_I = Y_I \Sigma_f \delta\Phi - \lambda_I \delta N_I \tag{9.47}$$

$$\omega N_{Xe} = Y_{Xe} \Sigma_f \delta\Phi + \lambda_I \delta N_I - \lambda_{Xe} \delta N_{Xe} - \sigma_{Xe} \delta N_{Xe} \Phi_0 - \sigma_{Xe} N_{Xe0} \delta\Phi. \tag{9.48}$$

Now we have three coupled space dependent equations. Assume that the spatial distribution of the equilibrium flux is flat, and expand the space dependent perturbations in terms of the eigenfunctions of the following operator:

$$M^2 f_n + (k-1) f_n - \alpha N_{Xe0} f_n + M^2 \nu_n = 0, n = 0, 1, 2, \ldots \tag{9.49}$$

The fundamental mode $n = 0$ corresponds to $\nu_0 = 0$ and f_0 is constant. Because N_{Xe0} is proportional to Φ_0, which is constant, from (9.39) and (9.40) we find that

$$N_{Xe0} = \frac{(Y_{Xe} + Y_I)\Sigma_f \Phi_0}{\lambda_{Xe} + \sigma_{Xe} \Phi_0} \tag{9.50}$$

is also a constant. Thus, actually the eigenfunctions introduced in (9.49) are the eigenfunctions of the Laplace operator, they are known to form a complete orthonormal system, so we expand the unknown functions as

$$\delta\Phi = \sum_n p_n f_n; \quad \delta N_I = \sum_n I_n f_n; \quad \delta N_{Xe} = x_n f_n. \tag{9.51}$$

Substituting (9.51) into (9.46)-(9.48), exploiting the orthogonality of f_n the eigenfunctions, we get a system of linear equations for p_n, I_n, x_n:

$$\begin{aligned} \Lambda\omega p_n &= -\nu_n p_n - \alpha x_n \Phi_0 && (9.52)\\ \omega I_n &= Y_I \Sigma_f p_n - \lambda_I I_n && (9.53)\\ \omega x_n &= Y_{Xe}\Sigma_f \phi_n + \lambda_I I_n - \lambda_{Xe} x_n - \sigma_{Xe} X_0 p_n. && (9.54) \end{aligned}$$

This is a system of homogeneous equations, non-trivial solution exists only when the determinant is zero, this given a third order equation for the frequency ω:

$$\Lambda\omega^3 + a_2\omega^2 + a_1\omega + a_0 = 0 \tag{9.55}$$

where:

$$a_2 = |\nu_n + \Lambda(\lambda_I + \lambda_{Xe} + \sigma_{Xe}\Phi_0)| \tag{9.56}$$

$$a_1 = \left|\nu_n(\lambda_I + \lambda_{Xe} + \sigma_{Xe}\Phi_0) - \alpha\Sigma_f\Phi_0\frac{Y_I\sigma_{Xe}\Phi_0 - Y_{Xe}\lambda_{Xe}}{\lambda_{Xe} + \sigma_{Xe}\Phi_0} + \lambda_I(\lambda_{Xe} + \sigma_{Xe}\Phi_0)\right| \tag{9.57}$$

$$a_0 = \left|\nu_n(\lambda_{Xe} + \sigma_{Xe}\Phi_0) + \alpha\Sigma_f\Phi_0 X_0\right|. \tag{9.58}$$

9.4.3. Samarium poisoning

A neodymium isotope ^{147}Nd is a fission product, its yield is $Y_{Nd} = 0.0109$ and β^- decays with $\lambda = 1.73\ \ h$ into ^{147}Pm, which undergoes a β^- decay with $\lambda = 53\ \ h$ into the stable ^{149}Sm. The total cross-section of ^{149}Sm in the thermal energy range exceeds 10^6 barn. Following the procedure we have applied to the xenon, the isotope balance takes the form of

$$\frac{dN_{Pm}}{dt} = Y_{Pm}\Sigma_f\Phi - \lambda_{Pm}N_{Pm} \tag{9.59}$$

and

$$\frac{dN_{Sm}}{dt} = \lambda_{Pm} - \Phi\sigma_{Sm}N_{Sm}. \tag{9.60}$$

The stationary solution is:

$$N_{Pm}(\infty) = \frac{Y_{Pm}\Sigma_f\Phi}{\lambda_{Pm}} \tag{9.61}$$

and

$$N_{Sm}(\infty) = \frac{Y_{Pm}\Sigma_f}{\sigma_{Sm}}. \tag{9.62}$$

The solutions are:

$$N_{Pm}(t) = \frac{Y_{Pm}\Sigma_f\Phi}{\lambda_{Pm}}\left(1 - e^{-\lambda_{Pm}t}\right). \tag{9.63}$$

$$N_{Sm}(t) = \frac{Y_{Pm}\Sigma_f}{\sigma_{Sm}}\left(1 - \frac{\sigma_{Sm}\Phi e^{-\lambda_{Pm}t} - \lambda_{Pm}e^{-\sigma_{Sm}\Phi t}}{\sigma_{Sm}\Phi - \lambda_{Pm}}\right) \tag{9.64}$$

The ratio of asymptotic N_{Pm} and N_{Sm} linearly depends on the flux:

$$\frac{N_{Pm}(\infty)}{N_{Sm}(\infty)} = \frac{\sigma_{Sm}\Phi}{\lambda_{Pm}} \tag{9.65}$$

and because $\lambda_{Pm} = 3.63\ 10^{-6}$, at large flux that ratio may reach 10. At the same time ^{149}Sm is stable, it does not decay as xenon does. To estimate the accumulated samarium in

the reactor, samarium poisoning, we have to adjust the time dependent solutions (9.63) and (9.64) to the following initial conditions:

$$N_{Pm}(0) = 0, \quad N_{Sm}(0) = N_{Sm}(\infty) + N_{Pm}(\infty) \tag{9.66}$$

because $N_{Sm}(\infty)$ is independent of the flux because ^{149}Sm is a stable isotope. Assuming constant flux Φ, the time dependent samarium concentration is:

$$N_{Sm}(t) = \frac{Y_{Pm}\Sigma_f}{\sigma_{Sm}} - \frac{Y_{Pm}\Sigma_f\Phi}{\lambda_{Pm}}\left(\frac{\lambda_{Pm}e^{-\lambda_{Pm}t} - \sigma_{Sm}\Phi e^{-\sigma_{Sm}\Phi t}}{\sigma_{Sm}\Phi - \lambda_{Pm}}\right). \tag{9.67}$$

The equilibrium samarium concentration is again $N_{Sm}(\infty)$ so the accumulated samarium poison burns during a fuel cycle and does not accumulate, provided the fuel cycle length is sufficiently long.

9.4.4. General treatment

We presented a couple of simple cases amenable to explicit discussion in the previous Subsections. When calculating the isotope inventory, we need an automated procedure, called burnup module, which determines the possible decay schemes from a nuclear data library, sets up the differential equations for the nuclear densities, solves those equations, and displays the resulting densities. To outline such a procedure, first we introduce a suitable notation.

The isotope balance is a first order, linear differential equation. We collect the nuclide densities into $\mathbf{N} = (N_1, N_2, \ldots, N_{n_{fuel}}, N_{n_{fuel}} + 1, \ldots, N_{iso})$ where N_{fuel} is the number of fissionable isotopes in the fuel, and N_{iso} is the total number of isotopes, which equals to the number of fissionable isotopes plus the number of fission products. The form of the equation is

$$\frac{d\mathbf{N}}{dt} = \mathbf{D}\mathbf{N}(t) + \mathbf{S}, \tag{9.68}$$

where all the transmutations are involved in matrix $\mathbf{D}$, $\mathbf{S}$ is a possible source vector that may be needed for example at core reload. The solution takes the following form:

$$N(t) = \exp\int_0^t \mathbf{D}(t')dt'\mathbf{N}(0) + \int_0^t \exp\int_{t'}^t \mathbf{D}(\tau)d\tau\mathbf{S}(t')dt'. \tag{9.69}$$

From the form of the solution it is clear that an efficient solution requires a simple $\mathbf{D}$ matrix.

We select the following partition. The first N_{fuel} nuclide densities belong to fuel isotopes, they vary in the depletion chains. The second block is $N_i, i > fuel$ for fission products, the equations for fission products contain source term linear in $N_i, i \leq fuel$. We deal first with the depletion equations. The depletion refers to a given region labeled by subscript r. In a given region the flux is represented by a constant value. The i-th line is

$$\frac{dN_i}{dt} = d_{ii}N_i + \sum_{j=1}^{i-1} d_{ij}N_j, i = 1, \ldots, N_{chain}, \tag{9.70}$$

where N_{chain} is the number of isotopes in the depletion chain. The diagonal term is negative and accounts of depletion:

$$d_{ii} = -\sum_{g=1}^{G}(\sigma_{cg} + \sigma_{fg} + \sigma_{(n,2n)g})_i\Phi_{rg} - \lambda_{j,i} - \lambda_i^*, \tag{9.71}$$

where σ_{cg} is the effective microscopic, self-shielded capture cross-section in energy group g; σ_{fg}-the effective microscopic, self-shielded fission cross-section in energy group g; $\sigma_{(n,2n)g}$-the effective microscopic, total self-shielded $(n,2n)$ cross-section in energy group g; λ_i^*-disintegration constant of isotope i; i,j-nuclide subscripts, the first refers to the daughter product, the second to the parent nuclide.

The non-diagonal term d_{ji} may stand for four different expressions depending on the relation between nuclide j and i. The relationship is given as input, the possibilities are

- $(n,2n)$ reaction:
$$d_{ji} = \sum_{g=1}^{G} \sigma_{(n,2n)gj} \Phi_{rg} \tag{9.72}$$
when the $(n,2n)$ reaction of isotope j produces isotope i;

- capture:
$$\sigma_{cjg} \Phi_{rg} \tag{9.73}$$
when the capture of isotope j results in production of isotope i;

- fission:
$$Y_{ij} N_j \sum_{g=1}^{G} \sigma_{fjg} \Phi_{rg}, \tag{9.74}$$
here Y_{ij} is the yield from fission of isotope j to isotope i;

- disintegration:
$$\lambda_{ij}, \tag{9.75}$$
the disintegration constant from isotope j to isotope i.

G is the number of energy groups.

The fission products originate from fuel isotopes. The source term S_j of isotope j is :

$$S_j = \sum_{i=1}^{n_{fuel}} d_{ij} N_j = \sum_{i=1}^{N_{iso}} Y_{ij} N_i \sum_{g=1}^{G} \sigma_{f_i}^g \Phi_{rg} \tag{9.76}$$

where N_{iso} is the number of isotopes in the fuel. The solution method for the depletion equation (9.68) may differ from isotope to isotope. Either analytical or finite difference solution may be chosen. We do not go into the technical details.

9.5. Problems

- The power is constant in the critical reactor. Calculate and plot the quantity of ^{235}U, ^{239}Pu, ^{240}Pu, ^{241}Pu in function of time! Neglect the change of ^{238}U nuclide number.

- How to change the amount of xenon if the flux is determined by
$$\phi(t) = \left\{ \begin{array}{rl} 0 & \text{if } t < 0 \\ \phi_0 t / T_1 & \text{if } 0 < t < T_1 \\ \phi_0 & \text{if } T_1 < t < T_2 \\ \phi_0 (T_3 - t) / (T_3 - T_2) & \text{if } T_2 < t < T_3 \end{array} \right\}$$
The initial conditions are $N_{Xe} = 0$ and $N_I = 0$ at $t = 0$. The parameters of problem: enrichment 3.6 %, $T_1 = 6$ h, $T_2 = 18$ h, $T_3 = 24$ h, $\phi_0 = 10^{12}$ $1/cm^2 s$.

- Solve the previous problem for ^{149}Sm isotope!
- The nuclear waste contains ^{134}Cs and ^{137}Cs isotopes which ratio depends on the operation of power plant. It follows that isotope ratio differs from the nuclear explosion and Chernobyl accident case. How can we separate the waste coming from Chernobyl accident from the waste coming from nuclear explosion according to Cs isotopes ratio?
- ^{148}Nd isotope is continuously produced during the operation of the reactor, the decay is negligible. The amount of ^{148}Nd can be accurately measured. How to infer the energy produced by the reactor?

10. fejezet

Global Calculation and In-Core Measurements

The subject of the present Chapter is the core surveillance. We shortly discuss the goals, the measurement methods, and the signal processing. The discussed topics are often summarized under the name Instrumentation and Control (I and C) although mostly the technical part (signal sampling, electrical processing of the signal, technical features of the electronics etc.) is discussed.

10.1. The goal of core surveillance

The regulation principles [98] limit among others the maximal coolant temperature in the core, and also the maximal pin wise power density. A nuclear power plant must be operated within strictly determined conditions. A part of the conditions fixes physical parameters in the reactor core: the maximum of power density, the maximum of coolant temperature, to mention a few. The maxima vary with time that makes impossible to designate beforehand the places where we expect the maximum and its value. Instead, the utility should implement measurement and post processing the measured values. The maxima should be estimated with a given accuracy. The limitations are global and local. Global limitations concern the gross power of the unit, the local limit concerns the temperature or power density at a given location. Usually large ionization chambers serve checking the nuclear power, which is subjected to global limitation. The in-core measurement serve checking the local power, which is a local limitation.

The limited space in the core and other technical difficulties set a limit to the number of measurements that can be implemented in the core. Thus an in-core measurement can not be a simple reading out of the measured values, a heavy statistical machinery [111], [109] is needed. Since the technical details may differ radically as they depend on the type of the reactor, we focus on the general principles of the measurement and the processing of the measured signal.

The present Chapter deals with the technical problems of the above outlined procedure. To reduce the size of the problem, we confine the investigation to two kinds of measurements: temperatures and neutron flux or power density.

One of the goals of in-core instrumentation is to inform the plant operator on the actual distance from the operational limit. It is impossible to measure the coolant temperature at every point, and it is impossible to measure the power distribution in every fuel pin henceforth we need a model in the frame of which the following question can be decided: Is it probable that we measured x_m and the quantity x is below a given limit x_L? Note that x_m and x may refer to different space points. It follows from the formulation of the problem that the answer must be based on statistics, and the limits should be set taking into consideration of the possible errors.

Another goal of the instrumentation is a kind of control. It should be discovered if the loaded core differs from the designed one. If there are tendencies in the core not foreseen at the core design stage, it should be indicated as early as possible to avoid later damages. This is called anomaly detection. Various anomalies may appear as a consequence of slow processes, like deformation of the coolant flow pattern, or fast processes like vibrations, crud[1] formation etc.

In the next two Sections, we assess the physical principles usable in measuring temperature and power density. The final goal is to determine W_{max}, the maximum power density in the core; and T_{max}, the maximum coolant temperature in the core.

[1]The crud is a precipitation from the coolant, its sources are mostly the corrosion products that are always present on the surface of the primary loop.

10.2. Measured fields

Before setting out for the measuring of the temperature or flux distribution in a reactor, let us analyze the problem. We have to determine a position dependent function $T(\mathbf{r})$ in a finite domain V and find its extremum, $\max_{\mathbf{r}\in V} T(\mathbf{r}) = T_{max}$, i.e. to find the position and value of the maximal temperature for example. The problem is aggravated by three major circumstances: The number of measured values is limited, the measured values may be deteriorated by errors, and the maximum may appear at any position. We investigate two problems, the first one is counter checking the measured values; the second one is to estimate non-metered positions. To simplify the problem, we set forth the following models.

We first deal with the the flux distribution in the core. Detailed calculational models are discussed in Chapter 6, here we put up with a simplified model to learn characteristic distances of flux (and power as well as temperature) variations in the core. Our model is a homogeneous disc, the flux is studied in diffusion theory, in two energy groups, the material distribution is assumed homogeneous. In the chosen model the flux distribution is obtained from the following equations:

$$D_1 \boldsymbol{\nabla}^2 \Phi_1(r,\phi) + \Sigma_1 \Phi_1(r,\phi) = \frac{\chi_1}{k_{eff}} \sum_{k=1}^{2} \nu\Sigma_{fk} \Phi_k(r,\phi) \tag{10.1}$$

$$D_2 \boldsymbol{\nabla}^2 \Phi_2(r,\phi) + \Sigma_2 \Phi_2(r,\phi) = \Sigma_{1\to 2} \Phi_1(r,\phi) + \frac{\chi_2}{k_{eff}} \sum_{k=1}^{2} \nu\Sigma_{fk} \Phi_k(r,\phi), \tag{10.2}$$

where χ_1, χ_2 is the fraction of neutron emerging from fission in group 1 and 2 respectively; k_{eff} is the estimated value of the criticality eigenvalue, see Chapter 1;D_1, D_2 are the diffusion constants; Σ_1, Σ_2 are the total cross-sections. No up-scattering is assumed in the model, thus $\Sigma_{2\to 1} = 0$ and $\Sigma_{1\to 2}$ is the scattering from the fast group to the thermal group. The radius of the disk is R and the boundary condition is

$$\Phi_k(R,\phi) = 0, k = 1,2; \;\; 0 \le \phi \le 2\pi. \tag{10.3}$$

In the solution, we exploit the eigenfunctions of the Laplace operator. The eigenvalue problem is formulated in the following from:

$$\boldsymbol{\nabla}^2 u(r,\phi) = -\lambda u(r,\phi), 0 \le r \le R; \;\; 0 \le \phi \le 2\pi. \tag{10.4}$$

Problem (10.4) has infinitely many $u_{jk}(r,\phi)$ solutions:

$$u_{jk}(r,\phi) = c_{kj} J_k(B_{kj} r) e^{ik\phi}. \tag{10.5}$$

Here $i = \sqrt{-1}$, c_{kj} is a normalization constant; and

$$B_{kj} = \frac{\mu_{jk}}{R}, \tag{10.6}$$

where μ_{jk} is the j-th root of the Bessel function $J_k(r)$. Note, that the $u_{jk}(r,\phi)$ functions are complex hence these real part and imaginary part is also an eigenfunction. With appropriate choice of the normalization constants, the eigenfunctions form an orthonormalized function set in the following sense:

$$\int_0^{2\pi} \int_0^R u_{jk}(r,\phi) u_{j',k'}(r,\phi) dr d\phi = \delta_{jj'} \delta_{kk'}, \tag{10.7}$$

where

$$\delta_{ij} = \begin{cases} 1 \text{ when } i = j \\ 0 \text{ otherwise.} \end{cases}$$

The fundamental eigenfunction $u_{00}(r, \phi)$ is independent of the azimuthal angle ϕ and is positive for $0 \leq r \leq R$ and thus has a physical meaning. Its explicit form is

$$u_{00}(r, \phi) = c_{00} J_0(B_{00} r). \tag{10.8}$$

The B_{00} buckling has been obtained from the boundary condition so it is called geometrical buckling. Below we investigate the solution of the form

$$\Phi_1(r, \phi) = C_1 J_0(Br); \;\; \Phi_2(r, \phi) = C_2 J_0(Br) \tag{10.9}$$

of the fundamental mode but now we determine the B buckling from (10.1)-(10.2). Let us replace the above forms of the fluxes into (10.1)-(10.2), we get the following two equations for the constants C_1 and C_2:

$$\begin{pmatrix} -D_1 B^2 + \Sigma_1 - \frac{\chi_1}{k_{eff}} \nu\Sigma f1 & -\frac{\chi_1}{k_{eff}} \nu\Sigma f2 \\ -\frac{\chi_2}{k_{eff}} \nu\Sigma f1 - \Sigma_{1\to 2} & -D_2 B^2 + \Sigma_2 - \frac{\chi_2}{k_{eff}} \nu\Sigma f2 \end{pmatrix} \begin{pmatrix} C_1 \\ C_2 \end{pmatrix} = 0. \tag{10.10}$$

Not identically zero solution exists when the determinant is zero:

$$\begin{vmatrix} -B^2 + \beta_1 & -\delta_2 \\ -\delta_1 & -B^2 + \beta_2 \end{vmatrix} = 0. \tag{10.11}$$

Here we introduced the following abbreviations:

$$\beta_1 = \frac{\Sigma_1 - \frac{\chi_1}{k_{eff}} \nu\Sigma_{f1}}{D_1} \tag{10.12}$$

$$\beta_2 = \frac{\Sigma_1 - \frac{\chi_2}{k_{eff}} \nu\Sigma_{f2}}{D_2} \tag{10.13}$$

$$\delta_1 = \Sigma_{1\to 2} + \frac{\chi_2}{k_{eff}} \nu\Sigma_{f1} \tag{10.14}$$

$$\delta_2 = \frac{\chi_1}{k_{eff}} \nu\Sigma_{f2}. \tag{10.15}$$

Equation (10.11) has two roots, B_1^2 and B_2^2:

$$\begin{pmatrix} B_1^2 \\ B_2^2 \end{pmatrix} = \beta_1 + \beta_2 \pm \mathcal{D} \tag{10.16}$$

where the plus sign is to be applied in the first line, the minus sign in the second line, furthermore, the discriminant is

$$\mathcal{D} = \sqrt{(\beta_1 - \beta_2)^2 + \frac{4\delta_1 \delta_2}{D_1 D_2}}. \tag{10.17}$$

Since B_1 and B_2 have been obtained from cross-sections, they are material bucklings. $B^2 > 0$ henceforth in the solution (10.9) we find $J_0(B_1 r)$, a "normal" Bessel function but B_2^2 may be negative and then the term containing B_2 is $J_1(iB_2) \equiv I_1(B_2)$, a modified Bessel function which is small compared to the term $J_0(B_1 r)$ and is negligible almost everywhere but near the

boundary. The flux in group $k =$ is shown in Fig. 10.1, where we see a slowly varying smooth curve. This indicates that if we have something unusual, the anomaly may be detected unless we are too far from the cause of the anomaly. The characteristic distances are

$$L_k = \sqrt{\frac{D_k}{\Sigma_k}}, \tag{10.18}$$

and $L_1 >> L_2$. The range of sensitivity of neutron flux measurement is maximum $3L_1$, the sensitivity exponentially decreases with the distance from the source. Actually, the current of a neutron detector, as a SPND, involves charges released from nuclear reactions with both thermal and epithermal neutrons, so the sensitivity range is usually closer to $2L_2$.

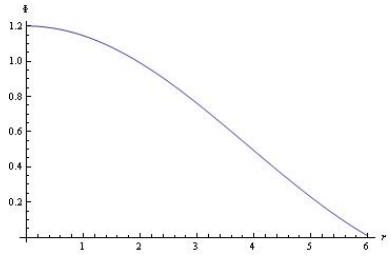

10.1. ábra. Radial flux in the fast group

The next issue we investigate is the detection of a perturbation. One of the goals on an in core surveillance is to detect

- a misplaced fuel assembly;
- flow anomalies;
- anomalies in the reactor behavior.

A possible model of the mentioned anomalies is the appearance of a perturbation. The mathematical model is the appearance of a perturbation in (10.1)-(10.2). There are local and global perturbations in the reactor core. A global perturbation is the change in the temperature of the inlet coolant, a local perturbation may be a control rod motion or a local blockage of the coolant flow in a given assembly.

We consider the anomaly to be detected as a local perturbation of the cross-sections. We keep the two energy group diffusion theory formalism. In the frame of the linear perturbation theory (c.f. Section 4.3) we estimate the flux perturbation caused by the anomaly. We change the notation for a form more suitable for the perturbation formalism. The spatial derivative is multiplied by a diagonal matrix $\mathbf{D}$ in (10.1)-(10.2). The rest of the mentioned equations is collected into another matrix $\mathbf{S}$:

$$\mathbf{D} = \begin{pmatrix} D_1 & 0 \\ 0 & D_2 \end{pmatrix}, \quad \mathbf{S} = \begin{pmatrix} \Sigma_1 - \frac{\chi_1}{k_{eff}}\nu\Sigma_{f1} & -\frac{\chi_1}{k_{eff}}\nu\Sigma_{f2} \\ -\Sigma_{1\to 2} - \frac{\chi_2}{k_{eff}}\nu\Sigma_{f1} & \Sigma_2 - -\frac{\chi_2}{k_{eff}}\nu\Sigma_{f2} \end{pmatrix}. \tag{10.19}$$

Finally, using $\mathbf{D}$ and $\mathbf{S}$, it is expedient to introduce a new matrix $\mathbf{A}$ with the following definition:

$$\mathbf{A} = \mathbf{D}^{-1}\mathbf{S}. \tag{10.20}$$

We represent the anomaly as a change of the cross-sections in matrices $\mathbf{S}, \mathbf{D}, \mathbf{A}$. The unperturbed core is described by

$$\mathbf{D}\boldsymbol{\nabla}^2\underline{\Phi}(r,\phi) + \mathbf{S}\underline{\Phi}(r,\phi) = 0, \tag{10.21}$$

where

$$\underline{\Phi}(r,\phi) = \begin{pmatrix} \Phi_1(r,\phi) \\ \Phi_2(r,\phi) \end{pmatrix} \tag{10.22}$$

comprises the space dependent fluxes in the energy groups.

After the anomaly, the flux distribution is determined from the equation

$$(\mathbf{D}+\delta\mathbf{D})\boldsymbol{\nabla}^2(\underline{\Phi}(r,\phi)+\delta\underline{\Phi}(r,\phi)) + (\mathbf{S}+\delta\mathbf{S})(\underline{\Phi}(r,\phi)+\delta\underline{\Phi}(r,\phi)) = 0. \tag{10.23}$$

In the linear perturbation it is assumed that the product of two perturbed variable is negligible. After rearranging and subtracting (10.21), we get the following expression for the flux perturbation:

$$\boldsymbol{\nabla}^2\delta\underline{\Phi}(r,\phi) + \mathbf{A}\underline{\Phi}(r,\phi) = \underline{Q}, \tag{10.24}$$

where

$$\underline{Q}(q,\phi) = \mathbf{D}^{-1}(\delta\mathbf{D}\boldsymbol{\nabla}^2 + \delta\mathbf{S})\underline{\Phi}(r,\phi). \tag{10.25}$$

It is typical in the first order perturbation theory that the perturbed solution is obtained from a non-homogeneous equation in which the source term is obtained from the solution before the perturbation. The typical solution technique is to find a complete function set and expand the perturbation against that functions. Now the perturbation has a space dependent part, and an energy dependent part. We express the space dependent part in terms of the eigenfunctions (10.5) of the Laplace operator. We express the energy dependent part in terms of the eigenvectors of matrix $\mathbf{A}$ hence our basis involves the functions $u_{jk}(r,\phi)\underline{t}_1, u_{jk}(r,\phi)\underline{t}_2$ where

$$\mathbf{A}\underline{t}_i = \tau_i\underline{t}_i, \quad i = 1,2. \tag{10.26}$$

Let us expand the source term on the chosen basis:

$$\underline{Q} = \sum_{j,k} q_{jk}^{(1)} u_{jk}(r,\phi)\underline{t}_1 + q_{jk}^{(2)} u_{jk}(r,\phi)\underline{t}_2, \tag{10.27}$$

with coefficients $q_{jk}^{(1)}$ and $q_{jk}^{(2)}$. We expand the flux perturbation analogously:

$$\delta\underline{\Phi}(r\phi) = \sum_{jk} c_{jk}^{(1)} u_{jk}(r,\phi)\underline{t}_1 + c_{jk}^{(2)} u_{jk}(r,\phi)\underline{t}_2 \tag{10.28}$$

with unknown coefficients $c_{jk}^{(1)}$ and $c_{jk}^{(2)}$. Exploiting the linear independence of the chosen basis functions, first we substitute (10.28) and (10.27) into equation (10.24), and obtain the following expression:

$$c_{jk}^{(m)} = \frac{q_{jk}^{(m)}}{\lambda_{jk} + \tau_m}. \tag{10.29}$$

Here λ_{jk} is the j-th root of the Bessel function J_k, thus λ_{jk} grows rapidly with j. The perturbation is orthogonal to the solution of the unperturbed solution, therefore $j \neq 0$ and the spatial dependence associated with the largest $c_{jk}^{(m)}$ are

$$J_1(r)\cos(\phi), \quad J_1(r)\sin(\phi).$$

From that we conclude that the lowest order higher harmonics are excited with the largest amplitude. Furthermore, a local perturbation has also non-local spatial effects because

$\cos\phi + \pi = -\cos(\phi)$ indicating that the sign of the perturbation in the solution has the opposite sign at the opposite side of the core. This observation allows for anomaly detection far from the actual place of the anomaly.

Consider a given sufficiently smooth function $f(\mathbf{r})$ in volume V. We measure values of function f at prefixed positions $\mathbf{r}_1, \mathbf{r}_2, \ldots, \mathbf{r}_N$, the measured values are $f(\mathbf{r}_1), f(\mathbf{r}_2), \ldots$ and find those functions that allow for reproducing the entire function in V. When f is a smooth function, we may use interpolation by low order polynomials between adjacent points. Smoothness means that if we have $f(\mathbf{r}_1)$ and $f(\mathbf{r}_2)$ measured so that $|\mathbf{r}_1 - \mathbf{r}_2| < d$ where distance d is derived from the smoothness criterion satisfied by f then we can reproduce f between $\mathbf{r}_1$ and $\mathbf{r}_2$ using linear interpolation:

$$f(\mathbf{r}_1 + a(\mathbf{r}_2 - \mathbf{r}_1)) = (1-a)f(\mathbf{r}_1) + af(\mathbf{r}_2); \;\; 0 \leq a \leq 1. \tag{10.30}$$

Besides the smoothness of f, we need considerations applicable to measured values at distant points. Such a consideration may be based on the symmetry of V.

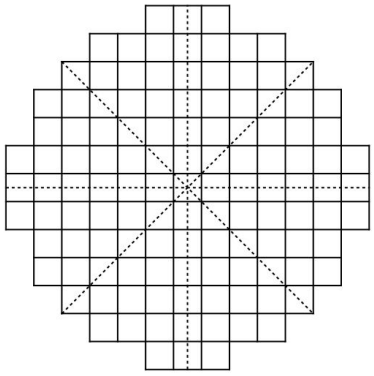

10.2. ábra. A PWR core

Figure 10.2 shows a PWR reactor core V. It is possible to build the core from a 45 degree segment by rotations and reflections. When $f(\mathbf{r})$ possesses the symmetries of V, it suffices to give values of f in one of the 45 degree segments.

But what if $f(\mathbf{r})$ is not symmetric? Then we have to know the $f(\mathbf{r})$ function in all the eight segments because there is no rule how to relate $f(\mathbf{r}_1)$ to $f(\mathbf{r}_2)$ when $\mathbf{r}_1$ and $\mathbf{r}_2$ reside in different segments. But it is known that an asymmetric distribution can not be reduced. In the worst case we have eight different $\mathbf{r}_1, \ldots, \mathbf{r}_8$ positions in the square where $f(\mathbf{r}_i), i = 1, 8$ are all different.

When operating an industrial reactor, the staff tends to establish a symmetric core although there are technical circumstances out of control, like the flow rate and temperature distributions, which are influenced by minor technical details. The result is a function $f(\mathbf{r})$ which is not exactly the same in the eight sectors but they are very close to each other.

A possible theoretical formulation of the situation is as follows. Consider the values of $f(\mathbf{r})$ in symmetric positions that can be transformed into each other by the symmetries allowed by the geometry of the core. Depending on $\mathbf{r}$, we get $1, 4$ or 8 values. One value is associated with $\mathbf{r} = 0$, the origin; four values belong to $\mathbf{r}$ lying on the x and y axes, and

other positions may have eight different values. We know that the fully symmetric function is invariant but what if a function is not invariant and what is the relevance of not invariant component functions?

The answer is obtained by perturbation theory. Studying the solution of a symmetric equation under perturbations, one arrives at the following conclusions:

1. even a symmetric equation has asymmetric solutions;
2. the asymmetric solutions associated with the smallest eigenvalues are stimulated first;
3. the asymmetric eigenfunctions are so similar to the Fourier components that the problem is often studied in a circular domain.

The above observations [113] lead to the below given orthogonal but unnormed vectors:

$$\begin{aligned}
\mathbf{e}_1 &= (1,1,1,1,1,1,1,1) && (10.31)\\
\mathbf{e}_2 &= (0,0,-1,1,0,0,1,-1) && (10.32)\\
\mathbf{e}_3 &= (-1,-1,0,0,1,1,0,0) && (10.33)\\
\mathbf{e}_4 &= (0,0,-1,-1,0,0,1,1) && (10.34)\\
\mathbf{e}_5 &= (-1,1,0,0,1,-1,0,0) && (10.35)\\
\mathbf{e}_6 &= (1,1,-1,-1,1,1,-1,-1) && (10.36)\\
\mathbf{e}_7 &= (1,-1,-1,1,1,-1,-1,1) && (10.37)\\
\mathbf{e}_8 &= (1,-1,1,-1,1,-1,1,-1). && (10.38)
\end{aligned}$$

By using the above vectors as basis, we find that the values of $f(\mathbf{r})$ in the eight sectors would result in decreasing coefficients. Formally, let $\mathbf{f} = (f_1, \ldots, f_8)$ with $f_i = f(\mathbf{r}_i)$, and in its expansion

$$\mathbf{f} = \sum_{i=1} c_i \mathbf{e}_i \tag{10.39}$$

we find c_i to be monotonously decreasing function of i. This leads us to the following conclusions:

- function $f(\mathbf{r})$ is reconstructible without loss of information if the number of nonzero c_i coefficients in the expansion (10.39) equals the number of measured values in the vector $\mathbf{f}(\mathbf{r})$ and the measured values unequivocally determine the missing coefficients.
- the missing values should be filled up by fitting as many c_i coefficients as we need to fill up the all missing values.
- one can estimate [75] the error of the reconstruction by considering all possible selections of the missing components in (10.39)

On the other hand, we may reverse the question. In a core as many measurement are required to reconstruct the measured field (temperature or power distribution) as many assures the reconstruction without information loss.

10.3. Measurement techniques

In-core measurements are used to measure the coolant temperatures and neutron flux or power at given locations. The present Section treats techniques to carry out the measurements and the processing of the measured data.

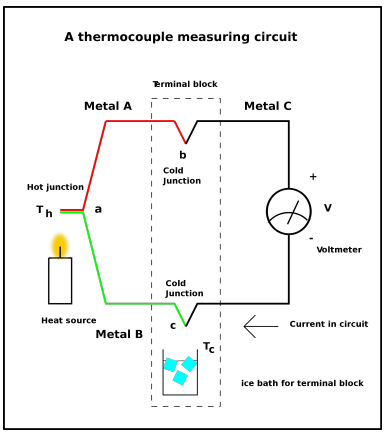

10.3. ábra. Principle of thermocouple (source:Wikipedia)

10.3.1. Temperature measurement

The coolant enters the core at the bottom and exits above the fuel elements. Therefore the temperature is monotonous in the axial variable z. As we need to estimate the maximum temperature, we have to look at the upper part of the core. The temperature of the coolant is measured above the exit from the fuel assemblies. To estimate the maximum, we have to guess the exit temperature of every non-metered assembly. At this point note that if the maximum happens to occur in a non-metered assembly, additional information may be needed.

Thermocouple exploits the thermoelectric effect. When a conductor is subjected to a thermal gradient, it will generate a voltage. This phenomenon is termed as the thermoelectric effect or Seebeck effect[96],[97]. Measure this voltage necessarily involves connecting another conductor to the "hot" leg. Thus a thermocouple is connected to a reference "cold" leg, and to the site where temperature is measured (hot leg). The metal connecting the hot leg to the cold leg will experience the temperature gradient, and for a given metal the voltage and the temperature difference are in a known functional relationship. The voltage needs electrical processing. In a power reactor the thermocouple should be resistive to neutron radiation. In the core, the gamma radiation varies less than for example the thermal neutron flux. That observation has led to a so called gamma temperature measurement method.

The gamma thermometer (GT) is a stainless steel rod with argon-filled annular chambers located at various levels. Differential thermocouples are embedded in the rod at each level so that a temperature difference, proportional to the gamma flux impinging on the rod, is effected between the thermocouple junctions. The gamma thermometer consists of a hollow, cylindrical stainless steel rod of length roughly equal to the reactor core height. Annuli of material are removed at intervals along the rod, and a cladding is swaged onto the exterior in an inert atmosphere. The thermocouple set and associated leads are contained in the rods central core. Basically, the idea behind the dual-purpose application of the gamma thermometer is to utilize the temperature difference between the hot and cold junctions as an indication of the local heat generation rate, and to utilize the shape of the temperature distribution to infer the thermal hydraulic environment exterior to the device.

The measuring system provides a voltage that should be converted to temperature. That step needs a procedure called calibration. During the startup of a reactor with fresh fuel,

there is a stationary state of the reactor. The kinetic energy of the coolant dissipates and warms the coolant up. In the stationary state the heat loss due to radiation and heat conductance equals the dissipated energy and in that state the temperature of the fuel is constant throughout the zone. That state is used for calibration of the thermocouples.

10.3.2. Flux or power measurement

Reaction rate is the only measurable information on the neutron gas therefore the reactor operation is based on reaction rate measurements. A reaction rate $R(\mathbf{r})$ is (see Section 4.3):

$$R_d(\mathbf{r}) = N_d \int_0^\infty \Phi(\mathbf{r}, E)\sigma_d(\mathbf{r}, E)dE. \tag{10.40}$$

To estimate the energy dependent flux, reaction rates R_d should be measured by a number of detectors. In principle, one should determine $\Phi(\mathbf{r}, E)$ from $R_d(\mathbf{r}), d = 1, 2, \ldots$ but only existing mixtures of isotopes are possible detector materials. The technique for reconstructing the energy dependence of the flux is called unfolding [112]. The signal processing technique allows for deriving both neutron flux or thermal, epithermal fluxes. To this end, the sensitivity coefficient ϵ_{ki} should be properly chosen.

Movable detectors were implemented in earlier reactor types, recent reactors are equipped with fixed detectors. The nucleus of the detector material should enter into a nuclear reaction with the neutron and emit a charged particle. Such nuclei are rhodium, vanadium, and platinum. The activation and decay scheme of rhodium is shown in Fig. 10.4. The newly formed nucleus suffers beta decay to ^{104}Pd with decay time $42.3\,s$. The beta decay may happen in more steps. Note that the majority of the electrons appears with a delay larger than $42\ s$. The detectors are arranged in strings so that the neutron distribution in the

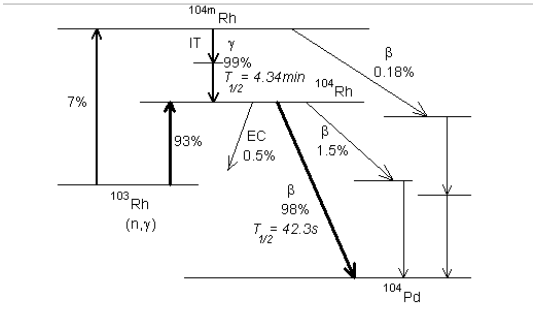

10.4. ábra. Rhodium detector decay scheme

majority of the core height the axial profile be measured. In a core of height $h \simeq 250\ cm$ the detector strings are shown in Fig. 10.5. Length are given in millimeter units in the figure. Note that there is a cable running down to the last detector. The role of that cable is to estimate the parasitic, i.e. current originating from elsewhere than the detector material and carry out a correction.

10.4. Core monitoring

The detector signals should be processed, to carry out corrections, transform the measured electric signal into a physical unit (Celsius degree for the temperature and W/cm for the detector) and check the reliability of the signal. The major steps of those processes are summarized in the two subsections below.

10.4.1. Determination of T_{max}-assembly level

The thermocouple gives a voltage $u_{tc}(t_i)$ which is sampled by an electronics at times $t_1, t_2, \ldots$. The voltage is usually a quadratic function of the temperature difference between the cold point temperature T_c and the temperature to be measured T:

$$u(T) = a_0 + a_1(T - T_c) + a_2(T - T_c)^2. \tag{10.41}$$

In principle, (10.41) holds for every time t_i, T_c is known, so to determine a_i, we have to measure u at T_1, T_2, T_3. This procedure is called calibration and is carried out during the reactor startup period.

From now on measuring $u(t_i)$ we know the $T(t_i)$ the temperature at the measured position at time t_i. The validity of $T(t_i)$ should be checked, if the indicated temperature is nonsensical the measurement should be discarded. Also the variation of the measured temperatures in two consecutive time points may not differ arbitrarily. The limits depend on the actual situation (core power, sampling frequency, reactor type). After that step we have a measured temperature at each position where the temperature measurement is reliable. The next step is to estimate the temperatures at non-metered positions.

In a well equipped core, appr. 60% of the fuel assemblies has temperature measurements and in an assembly usually there are appr. 100 sub-channels so only 1-2 sub-channels out of 1000 has measured info. That makes it clear that only with a suitable model can be stated that there is no limit violation in the given core.

Consider the details of the problem: the energy released from the fuel heats the coolant. To find the enthalpy rise, we have to know the flow rate and the inlet temperature. However, because of technical limitations, no reactor has so detailed instrumentation. The flow rate of a given assembly is derived from a mixing model. Main circulating pumps pump the coolant into the core, and using a simple mixing model, one can determine flow rates of the assemblies. The inlet temperature is determined analogously. But these are models, and we have to verify the model by comparing its results to measurements.

We have at our disposal a measured map T_{mi} for the set of measured positions I_M, i.e. $i \in I_M$. We have a calculated map T_{ci} for all i. Our goal is to estimate T_{mi} for all i. There are three possibilities:

1. We rely on the calculated temperatures;
2. We mix calculated and measured values;
3. We use exclusively the measured values.

The first method is the simplest. It is applicable if the measured values agree with the calculated values. This is formulated as a statistical hypothesis [103][Chapter 7]:

$$T_{mi} = T_{ci}. \tag{10.42}$$

for all metered positions. To verify our hypothesis, the following number is determined:

$$Q^2 = \sum_i \frac{(T_{mi} - T_{ci})^2}{T_{ci}}. \tag{10.43}$$

Here we assume that the "actual values" of the measurements is the calculated temperature. The probability distribution of Q^2 is complicated but in large number of measured points this distribution can be well approximated by a "chi-squared" distribution with $M-1$ degrees of freedom, where M is the number of measured positions. In MATHEMATICA, MATLAB, or MAPLE one can look up the percentage limits of the acceptance of the null hypothesis. For example, 0.05 is the probability that for a 21 element sample $Q^2 > 31.410$.

The second method fits precalculated trial functions to the measurements [100]. Those precalculated trial functions may include tilts, varied control rod positions, spectral variations etc. Let $\phi_k(i)$ signify the value of the kth trial function at position i. Then (10.43) is modified as

$$Q^2 = \sum_i \frac{(T_{mi} - \sum_k c_k \phi_k(i))^2}{T_{mi}}, \tag{10.44}$$

and now we have to minimize Q^2 by properly choosing the c_k coefficients. The method is capable of pointing out specific types of anomalies modeled by one of the trial functions.

In statistical tests, the individual differences between the fitted function and the measurement carries important information [105]. Denote Q^2_{min} the least value of (10.44) that we obtain by minimizing the $Q^2(c_1, c_2, \dots)$ function. Form the following random variable

$$t_i = \frac{t_{mi} - \sum_k c_k \phi_k(i)}{\sqrt{\frac{Q^2_{min}}{M-K}}}, \tag{10.45}$$

of Student distribution. t_i is called Student fraction. The Student distribution is fundamental in statistics, its features are readily available in MATHEMATICA, MATLAB, MAPLE, or other modern symbolic language. The t_i quantity offers a statistical test if the difference between the measured and fitted values is within statistically acceptable limits. From the Student distribution we can fix $\epsilon << 1$ and $\gamma > 1$ pairs such that

$$P\{|t_i| < \gamma\} = 1 - \epsilon. \tag{10.46}$$

The usual choice is $\gamma = 3$, the corresponding ϵ depends on the number of free parameters. If the reader has little experience in evaluating measurements, caution is recommended, it is rather easy to come to wrong conclusions. Usually wrong measurements can be associated with single large values, whereas model change is accompanied by a definite tendency in the Student fraction map, but the careful evaluation is a mixture of science and art [109].

Note that in the first two methods the evaluation relies on the assumption that the precalculated temperature distribution is the temperature distribution in the core. At the same time, the set of non-measured positions may share features. For example, if the geometry of the non-measured positions has a similar geometry (e.g. control rods) that kind of errors are rather hard to unveil.

The third method may be based on the statistical analysis of the temperature distribution in a given class of cores [2]. Using the principal components method [104], we carry out the evaluation in two steps. In the first step we analyze the statistics of a typical temperature distribution of the given class to be evaluated. In the second step, we not only give an estimation for the non-metered assemblies but also may point out outlier measured values.

[2] A fresh zone differs from a burned out zone, a low leakage zone differs from a traditional zone.

Assume that in the first step we analyze a temperature field of N temperature values $T_1, \ldots, T_N$. We define a segment of the field with K values and tally the K temperatures in a segment. We place the segment in every possible different ways on the field. In the first position of the segment we get $T_{11}, T_{12}, \ldots, T_{1K}$. The second time we place the segment elsewhere and get $T_{21}, T_{22}, \ldots, T_{2K}$. We seek new position for the segment until we find a new position different from any previous one. Assume that there are altogether P different positions in the field and we get

$$T_{11}, T_{12}, \ldots, T_{1K}, T_{21}, T_{22}, \ldots, T_{2K} \ldots T_{P1}, T_{P2}, \ldots, T_{PK}. \tag{10.47}$$

Since two positions of the segment in the field must differ, there may be joint points but at least one point must be different. Consequently the number of temperatures in the structure (10.47) is greater than N. When we regard the temperatures in a segment as a vector, it has K components. If the temperature distribution in the field has some kind of internal structure, the majority of the segment positions may be approximated by less than K vectors and we can reconstruct the field from less than N data.

The question is how to find the internal structure. This is done so that we form a $K \times K$ matrix from (10.47) in the following manner:

$$\begin{pmatrix} T_{11} & T_{21} & \ldots & T_{P1} \\ T_{12} & T_{22} & \ldots & T_{P2} \\ \vdots & \vdots & \vdots & \vdots \\ T_{1K} & T_{2K} & \ldots & T_{PK} \end{pmatrix} \begin{pmatrix} T_{11} & T_{12} & \ldots & T_{1K} \\ T_{21} & T_{22} & \ldots & T_{2K} \\ \ldots & \ldots & \ldots & \ldots \\ T_{P1} & T_{P2} & \ldots & T_{PK} \end{pmatrix}. \tag{10.48}$$

In short, we determine the

$$\mathbf{H} = \mathbf{T}^{+}\mathbf{T} \tag{10.49}$$

matrix, its elements are

$$H_{ij} = \sum_{p=1}^{P} T_{pi} T_{jp} = H_{ji} \quad i, j = 1, 2, \ldots, K. \tag{10.50}$$

Matrix $\mathbf{T}$ may be huge, but we have to determine $\mathbf{H}$ only once. The eigenvalues η_m and the associated eigenvectors $\mathbf{h}_m$ carry all information on the temperature field.

$$\mathbf{H}\mathbf{h}_m = \eta_m \mathbf{h}_m, m = 1, 2, ..., K. \tag{10.51}$$

Let the numbering of the eigenvalues be such that $\eta_1 > \eta_2 > \cdots > \eta_K$. Matrix $\mathbf{T}$ is actually an observation. It is a good approximation to place the observed values around their means and use the variance to measure how widely are the observations scattered.

Each eigenvalue is proportional to the portion of the "variance" (more correctly of the sum of the squared distances of the points from their mean) that is correlated with each eigenvector. The sum of all the eigenvalues is equal to the sum of the squared distances of the points from their multidimensional mean. For us this means that most segments can be well approximated as a linear expression of a few eigenvectors provided the eigenvectors are numbered as indicated above.

Originally, the principal component analysis deals with a random vector $\boldsymbol{\xi} = (x_1, \ldots, x_K)$. A linear combination of elements of $\boldsymbol{\xi}$ can be written as $\mathbf{a}^{+}\boldsymbol{\xi}$ and is called standard linear combination if

$$\sum_i a_i^2 = 1,$$

The method looks for a few linear combinations that can be used to summarize the data while losing as little information as possible. When we have missing measurements, it means that elements are missing from the measured values $\boldsymbol{\xi}$. Let $\boldsymbol{\xi}$ be a random vector with mean $\boldsymbol{\mu}$ and covariance matrix $\boldsymbol{\Sigma}$. Then the principal component transformation is

$$\boldsymbol{\xi} \to \mathbf{y} = \mathbf{G}^{+}(\boldsymbol{\xi} - \boldsymbol{\mu}), \tag{10.52}$$

where $\mathbf{G}$ is an orthogonal matrix, $\mathbf{G}^{+}$ is its adjoint, and the covariance matrix determines $\mathbf{G}$ as follows:

$$\mathbf{G}^{+}\boldsymbol{\Sigma}\mathbf{G} \tag{10.53}$$

is a diagonal matrix. The ith principal component of $\boldsymbol{\xi}$ is the ith element of vector $\mathbf{y}$ given as

$$y_i = \mathbf{g}_i^{+}(\boldsymbol{\xi} - \boldsymbol{\mu}). \tag{10.54}$$

Here g_i is the ith column of $\mathbf{G}$. The principal components have the following attractive properties[106]:

1. The sum of the first k eigenvalues divided by the sum of all the eigenvalues represents the the portion of total variation explained by the first k principal components.
2. The principal components of a random vector are not scale invariants.
3. The vector subspace spanned by the first k principal components $1 \leq k \leq K$ has a smaller mean square deviation from the population (or sample) variables than any other k-dimensional subspace.

When a given non-metered assembly falls into more copies of the segment as many predicted values are assigned to it as the number of segments it falls into. This offers an opportunity to reveal wrong measurement, and to estimate the accuracy of the applied method.

Finally a further possibility [107] [108] is mentioned. It is possible to fit parameters (usually one or two parameters) in an approximate equation (usually one- or two-group diffusion equation) so that the solution be closer to the measured values. The function to be minimized is in discretized form-

$$Q = (\Phi - F)^{+}(\Phi - F) + q(w^{+}\Phi - 1) + \Psi^{+}\mathbf{A}(p)\Phi) \tag{10.55}$$

where Φ is the vector of neutron fluxes, F-the vector of measured values, Ψ-the vector of adjacent fluxes; q-normalizing constant; w-weights; p-parameters to be fitted. We have to determine the parameters p, the fluxes Φ and adjoint flux Ψ which minimize Q. That condition gives three equations. The first one is:

$$\frac{\partial Q}{\partial \Psi} = \mathbf{A}(p)\Phi = 0, \tag{10.56}$$

i.e. the flux should be the solution of the diffusion equation. This is an equation for Φ provided p is known.

$$\frac{\partial Q}{\partial \Phi} = \Psi^{+}\mathbf{A}(p) + 2(\Phi - F)^{+}qw^{+} = 0, \tag{10.57}$$

showing that Ψ^{+} should be the solution of the adjoint equation; and finally

$$\frac{\partial Q}{\partial p_i} = \Psi^{+}\frac{\partial \mathbf{A}(p)}{\partial p_i}\Phi = 0. \tag{10.58}$$

The last equation formulates the condition that the parameters should minimize Q.

10.4.2. Determination of T_{max} -subchannel

The range of sensitivity depends on the thermometer but we may assume that it is smaller than the size of an assembly. On the other hand, when the thermometer is located above the assembly, the coolant mixes and we may assume that actually the average outlet temperature of the assembly is measured. Even in that case the following problem remains how to estimate the sub-channel temperature at the position of the measurement?

The answer is provided by a model. Two model types are in use: the sub-channel model and the porous model. The first sub-channel codes written in the sixties and seventies, calculated a one phase flow and took into account the heat and mass exchange among the channels. The next generation codes used two phase flows. The object of the calculation may be a single fuel assembly or the reactor core allowing for inter assembly flow and heat exchange. A well known code of the second generation to solve the sub-channel model is the COBRA code. As we know from thermal hydraulics [66], we can calculate the coolant temperature when the geometry and the flow rate distribution is given. In COBRA, the following model is applied, see Fig. 10.6. The model starts at the top, the power distribution in the selected region (subassembly, SA in the figure) is given as input, as well as the throttling (or driving) zones. From the powers and flow rates, the coolant temperature is calculated using the balance equations. The mixing factors, the fuel pin geometry, the inlet velocity distribution are also part of the input data. This makes it possible to study extreme situations, like bent fuel pins, extraordinary flow patterns.

1. The coolant flow rates are determined in the whole core;
2. flow rates and subassembly temperatures are determined along each sub-channel;
3. the temperature distribution is calculated along each fuel pin.

Some calculations allow for a change in the assembly geometry due to deformation or other reason. In Fig. 10.6 this is indicated by a dashed line.

The same equations govern the flow pattern in the sub-channels as the governing equations of the heat conduction problem. Thus the mass conservation equation, the momentum conservation, furthermore the energy conservation[66] are the basic equations to calculate the flow pattern, i.e. $\mathbf{v}(\mathbf{r}, t)$. The geometry is different, now the fuel is ordered into a regular lattice which is disturbed only at the assembly wall. In the heat balance, the heat generation rate is the energy released from fission and is determined in the neutron physical part of the calculation.

The set of equations to be solved in the sub-channel model is collected and rewritten below. First we set forth the underlying assumptions of the COBRA model.

1. The coolant flow is assumed to be one dimensional, one or two phase flow of slip type.
2. The two phase flow allows for describing the steam content of the coolant as function of the enthalpy, pressure, mass flow, axial position and time.
3. Between adjacent sub-channels turbulent cross-flow may occur. The net cross-flow is assumed to be zero.
4. We may superpose the turbulent and forced cross-flow.
5. Effects traveling with sound speed are neglected.
6. Speed of the cross-flow is negligible compared to the speed of the axial flow.

In a slip flow, the cross-section of the channel is occupied by either steam phase or a liquid phase. In the volume occupied a given phase, material properties and mass flux is assumed uniform. Note that this assumption may be violated, for example in an annular flow the speed of the liquid at the wall may be considerably lower than at other positions. At the same time, the cases having been analyzed by COBRA corroborate the above assumptions.

We study the flow in sub-channel i which is adjacent to sub-channel j. Using the above enlisted assumptions, we formulate the conservation equations. The mass conservation reads as

$$A_i \frac{\partial \rho_i}{\partial t} + \frac{\partial m_i}{\partial x} = -w_{ij}, \tag{10.59}$$

where A_i is the area of sub-channel i. ρ_i is the average sub-channel density:

$$\rho_i = \rho_s \alpha + \rho_l (1 - \alpha) \tag{10.60}$$

where ρ_s is the steam density, ρ_l is the liquid density and α is the steam volume fraction. m_i is the mass flow, w_{ij} is the cross-flow. The sign of w_{ij} is positive when mass flows out of volume i. The turbulent cross-flow does not contribute to the mass balance for it causes no mass change in subvolume i. The time derivative of the density accounts the mass change due to expansion or contraction.

The left hand side of equation (10.60) comprises two terms, the first one is the temporal enthalpy change, there u'' is the effective speed of enthalpy transport. Ultrasonic processes have been neglected, the second term is the enthalpy gradient.

The energy balance is written as

$$\frac{1}{u''} \frac{\partial h_i}{\partial t} + \frac{\partial h_i}{\partial x} = \frac{q_i'}{m_i} - (h_i - h_j) \frac{w_{ij}'}{m_i} - (t_i - t_j) \frac{C_{ij}}{m_i} + (h_i - h^*) \frac{w_{ij}}{m_i}. \tag{10.61}$$

The four terms on the right hand side are:

- The first term represents the heat streaming in from the adjacent sub-channels. Here $(h_i - h_j)$ is the enthalpy difference between sub-channels i and j.
- The second term represents the enthalpy change due to turbulent mixing, w_{ij}' is the turbulent cross-flow at the joint boundary of sub-channels i and j.
- The third term describes the enthalpy loss in consequence of the different sub-channel temperature. C_{ij} is the enthalpy loss caused by cross-flow.
- The fourth term is enthalpy conveyed by the forced cross-flow.

The momentum conservation is separated into axial and radial conservations. The conservation of the axial momentum is assured by the following equation:

$$\begin{aligned} \frac{1}{A_i} \frac{\partial m_i}{\partial t} - 2u_i \frac{\partial \rho_i}{\partial t} + \frac{\partial P_i}{\partial x} = &- \left(\frac{m_i}{A_i} \right)^2 \left[\frac{v_i f_i \phi}{2D_i} + \frac{k_j}{2\Delta x} + A_i \frac{\partial (v_i'/A_i)}{\partial x} \right] \\ &- \rho_l g \cos \vartheta - \frac{f_t}{A_i} (u_i - u_j) w_{ij}' + \frac{1}{A_i} (2u_i - u^*) w_{ij}. \end{aligned} \tag{10.62}$$

Here u_i is the speed of the mass in sub-channel i, P_i is the pressure, v_i is the specific volume of the liquid, v_i' is

$$v_i = \frac{(1-x)^2}{\frac{\rho_l}{1-\alpha}} + \frac{x^2}{\rho_s \alpha} \tag{10.63}$$

the so called momentum transfer effective specific volume. ϑ is the declination angle of the channel from the vertical, g is the gravitation constant, f_t- turbulent momentum correction factor.

The first two terms in equation (10.62) represent the transient component of the axial pressure drop. The right hand side comprises four terms:

1. The first term has three additive components, the first one is the loss due to friction, the second term is the loss due to deformation, the third component is the pressure difference caused by the acceleration.

2. The second term is the pressure drop.

3. The third term is due to the turbulent mixing. In that term the factor f_t is a correction.

4. The fourth term gives the momentum transfer caused by the forced cross-flow.

The radial momentum transfer between sub-channels i and j is expressed with the help of

$$\frac{\partial w_{ij}}{\partial t} + \frac{\partial u^*_{ij} w_{ij}}{\partial x} + \frac{s}{\ell} C_{ij} w_{ij} = \frac{s}{\ell}(p_i - p_j). \tag{10.64}$$

The first term is the effects of the temporal acceleration, the second one of the spatial acceleration, the third of the friction, and finally the fourth term of the pressure difference.

The COBRA model assumes that the cross-directional velocities are small compared to the axial flow, which is usually true in a reactor where the flow direction of the coolant is vertical. The last equation is the state equation

$$\rho_i = \rho(h_i, p^*, m_i, x, t) \tag{10.65}$$

which gives the mass density in sub-channel i as function of enthalpy h_i, the effective pressure p^*, mass flow m_i, position x and time t. Note that (10.65) gives the state equation for a two phase volume.

Equations (10.60) -(10.65) are transformed into a set of linear equations by a suitable numerical method, in COBRA the finite difference approximation is used [3]. The associated boundary conditions fix the entering enthalpy, mass flow, and cross-flow. The initial conditions fix a stationary state [92].

The equations are solvable with appropriate initial and boundary conditions. Initial conditions are required only at modeling transients, the usual initial state of a transient is a well defined stationary flow. The boundary conditions are only loosely determined. Most of the assemblies reside in asymmetric surroundings because the neighboring assemblies may differ (e.g. assemblies of different enrichment have different powers, if one of the neighbors of the assembly under consideration is a reflector, along the joint boundary the power distribution is different, the same holds for an assembly with absorber). That problem is treated in two different ways.

1. The boundary of the assembly calculation is extended so that a portion of each neighboring assembly is included in the calculation. Then the physical properties of the adjacent assemblies are explicitly accounted for but the solution domain increases and the calculation time increases.

2. The boundary conditions are derived from the neighboring assembly either from a separate calculation or only corrections are derived from model problems which take into account the actual properties of the assemblies.

[3]The above described version of COBRA is adapted to VVER-440 reactors by L. Szabados, Gy. Ézsöl, L. Maróti, I. Tóth, I. Trosztel, and J. Vigassy.

In most reactor types, there is no measurement indicating flow anomalies inside the fuel assemblies. Therefore the analysis of flow anomalies (partial or full blockage of sub-channels, the consequence of fuel pin deformation etc.) is carried out on experimental facilities or on computer models. Results of the analysis of sub-channel flow anomalies are used to set up limits for the safe operation and to detect departure from normal flow patterns in a power reactor.

Here we deal with two particular problems.

- Is the value measured by the thermocouples really the temperature T_{out}, the average coolant temperature over the measured fuel assembly?
- How to exploit the sub-channel model in the estimation of the coolant temperature maximum in the core?

The first problem has been analyzed by CFD codes [110] for VVER-440 reactors. The conclusion is that although the measured temperature fluctuates, and often is close to a sub-channel temperature, with minor correction in the evaluation of the measured values it can be considered as the measured average assembly outlet temperature.

The second question is answered by the details of the COBRA model. If the inlet and outlet coolant flow rates and temperatures are known, the assembly power equals the difference of the enthalpy difference. Thus, when running COBRA, the assembly powers can be given as input after the exiting temperatures have been estimated for each assembly. The detailed coolant temperature distribution is obtained from the COBRA calculation and the maximum of coolant temperature is determined.

10.4.3. Determination of W_{max}

The collector of the (SPN) detector gathers charge also from nuclear reactions taking place outside the detector material. To correct the false current called cable current, the measured detector current is subjected to corrections. Let subscript i stand for the assembly number of the SPND string under consideration and we know the α_{ki} correction for the k-th detector in the chain i. Then the corrected $I_{k,i}^{corr}$ is given by

$$I_{k,i}^{corr} = I_{ki}^{meas} - \alpha_{ki} I_i^{cable}, \tag{10.66}$$

where α_{ki} is simply the fraction of the cable current for the the k-th detector in chain i. It is generally accepted to assume that the cable current is proportional with the power density of the given assembly at the given elevation. Therefore

$$\alpha_{ki} = \frac{\int_{z_k}^{H} W_k(z)dz}{\int_{z_{k1}}^{H} W_k(z)dz} \tag{10.67}$$

where $W_k(z)$ is the power density at elevation z in assembly k, z_1 is the elevation of the lowest detector in chain k, H is the core height. The detector sensitivity is a slowly varying function of the detector total discharge, this is taken into consideration by another correction factor which is a multiplicative term in the sensitivity ϵ_{ki}:

$$W_{ki} = \epsilon_{ki} I_{ki}^{corr}, \tag{10.68}$$

and here

$$\epsilon_{ki} = \frac{K_1 K_{2ki} S_{ki}}{(1 - \eta G_{ki})^{\alpha}}, \tag{10.69}$$

and K_{2ki} is the individual sensitivity of detector ki,

$$G_{ki} = \int_0^t I_{ki}^{meas}(\tau) d\tau \tag{10.70}$$

is the total discharge of detector ki. The next correction factor, S_{ki} is responsible for transforming the flux at the position of the detector into assembly power integrated over the height of detector ik. That factor $S_{ki}(b, T_c, W_{ass,k}, C_B)$ depends on

- the local burnup B_k;
- coolant temperature T_c;
- the power $W_{ass,k}$ in assembly k;
- the boron concentration[4] in the coolant c_B.

Through S_{ki}, the sensitivity of the detector depends on global reactor parameters (T_c, c_B) and local parameters $(W_{ass,k}, B_k)$.

To determine the maximum of the axial profile, we create a continuous function by interpolation (for example using MATHEMATICA or MATLAB). Let $\Phi_1, \ldots, \Phi_K$ signify the axial measured values. The interpolating function, called third order spline, takes the form of

$$\Phi(z) = \sum_{i=1}^{3} c_i(\phi_1, \ldots, \Phi_K) z^i. \tag{10.71}$$

From $\frac{d\Phi(z)}{dz} = 0$ we find the locus of the maximum and the maximum itself. Repeating the procedure for each detector string, we get the axial flux profile in the metered assemblies. In practice, the axial core elevation is subdivided into 10 or 20 equidistant elevations and the maximum is picked up.

10.5. Measurement and safety

Reactor operation rests on two pillars: the measurements on the operating reactor and the calculations. The first one reflects the actual state of the reactor; the latter may reflect the actual state of the reactor when the input of the calculation model reflects the actual state of the reactor.

Note that both measured and calculated values rely on an underlying model. When the model is good both the calculation and the measurement reflects the real core state. The main features of the measured values are:

- a power plant is a noisy ambiance in every respect: vibrations, electrical noises, turbulent flow are typical.
- small detectors are subjected to local fluctuations large detectors are slow.
- most measurements are based on a secondary effect in which the physical parameter to be measured is involved. Example: the SPND detector has a long delay, the temperature measurements are exposed to changes in the temperature of the cold leg or the flow pattern, and the fluctuating flow above the assembly may influence the result of the measurement.

[4] subscript B in the boron concentration refers not to burnup but to boron.

- most measured signals go through a signal processing. Filters, amplifiers may bring in phantom effects.

Notwithstanding, the calculated values have the following features:

- the calculated result is at most as good as good is the input. From false input no precise calculated value can be obtained.
- Input is usually taken from measurements. Consequently, the calculated value we get from a deterministic model is actually aleatory.
- The calculations are rarely performed on the basis of first principles. Rather they rely on approximate models. Models usually lead to imprecise results.
- The models lead to mathematical problems that can not be solved in a closed form. Therefore numerical methods are used. The computers store the numbers in an approximate form, as simple operations like additions may lead to noticeable round-off errors. Numerical methods (solution of large linear equation sets, differentiations, integration, iterative methods etc) augment the error in the results.

At the same time, if we have two statistically independent values (distributions or other characteristics of the reactor) and they agree reasonably, we may say: the result is correct. To determine what a reasonable agreement is, one may apply the experimental technique or the calculation model to simple, well determined cases and estimate the maximum of the possible errors. To be on the safe side, when the operational limits are determined, in the case of the safety related key parameters an engineering reserve is added [115][p. 34], see Fig. 10.7 where four curves are shown. Each curve represents some anomalies. When a measured value (e.g. a temperature maximum) exceeds the curve, an alarm signal is sent to the plant operator to take some action in accordance with the hierarchy given below.

- Curve No. 1: Alarm Setting Exceeded. The operator is alerted to take measures to reduce the temperature.
- Curve No. 2: Operational Limit Exceeded. It is normal to have margins between alarm settings and operational limits in order to take account of routine fluctuations arising in normal operation. There may also be a margin between the operational limit and the safety system setting to allow the operator to take action to control a transient without activating the safety system.
- Curve No. 3: Safety System Setting Exceeded. The monitored parameter might reach the safety system setting at point A with the consequence that the safety system is actuated. This corrective action only becomes effective at point B owing to inherent delays in the instrumentation and equipment of the safety system. The response should be sufficient to prevent the safety limit being reached, although local fuel damage cannot be excluded.
- Curve No. 4: Safety Limit Exceeded. In the event of a failure that exceeds the most severe one that the plant was designed to cope with, or a failure or multiple failures in a safety system, it would be possible for the temperature of the cladding to exceed the value of the safety limit, and hence significant amounts of radioactive material could be released. Additional safety systems may be actuated by other parameters to bring other engineered safety features into operation to mitigate the consequences, and measures for accident management may be activated.

Note, that some planned transients may reach Curve No. 1, some failure may lead to reaching curve No. 2. The arrangement of the four mentioned curves allow time for the operator to take actions to prevent the aggravation of the conditions, see the bottom figure. The limits should be set so that the realistic response time would revert the curve before it would reach the next curve.

The same considerations apply for either one of the two measured distributions. The independent temperature and power measurements offer an error estimation as well. One can determine the assembly power from temperature measurement and from SPND signals. Comparing the two powers carries important information because if there is a flow anomaly, the power calculated from temperatures will be higher. The time variations of the temperature and W differ, all these carry important information for the analyst.

10.6. Problems

1. Assume that the detectors are equidistantly positioned. What is the importance of the detectors?
2. Determine the axial offset k_z when one detector gives false signal in the SPN string!
3. Determine the axial offset k_z when two detectors give false signal in the SPN string!
4. Estimate the radial power peaking factor k_q when all detectors are reliable!
5. Estimate the radial power peaking factor k_q when a fraction of the detectors are false!
6. Estimate the radial power peaking factor k_q when the detectors in a given zone are false!
7. Estimate the sector power ratios when the detectors in a given zone are false!
8. Estimate the maximal temperature rise ΔT in the core when all the detectors work!
9. Propose an estimation for the maximal subchannel temperature in the core!
10. Estimate the maximum power density in the core from the measured values!

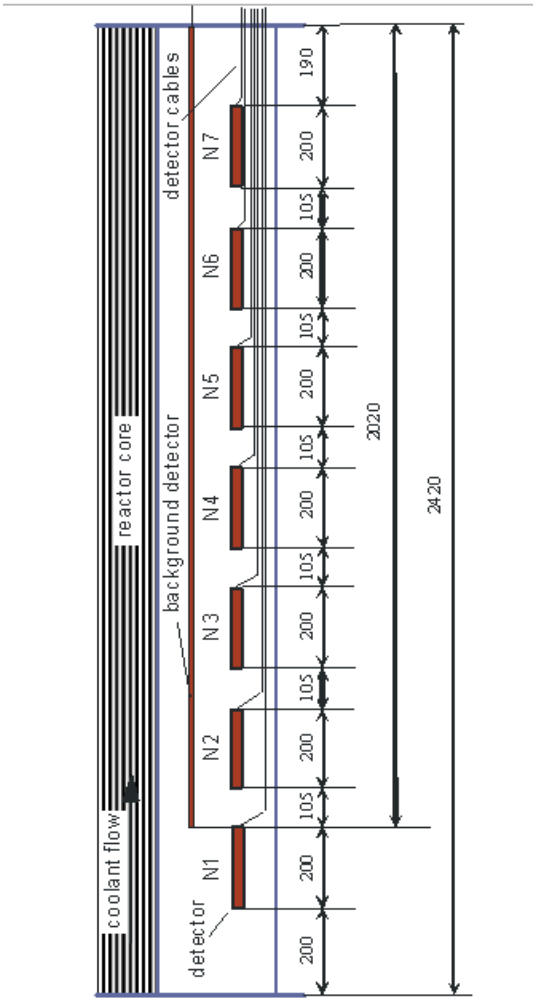

10.5. ábra. SPND detector string

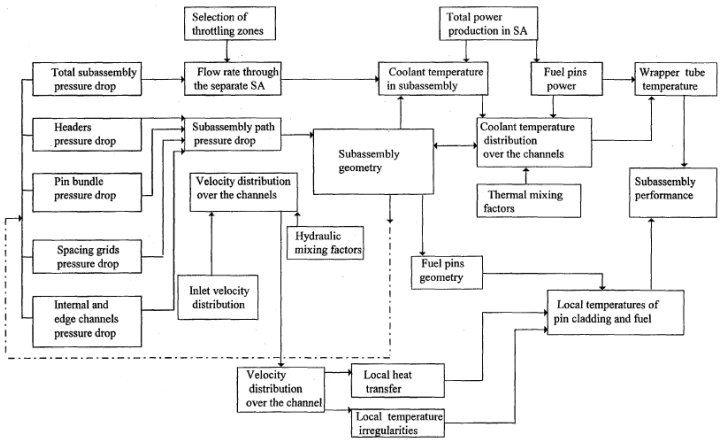

10.6. ábra. Thermal hydraulics analysis of an assembly (source: IAEA web site)

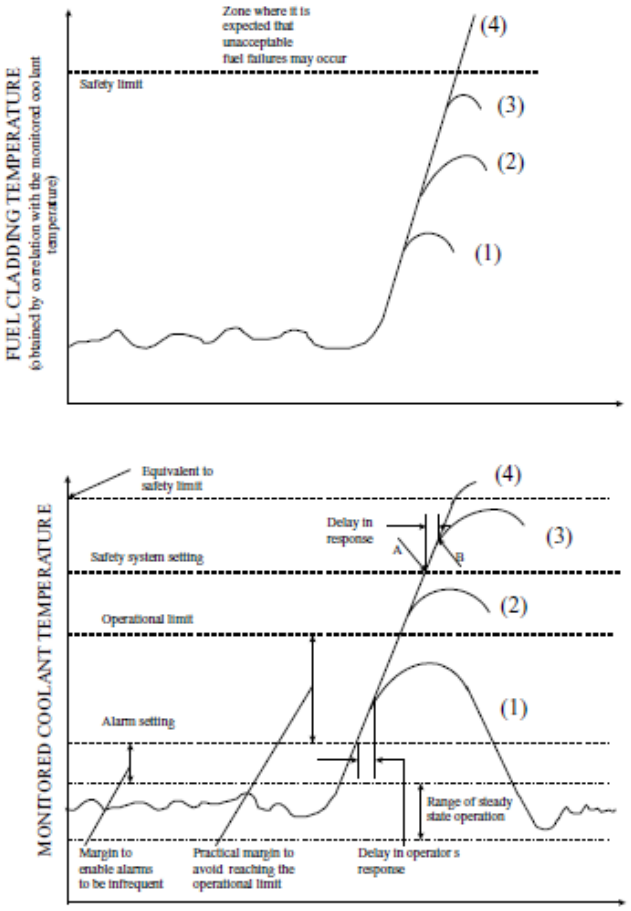

10.7. ábra. Interrelationship between a safety limit, a safety system setting and an operational limit.

11. fejezet

Appendix A: Mathematical Basics

A vector is written in bold: $\mathbf{u} = (u_1, u_2, u_3), \mathbf{v} = (v_1, v_2, v_3)$. A tensor is set in "mathrm" type: P and has three rows and three columns. Scalar variables are set in mathematical expressions in "italics" type. Dot product of two vectors gives a scalar:

$$\mathbf{u}^{+}\mathbf{v} = \sum_{i=1}^{3} u_i v_i. \tag{11.1}$$

dyadic product of two vectors gives a tensor T:

$$\mathbf{v}\mathbf{u}^{+} = \mathrm{T} \tag{11.2}$$

and $T_{ij} = v_i u_j$. The following products of tensor and vector are available:

$$(\mathbf{v}^{+}\mathrm{T})_i = \sum_{k=1}^{3} v_k T_{ki} \tag{11.3}$$

$$(\mathrm{T}\mathbf{v})_i = \sum_{k=1}^{3} T_{ik} v_k. \tag{11.4}$$

We use the following tensor products: the tensorial product

$$(\mathrm{S} \cdot \mathrm{T})_{ik} = \sum_{j} S_{ij} T_{jk} \tag{11.5}$$

and the scalar product:

$$(S : T)_{ik} = \sum_{i,j=1}^{3} S_{ij} T_{jk}. \tag{11.6}$$

A special vector is the Nabla operator $\boldsymbol{\nabla} = \left(\frac{\partial}{\partial x_1}, \frac{\partial}{\partial x_2}, \frac{\partial}{\partial x_3}\right)$. The usual operations are

$$\begin{aligned}
\boldsymbol{\nabla}\mathbf{v} &= \sum_{i=1}^{3} \frac{\partial v_i}{\partial x_i} \quad \text{the divergence of } \mathbf{v} \\
\boldsymbol{\nabla} a &= \left(\frac{\partial a}{\partial x_1}, \frac{\partial a}{\partial x_2}, \frac{\partial a}{\partial x_3}\right) \quad \text{the gradient of } a \\
\boldsymbol{\nabla} \times \mathbf{v} &= \Big(\frac{\partial v_z}{\partial x_2} - \frac{\partial v_y}{\partial z}; \\
\frac{\partial v_x}{\partial x_3} - \frac{\partial v_z}{\partial x}; &\frac{\partial v_x}{\partial x_2} - \frac{\partial v_y}{\partial x};\Big) \quad \text{the curl of } \mathbf{v}.
\end{aligned} \tag{11.7}$$

We need the following tensor operations:

$$\mathrm{Grad}\mathbf{v} = (\mathrm{Grad}\mathbf{v})^s + (\mathrm{Grad}\mathbf{v})^a \tag{11.8}$$

where the symmetric derivative is

$$(\mathrm{Grad}\mathbf{v})^s_{ik} = \frac{1}{2}\left(\frac{\partial v_k}{\partial x_i} + \frac{\partial v_i}{\partial x_k}\right), \tag{11.9}$$

the asymmetric derivative is

$$(\mathrm{Grad}\mathbf{v})^a_{ik} = \frac{1}{2}\left(\frac{\partial v_k}{\partial x_i} - \frac{\partial v_i}{\partial x_k}\right). \tag{11.10}$$

We need also the tensor derivative:

$$\boldsymbol{\nabla}\mathrm{T} \equiv \mathrm{DivT} = \sum_{k=1}^{3} \frac{\partial T_{ki}}{\partial x_k}. \tag{11.11}$$

The scalar operator of directional derivative $\mathbf{u}\boldsymbol{\nabla}$ applied to vector $\mathbf{v}$ is

$$(\mathbf{u}\boldsymbol{\nabla})\mathbf{v} = \sum_{k=1}^{3} u_k \frac{\partial}{\partial x_k}\mathbf{v}. \tag{11.12}$$

11.1 Theorem (Helmholtz theorem) *Any vector field* $\mathbf{v}$*, which is finite, uniform, and continuous and which vanishes at infinity, may also be expressed as the sum of a gradient of a scalar* ϕ *and a curl of a zero divergence vector* $\mathbf{A}$*:*

$$\mathbf{v} = \boldsymbol{\nabla}\phi + \mathbf{curlA}; \quad \boldsymbol{\nabla}\mathbf{A} = 0.$$

See Morse-Feschbach, I. p. 52-52.

$K_0(r)$ function. Ki_1 Bickley functions. The Bickley function of order n is defined as

$$Ki_n(x) = \int_0^{\pi/2} \cos^{n-1}\theta e^{-x/\cos\theta} d\theta = \int_0^{\infty} \frac{e^{-x\cosh(u)}}{\cosh^n(u)} du. \tag{11.13}$$

Properties:

1. Bickley functions decrease monotonously for $0 \leq x < \infty$;
2. the exponential behavior becomes pronounced for large arguments;
3. the n-th derivative has a logarithmic singularity at $x = 0$;
4. $Ki_0(x) = K_0(x)$ where $K_0(x)$ is the modified Bessel function of the second kind and order zero.

The Bickley functions are given by three polynomials $U_n(x), V_n(x), W_n(x)$:

$$Ki_n(x) = W_n(x) + (-x)^n \left(U_n(x) - V_n(x)\ln(x/2)\right). \tag{11.14}$$

The three polynomials are

$$W_n(x) = \sum_{m=0}^{n-1} w_{n,m} x^m; \;\; W_0(x) \equiv 0; \tag{11.15}$$

$$U_n(x) = \sum_{m=0}^{n-1} u_{n,m} \left(\frac{x}{2}\right)^{2m} \tag{11.16}$$

$$V_n(x) = \sum_{m=0}^{n-1} v_{n,m} \left(\frac{x}{2}\right)^{2m}. \tag{11.17}$$

The coefficients in the series are defined recursively:

$$w_{n.m} = -\frac{1}{m} w_{n-1,m-1}, m = 1, 2, \ldots, n-1; \tag{11.18}$$

$$u_{n,m} = \frac{(2m+n)u_{n-1,m} + v_{n-1,m}}{(2m+n)^2}; m = 0, 1, \ldots \tag{11.19}$$

$$v_{n,m} = \frac{1}{2m+n} v_{n-1,m}. \tag{11.20}$$

The initial values are defined as

$$w_{n,0} = \frac{1}{2}\sqrt{\pi}\frac{(n/2-1)!}{((n-1)/2)!} \tag{11.21}$$

$$v_{0,m} = \frac{1}{(m!)^2} \tag{11.22}$$

the third polynomial is defined with the help of the digamma function Ψ:

$$u_{0,m} = \frac{\Psi(m+1)}{(m!)^2} \tag{11.23}$$

$$\Psi(m+1) = 1 + \frac{1}{2} + \cdots + \frac{1}{m} - \gamma, \tag{11.24}$$

where γ is the Euler's constant

$$\gamma = 0.57721\ 56649\ 01533\ldots. \tag{11.25}$$

Fredholm theorem, Kreyszig, p. 451 A bounded linear operator $\mathcal{A}$ that maps $\mathbb{X}$ into itself is said to satisfy the Fredholm alternative if $\mathcal{A}$ is such that either (I) or (II) holds:

(I) The homogeneous equations

$$\mathcal{A}x = y\mathcal{A}^+ f = g, \tag{11.26}$$

where $\mathcal{A}^+$ is the adjoint operator of $\mathcal{A}$ have solutions x and f for every $y \in \mathbb{X}$ and $g \in \mathbb{X}^+$, the solutions being unique. The corresponding homogeneous equations

$$\mathcal{A}x = 0\mathcal{A}^+ f = 0 \tag{11.27}$$

have only trivial solutions $x = 0$ and $f = 0$, respectively.

(II) The homogeneous equations

$$\mathcal{A}x = 0\mathcal{A}^+ f = 0 \tag{11.28}$$

have the same number of linearly independent solutions $x_1, \cdots, x_n$ and $f_1, \cdots, f_n$, respectively. The nonhomogeneous equations

$$\mathcal{A}x = y\mathcal{A}^+ f = g, \tag{11.29}$$

are not solvable for all y and g, respectively; they have a solution if and only if y and g are such that the scalar products $(f_k, y) = 0$ and $(g, x_k) = 0$ $k = 1, \cdots, n$, respectively.

11.2 Theorem (Fredholm alternative) *Let operator $\mathcal{T}$ be a compact operator map the normed space $\mathbb{X}$ into itself and let $\lambda \neq 0$. Then operator T_λ satisfies the Fredholm alternative.*

Modified Bessel functions. A solution to the Laplace equation

$$\boldsymbol{\nabla}^2 \Phi(\mathbf{r}) = 0 \tag{11.30}$$

in cylindrical coordinates (ρ, ϕ, z), where

$$x = \rho\cos\phi; \quad y = \rho\sin\phi; \quad z = z \tag{11.31}$$

is often sought in separable form $\Phi(\phi, \rho, z)$, and when Φ is independent of ϕ, the separation is written as $\Phi(\rho, z) = R(\rho)Z(z)$. The involved functions are obtained from the following equations:

$$R'' + \frac{1}{\rho}R' + \lambda^2 R = 0 \tag{11.32}$$

$$Z'' = \lambda^2 Z. \tag{11.33}$$

This is a special case of the Bessel's differential equation:

$$x^2\frac{d^2y}{dx^2} + x\frac{dy}{dx} + (x^2 - p^2)y = 0, \tag{11.34}$$

its general solution is

$$y(x) = c_1 J_p(x) + c_2 Y_p(x) \tag{11.35}$$

where $J_p(x)$ the Bessel function of the first kind, $Y_p(x)$ is the Bessel function of the second kind.

The modified Bessel equation is obtained from (11.34) by the substitution $x \to ix, i^2 = -1$:

$$x^2\frac{d^2y}{dx^2} + x\frac{dy}{dx} - (x^2 + p^2)y = 0, \tag{11.36}$$

its general solution is

$$y(x) = c_1 I_p(x) + c_2 K_p(x). \tag{11.37}$$

Here $I_p(x)$ and $K_p(x)$ is the modified Bessel-function of the first and second kind, respectively. The modified Bessel functions I_p and K_p are defined as

$$I_p(x) = i^{-p}J_p(ix), \tag{11.38}$$

and

$$K_p(x) = \frac{\pi}{2}\frac{I_{-p}(x) - I_p(x)}{\sin(p\pi)}. \tag{11.39}$$

The J_p, Y_p, I_p, K_p Bessel functions are available in most symbolic algebra programs (e.g. MATHEMATICA, MATLAB, MAPLE).

The principal value integral serves the evaluation of the integral of a singular function. Let $f(x)$ have a singularity at $x = 0$, and $a, b > 0$, then

$$\int_{-a}^{+b} f(x)dx = \lim_{\varepsilon\to 0}\left[\int_{-a}^{+\varepsilon} f(x)dx + \int_{\varepsilon}^{+b} f(x)dx\right] \tag{11.40}$$

is called the Cauchy principal value integral [59] of the function $f(x)$.

Function $f(x)$ is Hölder continuous if

$$f(x_1) - f(x_2) = c||x_1 - x_2||^\alpha \tag{11.41}$$

where $0 \le \alpha \le 1$.

In the response matrix method, we used the so called Walsh functions. Consider a function $f(\alpha), 0 \le \alpha \le 2\pi$, which labels the boundary points of a regular n-gon. The Walsh

functions take values ± 1 on discrete subintervals of $[0, 2\pi]$, they are step functions. We are considering only the Walsh functions on $2n$ subintervals of equal length. There are 2^{2n} such distinct Walsh functions $W_i(\alpha)$.

Let $W_i(\alpha)$ be a Walsh function. A possible representation of $W_i(\alpha)$ is the $2n$-tuple $\mathbf{w}_i$ where element k of $w_i = +1$ if $W_i(\alpha) = +1$ when $(k-1)\beta \leq \alpha \leq k\beta$. A representation of function $f(\alpha)$ is $\mathbf{f}(\alpha)$ where element k of $\mathbf{f}(\alpha)$ is $f(\alpha), (k-1)\beta \leq \alpha \leq k\beta$.

The scalar product of $\mathbf{f}(\alpha)$ and $\mathbf{w}_i$ is the usual dot product of vectors:

$$(\mathbf{f}(\alpha), \mathbf{w}_i) = \sum_{k=1}^{2n} f_k(\alpha)_i w_{ik}, 1 \leq k, i \leq 2n; \tag{11.42}$$

a scalar function depending on α. Each $f_k(\alpha)$ is defined on a π/n wide interval so they can be mapped unequivocally onto the $[0, \pi/n]$ interval. When $f_k(\alpha)$ varies slowly, approximation by low order polynomials may be used.

Let $\mathcal{A}$ be a linear operator acting on variable x. The independent variable x involves the space variable $\mathbf{r}$ but may involve further variables (e.g. energy) as well. Consider the boundary value problem

$$\mathbf{A}\Phi(x) = Q(x); \tag{11.43}$$

in volume V and on the boundary $\mathbf{r} \in \partial V$ of V the boundary condition be $\Phi(x) = 0$.

The Green's function of (11.43) is the solution of the problem

$$\mathcal{A}\mathcal{G}(x, x') = \delta(x - x') \tag{11.44}$$

in V and

$$\frac{\partial \mathcal{G}(x, x')}{\partial \mathbf{r}} = 0, \quad \mathbf{r} \in \partial V. \tag{11.45}$$

The solution to (11.43) is given with the help of the Green's function as

$$\Phi(x) = \int_V \mathcal{G}(x, x') Q(x') dx'. \tag{11.46}$$

The Green's function is applied to solve the one group or multigroup diffusion equation in Chapter (6), the transport equation in Chapter (5).

12. fejezet

Appendix B: Basic Thermal Hydraulics Codes

The **ATHLET** code [91] was developed by GRS (Germany) for the thermal hydraulics analysis of leaks, breaks and transient processes in a power reactor. It is also applicable to severe accident modelling.

The **CATHARE** code [93] was developed by a French consortium including AREVA, CEA, EDF, IRSN. CATHARE is an advanced code for PWR modeling.

RELAP5 [94] is a best estimate system code suitable for the analysis of all transients and postulated accidents in LWRs.

COBRA [92] is a thermal hydraulics code for transient analysis of PWR nuclear reactor vessels and primary coolant systems. COBRA is capable of loss of coolant accident analysis as well.

MELCORE [95] is a severe accident analysis code, developed by Sandia Laboratory for the US Nuclear Regulatory Commission.

13. fejezet

Appendix C: Kolmogorov Forward and Backward Equation, Pál–Bell equation

Let ξ stand for a discrete random variable and let

$$p_k = P\{\xi = k\} \tag{13.1}$$

stand for the probability of the event $\xi = k$.

The function

$$g(z) = \sum_{k=0}^{\infty} p_k z^k \tag{13.2}$$

is called the generating function of the discrete variable ξ.

Using the generating function, we can obtain the mean value of the random variable ξ as

$$E\{\xi\} = \left.\frac{dg(z)}{dz}\right|_{z=1}. \tag{13.3}$$

In general, the derivatives of the generating function are connected to the moments of the discrete random variable ξ. As an illustration, the second derivative of the generating function is:

$$\frac{d^2 g(z)}{dz^2} = E\{\xi^2\} - E\{\xi\}. \tag{13.4}$$

From (13.3) and (13.4)

$$D^2\{\xi\} = g''(1) + g'(1)(1 - g'(1)). \tag{13.5}$$

where $D^2\{\xi\}$ is the variance and $D\{\xi\}$ is the standard deviation.

The autocorrelation function

$$R(x_1, x_2) = E\{\mathbf{\Phi}(x_1)\mathbf{\Phi}(x_2)\} = \int_{-\infty}^{+\infty} u_1 u_2 f(u_1, u_2; x_1, x_2) du_1 du_2. \tag{13.6}$$

The autocovariance of the random process $\mathbf{\Phi}(x)$ is

$$C(x_1, x_2) = E\{(\mathbf{\Phi}(x_1) - \eta(x_1))(\mathbf{\Phi}(x_2) - \eta(x_2))\}, \tag{13.7}$$

The power spectrum of the stochastic process $\mathbf{\Phi}(x)$ is the Fourier transform of its autocorrelation:

$$S(\omega_1, \omega_2) = \int_{-\infty}^{+\infty} e^{-i\omega_1 x_1} e^{-i\omega_2 x_2} R(x_1, x_2) dx_1 dx_2. \tag{13.8}$$

The cross-power spectrum of two random processes $\mathbf{\Phi}_1(x), \mathbf{\Phi}_2(y)$ is

$$S_{\Phi_1\phi_2}(\omega_1, \omega_2) = \int_{-\infty}^{+\infty} e^{-i\omega_1 x_1} e^{-i\omega_2 x_2} R_{\Phi_1\Phi_2}(x_1, x_2) dx_1 dx_2. \tag{13.9}$$

The Pál-Bell equation is a so called backward Kolmogorov type equation, its form is an integro-differential equation for the generating function $g(t_0, \mathbf{u}_0; t, z)$ of the neutron distribution:

$$\frac{\partial g(t_0, \mathbf{u}_0; t, z)}{\partial t_0} + \mathcal{T} g(t_0, \mathbf{u}_0; t, z) + Q_f(t_0, \mathbf{r}_0, v_0) q[s(t_0, \mathbf{r}_0, \mathbf{v}_0; t, z)|v_0] + Q_a(t_0, \mathbf{r}_0, v_0) = 0 \tag{13.10}$$

where $\mathcal{T}$ is the so called transport operator:

$$\begin{aligned} \mathcal{T} g(t_0, \mathbf{u}_0; t, z) &= -Q_0(t_0, \mathbf{r}_0, v_0) g(t_0, \mathbf{u}_0; t, z) + \mathbf{v}_0 \boldsymbol{\nabla} g(t_0, \mathbf{u}_0; t, z) + \\ &+ Q_s(t_0, \mathbf{r}_0, v_0) \int w_s(\mathbf{v}_0, \mathbf{v}') g(t_0, \mathbf{r}\mathbf{r}_0, v_0; t, z) d^3\mathbf{v}'. \end{aligned} \tag{13.11}$$

Here $\mathbf{u} = (\mathbf{r}, \mathbf{v})$ is a point in the configuration space composed of the position $\mathbf{r}$ and velocity $\mathbf{v}$ of the neutron. We assume the neutron to enter into interaction with the surrounding the reaction rate at time t, position $\mathbf{r}$ for a neutron having the speed v is $Q(t, \mathbf{r}, v)$ and three types of interactions are possible: absorbtion, scattering, and fission; the mention reactions exclude each other thus

$$Q(t, \mathbf{r}, v) = Q_a(t, \mathbf{r}, v) + Q_s(t, \mathbf{r}, v) + Q_f(t, \mathbf{r}, v). \tag{13.12}$$

The initial and boundary conditions associated with (13.10) are:

$$\lim_{t \to t_0} g(t_0, \mathbf{u}_0; t, z) = 1 - (1 - z)\Delta(\mathbf{u}_0, \mathbf{u}), \tag{13.13}$$

where $\Delta(\mathbf{u}_0, \mathbf{u})$ is Cronecker's delta function which is 1 when $\mathbf{u}_0 = \mathbf{u}$ and zero otherwise,

$$\lim_{\mathbf{r}_0 \to \mathbf{r}_s} g(t_0, \mathbf{u}_0; t, z) = 1 \tag{13.14}$$

provided the directions of speeds $\mathbf{v}_0$ and $\mathbf{v}_s$ are such that $\Omega_0 \Omega_s > 0$ holds for the directions.

The second term in the Pál-Bell equation (13.10) describes the fission process. Here the following model has been adopted. In a fission reaction ν_0 prompt neutron appears and $\nu_1, \ldots, \nu_\ell$ so called fragments which emit neutrons in a decay with decay time $\lambda_1, \lambda_2, \ldots, \lambda_\ell$. Let the fragment emitting prompt neutrons be of type A, the fragments emitting neutrons after a delay be of type $B_1, \ldots, B_\ell$. We define

$$P\{\nu_0 = k_0, \nu_1 = k_1, \ldots, \nu_\ell = k_\ell | v_0\} = f(k_0, k_1, \ldots, k_\ell | v_0) \tag{13.15}$$

giving the probability of k_0 fragments of type A, and $k'_j \leq k_j, j = 1, \ldots, \ell$ fragments of type B_j. We introduce the generating function

$$q(z_0, z_1, \ldots, z_\ell) = \sum_{k_0, k_1, \ldots, k_\ell} f(k_0, k_1, \ldots, k_\ell | v_0) z_0^{k_0} z_1^{k_1} \ldots z_\ell^{k_\ell}, \tag{13.16}$$

and the following concise notation

$$\{k_0, k_1, \ldots, k_\ell\} = \mathbf{k}, \quad \{z_0, z_1, \ldots, z_\ell\} = \mathbf{z},$$

and the generating function (13.16) takes as compact form as

$$q(\mathbf{z} | v_0) = \sum_{\mathbf{k}} f(\mathbf{k} | v_0) \mathbf{z}^k. \tag{13.17}$$

Tárgymutató

Irodalomjegyzék

[1] The Future of the Nuclear Fuel Cycle, An Interdisciplinary MIT Study, MIT, 2010

[2] Glasstone, S. and Edlund, M. C.: The Elements of Nuclear Reactor Theory, D. Van Nostrand, Princeton (1952)

[3] R. Soule and et al., Neutronic studies in support of accelerator-driven systems: The MUSE experiments on the MASURKA facility, Nuclear Science and Engineering, vol. **148**, pp. 124-152, 2004.

[4] Casti, J.: Nonlinear system theory, Academic Press, London, 1985

[5] Ronen, Y. (Ed.): *CRC Handbook of Nuclear Reactor Calculations*, vol. II, CRC Press, Boca Raton, 1986

[6] Csom, Gy.: *Nuclear power plant operation theory*, Volume II., Operation theory of nuclear power plants applied for energy production, Part 1, Műegyetemi Kiadó, Budapest, 2005 (in Hungarian)

[7] Z. Szatmáry: Are we running out of uranium at the Earth? *Fizikai Szemle* 2010/4. (in Hungarian)

[8] Nuclear Energy Institute (NEI), www.nei.org

[9] The nuclear power cycle (Areva brochure), www.areva.com

[10] `http://www.iaea.org/cgi-bin/db.page.pl/pris.charts.htm`, IAEA Power Reactor Information System (PRIS) Database

[11] `http://nuclear.gov/genIV/neGenIV1.html`

[12] UK-EPR Pre-Construction Environmental Report (PCER), Sub-chapter 1.2: General description of the unit, UKEPR-0003-012 Issue 01, Areva NP & EdF, September 2009

[13] Status of advanced light water reactor designs, IAEA-TECDOC-1391, IAEA, May 2004.

[14] EPR Technical Description, AREVA-NP, http://www.areva-np.com

[15] Schulz T.L.: Westinghouse AP1000 advanced passive plant, Nuclear Engineering and Design, 236 (2006), p. 1547-1557.

[16] http://www.ap1000.westinghousenuclear.com

[17] Modern Instrumentation and Control for Nuclear Power Plants: A Guidebook, IAEA Technical Report Series No. 387, IAEA, Vienna, 1999.

[18] Safety Objectives for New Power Reactors, WENRA Reactor Harmonization Working Group, December 2009.

[19] Defence in Depth in Nuclear Safety, Report INSAG-10, IAEA, Vienna, 1996.

[20] `http://www.tvo.fi`

[21] `http://www.mhi.co.jp`

[22] `http://www.nrc.gov`

[23] `http://www.wikipedia.org`

[24] Turso, J. A., March-Leuba, J., Edwards, R. M.: A modal-based reduced order model ov BWR out of physe instabilities, Ann. nucl. Energy, **24**, 921-934(1997)

[25] Cacuci, D. G.: Sensitivity Analysis and Uncertainty Analysis, Chapman and Hall/CRC Book, Boca Raton

[26] H. G. Schuster: Deterministic Chaos,Physik-Verlag, Weinheim, 1984

[27] recommended programming practices to facilitate the portability of scientific and engineering computer programs, an American National Standard, ANSI/ANS-10.2-1988, American Nuclear Society La Grange Park, IL, USA

[28] guidelines for the documentation of digital computer programs, an American National Standard, ANSI/ANS-10.3-1986, American Nuclear Society La Grange Park, IL, USA

[29] guidelines for the verification and validation of scientific and engineering computer programs for the nuclear industry, an American National Standard, ANSI/ANS-10.4-1987, American Nuclear Society La Grange Park, IL, USA

[30] guidelines for considering user needs in computer program development, an American National Standard, ANSI/ANS-10.5-1986, American Nuclear Society La Grange Park, IL, USA

[31] nuclear data sets for reactor design calculations,an American National Standard, ANSI/ANS-19.3-1983, American Nuclear Society La Grange Park, IL, USA

[32] the determination of neutron reaction rate distributions and reactivity of nuclear reactors,an American National Standard, ANSI/ANS-19.3-1983, American Nuclear Society La Grange Park, IL, USA

[33] the determination of thermal energy deposition rates in nuclear reactors, an American National Standard, ANSI/ANS-19.3.4-1976, American Nuclear Society La Grange Park, IL, USA

[34] a guide for acquisition and documentation of reference power reactor physics measurements for nuclear analysis verification, an American National Standard, ANSI/ANS-19.4-1978, American Nuclear Society La Grange Park, IL, USA

[35] requirements for reference reactor physics measurements,an American National Standard, ANSI/ANS-19.5-1976, American Nuclear Society La Grange Park, IL, USA

[36] Design of Reactor Cores of pressurized Water and Boiling Water Reactors; Part 1: Principles of Thermohydraulic Design, Nuclear Safety Standard Commission (KTA), Federal republic of Germany, 1980

[37] Marmier, P., Sheldon, E.: Physics of Nuclei and Particles, Vol. 1, Academic Press Naw York and London, 1969

[38] Bowler, M. G.: Nuclear Physics, Pergamon Press, (1973)

[39] Krane, K. S.: Introductory Nuclear Physics, John Wiley & Sons, New York, 1988.

[40] Cetnar, J.: General solution of Bateman equations for nuclear transmutations, *Annals of Nuclear Energy*, **33**, 640–645, 2006.

[Duder] J. J. Duderstadt, W. R. Martin: Transport Theory, Wiley Interscience, New York, 1979

[TIC1] Z. Szatmáry (ed): Final Report of Temporary International Collective (TIC), Vol. 1, Experimental Investigations of the Physical Properties of WWER-type Uranium-Water Lattices, Akadémiai Kiadó, Budapest, 1985

[TIC2] L. Maiorov (ed.): Final Report of Temporary International Collective (TIC), Theoretical Investigations of the Physical Properties of WWER-type Uranium-Water Lattices, Akadémiai Kiadó, Budapest, 1995

[Szatm] Szatmáry Zoltán: Bevezetés a reaktorfizikába, Akadémiai Kiadó, Budapest, 2000

[41] Marchuk, G. I. and Lebedev, V. I.: *Numerical methods in the theory of neutron transport*, Moscow, Atizdat, 1971, in Russian. English translation: Harwood, 1986, New York

[42] Birkhoff,G.: *Hydrodynamics*, Princeton University Press, 1950

[43] Varga R. S., *Matrix iterative analysis*, Prentice Hall Inc., Englewood Cliffs, New Jersey, 1962.

[44] Hegedűs Cs. J.: Generating conjugate directions for arbitrary matrices by matrix equations, I. *Comput. Math. Appl.* **21**, 71-85(1991)

[45] Wilkinson, J. H.: *The algebraic Eigenvalue Problem*, Clarendon Press, Oxford, 1964, p. 382

[46] Greenspan, H., Kelber, C. N. and Okrent, D.: *Computing Mathods in Reactor Physics*, Gordon and Breach, New York, 1968

[47] Hyman J. M. & Shashkov M., Adjoint operators for the natural discretizations of the divergence, gradient and curl on logically rectangular grids, *Appl. Numer. Math.*, **25** (1997), 413–442

[48] Hyman J. M. & Shashkov M., Natural discretizations for the divergence, gradient, and curl on logically rectangular grids, *Comput. Math. Applic.*, **33** (1997), 81–104

[49] Strang G. and Fix, G. J.: *An analysis of the finite element method*, Prentice-Hall, Englewood Cliffs, NJ, 1873

[50] Lautard, J. J.: New Finite Element Representation for 3D Reactor Calculations, p. 349-366, *Proc. Intl. Topical Mtg. on Advances in Mathematical Methods for the Solution of Nuclear Engineering Problems*, Műnchen, April 1981

[51] Lewis, E. E. and W. F. Miller: *Computational Methods of Neutron Transport*, Wiley, N.Y., USA, 1984

[52] Palmiotti, G., Lewis, E. E., and Carrico, C. B.: *VARIANT: VARiational Anisotropic Nodal Transport for Multidimensional Cartesian and Hexagonal Geometry Calculation*, Report ANL-95/40, October 1995, Argonne National Laboratory, IL, USA

[53] Laletin, N. I. and Elshin A. V.: *Derivation of finite difference equations for the heterogeneous reactor*, Report IAE-3281/5, 1, Square fuel assemblies, Kurchatow Institute, Moscow, 1980 and Laletin, N. I. and Elshin, A. V.: *Derivation of finite difference equations for the heterogeneous reactor*, Report IAE-3281/5, 2, Square, triangular, and double lattices, Kurchatow Institute, Moscow, 1981

[54] Makai M.: Symmetries Applied to Reactor Calculations, *Nucl. Sci. Eng.* **82**, 338-353(1982)

[55] Makai, M.: *Group theory applied to boundary value problems with applications to reactor physics*, Nova Science, New York, 2011

[56] Orechwa, Y. and M. Makai: Application of Finite Symmetry Groups to Reactor Calculations, INTECH, in: *Nuclear Reactors*, Mesquita, Z. (Ed), INTECH, 2012, http://www.intechopen.com/articles/show/title/applications-of-finite-groups-in-reactor-physics

[57] *Final Report of TIC, vol. 2*, Theoretical Investigations of the Physical Properties of WWER-Type Uranium-Water Lattices, Akadémiai Kiadó, Budapest, 1994

[58] Davison, B: *Neutron Transport Theory*, Oxford, Clarendon Press, 1957

[59] Duderstadt, J. J.; Martin, W. R.: *Transport Theory*, John Wiley, New York, 1979

[60] Lathrop, K. D. and Brinkley, W.: TWOTRAN-II, A*n Interfaced Exportable Version of the TWOTRAN Code for Two-Dimensional Transport*, Los Alamos Scientific Laboratory Report LA-4848-MS, 1973

[61] Lathrop, K. D.: *"THREETRAN: A Program to Solve the Multigroup Discrete Ordinates Transport Equation in (x,y,z) Geometry"*, Los Alamos Scientific Laboratory Report LA-6333-MS, 1976

[62] Ganapol, B. D.: *Analytical Benchmarks for Nuclear Engineering Applications*, NEA/DB(2008)1, OECD Nuclear Energy Agency

[63] *Argonne National Laboratory Benchmark Book*, Report ANL-7416, Argonne, IL, 1968

[64] *Final Report of TIC*, vol. 1, Akadémiai Kiadó, 1985, Budapest, Hungary

[65] Karlvik, I.: *Procedings of the Third International Conference on the Peaceful Uses of Atomic Energy*, Vol. 2, Vienna, 1965, p. 225

[66] Todreas,N. E.; Kazimi, M. S. *Nuclear Systems I.*, Thermal Hydraulics Fundementals, Taylor and Francis, 1990

[67] Kay J. M.;Nedderman R. M.: *An introduction to Fluid Mechanics and Heat Transfer*, Cambridge University Press, London, 1974

[68] Xiaoyi He and Li-Luo: Theory of the lattice Boltzmann method: From the Boltzmann Equation to the lattice Boltzmann equation, *Phys. Rev. E*, **56**, 6811-6817(1997)

[69] Huang, K.: *Statistical Mechanics*, John Wiley, New York, (1963)

[70] *ANSYS CFX*, Release 12.0, ANSYS Inc. Canonsburg, PA 15317, USA, April 2009

[71] Tennekes H.; Lumely J. L.: *A First Course in Turbulence*, MIT Press, 1972

[72] GeurtsB. J.: *Elements of direct and large eddy simulation*, Edwards, Philadelphia, 2004

[73] Batemann, G.: *MHD Instabilities*, The MIT Press, Cambridge (Mass.) and London, 1978

[74] Hyman, J. M., Shashkov. M.: Adjoint operators for the neutral discretizations of the divergence, gradient, and curl on logically rectangular grids, *Aplied Numerical Mathematics*, **25**, 413-442(1997)

[75] Makai M; Orechwa Y. Field reconstruction from measured values in symmetric volumes, *Nuclear Engineer. Design*, **199**, 289–301(2000),

[76] IAEA-TECDOC-1203: Thermohydraulic Relationships for Advances Water Cooled Reactors, IAEA, April 2001

[77] Williams, M. M. R,: *Random Processes in Nuclear Reactors*, Pergamon Press, Oxford, 1974

[78] Pál, L.: *Nuovo Cimento*, Supplemento, **7**, 25(1958)

[79] Bell, G. I.: *Annals of Physics*, **21**, 243(1962)

[80] Pázsit I.; L. Pál, L.: *Neutron Fluctuations*, Elsevier, Amsterdam, 2008

[81] Koblinger L.; Lux, I.: *Monte Carlo Particle Transport Methods*, CRC Press, Boca Raton, 1991

[82] Arnold, L.: *Stochastic Differential Equations*: Theory and Applications, Wiley, 1974

[83] Evans, L. C.: *An Introduction to Stochastic Differential Equations*, UC Berkeley, 2006

[84] Øksendal, B.: *Stochastic Differential Equations*, Springer, New York, 2010

[85] Papoulis, A.: *Probability, Random Variables, and Stochastic Processes*, McGraw Hill, Tokyo, 1965

[86] Doob, J. L.: *Stochastic Processes*, John Wiley, New York, 1953

[87] Pál, L.: *Randomly Evolving Trees* I.,arXiv:cond-mat/0205650, 30 May 2001

[88] Pál, L.: *Randomly Evolving Trees* II., arXiv:cond-mat/0211092, 5 Nov 2002

[89] Pál, L.: *Randomly Evolving Trees* III.,arXiv:cond-mat/0306540, 21 June 2003

[90] Pázsit,I.; Kuang Z. F.; Prinja A. K.: A unified theory of zero power reactor noise via backward master equations, *Ann. Nucl. Energy*, **29**(2002)169-192

[91] ATHLET Mod 2.2 Cycle A, *Program Overreview*, GRS, 2009, Gesellschaft für Anlagen- und Reaktorsicherheit (GRS) mbH, Germany, Garching

[92] COBRA-FLX: *A Core Thermal-Hydraulic Analysis Code*, Topical report, ANP-10311NP, AREVA NP Inc., 2010

[93] *CATHARE V1.3L-1*, CEA, Grenoble, France, 1997

[94] The RELAP5-3D Code Development Team: *RELAP5-3D Code Manual*, Volume IV: Methods and Correlations, INEEL-EXT-98-00834-V4, Revision 2.4, Idaho National Laboratory, Idaho Falls, Idaho, 2005

[95] Gauntt et al. (2000): *MELCORE Computer Code Manuals*, version 1.8.5, NUREG/CR-6119 Rev. 2, SAND2000-241761, Sandia Lab

[96] de Groot S. R.; Mazur,P.: *Non-Equilibrium Thermodynamics*, North-Holland, Amsterdam, 1962

[97] Kittel. Ch.: *Introduction to solid state physics*, John Wiley, 2004

[98] *Safety Series*, International Atomic Energy Agency, Vienna, 19xx-2xxx

[99] Végh, J.: *Application of standard in-core and ex-core instrumentation for monitoring safety related detector performance and for process surveillance in VVER-440 type reactors,* Ageing of Nuclear Reactor Protection Systems Hosted by the Institute of Nuclear Energy Technology in Tsinghua University (INET) 9-13 October 2007, Beijing, China

[100] Siltanen, P.; Antila, M.: *Combining in-core measurements with reactor theory for on-line supervision of core power distribution in the Loviisa reactors*, OECD NEA Specialists' Meeting on In-core Instrumentation and the Assessment of Reactor Nuclear and Thermal-hydraulic Performance, Fredrikstad, Norway, 10-13 October 1983

[101] Boyd, W. A., Miller R. W.: *The BEACON On-Line Core Monitoring System, Functional Upgrades and Applications*, OECD/NEASC INCORE-96 Specialists Meeting On In-Core Instrumentation and Reactor Core Assessment, Mito, Japan, 1996

[102] Zalesky K. et al.: *SCORPIO-VVER Core Surveillance System*, ENS International Topical Meeting on VVER Instrumentation and Control, Prague, Czech Republic, 21-24 April 1997

[103] Stanford, J. L. (Ed): *Statistical Methods for Physical Science*, Academic Press, San Diego, 1994

[104] E. Temesváry and M. Makai: The principal component method, *Nucl. Sci. Eng.* ****

[105] Green J. R.; Margerison, D.: *Statistical Treatment of Experimental Data*, Elsevier Scientific (1978)

[106] Mardia, K. V.; Kent J. T.; Bibby J. M.: *Multivariate Analysis*, Academic Press, London (1979)

[107] Bonalumi R. A.; Kherani, N. P.: Rational Mapping (RAM) of In-Core Data, *Nucl. Sci. Eng.* **90**, 47(1985)

[108] Temesváry, E.: *Evaluation of in-core measurements in nuclear reactors*, MSc Thesis, ELTE, Budapest, 1993, in Hungarian

[109] Szatmáry, Z.: *Data Evaluation Problems in reactor Physics, Theory of Program RFIT,* Report KFKI-1977-43, Central Research Institute for Physics, Budapest

[110] Aszódi,A. and Tóth S.: Numerical model of a steam generator feed water valve, V. Nuclear Technique Symposium, 30th November-1st December, 2006, Paks Hungary

[111] *Handbook of Parameter Estimation for Probabilistic Risk Assessment*, U. S. Nuclear Regulatory Commission, Washington, NUREG/CR-6823, 2003

[112] Perey, F. G.: *Spectrum unfolding by the least squares method*, Proc. of IAEA Technical Comittee Meeteng, Oak Ridge, 10-12 October, 1977

[113] Mackaey, G. W.: *Harmonic Analysis as the Exploitation of Symmetry–A Historical Survey, Bulletin of the American Mathematical Society*, **3**, No. 1, 543-698(1980)

[114] Robertazzi, T. G. and Schwartz, S. C.: *Best "Ordering" for Floating Point Addition*, ACM Trans. on Math. Software, **14**, 101-110(1988)

[115] *Operational Limits and Conditions and Operating Procedures for Nuclear Power Plants*, IAEA SAFETY STANDARDS SERIES, Safety Guide No. NS-G-2.2, Vienna, 2000

[116] *A Technology Roadmap for Generation IV Nuclear Energy Systems*, US DOE, 2002

[117] `http:\\www.world-nuclear.org`

[118] Kemeny, J. G. et al.: *Report of the President's Commission on the Accident at Three Mile Island*, October, 1979, Washington D.C.

[119] Levine, W. S., Ed (1996). *The Control Handbook*, New York: CRC Press

[120] Sacco, W. F., de Oliveira, C. R. E., and Pereira C. M.N. A.: Two stochastic optimization algorithms applied to nuclear reactor core design, *Progress in Nucl. Energy*, **48**, 525-539(2006)

[121] P. Collet and Rennard, J. P.: *Stochastic Optimization Algorithms*, in Rennard, J. P. (ed.): Handbook of Research on Nature Inspired Computing for Economics and Management, Hershley, IGR, 2006

[122] Hedayat, A., Davilu, H., Barfrosh, A. A. and Sepanloo, K.: Estimation of research reactor core parameters using cascade feed forward artificial meural nezworks, *Progress in Nucl. Energy*, **51**, 709-718(2009)

[123] Pereira, C. M. N. A, Sacco, W. F.: A parallel genetic algorithm with nichimg technique applied to a nuclear reactor core design optimization problem, *Progress in Nucl. Energy*, **50**, 740-746(2008)

[124] Bäck, T., Heistermann, J., Kappler, C., Zampelli, M.: *Evolutionary Algorithms to SUpport Refueling of Pressurized Water Reactors*, 3rd IEEE Conference on Evolutionary Computation. Piscataway, NJ, IEEE Press, 1996, pp. 104-108.

[125] Koza, J. R.: *Genetic Programming II., Automatic discovery of reusable programs*, MIT Press, 1994

[126] de Moura Meneses, A. A., Rancoita, P. Schirru R., Gambrardella L. M.: A Class-Based Search for the In-Core Fuel Management Optimization of a Pressurized Water Reactor, *Ann. Nucl. Energy*, **37**, 1554-1560(2010)

[127] Mizutani, A. and Sekimoto, H.: Calculational Method of One-Group Nuclear Constants in Nuclear Equilibrium State, *J. Nucl. Sci. and technology*, **34**, 596-602(1997)

[128] Artioli, A., Grasso, G., and Petrovich, C.: A new paradigm for core design aimed at the sustainibility of nuclear energy: The solution of the extended equilibrium state, *Ann. nucl. Energy*, **17**, 915-922(2010)

[129] Thie, J. A.: *Progress in Nuclear Energy*, Vol.**1**., p.283(1978)

[130] Honeck, H. C. The calculation of the thermal utilization and disadvantage factor in uranium-water lattices, *Nucl. Sci. Eng.* **18**, 49(1964)

[131] Lange, C., Hennig, D., and Hurtado, A.: An advanced reduced order model for BWR stability analysis, *Progress in Nucl. Energy*, **53**, 139-190(2011)

[132] Modern Instrumentation and Control for Nuclear Power Plants: A Guidebook, International Atomic Energy Agency, *Technical Report Series No. 387*, Vienna, 1999

[133] Waltar, A. E. and Reynolds A. B.: *Fast Breeder Reactors*, Pergamon, New York, 1981

[134] March-Leuba, J., Cacuci, D. G., Perez, R. B.: Nonlinear dynamics and stability of boiling water reactors, *Nucl. Sci. Eng.* **86**,401(1984), **93**,101(1986), **93**, 124(1986)

[135] Postnikov, N. S.: Dynamic Chaos in Reactor with Non-linear Feedback, *At. Ener.* **74**,328(1993)

[136] *Safety Analysis Report Series No. 55*, Safety Analysis for Research Reactors, IAEA Vienna, 2008

[137] *Reload Safety Evaluation Methods for Applications to Kewaunee*, Wisconsin Public Service Corporation, 1987, downloaded from `http://pbadupws.nrc.gov/docs/ML1117/ML111711546.pdf`

[138] Schuster, H. G.: *Determinisrtic Chaos*, Physik Verlag, Weiheim, 1984

[139] Pontryagin, L. S.: *Ordinary differential equations*, Nauka, Moscow, 1982, in Russian

[140] Kuchment, P.: *Floquet theory for partial differential equations*, Birkhäuser, Basel, 1993

[141] Sattinger. D. H.: *Group Theoretic Methods in Bifurcation Theory*, Springer, Berlin, 1979

[142] *Calculation and Measurement of the Moderator Temperature Coefficient of Reactivity for Water Moderated Power Reactors*, an American National Standard, ANSIOANS-19.11-1917, American Nuclear Society

[143] Bussac, J. Reuss, P.: *Traité de neutronique*, Hermann, Paris, 1985

[144] Bethe, H.: *Rev. Mod. Phys.* **9**,121(1937)

[145] Gadó J., Dévényi A., Kereszturi A., & Makai M. (1984), A new approach for calculating non-uniform lattices, *Ann. Nucl. Energy*, 11, 559–578.

[146] Gadó, J. et al. (1994). KARATE-A Code for VVER-440 Core Calculation, *Trans. Am. Nucl. Soc.*, 71 , 485.

[147] Case, K. M. and Zweifel, P. F.: *Linear Transport Theory*, Addison Wesley, Reading, Massachusetts, 1967

[148] Kreyszig, E.: *Introductory Functional Analysis with Applications,* John Wiley, 1989

[149] Shihov, S. B.: *Mathematical Problems of Reactor Theory*, Atomizdat, Moscow, 1973, in Russian

[150] Germogenova, T. A.: *Local features of the solution to the transport equation*, Nauka, Moscow, 1986, in Russian

[151] Habetler, G. J. and Martino, M. A.: Existence theorems and Spectral Theory for the Multigroup Diffusion Model, pp. 127-139, in: Proc. of the Eleventh Symposium in Applied Mathematics of the American Mathematical Society, 1959. Ed.: Birkhoff, G. and Wigner, E. P., American Mathematical Society, New York, 1961

[152] Lewins, J. : *Importance. The Adjoint Function*, Pergamon, Oxford, 1965

[153] Courant, R. and Hilbert, D.: *Methods of Mathematical Physics*, McDraw-Hill, New York, 1953

[154] Mika, J. R.: *Nucl. Sci. Eng.* **11**, 415(1961)

[155] Bowden, R. L., Sancaktar, S. Zweifel, P. F.: Multigroup neutron transport, I. Full range, *J. Math. Phys.* **17**,76-81(1976)

[156] Barry, R. F.: *LEOPARD- A spectrum dependent non-spatial depletion code*, Report WCAP-3269-29, 1963

[157] Laletin, N. I.: *At. En.* **14**,458(1963)(in Russian)

[158] Marsaglia, G.: Random numbers fall mainly in the plains, *Nat. Acad. Sci.* **61**, 25-28(1968)

[159] Bielajew, A. F.: *Fundamentals of the Monte Carlo method for neutral and charged particle transport*, The University of Michigan, 2001

[160] Katzgraber, H. G.: *Random Numbers in Scientific Computing: An Introduction,* arXiv:1005.4117v1[physics.comp-ph]22May2010

[161] Vladimirov, V. S.: *Equations of Mathematical Physics*, Marcel Dekker, New York, 1971, Chapter 5

[162] Rumyantzef, G. Ya.: Neutron Diffusion in Periodic Lattices, *At. Energiya,* **14**, 371(1963)

[163] Vladimirov, V. S.: *Mathematical problems of one-velocity transport theory*, Proceedings of the Stekhlov Institute of the Russian Academy, Moscow, 1961

[164] Weinberg, A. M. and E. P. Wigner: *The Physical Theory of Neutron Chain Reactors*, The University of Chicago Press, 1958, Chicago, IL

[165] Szatmáry, Z.: *Introduction to Reactor Physics*, Hungarian Academy of Sciences, Budapest, 2000, in Hungarian

[166] Landau, L. D. and Lisshitz, E. M.: *Course of Theoretical Physics*, vol. I., Butterworth-Heinemann, Amsterdam, 2003

[167] Shreydier, Yu. A. (Ed.): *Monte Carlo Methods*, Műszaki Könyvkiadó, Budapest, 1965, in Hungarian

[168] Nikolaev, M.N. and Hohlov, V. F.: *Subgroup constant system*, in: Bulletin of Nuclear Data Information Center, No. 4, p. 392, 1967

[169] Poole, G, and Boullion, t.: A Survey on M-matrices, *SIAM Review*, **16**. No. 4 (1974)

[170] Nikolaev, M. N., Ryazanov, B. G., Savoskin, M. M.: *Multi-group Approach in Neutron Transport Theory*, Egeroatomizdat, Moscow, 1984, in Russian

[171] Stam'ler, R. J. J.: *Fast Methods for Computing Thermal-neutron Group Constants in Single Pin Lattice Cells*, 1968, Wästeras, Sweden

[172] Honeck, H. C.: *THERMOS A thermalization transport theory code for reactor lattice calculations*, Report BNL-5826(1961)

[173] Akcasu, Z., Lellouche, S. G., Shorkin, L. M.: *Mathematical Methods in Nuclear Reactor Dynamics*, Academic Press, 1971

[174] Keepin, G., Wimelt, T., and Zeigler, R.: Delayed Neutrons from fissionable isotopes of uranium, plutonium, and thorium, *Phys. Rev.* **107**, 1044(1957)

[175] Henry, A. F.: *Nuclear Reactor Analysis*, MIT Press, Cambridge, 1975

[176] Makai, M. and Kollas, J.: Solution of the Diffusion Equation with Zero Average Boundary Values, *Transport Theory and Statistical Physics*, **18**, 313-329(1989)

[177] Larsen, E.: Neutron transport and diffusion in inhomogeneous media, I., *J. Math. Phys.*, **16**, 1421-1427(1975)

[178] Arkuszewski, J. J.: SIXTUS-2: A two-dimensional multigroup diffusion code in hexagonal geometry, *Progress in Nuclear Energy*, **18**, 123-136(1986)

[179] Simon, L. and Baderko, E. A.: *Second Order Partial Differential Equations*, Tankönyvkiadó, Budapest, 1982, p. 42, in Hungarian

[180] Polyanin, A. D.: *Handbook of Linear Partial Differential Equations for Engineers and Scientists*, Chapman and Hall/CRC, 2002

[181] Keresztúri A., Jakab, L.: *A Nodal Method for Solving the Time-Depending Diffusion Equation in the IQS Approximation,* Report KFKI-1991-35/G, 1991.

[182] Grundmann, U. Rohde, U. Mittag, S.: *"DYN3D - three dimensional core model for steady-state and transient analysis of thermal reactors"*, Proc. PHYSOR 2000, Pittsburgh, Pennsylvania, USA.

[183] Falicov, L. M.: *Group Theory and Its Physical Applications*, The University of Chicago Press, Chicago, IL (1996)